Climate Change in the Congo Basin: Evaluating Coupled Models

AMY CREESE

Keble College

A thesis submitted for the degree of Doctor of Philosophy

University of Oxford

Michaelmas Term 2018

Abstract

The convective region of the Congo Basin is a vital component of both the tropical and global circulation, but despite its importance, the climate system is the least studied of any African region. This is due in part to the severe scarcity of recent observational weather data, which in turn has consequences for the use of climate models for providing reliable future projections. Models are usually tested on their ability to reproduce the historical climate, but this approach is unsuitable where observations are lacking. To circumvent this issue, this thesis develops an alternative methodology of model evaluation which does not rely on observational data. This regionally-focussed, process-based approach determines the credibility of multiple state-of-the-art coupled model (CMIP5) simulations of rainfall by assessing the representation of physical processes known to be important for rainfall. The models diverge vastly in the historical period over the Congo Basin, with mean climatological rainfall differing by a factor of five across models in some months. In all seasons, the amount of rainfall in the basin is positively correlated ($p<0.05$) with low-level moisture flux convergence over the basin and low-level moisture flux into the basin across certain boundaries, which with targeted observational data could be used to provide one constraint on the spectrum of model rainfall. In the September-November (SON) wet season, model wetness in the west Congo Basin relates to the strength of the tropical Atlantic SST bias, casting doubt on models which are extremely wet. In the east, model wetness is related to the strength and structure of the African Easterly Jets. There is also uncertainty amongst models as to the direction and magnitude of future rainfall change. A process-based assessment of future change in SON finds that in some areas, spurious climatologies in the historical period result in distinct future rainfall change signals, casting doubt on the plausibility of those changes. This thesis finds that a process-based approach to climate model evaluation can be used to help determine model credibility in the historical period in the absence of observational data, and is a promising method for constraining uncertainty in the future climate signal.

Table of Contents

Abstract i

Table of Contents iii

Acknowledgements xi

List of Tables xiii

List of Figures xv

List of Acronyms xxxvii

1 Introduction 1

1.1 Motivations and Aims 2

1.1.1 Background and rationale 2

1.1.2 Aims and objectives 7

1.1.3 Thesis structure 8

1.2 The Congo Basin 9

1.2.1 Study area 10

1.2.2 1The Congo Basin climate regime 14

1.2.3 Regional influences on the Congo Basin climate 24

1.2.4 Observed recent rainfall change in the Congo Basin 33

1.2.5 Key challenges and knowledge gaps 35

1.3 Future climate change 40

1.3.1 Climate models 43

1.3.2 Projected tropical rainfall change 46

1.3.3 Projected Congo Basin rainfall change 49

1.3.4 Key challenges 52

1.4 Climate model evaluation 53

1.4.1 Performance-based model evaluation 54

1.4.2 Process-based model evaluation 59

1.4.3 Approach in this thesis 71

1.5 Summary of aims and objectives 72

Chapter 3: Assessing inter-model differences 73

Chapter 4: Processes differentiating models in SON 74

Chapter 5: Determining whether past capabilities informs future signal 75

Chapter 6: Identifying processes driving inter-model differences in projections 76

1.6 Thesis format 77

2 Data and Methods 79

2.1 Introduction 80

2.2 Data 80

2.2.1 CMIP5 data 80

2.2.2 Reanalysis, gauge and satellite data 83

2.3 Methods....85
2.3.1 Characterising the climatology....85
2.3.2 Process-based evaluation....86
2.3.3 Projected change....93

3 Using qflux to constrain modelled Congo Basin rainfall in the CMIP5 ensemble....95

Authorship Declaration....97
Abstract....98
3.1 Introduction....99
3.1.1 Congo climate regime....101
3.1.2 Coupled models....103
3.1.3 Aims....104
3.2. Data....105
3.3 Rainfall climatology....106
3.3.1 Annual cycle of rainfall....106
3.3.2 Rainfall distribution....110
3.4 Moisture flux convergence....118
3.4.1 Relationship to rainfall....120
3.4.2 Wet and dry model differences....123
3.5 Spatial limits to the convergence-rainfall relationship....125

3.5.1 Location of convergence maxima 125

3.5.2 Spatial limits at the subdomain scale 129

3.6 Origin of Water Vapour Transport 132

3.6.1 Direction of water vapour transport into the basin 132

3.6.2 Possible influences on water vapour transport at basin boundaries 136

3.7 Discussion 139

3.8 Conclusions 144

Acknowledgements 147

Supplementary Material 148

4 A process-based assessment of CMIP5 rainfall in the Congo Basin: the September-November rainy season 153

Authorship Declaration 155

Abstract 156

4.1 Introduction 157

4.1.1 Climate model evaluation in the Congo Basin 158

4.1.2 The September to November (SON) wet season 161

4.1.3 Aims 165

4.2 Data and Methods 165

4.3 Characterising model rainfall 169

4.4 Influence of Tropical Atlantic and Indian Ocean Sea Surface Temperatures 173

4.5 Identifying processes related to rainfall differences 177

4.5.1 Processes in the west 178

4.5.2 Processes in the east 185

4.6 Discussion 194

4.6.1 Rainfall differences between east and west 194

4.6.2 Influence of SSTs on the west of the basin 195

4.6.3 Dynamical processes affecting the east of the basin 198

4.7 Summary 201

Acknowledgements 203

5 The plausibility of September-November Congo Basin rainfall change in coupled climate models 205

Authorship Declaration 207

Abstract 208

5.1 Introduction 209

5.1.1 Regionally-focussed process-based assessments 210

5.1.2 Climate change in the Congo Basin 212

5.1.3 Tropical rainfall change 214

5.1.4 Aims 215

5.2 Data and Methods 216

5.3 Rainfall changes in SON 217

5.4 Rainfall change mechanisms in the west Congo Basin 221

5.4.1 Rainfall change 222

5.4.2 Processes associated with rainfall change 224

5.5 Rainfall change mechanisms in the east Congo Basin 232

5.5.1 Rainfall change 232

5.5.2 Processes associated with rainfall change 234

5.6 Discussion 242

5.6.1 Magnitude and patterns of rainfall change across models 243

5.6.2 Rainfall change in the west composites 245

5.6.3 Rainfall change in the east composites 249

5.7 Summary 254

Acknowledgements 257

Supplementary material 258

6 Climate change in the Congo Basin: Processes related to wetting in the December-February dry season 263

Authorship Declaration 265

Abstract 266

6.1 Introduction 267

6.1.1 Congo Basin rainfall change 269

6.1.2 Mechanisms of tropical rainfall change under warming 271

6.1.3 A process-based assessment of change 273

6.1.4 Aims 275

6.2 Data and Methods 276

6.3 Rainfall change across the annual cycle 278

6.4 Rainfall change in DJF 280

6.4.1 All models 281

6.4.2 Composites 286

6.5 Changes in large-scale vertical circulation 288

6.6 Low-level moisture flux changes 291

6.6.1 Moisture flux at 850 hPa 292

6.6.2 Moisture flux at 700 hPa 295

6.6.3 Flux across domain boundaries 296

6.7 Discussion and summary 298

6.7.1 Changes in rainfall magnitude and distribution 298

6.7.2 Circulation changes associated with rainfall change 299

6.7.3 Summary 305

Acknowledgements 306

Supplementary material 308

7 Conclusions 311

7.1 Model behaviour in the historical period 313

7.1.1 To what extent can the large-scale processes of water vapour transport, provision and convergence explain inter-model differences in the representation of rainfall in the Congo Basin? 314

7.1.2 Can the credibility of models be determined based on an assessment of regional processes related to rainfall? 318

7.2 Plausibility of model future climate projections 323

7.2.1 Does model credibility in the historical period give insights into the plausibility of future projections? 324

7.2.2 What processes contribute to inter-model uncertainty in future climate projections, and can an understanding of these processes help determine the plausibility of projections? 329

7.3 The value of process-based assessments 333

7.4 Avenues for future research 339

7.5 Concluding remarks 343

References 345

Acknowledgements

The experience of completing a DPhil has been a series of highs and lows. But while it was sometimes an isolating experience, the past four years have been made immeasurably better by a number of people, without whom I would not be writing this now.

The first thank you goes to my supervisor, Richard Washington. I'm not sure I would have believed, on meeting him nine years ago in an undergraduate interview, that I would be here now, finishing a PhD in African climate with him as my supervisor (especially since, when asked by Richard during that interview "Where does rain come from?", I panicked and answered, "The sky?!"). That he believed I could do this was never in doubt, and that has been a huge source of encouragement for me. It goes without saying that his scientific guidance has been second to none.

On the topic of science, this thesis wouldn't be what it is today without the countless discussions over the years with people in the Climate Research Lab. Special thanks must go to Ian Ashpole, Neil Hart and Rachel James, who have patiently listened to many a problem and always given considered advice. Emma Howard deserves a mention for her unending patience with maths questions, and help solving many a coding problem. I am not sure how we coped without a mathematician in the group before she came along. Thanks also to Sebastian Engelstaedter for teaching me to code in the first place, and for his ongoing help with coding and data access over the past four years.

None of this work would have been possible without funding, so I am extremely grateful to the Natural Environment Research Council for four years of support via the Oxford Doctoral Training Partnership, and to Victoria Forth and Claudia Azevedo in the DTP office for the unenviable task of managing this funding. Thanks also to the Met Office, for providing me with partial funding through a CASE studentship.

The experience of completing this DPhil has been greatly enhanced by my involvement in the NERC and DFiD funded UMFULA project. I feel incredibly fortunate that my DPhil began at the same time a large, international African climate project was starting, and I'd like to thank everyone in UMFULA for welcoming me into the fold, in particular Declan Conway and Estelle Rouhaud. Thanks also to the CCKE unit for funding two out of three wonderful trips to Cape Town for annual meetings, where alongside braais and beers some exceptional scientific collaboration has been undertaken. For this I must thank the

UMFULA climate science crew – Martin, Ross, Seshu, Fabien, Melissa, Chris and Rondro. I firmly believe scientists work best in teams, and I am delighted that this was my team.

My work has also been vastly improved through discussions with a number of excellent scientists and academics within and beyond Oxford. I was delighted to have Richard Jones on board as my Met Office supervisor, and his insights into the mysterious workings of models were invaluable on numerous occasions. I am much obliged to Wilfried Pokam, who has always had time to answer my questions about Central Africa, and whose work initiated some of the key hypotheses in this thesis. Thank you too to Ali Rogers at Keble, for my introduction to academic geography seven years ago, and for all his support since. I would also like to thank my two examiners – Simon Dadson, who has been a positive and enthusiastic assessor throughout my DPhil journey, and Sharon Nicholson, whose countless papers on African climate have underpinned a large part of the analysis in this thesis. Both made the examination process as pleasant as I think it is possible to be!

I would like to sincerely thank all my friends for their support over the last four years, and for consistently being proud of my achievements, which can feel small when you're in the thick of academia! Special thanks must go to Paige, Hannah, Fiona and Cara for just being wonderful friends, and thanks also to Josie and Boi in the climate lab, for providing tea and kindness when I've needed it most. Catherine Buckland has been an absolute rock in times of trouble, geography-related and otherwise, and I will very much miss our regular lunches in the common room putting the world to rights. A particularly special mention must go to Callum Munday, without whom this thesis probably would still have been completed, but with many more tears and a higher average heart rate. Doing a DPhil alongside your best friend is highly recommended.

My family have been consistently wonderful, not just during my DPhil but throughout my whole life. Special mentions must go to my grandparents and, of course, my Mum and Dad. They have not once stopped believing in me and being proud of me, and I cannot convey my thanks to them enough. I feel genuinely lucky to have them as my parents, and truly sorry for everyone who does not.

Finally, this DPhil would not have been completed without the support of my soon-to-be-husband James. His support over the past seven years has known no bounds; he even moved from his beloved North down to Oxford to be with me during this DPhil, which anyone who knows him will recognise as no small sacrifice. I feel incredibly lucky to have him to do life with.

List of Tables

Table 2.1 – CMIP5 model experiments used in this thesis 82

Table 2.2 - Reanalysis data used in this thesis 84

Table 2.3 – Observational data used in this thesis 85

Table 3.1 – CMIP5 models used in this study 107

Table 3.2 – Definition and characteristics of reanalysis and satellite/gauge datasets used in this study 108

Table 3.3 – Correlation (r-value) between model Congo Basin rainfall and a) specific humidity, b) wind convergence and c) qflux convergence at 850hPa and 700hPa, in the long term mean. * denotes significance at 95%. Bold indicates the highest correlation coefficient for each season and pressure level. 123

Table 4.1- CMIP5 models used in this study 167

Table 4.2 - Identity and charactertistics of reanalysis and satellite/gauge datasets used in this study 168

Table 4.3 - Models used in wet and dry composites 169

Table 5.1 – CMIP5 models used in this study 218

Table 6.1 – Calculations of qflux convergence (10^{-8} kg kg^{-1} s^{-1}) using different combinations of mean q and mean winds from the driest and wettest composites 303

List of Figures

Figure 1.1 - Number of rain gauges per year over the region 5°S–5°N, 12.5°E– 30°E in the CRU 0.5° rainfall dataset. Source: *Washington et al.* [2013] 4

Figure 1.2 - Standard deviation of long-term mean (1979-2005) rainfall (mm day^{-1}) across 19 CMIP5 models (listed in Chapter 6) for (a) MAM, (b) JJA, (c) SON and (d) DJF. The red, blue, green and purple boxes refer to the Congo Basin, East African, southern African and West African domains respectively. 5

Figure 1.3 - Map showing the study area, political boundaries and Congo Basin domains used in Chapter 3 (purple; 5°E to 35°E, 10°S to 10°N), Chapters 4 and 5 (red; 8°E to 35°E, 10°S to 10°N) and Chapter 6 (green; 10°E to 35°E, 10°S to 5°N)11

Figure 1.4 - Land surface height (m) over the Congo Basin domain (red box) and surrounding regions. Data is from the USGS GTOPO30 digital elevation model 13

Figure 1.5 - Schematic showing key features of the Congo Basin climate. Locations are approximate. AEJ-N = African Easterly Jet, north; AEJ-S = African Easterly Jet, south; TEJ = Tropical Easterly Jet 15

Figure 1.6 - Long term mean (1979-2005) rainfall (mm day^{-1}) from the Climatic Research Unit (CRU, version 3.23) dataset [*Harris et al.*, 2014], in (a) MAM, (b) JJA,

(c) SON and (d) DJF. The red box shows the main Congo Basin domain (8°E to 35°E, 10°S to 10°N) 16

Figure 1.7 - Schematic of the seasonal variability of the Intertropical Convergence Zone (ITCZ; green), Congo air boundary (red; not discussed), tropical rain-belt (blue), and surface winds (dark grey). The black box shows the location of Western and Central Equatorial Africa used by *Dezfuli* [2017]. Adapted from *Dezfuli* [2017]; shows approximate locations 17

Figure 1.8 - (a) Rainfall (mm day^{-1}) and (b) moisture flux at 850 hPa climatologies for (i) the driest (CNRM-CM5) and (ii) wettest (NorESM1-M) CMIP5 models in SON. Units are mm day^{-1} in (a) and g kg^{-1} ms^{-1} in (b) with contours of divergence (g kg^{-1} s^{-1}). Source: *Washington et al.* [2013] 21

Figure 1.9 - (a) Horizontal pattern of long-term mean zonal wind at 600 hPa in August to identify the African easterly jet (AEJ). (b) Latitude-height cross section of mean zonal wind in August, averaged over longitudes highlighted with the transparent strip in panel (a). Tropical easterly jet and low-level westerly (LLW) winds are evident. (c) and (d) are the same as (a) and (b), respectively, but for October. The black box in (a) and (c) shows the location of Western and Central Equatorial Africa used by *Dezfuli* [2017]. Grey shading in (b) and (d) represents topography, and dashed grey lines show the southern and northern limits of WCEA. Source: *Dezfuli* [2017] 25

Figure 1.10 - The global network of World Weather Watch (WWW) stations, colour coded to show reporting rates. Data-sparse areas and low reporting rates for Africa are clearly visible. Source *Washington et al.* [2006] (data from WMO 2003) 36

Figure 1.11 - Station data contributing to the Climatic Research Unit (CRU, version 2.23) precipitation (black) and Integrated Global Radiosonde Archive (IGRA) u wind at 1200 UTC (pink). (top) Coverage map for 1979–2013. Black squares indicate the location of 0.5° × 0.5° grid boxes that have at least one contributing station during at least 50% of the months; pink circles indicate stations with at least 10 records per month in at least 50% of the months. (bottom) Time series showing the number of stations contributing in each month (40°S–40°N, 30°W–60°E). Source: *James et al.* [2018].....37

Figure 1.12 - Long-term mean annual cycle of rainfall (mm day^{-1}) for Equatorial Central Africa over the region 58 S–58 N, 12.5–308 E for the following datasets: CMAP, TRMM, TAMSAT, CMORPH, NCEP, CFSR, ERA-40, ERA-Interim, ensemble mean of CMIP3 and CMIP5. Individual CMIP5 models are shown in grey. Averages over 1961-1990. Source: *Washington et al.* [2013] 38

Figure 1.13 - Maps of precipitation changes from IPCC AR5, for Africa in 2080–2099 with respect to 1986–2005 in June to September (top) and December to March (bottom) in the SRES A1B scenario with 24 CMIP3 models (left), and in the RCP4.5 scenario with 39 CMIP5 models (middle). Right figures are the precipitation changes in 2075–2099 with respect to 1979–2003 in the SRES A1B

scenario with the 12-member 60-km mesh Meteorological Research Institute (MRI)-Atmospheric General Circulation Model 3.2 (AGCM3.2) multi- physics, multi-sea surface temperature (SST) ensembles (Endo et al., 2012). Precipitation changes are normalized by the global annual mean surface air temperature changes in each scenario. Light hatching denotes where more than 66% of models (or members) have the same sign with the ensemble mean changes, while dense hatching denotes where more than 90% of models (or members) have the same sign with the ensemble mean changes. Source: *Christensen et al.* [2013] 42

Figure 1.14 - CMIP5, CMIP3 and CORDEX Ensemble-Median projected relative changes in annual total precipitation following the low (top row) and high (bottom row) emission scenario for the mid-21st (2036–2065; left column) and the end of 21st century (2071–2100; right column) with respect to the control period. The black stipples indicate regions in which at least 66 % of all projected changes agree in the sign of change. Source: *Haensler et al.* [2013a].....50

Figure 1.15 - Decomposition of RCP8.5-minus-historical precipitation change into dynamic and thermodynamic components, averaging data over three East African regions. Tick marks on each vertical line show results for individual CMIP5 models, and gray bars mark approximately the central 80% of datasets. The components are as follows: the change in q over land arising from increased moisture advection from the oceans + the weakening of the circulation (ΔPqadvw), residual changes in q over land (ΔPqres), spatial shifts in convection (ΔPshift), and a nonlinear cross term associated with interactions between other terms (ΔPcross). Source: *Rowell and Chadwick*, [2018] 69

Figure 2.1 - Schematic of the chain of processes related to higher rainfall in the wet composites compared with the dry composites in the west Congo Basin (purple box), as described in Chapter 4.....89

Figure 3.1 - Mean number of stations contributing to the CRU 3.23 gridded precipitation dataset (0.5° horizontal grid spacing). Red box indicates study domain for this research (5°E to 35°E, 10°N to 10°S).....101

Figure 3.2 - Schematic showing key features of the Congo Basin climate. Locations are approximate. The study area is shown by the green box. AEJ-N= African Easterly Jet – North and AEJ-S = African Easterly Jet South.....102

Figure 3.3 - 30 year mean rainfall (mm day^{-1}) for individual CMIP5 models, reanalysis and satellite data 1971-2000. The thick black line shows the ensemble of models; the dashed thick black line shows the ensemble of all observational and reanalysis datasets.....109

Figure 3.4 - Long term mean (1971-2000) rainfall (mm day-1) for a) MAM and b) SON for 17 CMIP5 models, the ensemble mean, reanalysis, gauge and satellite data sets. Models and reanalyses products are ordered from dry to wet (left to right, top to bottom) based on mean rainfall across the basin.....111

Figure 3.5 - For long-term mean (30-year) rainfall (mm day -1) (a) MAM and (b) SON: composite of five wettest models in Figure 4 (top left); composite of five

driest models in Figure 4 (top right); wet composite minus dry composite with stipples for agreement, (bottom left); dry composite minus wet composite, with stipples for agreement (bottom right). Large circles (crosses) indicate that all wet (dry) models are wetter (drier) than the maximum (minimum) of the dry (wet) models at that gridpoint. Small circles (crosses) indicate that all wet (dry) models are wetter (drier) than the mean of the dry (wet) models at that gridpoint. 113

Figure 3.6 - As for Figure 3.4 but for (a) JJA and (b) DJF 115

Figure 3.7- As for Figure 3.5 but for (a) JJA and (b) DJF 116

Figure 3.8 - Relationship between the long-term mean (30-year) rainfall (mm day^{-1}) in the wet seasons (MAM and SON mean) and dry seasons (JJA and DJF mean) for individual datasets. 118

Figure 3.9 - Average long-term mean (1971-2000) rainfall rank of CMIP5 models and reanalysis data sets for (a) wet seasons (MAM and SON), (b) dry seasons (JJA and DJF) and (c) all seasons. Rank 1 is the driest model; rank 17 is the wettest model. Circle denotes the mean rank. Solid lines denote the range in ranks each model occupies for the subset of seasons. 119

Figure 3.10 - Long-term mean (1971-2000) moisture flux divergence (10^8 kg kg^{-1} s^{-1}) and rainfall (mm day^{-1}) at (a) 850hPa and (b) 700hPa for CMIP5 models and reanalyses data 121

Figure 3.11 - For (a) 850hPa and (b) 700hPa: Difference in moisture flux convergence (shaded; 10^8 kg kg^{-1} s^{-1}) and moisture flux (vectors; kg kg^{-1} m s^{-1}) between composite of five wettest and five driest models in each season. Only vectors which are significantly different between the wet and dry ensembles (using the agreement metric described in Section 3.2.3) are shown 124

Figure 3.12 - Location of top 20% of rainfall values (blue), moisture flux convergence values (red), and areas of overlap (pink) in (a) MAM at 700hPa and (b) SON at 850hPa. The location of maximum rainfall (convergence) is denoted by a star (cross) 126

Figure 3.13 - As for Figure 3.12 but for (a) JJA at 850hPa and (b) DJF at 850hPa128

Figure 3.14 - Relationship between long term mean (1971-2000) moisture flux convergence (10^8 kg kg^{-1} s^{-1}) at (a) 850hPa and (b) 700hPa and rainfall (mm day^{-1}) for CMIP5 models, ensemble mean and two reanalysis data sets in: the north west (top left); north east (top right); south west (bottom left); and south east (bottom right) 129

Figure 3.15 – (a) Schematic showing the correlation coefficient between long-term mean rainfall over the basin and moisture (qflux) entering the basin across the northern, eastern, southern and western boundaries at 850hPa and 700hPa. Large arrows and bold text denotes r-values significant at the 95% level. Dashed arrows indicate a negative relationship. (b) Latitude/height and longitude/height cross-sections for flow across boundaries which feature significant correlations.

Individual vertical grid locations which feature significant correlations are stippled. 133

Figure 3.16 - Relationship between basin rainfall (5°E-35°E, 10°S-10°N; mm day-1) and SST bias (°C) at each gridbox, across 17 CMIP5 models 137

Figure 3.17 - (Top) a) Longitude/height (m) cross section of land surface height for 10 models at the equator. (Bottom) The relationship in MAM only between (b) land surface height (m) at 0°, 36°E and rainfall (mm day^{-1}); (c) land surface height at 0°, 36°E and qflux into the basin at 700hPa at 35°E (10^2 kg kg^{-1} s^{-1}); d) qflux from the east at 700hPa and rainfall. 139

Figure 3.S1 - for (a) 850 hPa and (b) 700 hPa - Composite of moisture flux convergence (shaded) and moisture flux (vectors) in the five wettest models (based on Figure 3.2) (left column) and the five driest models (right column) in each season at 850 hPa 148

Figure 3.S2 - Location of top 20% of rainfall values (blue), moisture flux convergence values (pink), and areas of overlap (purple) in a) MAM at 850hPa and b) SON at 700hPa. The location of maximum rainfall (convergence) is denoted by a star (cross) 150

Figure 3.S3 - As for Figure 3.S2 but for a) JJA at 700hPa and b) DJF at 700hPa ... 151

Figure 4.1 - Long term mean (1979-2005) SON rainfall (mm day^{-1}) for 17 CMIP5 models, ensemble mean, reanalysis and satellite-gauge products.....170

Figure 4.2 - Scatter plots showing relationship between long-term mean (1979-2005) rainfall (mm day^{-1}) in the west (8°E to 21°E, 10°S to 10°N) and in the east (21°E-35°E, 10°S to 10°N) Congo Basin. Blue (grey) plots show relationships that are significant (not significant) at the 95% level. 171

Figure 4.3 - Long term mean (1979-2005) rainfall (mm day^{-1}) composites of (a, d) four wettest models, (b, e) four driest models, and (c, f) the wet-minus-dry difference in the west and east of the basin respectively. The red box shows the location of the subdomain. Stipples occur under the following conditions: (1) where all wet model values are larger or smaller than all dry model values (large dots); (2) where all wet model values are greater or smaller than the dry mean, depending on the direction of difference (squares); (3) where all dry models are greater or smaller than the wet mean, depending on the direction of difference (crosses); and (4) where both (2) and (3) are true (small dots). 172

Figure 4.4 - Long term mean (1979-2005) SST bias (°C; model minus HadISST2) in SON, for all CMIP models, and HadISST2 observed SST (°C). Red box shows location of Atlantic SST mean bias in Figure 4.8. 174

Figure 4.5 - Long term mean (1979-2005) CMIP minus AMIP rainfall (mm day^{-1}) in SON, for all CMIP5 models and the ensemble mean.....175

Figure 4.6 - Annual cycle of long term mean (1979-2005): CMIP minus AMIP rainfall (mm day^{-1}) for all models (boxplot); the mean model Atlantic SST bias between 5°W to 8°E, 12°S to 3°N (°C ; purple line); and intermodel spread of Atlantic SST biases (purple shaded area; excluding CSIRO-Mk3-6-0). The dashed line shows the SST bias in CSIRO-Mk3-6-0, the only model to have a consistent cold bias. 176

Figure 4.7 - Long term mean (1979-2005) SST bias (°C) in SON in (a) HadISST2 (observed), (b) west Congo wet composite, (c) west Congo dry composite, and (d) wet-minus-dry difference between wet and dry composite..... 179

Figure 4.8 - Annual cycle of long term mean (1979-2005) SST bias (°C; model minus HadISST2) between 5°E and 8°E for the (a) west Congo wet composite, (b) west Congo dry composite, and (c) the wet-minus-dry difference. 180

Figure 4.9 - Long term mean (1979-2005) evaporation (mm day^{-1}) in SON in (a) ERA-I, (b) west Congo wet composite, (c) west Congo dry composite and (d) wet-minus-dry difference. Stipples are as described in Figure 4.3 caption. 181

Figure 4.10 - Long term mean (1979-2005) SON qflux convergence (10^{-8} kg kg^{-1} s^{-1}; shaded) and qflux (kg kg^{-1} m s^{-1}; vectors) at 925 hPa in (a) ERA-I, (b) west Congo wet composite, (c) west Congo dry composite and (d) wet-minus-dry difference. Vectors are only shown at gridboxes in (d) when the values in all wet models are greater than the values in all dry models, or all the values in all dry models are greater than the values in all wet models. 182

Figure 4.11 - Long term mean (1979-2005) SON omega between 3°S and 3°N (10^{-3} Pa s^{-1}; shaded) and divergent component of zonal wind (m s^{-1}) and omega (streamlines) in (a) ERAI, (b) west Congo wet composite, (c) west Congo dry composite, and (d) wet-minus-dry difference. Stipples are as described in Figure 3 caption. A bilinear interpolation scheme was used to fill missing values to calculate the divergent component of u-wind. Areas with high topography in models are masked (white); values below 900hPa are not shown due to large amounts of topography-related missing data. The purple box shows the extent of the west Congo domain.....183

Figure 4.12 - As in Figure 4.7 but for the east Congo composites.....186

Figure 4.13 - Long term mean (1979-2005) SON qflux convergence (10^{-8} kg kg^{-1} s^{-1}; shaded) and qflux (kg kg^{-1} m s^{-1}; vectors) at (i) 925 hPa and (ii) 700 hPa in (i) ERA-I, (ii) east Congo wet composite, (iii) east Congo dry composite and (iv) wet-minus-dry difference. Vectors in (iv) are as described in Figure 4.10 caption.....188

Figure 4.14 - Mean sea level pressure (hPa; shaded) and 925 hPa qflux (kg kg^{-1} ms^{-1}; vectors), in (a) ERA-I, (b) east Congo wet composite, (c) east Congo dry composite and (d) wet-minus-dry difference. Vectors and MSLP shading are only shown at gridboxes in (d) when the values in all wet models are greater than the values in all dry models, or all the values in all dry models are greater than the values in all wet models.....190

Figure 4.15 - As in Figure 4.11 but for east Congo composites. The green box shows the extent of the east Congo Basin domain. 191

Figure 4.16 - Latitude-height cross section of zonal wind averaged across 26°E-30°E (m s^{-1}; shaded) and location of -5 m s^{-1} contour in (a) ERA-I, (b) east Congo wet composite, (c) east Congo dry composite and (d) wet-minus-dry difference. Stipples in (d) are as described in Figure 4.3 caption. 193

Figure 4.17 - Long term mean (1979-2005) meridional potential temperature gradient (10^{-6} K m^{-1}; shaded) at 850 hPa in (a) ERA-I, (b) east Congo wet composite, (c) east Congo dry composite and (d) wet-minus-dry difference. Lines show latitudinal location of maximum easterly wind speed (≤ -5 m s^{-1}) at 700 hPa in region of AEJ-N (cyan) and AEJ-S (magenta). Stipples in (d) are as described in Figure 4.3 caption. 194

Figure 5.1 - Long term mean SON rainfall (mm day^{-1}) in individual CMIP5 models in (a) the west Congo Basin (8°E to 21°E, 10°S to 10°N) and (b) east Congo Basin (22°E to 35°E, 10°S to 10°N), in: the historical period (1979-2005; red); the future period (2074-2100; light blue); and the 2074-2100 minus 1979-2005 (ΔP; dark blue). Ordered by mean historical rainfall (low to high). Models used in the wet (dry) composites are denoted by hatching (stipples). CSIRO-Mk3-6-0 is excluded from the dry composite (as in Creese and Washington 2018) due to the opposite signal of the historical SST bias 220

Figure 5.2 - Future (2074-2100) minus historical (1979-2005) long-term mean rainfall (ΔP; mm day^{-1}) in individual CMIP5 models. Stipples in the ensemble mean plot show gridboxes where 14 out of 17 models agree on the sign of change. 221

Figure 5.3 - Long term mean SON rainfall (mm day^{-1}) in the west Congo Basin wet composite (top row) and dry composite (middle row) in (a), (d) 2074-2100, (b), (e) 1979-2005; and (c), (f) 2074-2100 minus 1979-2005 (ΔP); (g) 2074-2100 wet minus dry composite; (h) 1979-2005 wet minus dry composite; and (i) wet ΔP minus dry ΔP. Stipples in (c) and (f) indicate where all four models in the composite agree on the sign of change. Stipples in (g-i) occur at gridboxes where: 1) all wettest composite values are larger or smaller than all driest composite values (large dots); 2) all wettest composite values are greater or smaller than the driest composite mean (squares); 3) driest composite values are greater or smaller than the wettest composite mean (crosses); and 4) both (2) and (3) are true (small dots). The purple box indicates the location of the west Congo Basin domain. 223

Figure 5.4 - Long term mean SON SST (°C) in the west Congo Basin wet composite (top row) and dry composite (middle row) in (a), (d) 2074-2100, (b), (e) 1979-2005; and (c), (f) 2074-2100 minus 1979-2005 (ΔSST); (g) 2074-2100 wet minus dry composite; (h) 1979-2005 wet minus dry composite; and (i) wet ΔSST minus dry ΔSST. Stipples as in Figure 5.3. The purple box indicates the location of the west Congo Basin domain..... 226

Figure 5.5 - Long term mean SON qflux convergence (10^{-8} kg kg^{-1} s^{-1}; shaded) and qflux (kg kg^{-1} m s^{-1}; vectors) at 925 hPa in the west Congo Basin wet composite

(top row) and dry composite (middle row) in (a), (d) 2074-2100, (b), (e) 1979-2005; and (c), (f) 2074-2100 minus 1979-2005; (g) 2074-2100 wet minus dry composite; (h) 1979-2005 wet minus dry composite; and (i) wet change minus dry change. Vectors in (c) and (f) indicate where all four models in the composite agree on the sign of change. Vectors in (g), (h) and (i) occur at gridboxes where all wettest composite values are larger or smaller than all driest composite values. The red box indicates the location of the west Congo Basin domain. 228

Figure 5.6 - Long term mean SON omega (10^{-3} Pa s^{-1}; shaded) averaged between 3°S and 3°N and divergent component of zonal wind (m s^{-1}) and omega (10^{-3} Pa s^{-1} streamlines), in the west Congo Basin wet composite (top row) and dry composite (middle row) in (a), (d) 2074-2100, (b), (e) 1979-2005; and (c), (f) 2074-2100 minus 1979-2005; (g) 2074-2100 wet minus dry composite; (h) 1979-2005 wet minus dry composite; and (i) wet change minus dry change. Areas with high topography in models are masked (white). The purple box shows the extent of the west Congo Basin domain (8°E to 21°E). Stipples as in Figure 5.4 and refer to omega values. 229

Figure 5.7 - Annual cycle of long term mean omega at 500hPa (10^{-3} Pa s^{-1}; shaded) and rainfall (mm day^{-1}; contours), averaged between 8°E and 21°E in the west Congo Basin wet composite (top row) and dry composite (bottom row) in (a), (d) 2074-2100, (b), (e) 1979-2005; and (c), (f) 2074-2100 minus 1979-2005. Stipples as in Figure 5.4 and refer to omega values. Dashed lines indicate the northern and southern boundaries of the domain. 231

Figure 5.8 - Frequency distribution of daily rainfall (mm day^{-1}) in all SON days in the northwest of the basin (8°E to 21°E, 0° to 10°N) in all composite member models in (a) the west Congo Basin wet composite and (b) the dry composite, between 2074 and 2100 (blue) and 1979-2005 (orange). Pink denotes overlap between the orange and blue distributions. 232

Figure 5.9 - As in Figure 5.3 but for the east Congo Basin composites. The green box indicates the location of the east Congo Basin domain. 233

Figure 5.10 - Long term mean SON sea level pressure (hPa; shaded) and qflux at 925 hPa (kg kg^{-1} m s^{-1}; vectors) in the west Congo Basin wet composite (top row) and dry composite (middle row) in (a), (d) 2074-2100, (b), (e) 1979-2005; and (c), (f) 2074-2100 minus 1979-2005; (g) 2074-2100 wet minus dry composite; (h) 1979-2005 wet minus dry composite; and (i) wet change minus dry change. Vectors as in Figure 5.5. SLP shading is only shown at grid boxes in (i) when the values in all wet models are greater than the values in all dry models, or all the values in all dry models are greater than the values in all wet models. 235

Figure 5.11 - As in Figure 5.6 but for the east Congo Basin composites. The green box indicates the location of the east Congo Basin domain. 237

Figure 5.12 - As in Figure 5.7 but for the east Congo Basin composites. Dashed lines indicate the northern and southern boundaries of the domain. 238

Figure 5.13 - As in Figure 5.5, but for the east Congo Basin composites at 700 hPa. The green box indicates the location of the east Congo Basin domain. 240

Figure 5.14 - Latitude-height cross section of zonal wind averaged across 26°E-30°E (m s^{-1}; shaded) and location of -5 m s^{-1} contour in the east Congo Basin wet composite (top row) and dry composite (middle row) in (a), (d) 2074-2100, (b), (e) 1979-2005; and (c), (f) 2074-2100 minus 1979-2005; (g) 2074-2100 wet minus dry composite; (h) 1979-2005 wet minus dry composite; and (i) wet change minus dry change. Stipples as in Figure 5.4. 242

Figure 5.15 - Box plot of 2074-2100 minus 1979-2005 long-term mean rainfall (mm day^{-1}; ΔP) averaged over (a) the west Congo Basin domain (8°E to 21°E, 10°S to 10°N) and (b) the north west Congo Basin domain (8°E to 21°E, 0° to 10°N). The first boxplot includes all models, the second excludes the wet composite models, and the third excludes the dry composite models. 247

Figure 5.16 - Box plot of 2074-2100 minus 1979-2005 long-term mean rainfall (mm day^{-1}; ΔP) averaged over (a) the east Congo Basin domain (22°E to 35°E, 10°S to 10°N) and (b) the north east Congo Basin domain (22°E to 35°E, 0° to 10°N). The first boxplot includes all models, the second excludes the wet composite models, and the third excludes the dry composite models. 252

Figure 5.S1 - Long term mean SON evaporation (mm day^{-1}) in the west Congo Basin wet composite (top row) and dry composite (middle row) in (a), (d) 2074-2100, (b), (e) 1979-2005; and (c), (f) 2074-2100 minus 1979-2005 (ΔE); (g) 2074-

2100 wet minus dry composite; (h) 1979-2005 wet minus dry composite; and (i) wet ΔE minus dry ΔE. Stipples in (c) and (f) indicate where all four models in the composite agree on the sign of change. Stipples in (g-i) occur at gridboxes where: 1) all wettest composite values are larger or smaller than all driest composite values (large dots); 2) all wettest composite values are greater or smaller than the driest composite mean (squares); 3) driest composite values are greater or smaller than the wettest composite mean (crosses); and 4) both (2) and (3) are true (small dots). The purple box indicates the location of the west Congo Basin domain. 258

Figure 5.S2 - Long term mean SON omega (10^{-3} Pa s^{-1}; shaded) averaged between 0° and 10°N and divergent component of zonal wind (m s-1) and omega (10^{-3} Pa s^{-1} streamlines), in the west Congo Basin wet composite (top row) and dry composite (middle row) in (a), (d) 2074-2100, (b), (e) 1979-2005; and (c), (f) 2074-2100 minus 1979-2005; (g) 2074-2100 wet minus dry composite; (h) 1979-2005 wet minus dry composite; and (i) wet change minus dry change. Areas with high topography in models are masked (white). The purple box shows the extent of the west Congo Basin domain (8°E to 21°E). Stipples as in 5.S1 and refer to omega values. 259

Figure 5.S3 - Frequency distribution of daily omega (10^{-3} Pa s^{-1}) in the northwest of the basin (8°E to 21°E, 0° to 10°N) in all SON days in all composite member models in the west wet composite, in 2074-2100 (blue) and 1979-2005 (orange). Pink denotes overlap between the orange and blue distributions. The dry composite is not shown as daily omega data is unavailable for two composite member models. 260

Figure 5.S4 - As in Figure 5.S2 but averaged between 5°S and 10°S.....260

Figure 5.S5 - As in Figure 5.S2 but for the east Congo Basin composites. The green box shows the extent of the east Congo Basin domain 261

Figure 6.1 - Box plot of long term mean rainfall (mm month $^{-1}$) across CMIP5 models in the historical (1979-2005; red) and future (2074-2100; blue) periods for each month, averaged over 8°E to 35°E, 10°S to 10°N.....279

Figure 6.2 - Scatterplots of long term mean rainfall (mm season^{-1}) in the future (2074-2100, RCP8.5) and historical (1979-2005) periods, averaged over 8°E to 35°E, 10°S to 10°N. Asterisks indicate r-values significant at the 99.9% level. 280

Figure 6.3 - Long term mean DJF rainfall (mm season^{-1}) in the historical period (1979-2005; red) and future (2074-2100) minus historical rainfall change (ΔP; blue) in individual CMIP5 models, averaged over 10°E to 35°E, 10°S to 5°N. Models are displayed in order of ΔP values (low to high). Models used in the wettest (driest) composites in Section 6.4 are denoted by hatching (stipples).....281

Figure 6.4 - Long term mean DJF rainfall (mm day^{-1}) in (a) 2074-2100, (b) 1979-2005 and (c) ΔP. The red (green) box is the location of the 8°E to 35°E, 10°S to 10°N (10°E to 35°E, 10°S to 5°N) domain. Stipples in (c) indicate where 15 out of 19 models agree on the sign of change.....282

Figure 6.5 - DJF ΔP (mm day^{-1}) in individual CMIP5 models, ordered by mean ΔP (low to high) calculated over the domain 10°E to 35°E, 10°S to 5°N (green box). 284

Figure 6.6 - Annual cycle of long term mean rainfall (mm day^{-1}) averaged between 10°E and 35°E, in (a) 2074-2100, (b) 1979-2005 and (c) ΔP. Dashed lines denote the northern and southern boundaries of the domain. Stipples as in Figure 6.4 caption..... 285

Figure 6.7 - Long term mean DJF rainfall (mm day^{-1}) in the wettest composite (top row) and the driest composite (middle row) in: (a), (d) 2074-2100; (b), (e) 1979-2005); and (c), (f) ΔP; (g) wettest composite ΔP minus driest composite ΔP. Stipples in (c) and (f) indicate where all four models in the composite agree on the sign of change. Stipples in (g) occur at gridboxes where: 1) all wettest composite values are larger or smaller than all driest composite values (large dots); 2) all wettest composite values are greater or smaller than the driest composite mean (squares); 3) driest composite values are greater or smaller than the wettest composite mean (crosses); and 4) both (2) and (3) are true (small dots)..... 286

Figure 6.8 - Long term mean DJF omega (Ω, 10^{-3} Pa s^{-1}) averaged between 10°E and 35°E, in the wettest composite (top row) and the driest composite (middle row) in: (a), (d) 2074-2100; (b), (e) 1979-2005); and (c), (f) ΔΩ; (g) wettest composite ΔΩ minus driest composite ΔΩ. Areas with high topography in models are masked (white). The green box shows the extent of the Congo Basin domain (10°E to 35°E). Stipples are as described in Figure 6.7 caption. 289

Figure 6.9 - Long term mean DJF omega (10^{-3} Pa s^{-1}) averaged between 10°S and 5°N, in the wettest composite (top row) and the driest composite (middle row) in: (a), (d) 2074-2100; (b), (e) 1979-2005); and (c), (f) ΔΩ; (g) wettest composite ΔΩ minus driest composite ΔΩ. Areas with high topography in models are masked (white). The green box shows the extent of the Congo Basin domain (10°S to 5°N). Stipples are as described in Figure 6.7 caption.....290

Figure 6.10 - Long term mean DJF qflux convergence (10^{-8} kg kg^{-1} s^{-1}; shaded) and qflux (kg kg^{-1} m s^{-1}; vectors) at 850 hPa in the wettest composite (top row) and the driest composite (middle row) in: (a, d) 2074-2100; (b, e) 1979-2005); and (c, f) Δqflux and Δqflux convergence; (g) wettest composite minus driest composite Δqflux and qflux convergence. Vectors in (c) and (f) are only present where all four models in the composite agree on the sign of change. Vectors in (g) are only present at gridboxes where all wettest composite values of qu or qv are larger or smaller than all driest composite values. The green box indicates the location of the 10°E to 35°E, 10°S to 5°N domain. 293

Figure 6.11 - As in Figure 6.10 but for 700 hPa.....296

Figure 6.12 - Latitude/height and longitude/height cross-sections showing the correlation (r-values) across CMIP5 models between long term mean ΔP over the Congo Basin and long term mean Δqconv across the: (a) western; (b) eastern; (c) northern; and (d) southern boundaries of the Congo Basin. Stipples indicate vertical grid locations which feature significant correlations at the 95% level.....297

Figure 6.S1 - Long term mean DJF *qflux* convergence (10^{-8} kg kg^{-1} s^{-1}; shaded) and *qflux* (kg kg^{-1} m s^{-1}; vectors) at 850 hPa in (a) the wettest composite and (b) the driest composite. Swapped values of q and winds: (c) q from the driest models, winds from the wettest models; (d) q from the wettest models, winds from the driest models. 308

Figure 6.S2 - As in Figure 6.S1 but for 700 hPa. 309

Figure 6.S3 - Future minus historical SST (°C; ΔSST) in (a) wettest composite, (b) driest composite; (c) wettest composite ΔSST minus driest composite ΔSST. RCP8.5 data for FGOALs is missing, so driest composite includes only 3 models. Stipples in (c) occur at gridboxes where: 1) all wettest composite values are larger or smaller than all driest composite values (large dots); 2) all wettest composite values are greater or smaller than the driest composite mean (squares); 3) driest composite values are greater or smaller than the wettest composite mean (crosses); and 4) both (2) and (3) are true (small dots). Due to missing data the dry composite contains only 3 models. 309

Figure 6.S4 - Long term mean DJF vertically integrated (surface to 300 hPa) q (kg kg^{-1}) in the wettest composite (top row) and the driest composite (middle row) in: (a), (d) 2074-2100; (b), (e) 1979-2005); and (c), (f) Δq; (g) wettest composite Δq minus driest composite Δq. Stipples in (c) and (f) indicate where all four models in the composite agree on the sign of change. Stipples in (g) occur at gridboxes where: 1) all wettest composite values are larger or smaller than all driest composite values (large dots); 2) all wettest composite values are greater or

smaller than the driest composite mean (squares); 3) driest composite values are greater or smaller than the wettest composite mean (crosses); and 4) both (2) and (3) are true (small dots). Due to missing data the dry composite contains only 3 models 310

Figure 7.1 – Schematic of the difference between the location and strength of the AEJs in wet and dry models in Chapter 4 (top row) and the changes to the AEJs in the future described in Chapter 5 (bottom row). 328

List of Acronyms

AEJ	African Easterly Jet
AEJ-N	African Easterly Jet - North
AEJ-S	African Easterly Jet - South
AEW	African Easterly Wave
AMIP	Atmospheric Model Intercomparison Project
AMMA	African Monsoon Multidisciplinary Analysis
AR5	IPCC Fifth Assessment Report
CMAP	Climate Prediction Centre Merged Analysis of Precipitation
CMIP3	Coupled Model Intercomparison Project 3
CMIP5	Coupled Model Intercomparison Project 5
CORDEX	Coordinated Regional Climate Downscaling Experiment
CRU	Climate Research Unit (University of East Anglia)
DFID	Department for International Development
DJF	December-January-February
DRC	Democratic Republic of the Congo
ECMWF	European Centre for Medium-Range Weather Forecasts
ENSO	El Nino Southern Oscillation
ERA-I	ERA-Interim (ECMWF Interim reanalysis)
ESGF	Earth System Grid Federation
ESM	Earth System Model
FCFA	Future Climate for Africa
GCM	Global Climate Model

GDP	Grodd Domestic Product
GoG	Gulf of Guinea
GPCC	Global Precipitation Climatology Centre
GPCP	Global Precipitation Climatology Project
IMPALA	Improviing Model Processes for African Climate (FCFA project)
IOD	Indian Ocean Dipole
IPCC	Intergovernmental Panel on Climate Change
ITCZ	Inter Tropical Convergence Zone
JJA	June-July-August
LLW	Low Level Westerlies
MAM	March-April-May
MASC	Mean Advection of Stratification Change
MCS	Mesoscale Convective System
MME	Multi-Model Ensemble
MMM	Multi-Model Mean
MSLP	Mean Sea Level Pressure
NCAR	National Centre for Atmospheric Research (USA)
NCEP	National Centers for Environmental Prediction (USA)
NERC	Natural Environment Research Council
OND	October-November-December
PCMDI	Program for Climate Model Diagnosis & Intercomparison
RCM	Regional Climate Model
RCP	Representative Concentration Pathway
RMSE	Root Mean Square Error

SAH	South Atlantic High
SLP	Sea Level Pressure
SON	September-October-November
SST	Sea Surface Temperature
SSTA	Sea Surface Temperature Anomaly
TAMSAT	Tropical Applications of Meteorology using Satellite Data and Ground-Based Observations
TEJ	Tropical Easterly Jet
TRMM	Tropical Rainfall Measuring Mission
UMFULA	Uncertainty Reduction in Models for Understanding Development Applications (FCFA project)
USGS	United States Geological Survey
WAM	West African Monsoon
WCRP	World Climate Research Programme
WIO	West Indian Ocean
ZAP	Zonal Asymmetry Pattern

1 Introduction

1.1 Motivations and Aims

1.1.1 Background and rationale

The Congo Basin is one of the most convectively active regions on the planet, and thus a driver of both the regional and global climate system [*Webster*, 1983; *Liu and Zipser*, 2005]. The majority of rainfall is the result of deep convection, and during the transition seasons, March-May (MAM) and September-November (SON), the Congo Basin dominates global rainfall totals as the wettest place on the planet [*Xie et al.*, 2003]. The climate regime supports the world's second largest rainforest, a globally significant carbon sink and thus an important element of the global carbon cycle [*FAO*, 2011]. The Democratic Republic of the Congo (DRC) holds the world's second largest above-ground carbon stock (22 Pg), and the amount of carbon stored in Africa (60-70 Pg) is second only to Amazonia [*Baccini et al.*, 2012]. The region is also home to a large population, the majority of whom rely on rain-fed agriculture for food and income [*Samba and Nganga*, 2012].

It follows that understanding the climate of this region, and how it may change in the future, is of vital importance. Africa as a whole is one of the most vulnerable continents to the effects of climate change [*Niang et al.*, 2014]. The dependence of the population and economy on subsistence farming, rain-fed agriculture and hydro-electricity [*Vogel*, 2005; *World Bank*, 2017a], combined with the region's already high climatic variability, means Africa is highly exposed to the risks

associated with climate change, while having a low capacity to mitigate such risks [*Collier et al.*, 2008; *Niang et al.*, 2014]. Across the continent, the direct contribution of agriculture to the economy is high: in some countries, such as the Central African Republic, it accounts for up to 40% of GDP [*World Bank*, 2017a]. Climate change is expected to have an impact on crop yields across the continent, including in Central Africa [*Fuller et al.*, 2018]. There is also dependency on rainfall-sensitive hydroelectric sources for energy across the continent and especially in the Congo Basin; in the DRC, almost 100% of energy comes from hydroelectricity [*World Bank*, 2017b]. In addition, changes in future rainfall could have profound impacts on rainforest extent. The forest boundaries in the dry seasons are already thought to be close to the lower threshold of rainforest viability, and so relatively small changes in the future have the potential to cause large changes in land cover [*James et al.*, 2013; *Malhi et al.*, 2013]. Understanding the likely hydrological changes in the region over the next century is therefore crucial.

Despite its importance, there remains a dearth of scientific research into the historical and future climate of the Congo Basin, which has been subject to less targeted research that any other African or tropical region [*Washington et al.*, 2006]. Analysis by *Alsdorf et al.* [2016] found that as of 2013 there were only 33 peer-reviewed articles focusing on the climate, hydrology or biogeochemistry of the Congo Basin in a sample of ten international Earth science journals, compared to almost 300 papers on the Amazon Basin. This lack of attention, and resulting limited understanding of the climate system, is concerning given the crucial role the Congo Basin plays in both the regional and global climate systems.

Limited scientific attention to the climate of the Congo Basin is due in part to the extreme scarcity of observational data in the region [*Washington et al.*, 2006, 2013], particularly in recent years when there has been a stark decline in reporting weather stations, and as a result, their inclusion in datasets (Figure 1.1). The reasons for this include the extreme ratio of size to access, and longstanding and ongoing political instability, in addition to a lack of investment in weather networks in some countries where there may be perceived greater priorities for limited resources [*Washington et al.*, 2006].

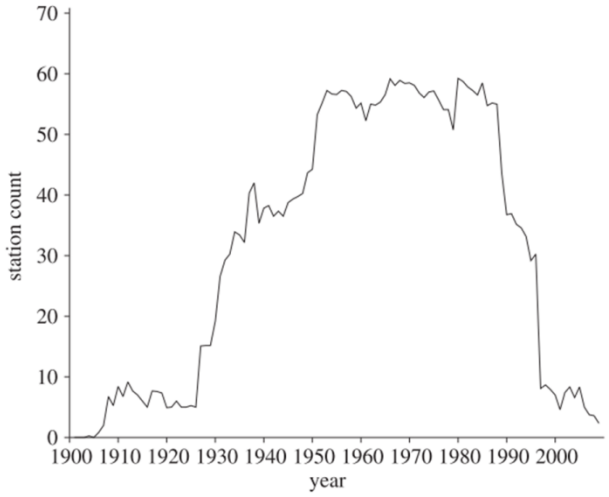

Figure 1.1 - Number of rain gauges per year over the region 5°S–5°N, 12.5°E– 30°E in the CRU 0.5° rainfall dataset. Source: *Washington et al.* [2013]

In addition to limiting our understanding of the climatology of the region, the lack of recent observational data also has consequences for numerical models, the tools through which we diagnose and project future climate changes. Without long-term, spatially homogeneous climate data, it is difficult to test models' abilities to accurately simulate the historical climate, an assessment which is frequently used to ensure model adequacy for producing reliable future projections. The lack of

recent observational data is likely to be one reason that numerical model simulations of historical climate diverge significantly in this region [*Washington et al.*, 2013]. Model divergence is stark; in both wet and dry seasons mean model rainfall varies by greater than a factor of two across coupled models, and up to an order of magnitude in some seasons [*Washington et al.*, 2013]. In three seasons out of four, the Congo Basin features the highest standard deviation of rainfall across models of any African region (Figure 1.2).

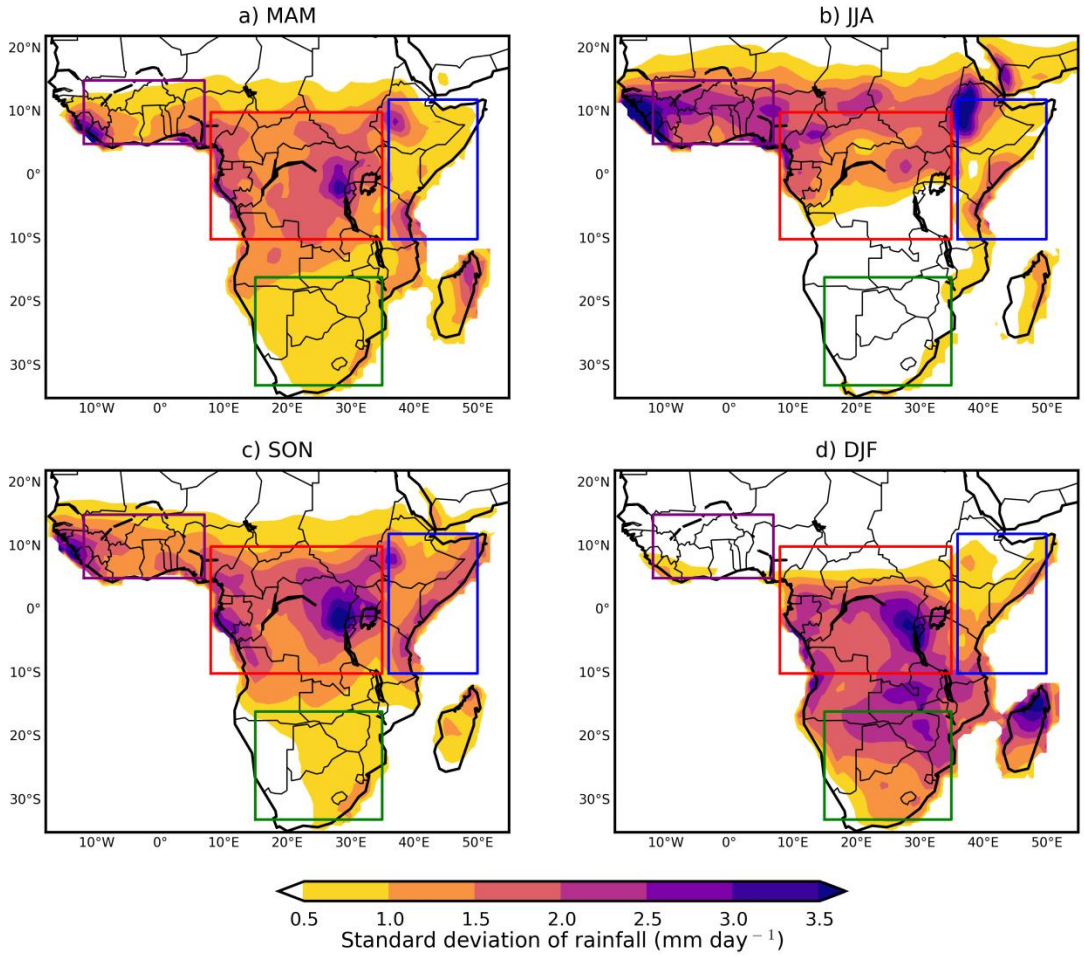

Figure 1.2 - Standard deviation of long-term mean (1979-2005) rainfall (mm day^{-1}) across 19 CMIP5 models (listed in Chapter 6) for (a) MAM, (b) JJA, (c) SON and (d) DJF. The red, blue, green and purple boxes refer to the Congo Basin, East African, southern African and West African domains respectively.

In order to ascertain the capabilities of models in this region, novel methods of model evaluation that do not depend on observational data need to be developed and deployed [*James et al.*, 2018]. This is a vital first step in ensuring these models are fit for purpose for use in climate change projections over this region. Regionally-focused process-based model evaluation is an emerging method that assesses the ability of models to represent important regional climatic features which are of importance to the variable of interest; in this case, rainfall. Such processes may be better observed and understood than rainfall itself, and therefore can be used to help to determine the credibility of a model's rainfall climatology. Research by *Washington et al.* [2013] has identified water vapour transport and convergence as potentially useful processes in this regard. Moisture is embedded in the low-level large-scale wind field, which is better constrained in the reanalysis data than rainfall, a highly parameterised field. If a model's representation of water vapour transport can be linked to its representation of rainfall, the credibility of rainfall simulations in this region can be established.

Process-based approaches may also be useful in helping to constrain uncertainty in the range of future projections by assessing the plausibility of the processes associated with future change. Across Africa there is considerable uncertainty in the signal of rainfall change simulated by the end of the 21st century, with disagreements amongst models in the sign or magnitude of rainfall change in many regions [*Niang et al.*, 2014]. This thesis will contribute to the development of both historical and future-focused process-based assessments and thus aims to play an important role in providing regional decision makers in the Congo Basin with usable climate information for long-term planning.

1.1.2 Aims and objectives

This thesis has two overall aims. First, it aims to contribute to an improved understanding of the credibility of coupled model representations of rainfall in the Congo Basin. The work in this thesis will constitute the first thorough assessment of the differences amongst CMIP5 coupled climate models in this region and will attempt to elucidate the physical climatic processes which drive these differences. An understanding of the representation of these processes across models will be used to try to determine the credibility of different model representations of the Congo Basin, in the absence of recent and homogeneous observational data.

To achieve this aim, the first two overarching research questions for this thesis are therefore:

i. To what extent can the large-scale processes of water vapour transport, provision and convergence explain inter-model differences in the representation of rainfall in the Congo Basin?
ii. Can the credibility of models be determined based on an assessment of regional processes related to rainfall?

The second aim of this thesis is to determine the plausibility of different climate projections produced by models. Coupled models are the primary tool available to make projections of future climate change, but there has been limited research into their fidelity in understudied and poorly-observed regions such as the Congo Basin. This work will contribute towards a better understanding of why climate

projections may differ in this region, and will be an important first step towards providing usable information for regional decision makers.

In light of this aim, two further research questions are therefore:

iii. Does model credibility in the historical period give insights into the plausibility of future projections?

iv. What processes contribute to inter-model uncertainty in future climate projections, and can an understanding of these processes help determine the plausibility of projections?

1.1.3 Thesis structure

The analysis in this thesis falls into two sections. The first section, comprising Chapters 3 and 4, focuses on the capabilities of models in the historical period, and will address research questions 1 and 2. The second section, comprising the results in Chapters 5 and 6, analyses projections of future climate and, extending the methodology developed in the first section, attempts to assess the plausibility of these projections, thus addressing research questions 3 and 4.

The present chapter will make the case for the forthcoming analysis, beginning by describing the study area and outlining its importance as a climatic region. It will then summarise what is known about the current climate of the Congo Basin, explaining the key regional processes driving rainfall variability, before highlighting the key challenges facing climate research in this region (Section 1.2). It will then introduce the tools (climate models) that are used to make projections

about future climate, before discussing the limitations of their use in data scarce regions such as the Congo Basin and outlining the ways in which this thesis aims to overcome these limitations via novel methods of model evaluation (Section 1.3). Next, it will assess the current state of understanding about future climate in the region, drawing out the knowledge gaps, and highlighting how this thesis will attempt to address these via an improved understanding of model capabilities (Section 1.4). Finally, the specific research questions for each chapter of analysis will be outlined in detail (Section 1.5). Notes on the format of this thesis are given in Section 1.6.

1.2 The Congo Basin

The Congo Basin is a large and globally important climatic region, predicated on three key considerations. First, it is one of three convective hotspots, along with the Amazon and Maritime Continent, which together constitute the wettest regions on Earth. The Congo Basin itself experiences the highest lightning strike frequency of anywhere on the planet, and during the rainy seasons (March-May, September-November), it dominates global rainfall totals [*Xie et al.*, 2003; *Williams and Sátori*, 2004; *Jackson et al.*, 2009]. Second, the region supports the planet's second-largest rainforest, a globally significant carbon sink and thus a crucial element of the global carbon cycle [*Williams et al.*, 2007]. However, during the dry seasons the Congo rainforests exist close to the climatic threshold between rainforest and savannah, making it potentially vulnerable to climatic shifts at the rainforest edge [*Malhi et al.*, 2013]. Finally, the Congo Basin supports a large population, the

majority of whom rely on rain-fed agriculture. The region has already experienced significant land degradation due to drought in recent years, and, alongside pressures from deforestation, is vulnerable to external stressors [*Kotir*, 2011; *Samba and Nganga*, 2012; *Megevand et al.*, 2013]. Understanding the current climate, and likely future changes, is therefore crucial to this region.

This section will first outline the study area used throughout this thesis, before assessing the available literature on the climate regime of the Congo Basin. It will then discuss the wider regional influences on the climate, as well as remote drivers, and go on to summarise the observed trends in the available observational data. Finally, it will outline the most pressing challenges for climate research in this region, and the gaps in our understanding of the current climate of the Congo Basin, some of which this thesis attempts to address.

1.2.1 Study area

The 'Congo Basin' as referred to in this thesis covers the broad area around the sedimentary basin of the Congo River in Central Africa, which contains part or all of the following countries: the Democratic Republic of the Congo, the Republic of the Congo, Rwanda, Burundi, Cameroon, Central African Republic, South Sudan, Angola, Zambia, Equatorial Guinea, Gabon, Tanzania and Uganda. The largest domain used in this thesis is 5°E to 35°E, 10°S to 10°N, chosen to represent a broad Central African region. Individual chapters use slightly different domains where appropriate; for example, the domain used in Chapter 6 has a more southerly northern boundary, to account for the location of the rain-band during the

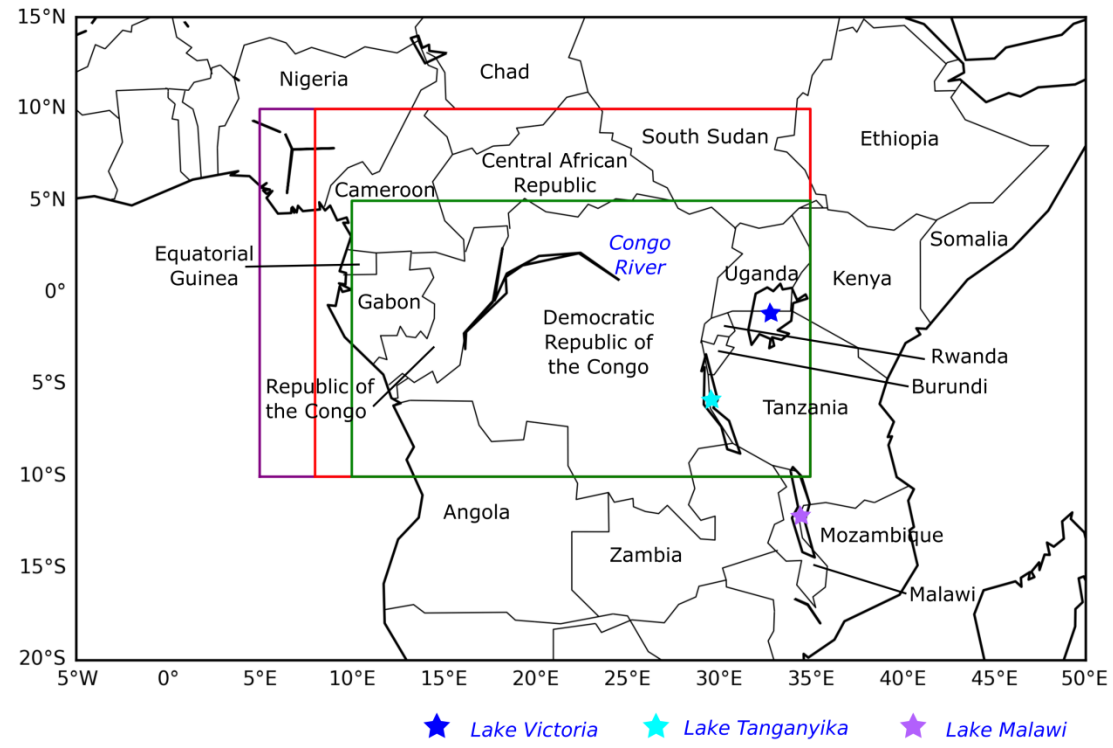

Figure 1.3 - Map showing the study area, political boundaries and Congo Basin domains used in Chapter 3 (purple; 5°E to 35°E, 10°S to 10°N), Chapters 4 and 5 (red; 8°E to 35°E, 10°S to 10°N) and Chapter 6 (green; 10°E to 35°E, 10°S to 5°N)

December-February dry season, which is the focus of that chapter. Additional analysis for the results in Chapter 3 found the results were not sensitive to the chosen domain size (not shown). The domains and the national political boundaries are shown in Figure 1.3. In the literature, other terms used to describe the same general region include Central Africa, West Equatorial Africa and Central Equatorial Africa. For simplicity, this thesis will use 'Congo Basin' to describe this broad region.

1.2.1.1 Land surface characteristics

Rainforest

The Congo Basin is characterised by a warm, humid climate, high rainfall, and dense rainforest coverage, which extends between roughly 5°S and 7°N and the Atlantic coast to 30°E [*Mayaux et al.*, 2013]. It is the second largest contiguous rainforest on the planet, constituting nearly 20% of global tropical rainforest area and containing ~60-70 Pg of above-ground carbon stock, second only to Amazonia (~110-125 Pg) [*FAO*, 2011; *Baccini et al.*, 2012]. The Democratic Republic of the Congo, the largest country within the Congo Basin, has the second-largest national carbon stock (22 Pg) after Brazil (53.2 Pg). The region is a net carbon sink via uptake from rainforests and savannahs, although fires and deforestation contribute to carbon losses [*Bombelli et al.*, 2009; *Ciais et al.*, 2011].

In all tropical rainforests, deforestation is a prominent environmental concern [*FAO*, 2011]. Historically, deforestation rates in the Congo Basin (0.23% between 1990 and 2000) have been less pronounced than in the Amazon (0.45%) and Southeast Asia (0.96%) [*FAO*, 2011]. This has been attributed primarily to political instability, poor infrastructure, and a relatively low population density [*Megevand et al.*, 2013; *Zhou et al.*, 2014]. There is uncertainty in the literature as to whether deforestation rates have increased or decreased in recent years; *Megevand et al.* [2013] report a doubling in the rate of deforestation since 1990; however, *Malhi et al.* [2013] report a decrease in the deforestation rate in Central Africa from 0.19% to 0.11% between 1990-2000 and 2000-2010. Nevertheless, there is consensus that as barriers to deforestation activities (e.g. poor infrastructure) reduce and

economic incentives (e.g. expansion of agriculture and energy activities, including palm oil) and population pressures increase, rates are likely to increase in the near future [*Ernst et al.*, 2013; *Megevand et al.*, 2013; *Mosnier et al.*, 2014]. Modelling studies have suggested that deforestation may result in drier and warmer conditions in parts of the Congo Basin, by affecting evapotranspiration, cloud physics and moisture circulation patterns [*Maynard and Royer*, 2004; *Werth and Avissar*, 2005; *Bala et al.*, 2007; *Akkermans et al.*, 2014; *Bell et al.*, 2015].

Orography

The land surface height in the Congo Basin region is shown in Figure 1.4. The average elevation of the basin is over 700m, around 300-400m higher than the Amazon Basin, which is hypothesized to contribute to the considerable climatic

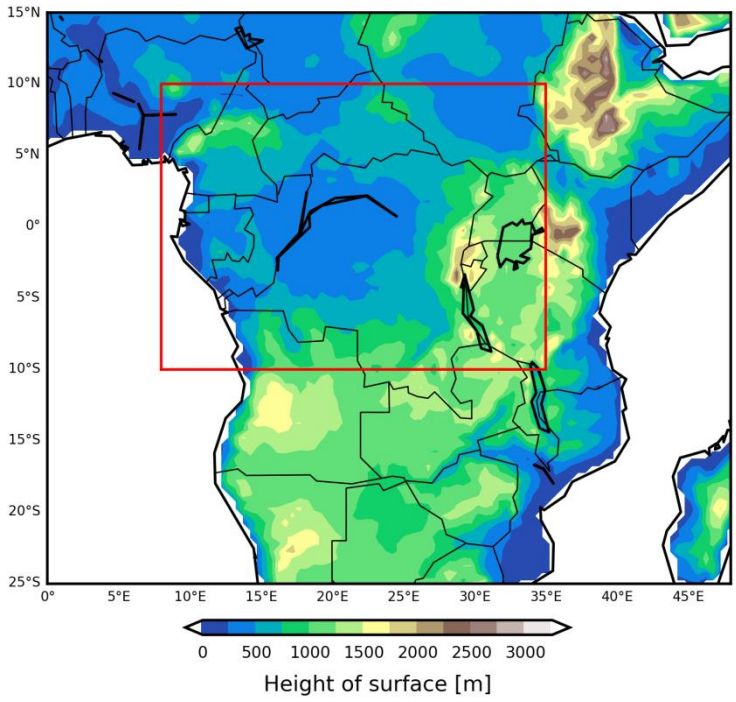

Figure 1.4 - Land surface height (m) over the Congo Basin domain (red box) and surrounding regions. Data is from the USGS GTOPO30 digital elevation model

differences between the two convective regions [*Williams and Sátori*, 2004]. The basin is separated from the climatologically and geographically distinct region of East Africa by the African Rift Valley highlands and Great Lakes at its eastern edge, including Lake Victoria and Lake Tanganyika, the world's largest tropical lakes by area and volume respectively [*Schubert et al.*, 2006; *Kitchell et al.*, 2011]. The Rift Valley mountains reach a peak height of 5895m (Mount Kilimanjaro in Tanzania), and the presence of this high terrain is likely to influence the climate, including influencing the amount of moisture than can reach the basin from the Indian Ocean [*McCollum et al.*, 2000]. The Rift Valley mountains have also been identified as a preferential location of convection in the region [*Jackson et al.*, 2009; *Dezfuli et al.*, 2015]. To the west, the Congo Basin borders the Atlantic Ocean, and in the northwest of the region the Cameroon highlands reach a peak height of 4040m (Mount Cameroon). It has been suggested that this terrain may block some low-level incoming moisture from the Atlantic [*Balas et al.*, 2007; *Jackson et al.*, 2009].

1.2.2 The Congo Basin climate regime

The key features of the Congo basin climate regime are shown in Figure 1.5. The following two sections describe the previous research into these key features.

1.2.2.1 Rainfall regime

General characteristics of the basin's rainfall regime are understood, though some uncertainty stems from limited observational data (discussed further in Section

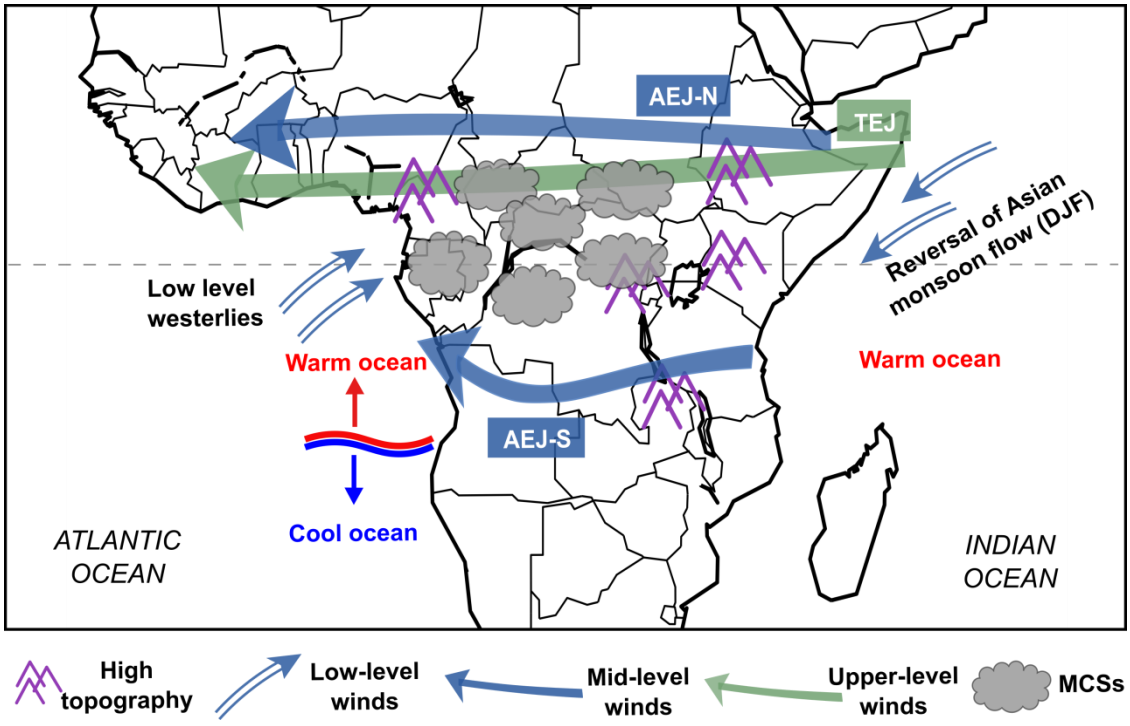

Figure 1.5 - Schematic showing key features of the Congo Basin climate. Locations are approximate. AEJ-N = African Easterly Jet, north; AEJ-S = African Easterly Jet, south; TEJ = Tropical Easterly Jet

1.2.5.1). The Congo Basin is estimated to receive around 1500-2000 mm of rainfall per year, with some areas (the Atlantic coast, east Congo Basin and Lake Victoria) receiving more than 2000mm per year [*Dezfuli*, 2017]. During the transition seasons, March to May (MAM) and September to November (SON), it is the wettest place on earth [*Xie et al.*, 2003]. The zone of maximum rainfall occurs over the western central African region, covering almost the entirety of the Congo rainforest [*Pokam et al.*, 2012].

Throughout the annual cycle, the Congo Basin climate regime is influenced by the meridional oscillation of tropical convection, which lags solar heating by roughly a month [*Okoola and Ambenje*, 2003]. This results in a rainfall cycle with two wet

seasons (MAM and SON) and two dry seasons between June and August (JJA) and December and February (DJF) (Figure 1.6). During the wet seasons mean rainfall is approximately double that in the dry seasons in satellite, gauge and reanalysis data [*Washington et al.*, 2013]. SON is generally regarded as the primary wet season over the Congo. This is contrast with East Africa, where MAM is known as the 'long rains' and features higher magnitude and more intense rainfall [*Dezfuli*, 2017]. Different characteristics of the two seasons have been documented in the Congo Basin; *Sandjon et al.* [2012] note that rainfall events in MAM are heavier and more

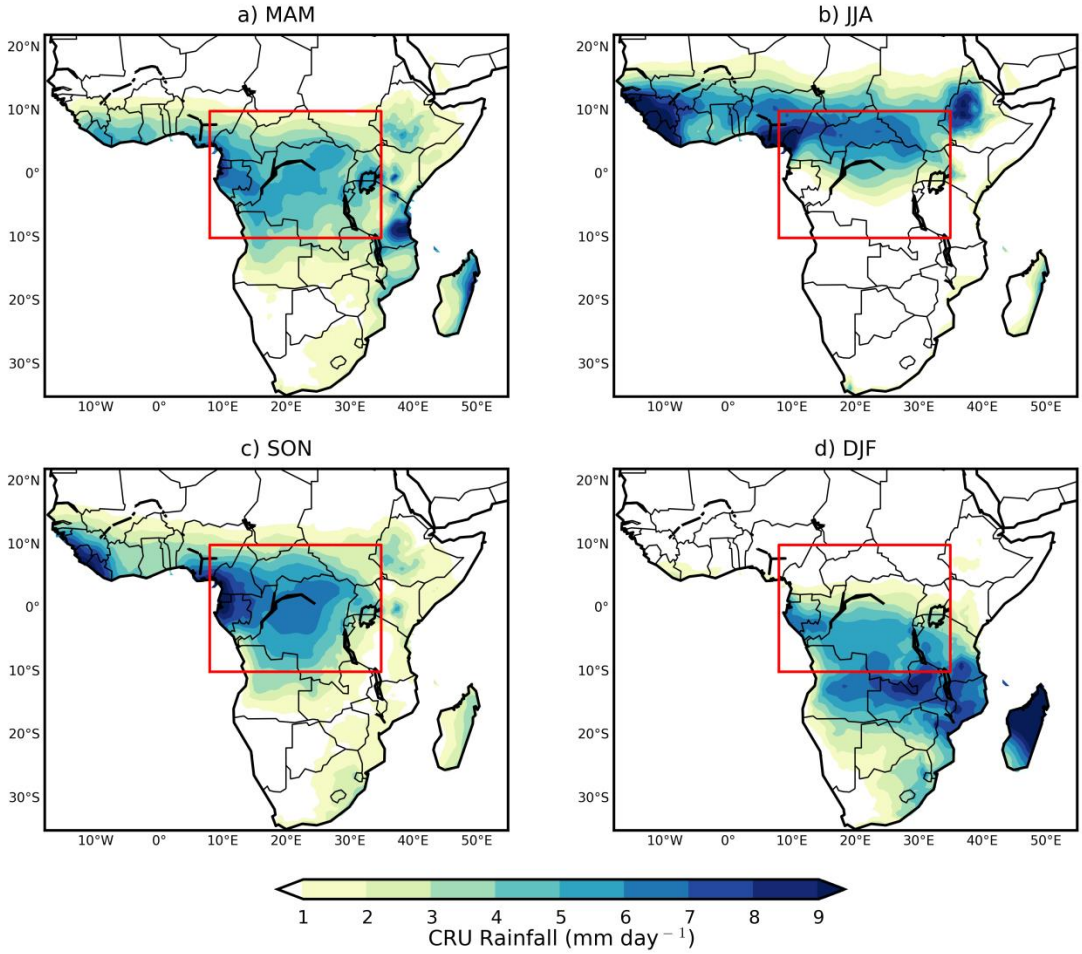

Figure 1.6 - Long term mean (1979-2005) rainfall (mm day^{-1}) from the Climatic Research Unit (CRU, version 3.23) dataset [*Harris et al.*, 2014], in (a) MAM, (b) JJA, (c) SON and (d) DJF. The red box shows the main Congo Basin domain (8°E to 35°E, 10°S to 10°N)

prolonged than the shorter and more intense rainfall events in SON, while *Jackson et al.* [2009] suggest SON is wetter than MAM due to enhanced mesoscale convective system (MCS) activity. This is also the case in coupled models; *Washington et al.* [2013] found that SON was the wettest season in the majority of CMIP5 and CMIP3 coupled models.

Traditional explanations for the rainfall regime of the Congo Basin have emphasized the dominance of the north-south displacement of the tropical rain-belt, often broadly referred to as the movement of the Inter Tropical Convergence Zone (ITCZ). The ITCZ is a zone of converging winds near the equator, the

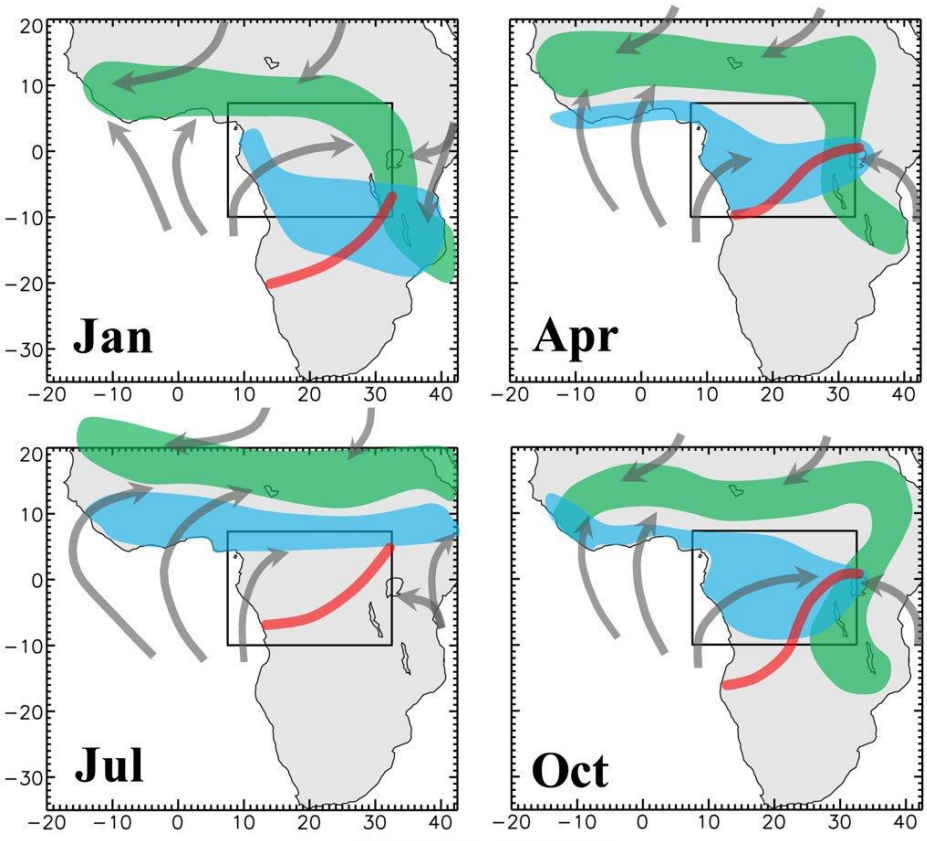

Figure 1.7 - Schematic of the seasonal variability of the Intertropical Convergence Zone (ITCZ; green), Congo air boundary (red; not discussed), tropical rain-belt (blue), and surface winds (dark grey). The black box shows the location of Western and Central Equatorial Africa used by *Dezfuli* [2017]. Adapted from *Dezfuli* [2017]; shows approximate locations

latitudinal location of which follows solar heating, contributing to deep convection in this region. However, while the ITCZ holds as an explanation for the rainfall structure over the tropical oceans, recent work has suggested that it is not a precise enough explanation for the spatial and seasonal variation experienced over Africa and the Congo Basin [*Nicholson*, 2017a]. A wide number of datasets indicate that the distribution of rainfall across the basin is in fact strongly spatially heterogeneous, with stark zonal differences. These spatial differences also vary considerably between seasons. *Nicholson* [2017a] finds that the location of low-level wind convergence does not map well onto the location of maximum rainfall over the continent, and argues that other regional features are more important drivers of rainfall patterns (Figure 1.7, from *Dezfuli* [2017]; note that the ITCZ is not as contiguous as suggested by this schematic). These may include forcings from local and remote ocean basins, zonal overturning circulations, mesoscale convective systems, regional atmospheric circulations, topography interactions, and equatorial wave dynamics [*Dezfuli*, 2017; *Nicholson*, 2017a]. The varying degree of influence of these drivers across seasons may better explain the differences between the two wet seasons than the annual cycle of the ITCZ.

In line with the emerging paradigm, this thesis will not use the term ITCZ to explain the latitudinal movement of rainfall; instead it will use the term 'tropical rain-belt' to signify the region with maximum rainfall over the continent.

1.2.2.2 Moisture availability and transport

One of the drivers of rainfall variability in any region is the availability, transport and accumulation of moisture in the atmosphere. Moisture for precipitation has three main sources: moisture already in the atmosphere, advection and convergence of moisture from outside the region, and rainfall recycling via evaporation [*Brubaker et al.*, 1993; *Pokam et al.*, 2012]. The relative importance of each of these sources in the Congo Basin is not fully understood. Estimates of the amount of rainfall recycling in the region vary considerably, from 45% [*Van Der Ent et al.*, 2010], to 38% [*Pokam et al.*, 2012], to less than 20% [*Trenberth*, 1998]. Isotope analysis conducted by *Balagizi et al.* [2018] finds that moisture from the East African Great Lakes is the primary source during drier periods, while evapotranspiration is the dominant source during wetter periods.

In terms of the influence of these sources on rainfall variability, *Shem* [2006] find in a modelling study that locally-recycled moisture is not the dominant contributor to high rainfall in the wet seasons, and that moisture influx from the surrounding regions and oceans is a more significant influence in this region. Using a water tagging scheme in the Community Earth System Model, *Dyer et al.* [2017] find that along with recycling from the basin itself, advection from the Indian Ocean is a major source of moisture for the region; this is despite *Van Der Ent et al.*'s [2010] hypothesis that the high terrain in East Africa acts to block the inflow of much of this moisture. Other studies have indicated low-level advection from the Atlantic Ocean is an important moisture source for the Congo Basin and contributes to interannual rainfall variability [*Balas et al.*, 2007; *Pokam et al.*, 2014; *Sorí et al.*,

2017]. The influence of adjacent oceans on the basin is discussed further in Section 1.2.4. The Congo Basin itself also acts as a moisture source for, and plays a role in, modulating rainfall variability in other regions, including East Africa [*Levin et al.*, 2009; *Van Der Ent et al.*, 2010; *Williams et al.*, 2012; *Dyer et al.*, 2017].

The magnitude and location of moisture flux convergence has also been linked to rainfall amounts in the Congo Basin. *Pokam et al.* [2012] find that total column moisture flux (qflux) convergence is stronger in wet years than dry years, and is dominated by convergence at low-levels. Other studies have indicated that the interannual variability of rainfall is more strongly associated with moisture convergence in the region than moisture already in the atmosphere, as the latter does not change significantly between extremely wet and dry years [*Vigaud et al.*, 2007; *Dezfuli and Nicholson*, 2013; *Vizy and Cook*, 2016]. Within the annual cycle, seasonal variations in the relative contribution of moisture sources have also been identified. *Pokam et al.* [2012] identify two maxima in the seasonal cycle of moisture convergence in the Congo Basin: one during MAM at mid-to-upper-levels, and the second during SON at low-levels. They found that the former is embedded in the northern component of the African Easterly Jet, which acts to increase the mid-to-upper-level convergence over the Congo Basin, while the latter is dominated by advection from the Atlantic.

Such research suggests that water vapour flux is likely to be a useful variable for analysing model rainfall. A positive relationship between rainfall and low- to mid-level convergence has already been identified between climate models in the wet seasons: in their sample of CMIP5 models, the wettest models features greater

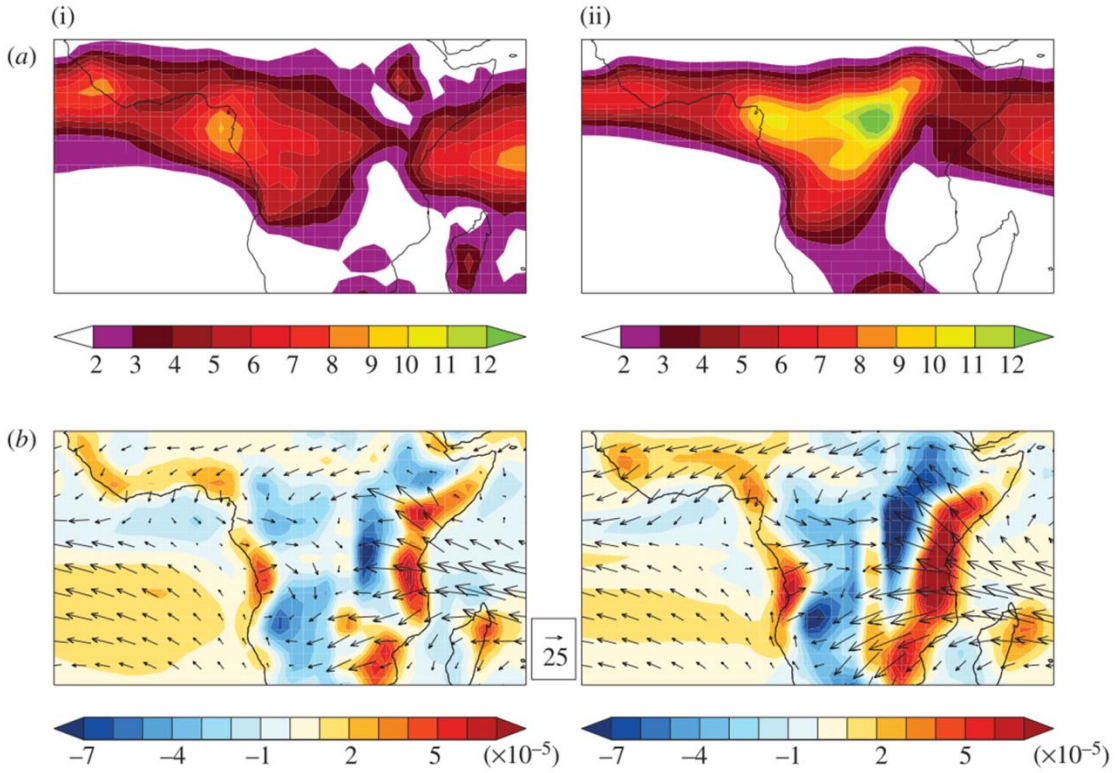

Figure 1.8 - (a) Rainfall (mm day^{-1}) and (b) moisture flux at 850 hPa climatologies for (i) the driest (CNRM-CM5) and (ii) wettest (NorESM1-M) CMIP5 models in SON. Units are mm day^{-1} in (a) and g kg^{-1} ms^{-1} in (b) with contours of divergence (g kg^{-1} s^{-1}). Source: *Washington et al.* [2013]

convergence than the driest models (Figure 1.8, *Washington et al.* [2013]). Similarly, in the Amazon, *Yin et al.* [2013] found that models with the most realistic moisture convergence climatologies also feature the most realistic rainfall, indicating the importance of these processes for simulating tropical rainfall accurately.

1.2.2.3 Convection and Mesoscale Convective Systsems

Most of the rainfall in the Congo Basin is produced by mesoscale convective systems (MCSs), which account for 70-80% of rainfall in tropical Africa [*Schumacher and Houze*, 2003; *Nesbitt et al.*, 2006]. MCSs are collections of

cumulonimbus clouds that organise into a large, contiguous rainfall-producing system, with the resulting rainfall covering areas in the order of 100km or more in at least one direction [*Houze*, 2004a; *Markowski and Richardson*, 2011; *Trapp*, 2013; *Dezfuli*, 2017]. MCSs propagate horizontally via new cell development on the flank of the updraft region, the result of the system interacting with the surrounding environment, including via cold-pool outflows, low-level jets and gravity-wave interactions [*Houze*, 2004b; *Laing and Evans*, 2015]. They tend to last in the atmosphere for around 12-24 hours [*Yang et al.*, 2017]. The systems produce intensive rainfall, the cycle of which is strongly diurnal [*Jackson et al.*, 2009].

In tropical Africa, there are four regions of MCS maxima; over local orographic maxima (Ethiopian Highlands, Mount Cameroon), over Lake Victoria, and across a large region in the central-west Congo Basin near the equator [*Jackson et al.*, 2009]. In the east Congo Basin, MCSs preferentially form on the western slopes of the Rift Valley mountains, and propagate westward at a rate of between 8 and 20 m s^{-1} [*Nguyen and Duvel*, 2008; *Laing et al.*, 2011]. High MCS activity in the Cameroonian Highlands contributes to some of the world's highest rainfall totals; at the Debundscha station in Cameroon, mean annual rainfall often exceeds 10m [*ORSTOM*, 1978; *Jackson et al.*, 2009].

Seasonal differences over the basin in the amount and location of rainfall may be attributable to MCS activity. *Jackson et al.* [2009] found that there are more MCSs during SON, particularly over the Ethiopian Highlands and Mount Cameroon, which are not significant regions of MCS activity during MAM. Conversely, maximum MCS activity over Lake Victoria occurs during MAM. The interaction of

these systems with seasonally-varying regional climate features may explain the higher rainfall amounts and different rainfall distributions across seasons [*Jackson et al.*, 2009]. These features this will be discussed further in Section 1.2.3.

The high occurrence of MCSs in the basin may also explain why the Congo Basin experiences the highest lightning strike frequency of anywhere on the planet [*Toracinta and Zipser*, 2001; *Williams and Sátori*, 2004; *Zipser et al.*, 2006; *Albrecht et al.*, 2016]. Despite this, the Congo Basin receives less rainfall annually than the Amazon and Maritime Continent convective hotspots [*Petersen et al.*, 2001; *Christian et al.*, 2003; *Zipser et al.*, 2006]. The reasons for this apparent paradox are a matter of ongoing research, though some explanations have been proposed. The Congo Basin has higher levels of aerosols than other tropical land regions, which may influence convective activity by reducing cloud droplet radii, and as a result reduce rainfall efficiency [*McCollum et al.*, 2000]. Lower rainfall may also be associated with higher cloud base heights in the Congo Basin than the Amazon, which has been linked to the greater continentality of the region, as well as the formation and structure of the African Easterly Jets (AEJs) [*Pokam and Washington*, forthcoming; *Williams and Sátori*, 2004]. Finally, the relative aridity of neighbouring East Africa and the high terrain to the east of the basin may reduce or block the available moisture transport from the Indian Ocean [*McCollum et al.*, 2000], limiting total rainfall amounts.

1.2.3 Regional influences on the Congo Basin climate

As discussed in Section 1.2.2.1, the north-south oscillation of solar heating and the ITCZ cannot explain fully the distribution of rainfall in this region. Several regional features act to modulate the climate, including the regional atmospheric circulation and the influence of sea surface temperatures (SSTs) in both adjacent and remote oceans. These are highlighted in Figure 1.5 and discussed in turn below.

1.2.3.1 Atmospheric circulation

Low-level westerlies

The horizontal and vertical zonal wind structure over the Congo Basin in August and October are shown in Figure 1.9 [*Dezfuli*, 2017]. The low-level westerlies (LLWs), which form over the Atlantic coast and penetrate into the basin, are a persistent feature of the region's climate [*Dezfuli and Nicholson*, 2013; *Nicholson and Dezfuli*, 2013; *Pokam et al.*, 2014]. They occur in all months with varying strength, and are particularly active during the SON wet season, whilst weaker during MAM [*Pokam et al.*, 2012, 2014]. The LLWs transport moisture from the Atlantic Ocean into the Congo Basin, and are stronger during years with above-average rainfall [*Pokam et al.*, 2012; *Dezfuli and Nicholson*, 2013; *Nicholson and Dezfuli*, 2013]. *Pokam et al.* [2012] identified a maximum in low-level convergence during SON, associated with the strength of the LLWs, and contributing to rainfall in the region. Between June and October, the LLWs appear to form the lower

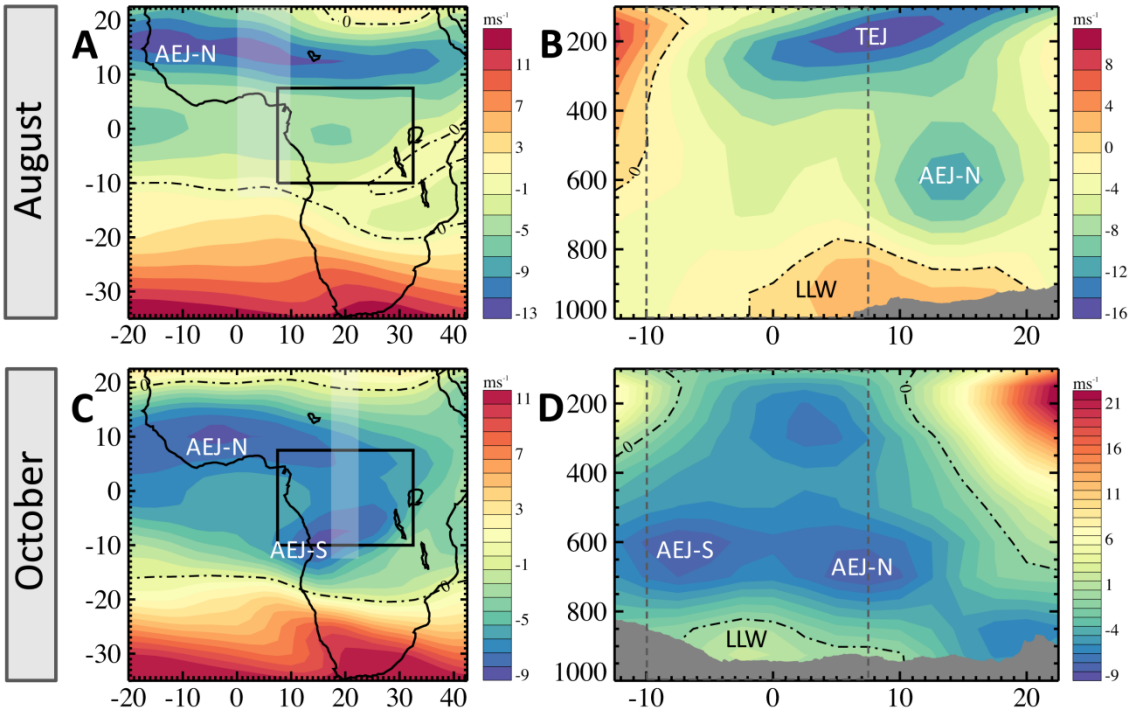

Figure 1.9 - (a) Horizontal pattern of long-term mean zonal wind at 600 hPa in August to identify the African easterly jet (AEJ). (b) Latitude-height cross section of mean zonal wind in August, averaged over longitudes highlighted with the transparent strip in panel (a). Tropical easterly jet and low-level westerly (LLW) winds are evident. (c) and (d) are the same as (a) and (b), respectively, but for October. The black box in (a) and (c) shows the location of Western and Central Equatorial Africa used by *Dezfuli* [2017]. Grey shading in (b) and (d) represents topography, and dashed grey lines show the southern and northern limits of WCEA. Source: *Dezfuli* [2017]

branch of an Atlantic-Congo Walker-type circulation, with its ascending branch over the basin and subsiding branch over the Gulf of Guinea [*Pokam et al.*, 2014; *Cook and Vizy*, 2015; *Neupane*, 2016]. The strength of the overturning circulation, and related low-level flow, is related to variability in tropical Atlantic SST, whereby years with anomalously warm SSTs in the Gulf of Guinea region also feature enhanced evaporation and subsequent moisture transport into the continent, intensifying the convection in the ascending branch of the overturning circulation [*Cook and Vizy*, 2015]. However, *Cook and Vizy* [2015] note that the initial formation of a closed Walker-type circulation is dependent on the formation of the

Atlantic cold tongue. There is some controversy around the structure of Walker-like cell, with some studies suggesting there is not a low-level closing branch of of cell [*Longandjo*, 2017], and highlighting the presence of a shallow zonal overturning circulation with an ascending branch near 24°E and descending branch near 2°E, over the Atlantic Ocean [*Pokam et al.*, 2014; *Longandjo*, 2017].

There are two complementary ideas as to why the LLWs form in this region, and why their strength varies seasonally. One hypothesis is that they are modulated by the strength of the South Atlantic High (SAH), a high pressure system which forms in the south tropical Atlantic Ocean. South-easterlies on the northeast flank of the SAH turns into westerlies as they cross the equator [*Nicholson and Grist*, 2003]. In an alternative theory, *Pokam et al.* [2014] suggest that the LLWs are instead driven by the differential heating between the Atlantic and Congo Basin, the former serving as a heat sink due to subsidence and the latter a heat source due to strong latent heat release. This temperature gradient can reach 6K in July [*Cook and Vizy*, 2015], and seasonal variation in strength of the LLWs has been found to be related to variability in this thermal contrast [*Pokam et al.*, 2014; *Cook and Vizy*, 2015].

African Easterly Jets

The African Easterly Jets (AEJs) in the mid-troposphere are another important feature of the regional climatology. Both the northerly (AEJ-N) and southerly (AEJ-S) components have cores between 700 and 600 hPa, centred between 10°-15°N and 5°-10°S respectively. The AEJ-N is present throughout the year, peaking in strength between June and September, whilst the AEJ-N is most clearly defined between August and November [*Nicholson and Grist*, 2003]. The AEJ-N tends to be

stronger than the AEJ-S, reaching core speeds of 12 m s^{-1} in June, whereas the highest mean core speed of the AEJ-S is around 8 m s^{-1} in October and November. Both jets are generally considered to form due to strong meridional temperature gradients between the equator and subtropics, though further research has also highlighted the importance of soil moisture gradients in maintaining the AEJ-N strength and structure [*Burpee*, 1972; *Cook*, 1999]. *Thorncroft and Blackburn* [1999] also highlight the role played by diabatically-forced meridional circulations in influencing the gradient and maintaining the AEJ-N; one related to dry convection over the Saharan Heat Low region, and one associated with moist convection close to the equator.

The AEJs play a role in rainfall variability in both the Congo Basin and West Africa, where the AEJ-N is strongest and most active. In the Sahel, wet years are associated with a weaker and more poleward AEJ-N, whereas during dry years the jet is stronger and more equatorward [*Kanamitsu and Krishnamurti*, 1978; *Newell and Kidson*, 1984; *Fontaine et al.*, 1995; *Grist and Nicholson*, 2001]. The AEJ-N is also important for creating the conditions for AEW formation [*Rennick*, 1976; *Thorncroft and Hoskins*, 1994] and thus the jet's variability will likely influence rainfall variability over the broad region [*Payne and McGarry*, 1977; *Rowell and Milford*, 1993; *Grist et al.*, 2002; *Fink*, 2003]. Over the Congo Basin, *Jackson et al.* [2009] suggest that the presence of the AEJ-S during SON acts to enhance convection. They identified a maximum in MCS activity to the right of the entrance region of the AEJ-S, where the jet streak model of [*Uccellini and Johnson*, 1979] would place a region of strong convergence. This strong mid-level convergence enhances uplift from the surface and results in greater MCS activity. There is also

evidence that the presence of both jets during SON is linked to the increased intensity of the tropical rain-belt during this season [*Pokam and Washington*, forthcoming.; *Nicholson and Grist*, 2003; *Jackson et al.*, 2009], and thus may explain why SON is wetter than MAM.

Tropical Easterly Jet

The Tropical Easterly Jet (TEJ) in the upper troposphere develops in response to the temperatue gradient between the Himalayan Plateau and Indian Ocean between June and September, extending westward into Africa [*Dezfuli*, 2017]. Its core is centred at around 7°N and 200 hPa, and it reaches maximum wind speeds of around 20 m s^{-1}. The TEJ tends to be stronger in wet years over the Sahel, in opposition to the AEJ-N which tends to be weaker and more poleward [*Grist and Nicholson*, 2001; *Nicholson and Grist*, 2003]. Upper-level easterly flow is evident throughout the year, and there is a weak secondary maximum south of the equator during January and February. However this is not usually referred to as the TEJ and is much waeker than the upper level flow during the boreal summer. The TEJ appears to both modulate, and be modulated by, convective rainfall; studies suggest that upper-level divergence in the exit region of the jet over west Central Africa may promote convection at the surface [*Druyan and Hall*, 1996; *Dezfuli and Nicholson*, 2013; *Nicholson and Dezfuli*, 2013], whilst *Thorncroft and Blackburn* [1999] suggest the TEJ forms partially in response to convection over the continent.

1.2.3.2 Adjacent oceans

The regional climates within Africa are modulated and influenced by the adjacent Atlantic and Indian Oceans, where variability in SSTs can influence moisture availability, moisture advection, and the static stability of the lower troposphere [e.g. *Camberlin et al.*, 2001; *Pokam et al.*, 2014; *Yang et al.*, 2015a]. The tropical Atlantic has long been established as an important influence on African rainfall [e.g. *Nicholson and Entekhabi*, 1987; *Balas et al.*, 2007; *Pokam et al.*, 2012], and a recent modelling study using a Lagrangian transport model identified the Atlantic as the most important oceanic source of moisture for the region [*Sorí et al.*, 2017]. Climate features in the tropical Atlantic include the Atlantic Niño, the Atlantic cold tongue, and the south Atlantic High (SAH) [*Nobre and Srukla*, 1996; *Xie and Carton*, 2004; *Okumura and Xie*, 2006].

Variability in tropical Atlantic SSTs has been linked to rainfall variability over Central Africa [*Nicholson and Entekhabi*, 1986, 1987; *Okumura and Xie*, 2006; *Balas et al.*, 2007; *Nicholson and Dezfuli*, 2013], in particular the western part [*Pokam et al.*, 2012; *Dezfuli et al.*, 2015], as well as adjacent West Africa [e.g. *Folland et al.*, 1986; *Vizy and Cook*, 2001] and southern Africa [e.g. *Hirst and Hastenrath*, 1983a; *Nicholson and Entekhabi*, 1987; *Reason et al.*, 2006; *Vigaud et al.*, 2007; *Hansingo and Reason*, 2009]. Coastal rainfall in Central and southern Africa has been found to be enhanced in years with positive SST anomalies (SSTAs), and suppressed in years with negative SSTAs, in response to both indirect atmospheric mechanisms and direct local forcings [*Nicholson and Entekhabi*, 1987; *Nicholson and Dezfuli*, 2013]. *Hansingo and Reason* [2009] conducted idealised model experiments to

identify the mechanisms relating SST and rainfall in southern Africa, which include enhanced latent heat flux from the ocean surface over regions of forced SSTs and local enhanced uplift. Their work highlighted the importance of a local, direct relationship between SSTAs and rainfall.

In west equatorial Africa, *Balas et al.* [2007] found that the influence of Atlantic SSTs on rainfall is strongest during boreal summer and fall. They assert that the sign of the relationship between SSTAs in the Atlantic and rainfall depends on whether it is a direct influence (which results in a warm/wet relationship), or indirect (which can be both warm/wet and cold/wet). They are also in agreement with *Camberlin et al*. [2001] that warm Atlantic SSTAs can modulate the north-south position of the tropical rain-belt over the continent. Variability in Atlantic SSTs has also been found to modulate a local Atlantic-Congo overturning circulation, where warm SSTAs result in enhanced evaporation, enhanced low-level onshore flow and enhanced convection over the continent [*Cook and Vizy*, 2015; *Neupane*, 2016].

The Indian Ocean also influences the climate of the Congo Basin and adjacent regions [*Hastenrath*, 2000; *Black et al.*, 2003; *Ummenhofer et al.*, 2009; *Dyer et al.*, 2017]. Variability in rainfall over the Indian Ocean region is dominated by the monsoon systems, which produce southeasterly flow along the east coast of Africa during boreal summer, and northeasterlies during boreal winter [*Schott et al.*, 1997; *Schott and McCreary*, 2001]. These easterly flows directly affect moisture advection into the region, which in turn is modulated by the East Africa Highlands, which are likely to block some moisture penetrating inland to the Congo Basin

[*Van Der Ent et al.*, 2010]. *Dyer et al.* [2017], using the Community Earth System Model, identified the Indian Ocean as a dominant oceanic moisture source for the Congo Basin, contributing 21% during the rainy seasons.

Variability in Indian Ocean SSTs has long been linked to variability in East African rainfall [*Beltrando and Camberlin*, 1993; *Goddard and Graham*, 1999; *Endo and Tozuka*, 2015]. The Indian Ocean Dipole (IOD), an SST phenomenon which features warm SSTAs in the west Indian Ocean and cold SSTAs in the east during its positive phase, has been linked to both East and Central African climate variability [*Ogallo et al.*, 1988; *Ummenhofer et al.*, 2009; *Dezfuli and Nicholson*, 2013], and a modelling study has indicated that the influence of the IOD on the East African short rains (October-December) is much stronger than that of the El Niño Southern Oscillation (ENSO) [*Behera et al.*, 2005]. Positive phases of the IOD have been linked to increased wetting over East Africa, via enhanced low-level moisture convergence and uplift over the region [*Ummenhofer et al.*, 2009; *Nicholson*, 2017b].

A similar relationship is identified by *Dezfuli and Nicholson* [2013] between positive IOD years and enhanced rainfall in the east Congo Basin during SON, while the opposite pattern (negative IOD in wet years) is observed in the west of the basin at the Angola coast. Pressure gradients between the Atlantic and Indian Ocean have also been found to relate to zonal differences in rainfall across the Congo Basin. *Dezfuli et al.* [2015] identify a Zonal Asymmetry Pattern (ZAP) in the south Congo Basin between boreal winter and spring, where opposite signs of rainfall anomalies occur in the western and eastern portions of the subdomain. During wet years, the strong contrast between high pressure over the equatorial

Atlantic and low pressure in the southwest Indian Ocean leads to enhanced westerlies into the Congo Basin, which converge at the East African highlands. This leads to high rainfall in the east of the basin, and drying in the west of the basin, as a subsiding branch forms in response to enhanced uplift in the east. This previous research indicates an important role for SSTs, and associated moisture transport, in modulating rainfall over the Congo Basin.

1.2.3.3 Remote oceans

In addition to the influence of adjacent ocean basins, climate variability in Africa can be influenced by forcings from remote oceans, in particular the tropical Pacific. The influence of remote forcings can be direct, by influencing the global atmospheric circulation, or indirect, by inducing changes in the SST of adjacent oceans [*Alexander et al.*, 2002; *Giannini et al.*, 2008]. Some studies suggest the latter mechanism dominates over Central Africa, whereby the Pacific influences African rainfall indirectly via its influence on the Atlantic and Indian Oceans [*Nicholson*, 1997; *Goddard and Graham*, 1999; *Nicholson and Dezfuli*, 2013]. Modelling studies support this, finding that in east equatorial Africa the patterns of rainfall variability can be reproduced with observed Indian Ocean SSTs only, whilst they cannot be produced with Pacific SSTs alone [*Goddard and Graham*, 1999; *Behera et al.*, 2005].

On interannual timescales, the strongest association between Pacific SST variability via ENSO and rainfall are found in eastern equatorial and south-eastern Africa, though the strength of these connections varies both seasonally and

spatially [*Ropelewski and Halpert*, 1987; *Lindesay*, 1988; *Nicholson and Kim*, 1997; *Camberlin et al.*, 2001]. *Ropelewski and Halpert* [1987] found that rainfall in East Africa during boreal autumn and the following spring is enhanced (reduced) during El Niño (La Niña) phases. There is also some evidence of teleconnections with the Congo Basin. *Dezfuli and Nicholson* [2013] found that wet years in the east Congo Basin are associated with Pacific SST patterns similar to that of El Niño (warm SSTAs in the east, cool in the west), while dry years feature La Niña-like SST patterns. An opposite pattern is observed in the western coastal region of Central Africa: La Niña (El Niño) conditions are associated with wet (dry) years. This is supported by recent work which has suggested that ENSO phase is related to convective activity across Africa; *Hart and Washington*, [forthcoming] find that convective activity in satellite data over the eastern Congo Basin is enhanced during El Niño years, while in the west of the basin it is enhanced during La Niña years. However, the precise influence of ENSO on interannual variability in the region is unclear, with some studies finding no significant teleconnections [e.g. *Camberlin et al.*, 2001]. Relationships have also been identified between Congo Basin rainfall and remote SSTs at multiannual scales; *Todd and Washington* [2004] find that positive rainfall anomalies are related to anomalous westerly winds at mid-levels between the Atlantic and Central Africa, which may be associated with tropical North Atlantic SST forcing.

1.2.4 Observed recent rainfall change in the Congo Basin

Compared to other tropical and Africa regions, little attention has been paid to recent climate change in the Congo Basin [*Washington et al.*, 2006, 2013; *James et*

al., 2013]. Analysis of the available observational data (both gauge and satellite products) in the region indicates a possible drying trend in the region since the mid-1980s [*Sanga-Ngoie and Fukuyama*, 1996; *Laraque et al.*, 2001; *Malhi and Wright*, 2004; *Samba et al.*, 2008; *Samba and Nganga*, 2012; *Diem et al.*, 2014], particularly in the south of the region [*Yin and Gruber*, 2010]. The impact of this drying on the Congo rainforest is unclear, with some studies reporting reduced greenness and photosynthetic capacity in the region [e.g. *Zhou et al.*, 2014] and others finding no significant impacts [e.g. *Asefi-Najafabady and Saatchi*, 2013]. There is also evidence to suggest extremes in rainfall have changed: digitisation efforts in the central African region have unearthed data which indicate that wet extreme indices have been decreasing in the central and western part of the basin [*Aguilar et al.*, 2009].

Recent studies have attempted to identify the mechanisms that are driving this possible drying trend, which could be due to either anthropogenic forcings or natural variability. In an assessment of the drought and associated circulation features in several observational and reanalysis datasets, *Hua et al.* [2016] suggest that the regional drying trend (-0.21 mm day^{-1} decade^{-1}) between 1979 and 2014 in April to June may reflect the response of the large-scale circulation to tropical SST variations. Their results suggest that relatively greater warming of west Pacific SSTs compared to central Pacific SSTs, as well as rapid warming over the Indian Ocean, has resulted in a westward extension of the tropical Walker circulation (as also proposed by *Williams and Funk* [2011]), resulting in anomalous subsidence over equatorial Africa in recent decades. The drying trend has also been related to the Atlantic Multi-Decadal Oscillation [*Diem et al.*, 2014], which has been in its

positive phase since the mid-1990s, and decreased moisture recycling as a result of deforestation [*Nogherotto et al.*, 2013; *Lawrence and Vandecar*, 2015].

1.2.5 Key challenges and knowledge gaps

1.2.5.1 Data access and availability

One of the key challenges facing climate research in the Congo Basin is the extreme scarcity of recent observational data in the region. Africa as a whole is considered to have the most sparse climate-observing system of any inhabited continent, with an average density of just one weather station per 26,000 km^2 [*Washington et al.*, 2004, 2006]. This is particularly stark in the Congo Basin, which has some of the lowest reporting rates of any land region [*Washington et al.*, 2004] (Figure 1.10). The situation has worsened in recent years; between 1980 and 2010, the number of rain gauges included in the CRU rainfall dataset from the Central African region declined from around 60 to fewer than 10 [*Washington et al.*, 2013], compared to more than 20 in 2010 in the UK, an area roughly 1/40th of the size of the Congo Basin (Figure 1.11, *James et al.* [2018]). There are also very few radiosondes released in the region, limiting our understanding of atmospheric processes above the surface (Figure 1.11). The scarcity of data can be traced in part to decades of political instability in the region, which, along with the extreme size-to-access ratio, have meant maintaining a network of weather stations is a low priority for national and regional governments, resulting in discontinuities in the weather record [*Nicholson et al.*, 2018a]. Even where there are maintained rain gauges, the

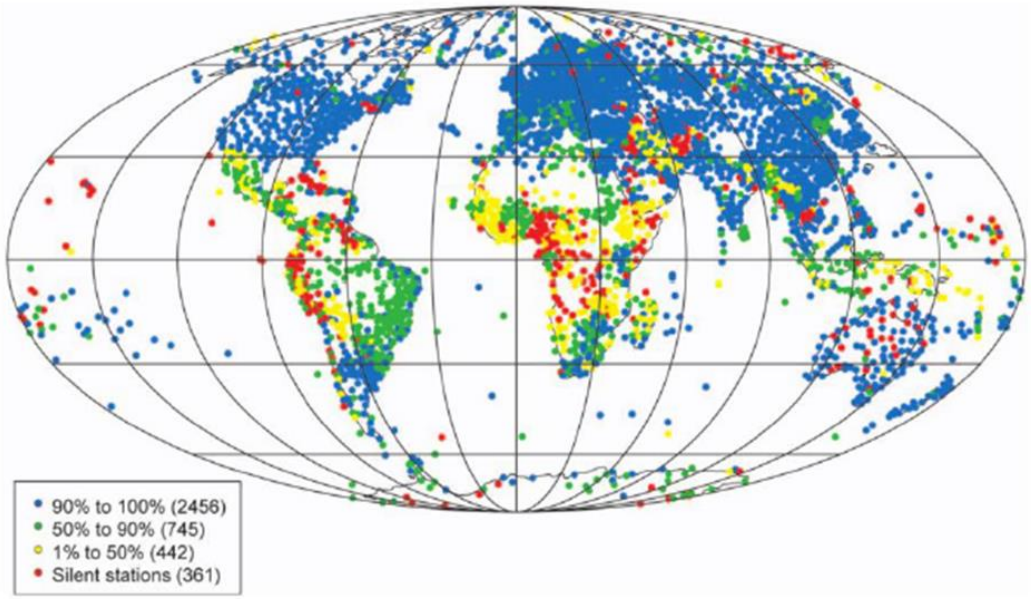

Figure 1.10 - The global network of World Weather Watch (WWW) stations, colour coded to show reporting rates. Data-sparse areas and low reporting rates for Africa are clearly visible. Source: *WMO* [2003]

data is not always widely accessible; in 2013 only three stations in the DRC reported to the Global Telecommunications Service for international use [*Washington et al.*, 2013]. In addition, regional weather services are increasingly choosing to monetise meteorological data, meaning it may be too expensive to use for research purposes [*Nicholson et al.*, 2018b].

Thus, while general characteristics of the region's climatology are well known, there remain significant gaps in our understanding of the climate system. To some extent, reanalysis data has been used to try to fill this knowledge gap and is the basis for a considerable amount of the climatological research discussed in Section 1.2. Reanalysis data is a combination of observations, assimilation schemes and numerical models, and is commonly used as a proxy for observations, especially in regions with sparse observational coverage. It has two main advantages: it

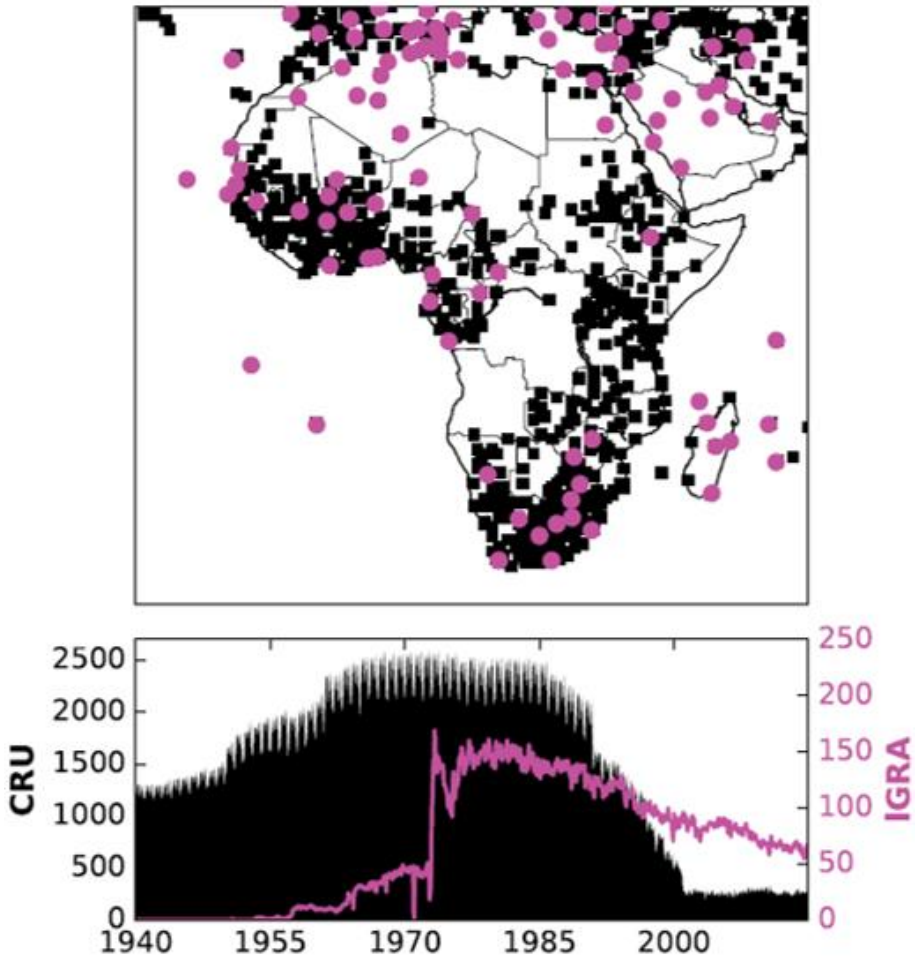

Figure 1.11 - Station data contributing to the Climatic Research Unit (CRU, version 2.23) precipitation (black) and Integrated Global Radiosonde Archive (IGRA) u wind at 1200 UTC (pink). (top) Coverage map for 1979–2013. Black squares indicate the location of 0.5° × 0.5° grid boxes that have at least one contributing station during at least 50% of the months; pink circles indicate stations with at least 10 records per month in at least 50% of the months. (bottom) Time series showing the number of stations contributing in each month (40°S–40°N, 30°W–60°E). Source: *James et al.* [2018]

provides global spatial coverage, including over oceans; and it provide outputs over a wide number of variables, including rainfall, temperature, horizontal and vertical wind, specific humidity and geopotential height. However, in extremely data scarce regions such as the Congo Basin, reanalysis relies heavily on the assimilation scheme and model physics rather than observational data inputs. This has resulted in divergence amongst reanalysis products themselves (Figure 1.12, *Washington et al.* [2013]), casting doubt on their ability to represent the true

climate of the region. Similarly, satellite and merged satellite-gauge products also show divergence in the region, given the limited amount of ground-data with which to validate them, with some products differing in mean rainfall estimates by a factor of two [*McCollum et al.*, 2000; *Nicholson et al.*, 2003; *Washington et al.*, 2013]. A recent review of global precipitation datasets by *Sun et al.* [2017] highlighted the Congo Basin as a region which features large discrepancies amongst datasets, including Global Precipitation Climatology Centre (GPCC) station data and CPC Merged Analysis of Precipitation (CMAP) merged data, in terms of interannual and decadal variability.

There have been ongoing efforts to improve the data situation in the Congo Basin. A number of datasets have been compiled in recent years with the aim of making the data that is available more accessible [e.g. *Nicholson et al.*, 2012, 2018a, 2018b;

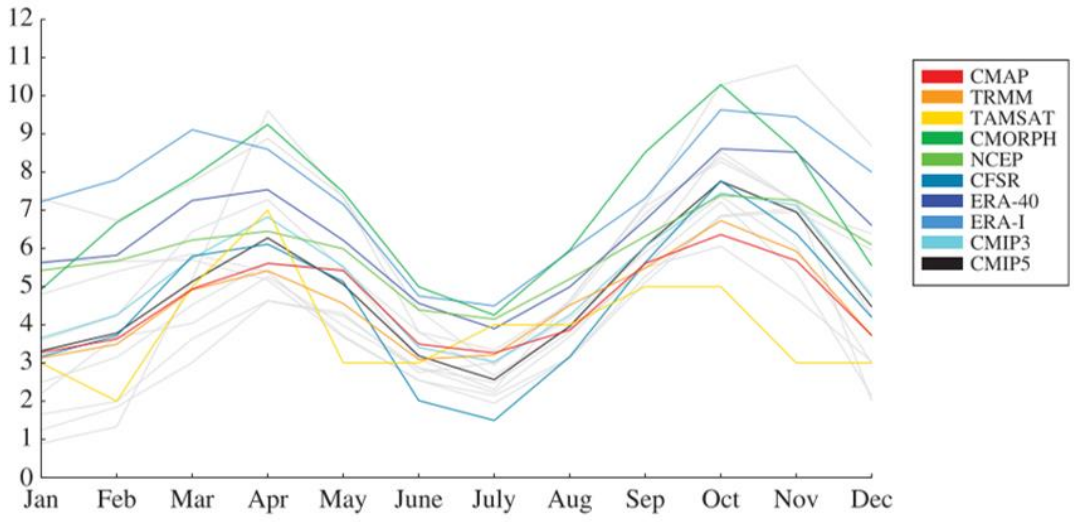

Figure 1.12 - Long-term mean annual cycle of rainfall (mm day^{-1}) for Equatorial Central Africa over the region 58 S–58 N, 12.5–308 E for the following datasets: CMAP, TRMM, TAMSAT, CMORPH, NCEP, CFSR, ERA-40, ERA-Interim, ensemble mean of CMIP3 and CMIP5. Individual CMIP5 models are shown in grey. Averages over 1961-1990. Source: *Washington et al.* [2013]

Funk et al., 2015]. For example, *Nicholson et al.* [2012] compiled all available nineteenth-century gauge records across the region, including data from stations established by colonial governments, in addition to temporary observations taken by nongovernmental groups like expeditions. In some sites regular observations have been taken from the end of the nineteenth century, including Douala and Yaoundé in Cameroon, and Luanda in Angola, at the western and southern edges of the Congo Basin. More recently, *Nicholson et al.* [2018] have compiled a new rainfall dataset across the Congo Basin, which incorporates newly acquired station data and uses spatial reconstruction to create a gridded dataset. There have also been efforts to develop methods of satellite calibration which use limited or sparse ground-based data [e.g. *Munzimi et al.*, 2015].

1.2.5.2 Representation in climate models

The scarcity of observational data has consequences for the representation of the region in climate models. Climate models are the primary tool available to identify and diagnose changes in climate and are thus vitally important in regions especially vulnerable to climate change, such as Africa. Before we can trust the outputs of climate models, however, they need to be assessed to determine if they are fit for purpose [*Flato et al.*, 2013]. The lack of recent, homogeneous climate data in the Congo Basin poses a significant problem for climate model evaluation, as they are normally tested by checking their ability to reproduce the historical climate [*Flato et al.*, 2013]. Given that even observational and reanalysis datasets can vary considerably in this region, the ability to perform such tests on models over the Congo Basin is severely limited. This has likely contributed to the

widespread divergence amongst coupled model climatologies in this region, where in some seasons, model datasets differ by a factor of three [*Washington et al.*, 2013]. Model divergence is not unique to data-scarce regions; it also occurs in regions which have not historically been the subject of focus by the model development community, such as southern Africa [e.g. *Munday and Washington*, 2017]. However, the extreme scarcity of recent observational data compounds this problem significantly in the Congo Basin.

There are two possible approaches to improving the representation of the Congo Basin in climate models in light of observational scarcity. The first is to improve the availability and usability of the available climate data in the region. This will be an important contribution to improving our understanding of the climate in this region, as well as providing better quality data for climate model evaluation. The second approach is to develop ways to evaluating climate models in the absence of observational data. This is the dominant approach taken in this thesis, and it intended to be complementary to the data-rescue projects that are ongoing in this region. Model evaluation approaches are discussed further in Section 1.4.

1.3 Future climate change

Africa is one of the most vulnerable continents to the effects of climate change [*Niang et al.*, 2014], and so understanding the likely climatic changes across the continent in the next century is crucial. The importance of advancing climate research in Africa is increasingly being recognised; in the past decade, multiple

research projects have been dedicated to better understanding regional climates within the continent (e.g. AMMA, Fennec, Future Climate for Africa), and both the Internatiolnal Panel on Climate Change (IPCC) and the World Climate Research Programme's (WCRP) Coordinated Regional Climate Downscaling Experiment (CORDEX) have emphasized Africa as a regional focus. Despite this progress, there remain large uncertainties in the outlook for the region (Figure 1.13), particularly concerning rainfall projections, which are more uncertain than those for temperature [*Rowell*, 2012; *Niang et al.*, 2014]. These uncertainties are in part associated with the capabilities of climate models, especially in tropical regions [*Rowell*, 2012].

The current section will introduce the climate models most commonly used for climate change projections and those that are used in this thesis. It will then summarise the previous research into the possible changes the Congo Basin, and the wider tropical region, may experience under anthropogenic warming, which has been conducted using climate models. This section does not attempt to critically assess the uncertainties of using climate models for this purpose; this will be examined thoroughly in Section 1.4. Instead, it seeks to outline the range of modelled climate futures for this region, and the climate processes which may be particularly important for those changes.

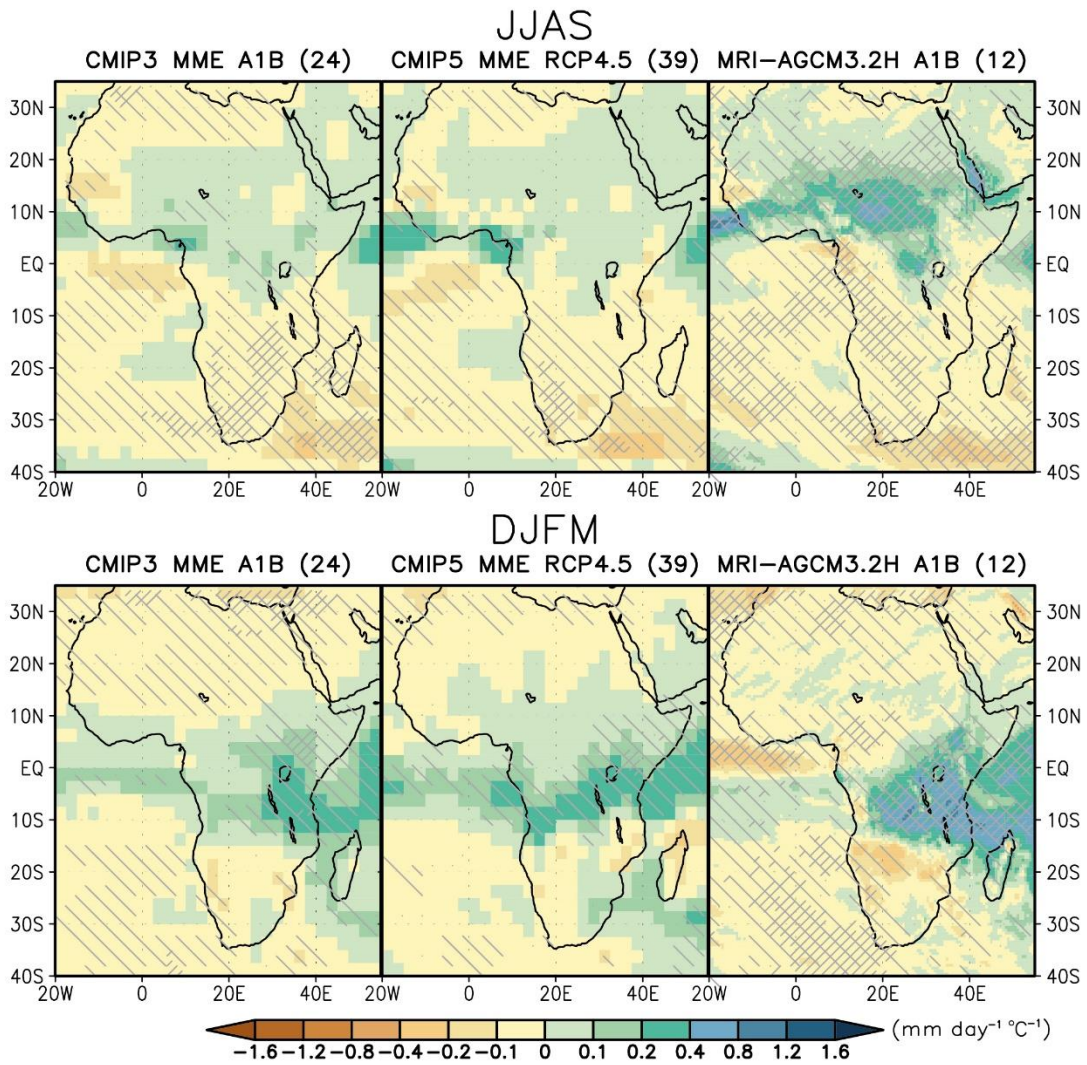

Figure 1.13 - Maps of precipitation changes from IPCC AR5, for Africa in 2080–2099 with respect to 1986–2005 in June to September (top) and December to March (bottom) in the SRES A1B scenario with 24 CMIP3 models (left), and in the RCP4.5 scenario with 39 CMIP5 models (middle). Right figures are the precipitation changes in 2075–2099 with respect to 1979–2003 in the SRES A1B scenario with the 12-member 60-km mesh Meteorological Research Institute (MRI)-Atmospheric General Circulation Model 3.2 (AGCM3.2) multi- physics, multi-sea surface temperature (SST) ensembles (Endo et al., 2012). Precipitation changes are normalized by the global annual mean surface air temperature changes in each scenario. Light hatching denotes where more than 66% of models (or members) have the same sign with the ensemble mean changes, while dense hatching denotes where more than 90% of models (or members) have the same sign with the ensemble mean changes. Source: *Christensen et al.* [2013]

1.3.1 Climate models

Most climate projections are created using either global (GCM) or regional (RCM) climate models. The former have comparatively lower spatial and temporal resolution, and can have coupled atmosphere and ocean components (AOGCMs). More complex versions of GCMs, Earth System Models (ESMs), simulate interactions between the climate, biosphere and cryosphere, as well as modelling the carbon cycle and other elements of atmospheric chemistry [*Flato*, 2011; *Heavens et al.*, 2013]. RCMs have higher spatial and temporal resolution than GCMs, allowing them to simulate some processes which are too small for GCMs to capture. However, this vastly increases the computational power required to run the model, and so RCM outputs are often limited to small spatial areas. In addition, RCMs are generally driven by GCM models, so they are not independent of biases found in GCMs.

1.3.1.1 Multi-model ensembles

More than 20 research centres worldwide have produced their own climate models, which differ in terms of horizontal and vertical resolution, parameterisations and core physics [*Easterbrook*, 2012]. Comparing the results from different models via multi-model ensembles (MMEs) has long been considered a useful component of model evaluation and development [*Palmer et al.*, 2005; *Collins*, 2007; *Stainforth et al.*, 2007; *Tebaldi and Knutti*, 2007]. Climate model intercomparison projects, such as those coordinated by the WCRP have ensured that the outputs of a wide range of GCMs are both widely accessible and

easily comparable. The two most recent iterations of the Coupled Model Intercomparison Project (CMIP3 and CMIP5) now constitute a large portion of the data used for global climate change research, and CMIP5 is the core model suite used in the most recent IPCC assessment report (AR5) [*Taylor et al.*, 2012]. The Coordinated Regional Climate Downscaling Experiment (CORDEX) is a similar intercomparison project for RCMs [*Giorgi et al.*, 2009].

A key feature of MMEs is that they allow for the creation of ensemble means. These have been found to produce a better representation of the historical climatology than any of the individual ensemble members, based on the theory that errors in individual models will be cancelled out by the averaging process (i.e. reducing structural uncertainty) [*Hagedorn et al.*, 2005; *Palmer et al.*, 2005; *Reichler and Kim*, 2008; *Knutti et al.*, 2010]. MMEs also allow for a greater incorporation of uncertainty in climate projections than studies which use individual models; as such, they are the dominant method used to represent climatic changes in the IPCC assessment reports [*Tebaldi and Knutti*, 2007].

However, there are challenges facing the use of MMEs and ensemble means, particularly in understudied regions such as Africa. First, MMEs such as CMIP5 are 'ensembles of opportunity', meaning that the ensemble is composed only of models from groups that are willing or able to contribute, and as such does not comprise a systematic, scientific sample [*Tebaldi and Knutti*, 2007; *Knutti*, 2010]. Second, and relatedly, coupled models are not all independent from one another: some modelling groups provide multiple, related models to the ensemble, and some share code or build new models based on model code developed elsewhere

[*Masson and Knutti*, 2011; *Leduc et al.*, 2016]. This means that biases or errors can be amplified across the ensemble, which may result in spurious indications of model agreement. Third, analysis of climate signals from MMEs often gives individual models equal weight (known as 'one-model-one-vote'), despite the fact it is unlikely that all models in the ensemble are equally as skilful or capable [*Collins*, 2017; *Knutti et al.*, 2017]. This is where model evaluation becomes particularly important, as weighting models, or choosing which models to include or exclude in an ensemble, requires an understanding of how capable or credible individual models are. This will be discussed further in Section 1.4.

1.3.1.2 Models used in this thesis

The analysis in this thesis will use models from the latest iteration of the Coupled Model Intercomparison Project (CMIP5) [*Taylor et al.*, 2012]. This is a suite of over 40 GCMs from more than 20 modelling groups. It is one of the most widely used datasets in climate change research, forming the basis of the IPCC fifth assessment report, and is easily accessible for researchers via the WCRP. Given the extremely limited understanding of climate model performance in the Congo Basin, GCMs are considered a good starting point for this thesis for a number of reasons. First, whilst RCMs have higher resolution, they are not independent of biases in parent GCMs, and so it is important to first analyse the behaviour of GCMs. Second, GCMs, unlike RCMs, allow for scale-dependent feedbacks from the regional to the global; a perspective which is particularly important in convective regions such as the Congo Basin. Finally, there is currently limited evidence over Africa that higher resolution models offer improved performance [e.g. *Moufouma-Okia and Jones*,

2014; *Vondou and Haensler*, 2017]. Analysing the mostly commonly used and available models is thus considered the most sensible starting point.

1.3.2 Projected tropical rainfall change

The response of the tropical climate system to warming will be complex and is not yet fully understood [*Collins et al.*, 2013]. It is likely that the global distribution of water resources will shift in a warmer world, creating wetter conditions in some areas and drier in others [*Held et al.*, 2005; *Zhang et al.*, 2007; *Hegerl et al.*, 2015]. Analysis of future projections from climate models has identified a number of mechanisms which may play a role in the response of tropical rainfall to warming. These mechanisms will be interlinked, and in some cases will contribute to opposite signals of change. They can be broadly split into two categories: *thermodynamic* and *dynamic* mechanisms of change [*Ma et al.*, 2018].

The dominant thermodynamic mechanism of tropical rainfall change diagnosed in coupled models is an increase in atmospheric moisture content (q) under warming, in line with the Clausius-Clapeyron relationship (~7% increase per K warming). This may result in a 'wet-gets-wetter' (or 'rich-gets-richer') response, where enhanced atmospheric moisture leads to enhanced moisture transport, and thus increased moisture convergence in regions which are already convergent, and divergence in areas which are already divergent [*Chou and Neelin*, 2004; *Held and Soden*, 2006]. *Chou et al.* [2007] note that this mechanism may enhance the seasonal rainfall differences, resulting in longer dry seasons. At large (zonal mean) scales this pattern of change has been identified in both observations and models

[*Allan et al.*, 2010; *Allan*, 2012; *Durack et al.*, 2012]. Relatedly, the 'upped-ante' mechanism posited by *Chou and Neelin* [2004] suggests that a warmer troposphere will increase the moisture threshold required for convection. This will have little impact on regions of deep convection where there is more than enough moisture to reach this threshold, but it may induce drying at the margins of convective regions.

The wet-gets-wetter mechanism is found to be opposed to some extent in models by the dynamical weakening of the tropical circulation under warming [*Held and Soden*, 2006; *Vecchi and Soden*, 2007; *Ma et al.*, 2012; *Chadwick et al.*, 2013]. A weakening of the tropical circulation is necessitated by the differential rate of increase in q (7% per K) and precipitation (1-2% per K). *Ma et al.* [2012] posit the mean advection of stratification change (MASC) theory as a dynamical explanation for why this occurs. As warming across the tropics increases with height, the atmosphere is stabilised. This leads to relative cooling in areas of ascent, as relatively-cooler air at the surface is advected upwards, and relative warming in areas of descent, as relatively-warmer upper air is advected downwards. This reduces the pressure gradients between ascent and descent regions, acting to slow down the climatological circulation. The weakening of the tropical circulation appears more robustly in the Walker cell than the Hadley cell [*Vecchi and Soden*, 2007].

A further dynamical mechanism of rainfall change is the 'warmer-gets-wetter' mechanism, whereby the spatial pattern of SST change influences regional rainfall and circulation patterns [*Xie et al.*, 2010]. As the moisture threshold for tropical

rainfall is raised under warming, it is expected that the greatest increases in rainfall will occur where SST warming is greater than the mean tropical warming, and decreases will occur where there is weaker-than-average SST warming. Further work has suggested that the balance of mechanisms may vary depending on the time-scale analysed. For example, *Huang et al.* [2013] find that the warmer-gets-wetter mechanisms dominates tropical rainfall change in the annual mean, but over the seasonal cycle, changes are dominated by the wet-gets-wetter mechanism, with the greatest increases in rainfall occurring in the regions of climatologically-maximal rainfall.

Whilst our understanding of the physical processes which drive rainfall responses to warming in models has improved, there remain large uncertainties in which of these mechanisms will dominate [*Meehl et al.*, 2007a; *Rowell*, 2012]. *Chadwick et al.* [2013] suggest that at a tropics-wide scale, the weakening tropical circulation and wet-gets-wetter mechanism almost entirely cancel each other out; leaving dynamical mechanisms relating to shifts in the location of convection to dominate the spatial pattern of rainfall change. Using a similar framework, *Lazenby et al.* [2018] find that spatial patterns of rainfall change over southern Africa are also primarily related to dynamical mechanisms of change, which affect the location of convection over land and the adjacent oceans. Both studies conclude that further work is required to determine the specific balance of these mechanisms, and to identify the important processes that are driving dynamical rainfall changes, particularly at regional scales and over land.

1.3.3 Projected Congo Basin rainfall change

Despite increasing scientific focus on tropics-wide rainfall change, there has been considerably less work analysing the projections of tropical rainfall change at a regional scale, particularly in the Congo Basin. Two studies have examined the range of projections over the region in multi-model datasets. *Haensler et al.* [2013a] assess projections from CMIP3, CMIP5 and CORDEX and find that the mean of the projections does not indicate significant changes in Congo Basin rainfall in the future. *Aloysius et al.* [2016] find mean precipitation increases across CMIP5 models of 2.4 to 2.8 % under medium and high-emissions scenarios respectively, by the end of the century. However, both studies show large uncertainties amongst models, with *Aloysius et al.* [2016] finding a range of -9% to 27%. In a study of the possible changes under 1.5°C and 2°C of warming, *Pokam et al.* [2018] find that while global models generally project wetting in the region, regional models in the ensemble show an equal number of positive and negative rainfall changes. The studies also highlight differences amongst models in the sign and magnitude of change across the basin (Figure 1.14).

There have also been a few studies analysing possible changes in rainfall extremes in numerical models over the Congo Basin. Analysis of the latter half of the 20th century indicates a reduction in total rainfall in the region, dominated by a reduction in the number of heavy rainfall days [*Aguilar et al.*, 2009]. However, multiple analyses of future projections have found increases in rainfall extremes under warming., Using a 90-km resolution regional model with a midline emissions forcing, *Vizy and Cook* [2012] find that the number of dry days over the Congo Basin by the mid-21st century are projected to decrease by 15-25%,

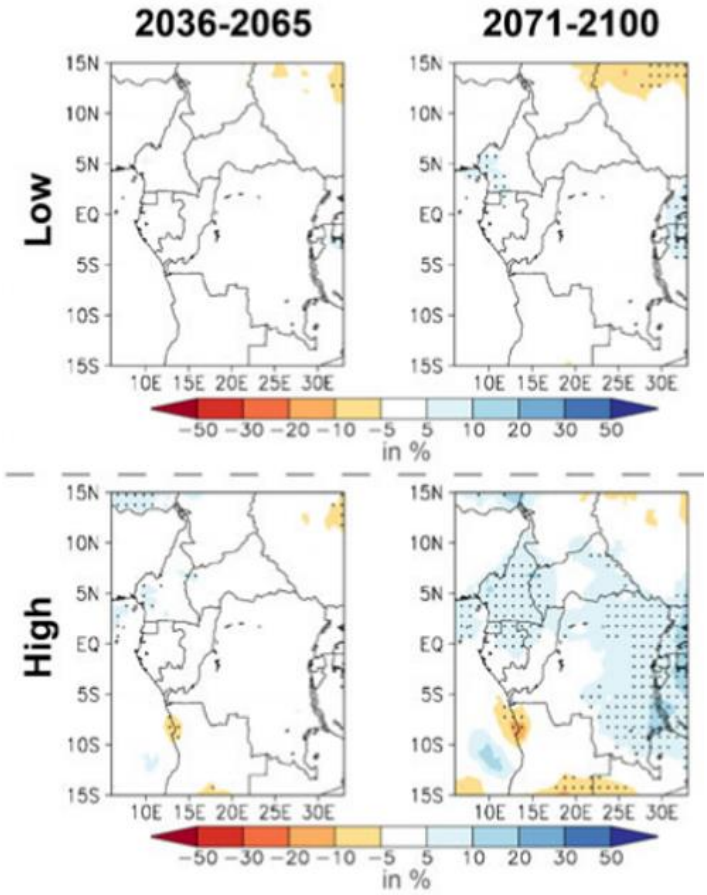

Figure 1.14 - CMIP5, CMIP3 and CORDEX Ensemble-Median projected relative changes in annual total precipitation following the low (top row) and high (bottom row) emission scenario for the mid-21st (2036–2065; left column) and the end of 21st century (2071–2100; right column) with respect to the control period. The black stipples indicate regions in which at least 66 % of all projected changes agree in the sign of change. Source: *Haensler et al.* [2013a]

dominated by a reduction of dry days in the rainy seasons. They also find a 30-60% decrease in the number of extreme wet days in the SON rainy season, with an increase of extreme wet days during MAM. In a recent analysis of 20 CMIP5 models under the RCP8.5 pathway, *Fotso-Nguemo et al.* [2018] identify increases in the 90th and 99th percentiles of rainfall events, particularly in the north and east of the basin. *Diedhiou et al.* [2018] compare changes in extremes in CMIP5 models under 1.5°C and 2°C of warming, finding that at both temperatures the majority of models project heavier rainfall and fewer rainfall days.

There is also evidence that the representation of extremes in models may contribute to diverging rainfall change signals. In a comparison between an RCM (REMO) and its parent GCM (MPI-ESM), *Saeed et al.* [2013] find that the former tends to simulate more extreme rainfall events, leading to higher surface run-off, less soil moisture, and lower total rainfall. In contrast, the GCM simulates fewer extreme events, reducing surface run-off and contributing to higher rainfall overall.

In terms of the mechanisms driving rainfall change in the Congo Basin, it is expected that dynamical mechanisms will play an important role, as in other tropical regions [*Chadwick et al.*, 2013; *Lazenby et al.*, 2018]. In addition, the large number of regional processes influencing rainfall in the region (see Section 1.2.3) may complicate the overall picture of rainfall change. In an analysis of numerous model products, including CMIP3 and perturbed physics ensembles from the UK Met Office, *James et al.* [2013] find that most models project drying in the west of the region during SON, whereas there is little change in the east of the basin. They

associate the drying in the west with enhanced subsidence under warming as part of a shift in the zonal circulation. However, they conclude that large differences in model historical climatologies within the ensemble may influence how models respond to greenhouse gas warming, and conclude that further work is needed to assess whether such responses are plausible.

The differences in rainfall change projected by models could have a wide range of impacts across the basin. Constraining the range of uncertainty in future rainfall change is therefore a critical task, and will be a central aim of the analysis in this thesis.

1.3.4 Key challenges

1.3.4.1 Establishing the plausibility of future climate projections

As discussed in Section 1.3.2, work on tropical rainfall change has predominantly focussed on understanding the balance of the mechanisms of change within models (e.g. wet-gets-wetter, warmer-gets-wetter, weakening of the circulation). Uncertainties amongst climate models are likely to contribute a large part of the uncertainty in the balance of tropical-rainfall mechanisms [*Chadwick et al.*, 2013]; however, there has been much less attention to model uncertainties, and whether all models used for such projections are fit for purpose. Across Africa there is considerable disagreement between models on how the climate will change in response to warming (Figure 1.13), and this divergence may to be compounded in

the Congo Basin by the significant divergence in the historical climatologies across models [*Washington et al.*, 2013; *James et al.*, 2018].

In order to improve our understanding of the plausibility of model projections in this region, and by extension, the most likely changes to rainfall, understanding uncertainties amongst models is a logical place to begin. While a wide ensemble of model projections of future climate have been assessed in this region [*Haensler et al.*, 2013a; *Aloysius et al.*, 2016], such assessments have not been able to establish the plausibility of any of these projections. The following section will introduce a methodology of climate model evaluation which this thesis will use to attempt to address this knowledge gap.

1.4 Climate model evaluation

The preceding section justifies the focus on the Congo Basin in this thesis and summarises what is already known about the climate of this region. It also outlines the particular challenges to climate research in the Congo Basin: a lack of recent, homogeneous climate data, a general lack of scientific attention to the climate regime, and stemming from these, the questionable ability of climate models to represent this region and to produce reliable future projections. Given that data availability is unlikely to improve in the near future, it is imperative we develop methods for evaluating and improving climate models which do not rely on this. Recent efforts have highlighted the importance of evaluating models with an

'African lens' [*James et al.*, 2018]; taking into account the particular challenges facing model development in this region, and recognising that none of the current generation of coupled models was developed in Africa itself [*Watterson et al.*, 2014].

This section will first describe the most common approach to climate model evaluation and the progress that has been made in determining model capabilities over Africa. It will then describe an emerging method of model evaluation, regionally-focussed process-based assessments, and the ways in which they may provide additional insights to this region.

1.4.1 Performance-based model evaluation

James et al. [2018] divide model evaluation into two main approaches: 1) quantification of model performance, and 2) analysis of physical processes. The former is a widely-used method of model evaluation, and consists of comparing the output of individual models in the historical period with observational and reanalysis data in the variables of interest (sometimes known as 'hindcast validation') [*Boer and Lambert*, 2001; *Taylor*, 2001; *Reichler and Kim*, 2008]. Checking a model's ability to reproduce the known climate is an important aspect of model assessment, as it identifies biases in the model and can direct efforts for model development [*Flato et al.*, 2013]. Regular hindcast validation of progressive model versions also allows for tracking the development of models over time [*Reichler and Kim*, 2008]. Standard statistical tests, such as mean square error (MSE), root-mean square error (RMSE) and correlation are used to quantify the

differences between models and observations, and these can be represented in various forms (e.g. Taylor diagrams [*Taylor*, 2001]). Models are usually tested on their ability to reproduce the climatological mean state of the variable, but can also be tested on their ability to reproduce other features such as temporal variability. Some studies have attempted to create a standardised set of 'performance metrics', by which suites of models can be objectively assessed [e.g. *Gleckler et al.*, 2008; *Baker and Taylor*, 2016]. Performance-based evaluation methods frequently calculate a 'skill-score' for individual models, which can be used to rank models and to assess models' performance relative to one another [e.g. *Watterson et al.*, 2014].

1.4.1.1 Performance-based evaluation in Africa

Performance-based model analysis has been used across Africa to identify and quantify errors in models. The ability of models to reproduce the spatial and seasonal distribution of rainfall across the African continent has been assessed in numerous model datasets, including CMIP5 [e.g. *Brands et al.*, 2013; *Mehran et al.*, 2015] and CORDEX [e.g. *Nikulin et al.*, 2012]. Recent work by *Dunning et al.* [2017] evaluated CMIP5 models on their ability to capture the timings of the seasonal cycle of rainfall across the continent, finding that the majority of models are able to capture the overall cycle. Other studies have combined multiple regionally-relevant metrics to create an overall assessment of model skill in Africa. For example, *Rowell et al.* [2015] test 39 CMIP5 models against 23 metrics, including RMSE of precipitation and RMSE of the annual cycle of SSTs, in order to rank model performance across East and West Africa. In East Africa, assessments have focused

on the ability of models to capture the climatological annual cycle of observed differences between the two rainy seasons [*Yang et al.*, 2015b; *Ongoma et al.*, 2018]. Such studies over East Africa have found that CMIP3 and CMIP5 models tend to underestimate rainfall during MAM and overestimate rainfall during the October to December (OND) rainy season [e.g. *Anyah and Qiu*, 2012; *Yang et al.*, 2014]. Over the Sahel, *Lau et al.* [2006] evaluate the ability of 19 coupled GCMs to reproduce the historical climate, in particular during the 1970s-1980s drought, via correlation analysis with rainfall and SST in the Atlantic and Indian Oceans. They find that only eight models are able to reproduce the drought signal based on these metrics.

The limited amount of model evaluation performed over the Congo Basin is largely performance based. In their analysis of projected rainfall changes in Central Africa, *Haensler et al.* [2013b] first assessed the ability of the CMIP3, CMIP5 and CORDEX models in a large ensemble to simulate the observed climatology in the region. When compared to the Climate Research Unit (CRU) gridded dataset and WATCH forcing dataset, they found that each ensemble was able to capture the broad seasonal variations in each sub-region. However, large ranges in precipitation values were present, particularly in CMIP3 and CMIP5, which they attribute mostly to outlier models. *Aloysius et al.* [2016] also tested the performance of 25 CMIP5 models compared with observations (a combination of NCEP-NCAR reanalysis, satellite and gauge datasets). Using statistical comparison techniques, including MSE and spatial correlation, they calculated skill scores and ranked individual models. The analysis indicates that many models are able to represent the annual cycle of rainfall in the Congo Basin, and that the pattern correlation between

modelled and observed annual precipitation varies between 0.6 and 0.94. However, their results also suggest that the majority of models overestimate rainfall compared to the observational data used, particularly in the centre of the basin. In agreement with work by *Palmer et al.* [2005], *Knutti et al.* [2010a] and others, they find that the multi-model ensemble outperforms individual models when compared to observational estimates.

1.4.1.2 Limitations of performance-based evaluation

Performance-based model evaluation is an important element of testing the capabilities of models, and such studies have revealed a number of biases present across models which need addressing by the model development community. However, there are some caveats to performance-based model evaluation, limiting the extent to which it can inform our understanding of model credibility. First, while comparisons to observations help to identify biases in models, they are on their own unable to demonstrate the causes of biases, or point to possible fixes [*Gleckler et al.*, 2008; *James et al.*, 2018]. Even where models are able to reproduce observed features of the climate, performance-based assessments cannot determine whether they are doing so for the correct reasons. Second, identifying the most important metrics to test against observations is a difficult task, particularly in regions where there is a limited understanding of the climate system, such as Africa [*James et al.*, 2018]. Third, assessing models' abilities across a spectrum of metrics can sometimes return contradictory results, with models performing well in some metrics and poorly in others [*Rowell et al.*, 2016].

Without further investigation into the relative importance of the processes underlying such metrics, their use can create additional uncertainty.

Performance-based model evaluation is also particularly limited in regions like the Congo Basin, where recent, homogeneous observational data is scarce [*James et al.*, 2018]. *Sylla et al.* [2013], in their comparison of gridded rainfall datasets, highlight uncertainty in observations as a key factor limiting the evaluation of climate models in Africa. In the Congo Basin, there are considerable discrepancies in rainfall magnitude and distribution across rain-gauge, satellite and reanalysis products [*Washington et al.*, 2013], and so determining which "version" of observations to compare models with is problematic (Figure 1.12). In addition to ground-based rainfall data, there is also limited radiosonde data in the region, limiting our understanding of processes within the atmospheric column, such as deep convection and, as our result, our ability to test the representation of these processes in models.

Finally, there is currently limited evidence that selecting models which show skill in reproducing observed climatological metrics leads to a narrower range of projection uncertainty in the future [*Rowell et al.*, 2016]. This may also be a function of the possibility that some models are producing the right climatology but for the wrong reasons. This thesis will test the hypothesis that other, non-performance-based methods of model evaluation, might provide greater constraints on the range of rainfall projections in the future.

1.4.2 Process-based model evaluation

Process-based, or process-oriented, model evaluation is the second main branch of climate model evaluation [*James et al.*, 2018], which aims to offer additional insights into model behaviour to performance-based model evaluation. Process-based assessments are used primarily in two ways: to investigate the ability of models to represent physical processes which are known to be important to the climatological variable of interest; and to determine the processes which cause model differences and biases. They can be used to address the capability of models to produce the mean-state climatology [*Cook and Vizy*, 2006], the temporal variability [e.g. *Dieppois et al.*, 2015], or trends over time in the variable of interest [e.g. *Williams et al.*, 2012]. A key advantage of such an approach is that we can use an understanding of the links between these processes and the variable of interest, such as rainfall, to help determine model credibility, even if rainfall is poorly observed.

At a global scale, considerable effort has gone into investigating the ability of models to represent important climatic processes, including tropical circulation [*Niznik and Lintner*, 2013], modes of tropical variability [*Guilyardi et al.*, 2009; *Kim et al.*, 2009], and clouds and water vapour [e.g. *Jiang et al.*, 2012; *Klein et al.*, 2013]. Such work has been fundamental to model development through the identification of model errors and possible improvements. Where there has been less work is in identifying and analysing processes which are important at a regional scale. *James et al.* [2018] argue that regionally-focussed process-based assessments are vital for better understanding model behaviour in understudied or poorly observed regions

such as Africa. Regionally-focussed process-based evaluation involves first identifying regionally-important processes which relate to the variable of interest, such as atmospheric jets, SST interactions, and local overturning circulations, before assessing if modelsare capabale of representing these processes.

1.4.2.1 Uses of regional process-based assessments

There are two, related ways in which process-based assessments can be used at a regional scale: to assess the *credibility* of models in the historical period and reasons for model divergence; and to examine the *plausibility* of future climate projections and the processes driving uncertainty. The former can inform the latter by helping to determine the trustworthiness of models to be used in future projections. These two approaches are discussed in turn below.

Model credibility in the historical period

The overall aim of this approach is to establish the credibility of model in the historical period. This is generally considered an important step in ensuring their adequacy for use in future projections, based on the assumption that if a model exhibits a questionable underlying mean-state, the direction and amplitude of rainfall change may also be questionable. Compared to performance-based evaluation, process-based assessments can provide more detailed reasoning for trusting models, and by extension, choosing which models to include or exclude from use in projections [*Overland et al.*, 2011; *McSweeney et al.*, 2014]. In addition, process-based analyses can help direct efforts for model development by identifying biases or errors in important processes. They can also offer additional

value by improving our understanding of the mechanics of climate processes in reality.

A process-based understanding of model behaviour in the historical period can be conducted in several ways. Such assessments can be used in combination with performance-based assessments, for example to determine whether models which can reproduce the historical climatology are doing so for the correct reasons. This is an important step in establishing the fidelity of models, and one that cannot be achieved by performance-based methods alone. Process-based evaluation can also be used in an exploratory manner to discover why different models produce different historical climatologies. Exploratory approaches are useful for identifying processes which should be the focus of future research, and in some cases can be used to guide the collection of observational data that will be of greatest use for model evaluation, a consideration which is especially important given the limited resources available for such endeavours. For example, *Munday and Washington* [2017] assess the regional circulation processes related to southern African rainfall across CMIP5 models, finding that the representation of the strength of the Angola Low is highly correlated with rainfall across models. This research highlights the importance of further research into this understudied phenomenon, given its importance with regard to rainfall, and led to a study by *Howard and Washington* [2018] which aimed to better understand the Angola Low in reality. In another example, *Washington et al.* [2013] identify moisture flux convergence as an important regional process relating to modelled rainfall over the Congo Basin, and argue that data from a targeted observational campaign of moisture flux

convergence in this region could be used to constrain the wide spread of modelled values.

Process-based assessments can also be used to identify biases in regional processes which may be the source of model differences. While many biases in GCMs are well-documented [e.g. *Wang et al.*, 2014], there has been little work to determine the impact of the biases on rainfall at a regional scale. Establishing the influence of these biases at a regional scale both informs our determination of model credibility and helps direct efforts for model development. For example, *Munday and Washington* [2018] find that the representation of regional topography, and its interactions with moisture transport, is a key cause of CMIP5 model divergence over southern Africa. They conclude that in order to reduce rainfall differences across models, both should be a focus for model development.

A further benefit of regionally-focused process-based assessments in the historical period is that they can help to improve our understanding of the climate system itself. The fact that ensembles of models often produce a range of climatologies, and a corresponding range in process behaviour, can in some cases be used to better understand how those processes are physically linked to the variables of interest. For example, *Hua et al.* [2018] use an ensemble of AMIP-style simulations from the ECHAM4.5 model to investigate the processes driving the drying trend over Central Africa in the past two decades. It has already been hypothesized that the drought was related to SST variations in the Indian and Pacific Oceans [*Hua et al.*, 2016], but the processes linking this to rainfall were poorly understood, in part due to limited observations. They found that the ability of a model to capture the

drought is tightly coupled with its representation of the Walker circulation and associated atmospheric teleconnections, suggesting that these are key processes driving the drying trend.

Plausibility of model projections

The second main use of process-based assessments is to identify and analyse the plausibility of processes related to future climate change in a region [*James et al.*, 2018]. An understanding of whether models produce climate signals based on plausible processes is important for checking the adequacy of models for this task [*Baumberger et al.*, 2017]. While performance-based evaluation identifies which models are most similar to observations, as yet it is unclear whether this helps to narrow the range of uncertainty in future projections [*Rowell et al.*, 2016]. This may be because the chosen metrics do not adequately capture models' capabilities, or that models are producing the right rainfall climatology for the wrong reasons. Both indicate that process-based evaluation may provide a better method for constraining the uncertainty in future climate signals.

There are two ways of conducting future-focussed process-based assessments. In the first approach, more or less credible models in the historical period are identified using a historical process-based assessment, and future changes in these models are assessed. If the historically credible and less-credible models produce difference climate signals, further analysis is conducted to check if the processes driving these differences are similar to those relating to model divergence in the historical period. If they are, this is powerful evidence that projections from the historically less-credible models are implausible, as they build on known

deficiencies in the models. On the other hand, if models produce similar climate change signals regardless of their climatological differences, the assumption that credibility in the climatological period results in more plausible projections is under question. As this assumption underpins a considerable amount of climate model evaluation research [*Räisänen*, 2007], this would be an equally important finding.

In the second approach, analysis starts by identifying the processes driving differences in projections across a suite of models, or in the models at the extreme ends of the projection spectrum. It then assesses whether these processes are plausible, based on what we already understand about the processes in that region. An example is the study by *James et al.* [2015], which uses a process-based assessment to examine the plausibility of the drying signal projected by Hadley Centre GCMs and RCMs over West Africa. They first identified the processes associated with historically dry years in the Sahel in models, finding that these were not the same processes present in dry years in reanalysis data. They then analysed the processes associated with the future drying signal in the models and found that models were producing drying via the same mechanism as in the historical period. They concluded that the drying projections were therefore untrustworthy, as they were related to spurious drying mechanisms which are not evident in observations.

Both historical and future-focussed process-based assessments are likely to enhance our understanding of the climatology of the Congo Basin, and future climate changes in the region. While limited research has been conducted in

Central Africa, studies from other regions demonstrate the potential promise of this method, as well as highlighting regional processes which may also be of importance in the Congo Basin. The following sections will summarise the previous research conducted over Africa in both historically and future-focussed process-based assessments, before outlining the possibilities this approach offers in the Congo Basin.

1.4.2.2 Historical process-based evaluation in Africa

Regionally-focussed process-based model evaluation has been conducted across Africa, including in East Africa, southern Africa, and West Africa. In East Africa, process-based evaluations have been used to better understand the models' representations of the region's climatology. Performance-based evaluation has established that models tend to underestimate the MAM long rains and overestimate the OND short rains [e.g. *Yang et al.*, 2014; *Tierney et al.*, 2015], but such studies are not able to determine the causes of these biases. In a process-based assessment of the short rains, *Hirons and Turner* [2018] find that the ability of models to capture the historical rainfall climatology is closely related to their representation of the Indian Ocean Dipole (IOD) and the related equatorial-westerlies in the Indian Ocean. They find that models which are too wet have anomalous easterlies at the equator, resulting in erroneous moisture advection into East Africa. The coupled models analysed also have an enhanced zonal SST gradient in the Indian Ocean, which acts as a positive feedback, further strengthening the easterlies.

Historical process-based assessments have also proven fruitful in southern Africa, where efforts have largely focussed on understanding the causes of model wet biases across the region. Model deficiencies in simulating rainfall have been linked to numerous processes, including topography interactions [e.g. *Pinto et al.*, 2016; *Munday and Washington*, 2018], low-level moisture circulation [e.g. *Kalognomou et al.*, 2013; *Lazenby et al.*, 2016; *Munday and Washington*, 2017], SST teleconnections [e.g. *Dieppois et al.*, 2015], and the location of the subtropical jet [e.g. *Tennant*, 2003; *Bracegirdle et al.*, 2013]. Process-based evaluation has also been used to better understand the processes accounting for model divergence in the region, and to point to ways to reduce this spread of model behaviours. For example, *Munday and Washington* [2017] identify the Angola Low as an important circulation feature relating to the relative wetness of models, indicating that improving the simulation of the low might narrow the spread of model climatologies.

In West Africa, process-based assessments have been used to investigate model representation of the West African Monsoon (WAM) [e.g. *Cook and Vizy*, 2006], the AEJs [e.g. *Caminade et al.*, 2006; *Abiodun et al.*, 2011], AEWs [e.g. *Bain et al.*, 2014; *Martin and Thorncroft*, 2015], Gulf of Guinea SSTs [e.g. *Roehrig et al.*, 2013], the Saharan heat low [e.g. *Biasutti et al.*, 2009] and other regional features. Research focussing on the capabilities of models in the climatological period has found that most models either poorly represent or are unable to represent the WAM, casting doubt on their ability to produce sensible climate projections in the region, given the dominance of the WAM in the region's climate system [e.g. *Cook and Vizy*, 2006].

To date there have been no peer-reviewed papers attempting a dedicated process-based evaluation of model behaviour in the historical period over the Congo Basin. *Washington et al.*'s [2013] study highlighted the potential importance of moisture flux for establishing model credibility; this thesis will follow on from this work by conducting process-based evaluation based on model representations of the large-scale moisture circulation.

1.4.2.3 Future-focussed process-based assessments in Africa

Considerably less work has been undertaken to assess the plausibility of future climate changes over Africa from a process-based perspective. In a study of GCMs, *Cook and Vizy* [2006] analyse future projections from a subset of models which were found to be capable of simulating the climatology and variability of the West African Monsoon. By analysing the processes related to future rainfall change in each simulation, they determine that the responses to changes under warming in one model (MRI-CGCM2.3.2) are more consistent with responses observed to similar patterns in the present-day climate. They conclude that this model therefore provides a more reliable simulation of future changes than the others sampled. Of the more recent work that has been undertaken, the majority falls into the second category outlined above: assessing the processes driving inter-model uncertainty in rainfall projections. In East Africa, recent work has focussed on addressing the 'East African climate paradox': the apparent mismatch between recent drying trends during the long rains and projected wetting over this region [*Shongwe et al.*, 2011; *Williams and Funk*, 2011; *Taylor et al.*, 2012]. *Rowell et al.* [2015] suggest that this paradox could be due to model deficiencies in producing

important processes in this region and call for a process-based investigation into the plausibility of these projections.

Recent research has suggested that changes in patterns of atmospheric circulation may be the dominant processes driving future wetting in several African regions. For example, *Giannini et al.* [2018] find that the wet-gets-wetter thermodynamic mechanism does not explain wetting in tropical East Africa; instead, increased rainfall is predominantly associated with dynamical mechanisms consisting of changes to circulation patterns which result in the export of moisture from the convective core of the continent towards East Africa. This is also found to be the case in southern Africa [*Lazenby et al.*, 2018]. While the predominance of dynamical mechanisms in driving spatial patterns of rainfall change is in line with previous work [e.g. *Chadwick et al.*, 2013], analysis by *Rowell and Chadwick* [2018a] emphasises that representations of the dynamical component of rainfall change are also where model uncertainties are largest (Figure 1.15).

1.4.2.4 Opportunities for process-based evaluation in the Congo Basin

Process-based assessments are hypothesized to be particularly useful in the Congo Basin for evaluating model behaviour. Given the lack of observational data with which to perform extensive performance-based evaluation, process-based methods instead allow for the evaluation of related fields, which may be better understood or observed than the variable of interest. In the case of the Congo Basin, this is likely to include analysis of moisture transport, atmospheric jets and SST interactions, which may be better understood than rainfall due to more

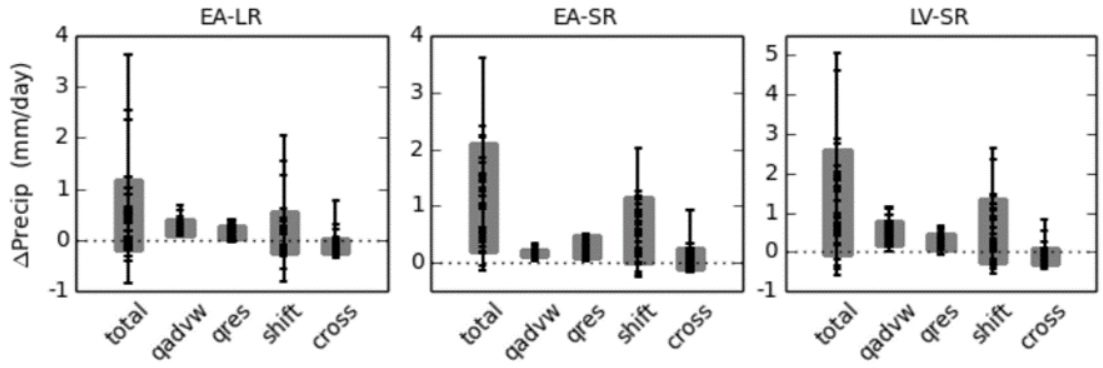

Figure 1.15 - Decomposition of RCP8.5-minus-historical precipitation change into dynamic and thermodynamic components, averaging data over three East African regions. Tick marks on each vertical line show results for individual CMIP5 models, and gray bars mark approximately the central 80% of datasets. The components are as follows: the change in q over land arising from increased moisture advection from the oceans + the weakening of the circulation (ΔPqadvw), residual changes in q over land (ΔPqres), spatial shifts in convection (ΔPshift), and a nonlinear cross term associated with interactions between other terms (ΔPcross). Source: *Rowell and Chadwick*, [2018]

extensive study in surrounding regions or better observational records (e.g. SST satellite observations). A process-based approach may also reveal biases in model simulations of these processes which in turn influence how the model simulates rainfall. Little is currently known about the ways in which model biases may erroneously influence the representation of rainfall in the region; identifying the linkages between biases and rainfall is therefore an opportunity to guide model development towards rectifying features which may be contributing to spurious rainfall climatologies. In the Congo Basin, investigation of the well-documented tropical Atlantic SST bias [*Richter and Xie*, 2008; *Richter et al.*, 2012; *Wang et al.*, 2014] would be well justified, given its proximity to the region and the known influence of SSTs on rainfall variability.

Process-based evaluation will also help guide research into the important features of the region's climate, as well as suggesting locations and variables that could be targeted by observational work. A preliminary process-based assessment of coupled models in the Congo Basin by *Washington et al.* [2013] identified a link between rainfall and low-level moisture flux convergence in models. This has contributed to increased attention to this process in the region, including in the model evaluation work conducted by *James et al.* [2018] and in this thesis. Further, their work has indicated the value that might be gained from a targeted observational campaign of moisture flux in this region. Given that a network of weather stations sufficient to support conventional model evaluation is unlikely to be implemented in the Congo Basin any time soon, targeted approaches are a more practical endeavour, which would offer a better understanding of the Congo Basin's climatology, as well as helping constrain the wide spectrum of model climatologies. Process-based approaches could be used to identify specific locations over which such data collection would be of most use.

Finally, process-based approaches are likely to further our understanding of possible future changes in the region. Given the large model differences that are observed in the historical period, such divergence may extend into the future. There has been limited research into the plausibility of future changes in the Congo Basin, with all work so far focussing on the extent to which models agree across the ensemble [*Haensler et al.*, 2013a; *Aloysius et al.*, 2016]. As *Aloysius et al.* [2016] highlight in their performance-based analysis of models in Central Africa, a deeper understanding of model plausibility requires an assessment of the causal mechanisms of change, including SST departures, and sources and fluxes of

atmospheric moisture. Process-based assessments of future change in the region can therefore be expected to add scientific value in two ways: first, by offering an understanding of whether a model's behaviour in the historical period influences its projections of future change; and second, by identifying the changes in regional processes which contribute most to uncertainty in future projections, and assessing the plausibility of these changes. Previous work has indicated that patterns of tropical rainfall change across coupled model ensembles are dominated by dynamical mechanisms [e.g. *Chadwick et al.*, 2013], and work over Africa has indicated that inter-model uncertainty is largely a result in model differences in representing these dynamical mechanisms [e.g. *Lazenby et al.*, 2018; *Rowell and Chadwick*, 2018]. This further justifies a focus on dynamical processes, such as moisture transport and atmospheric circulation, in this thesis.

1.4.3 Approach in this thesis

Section 1.2.3 highlights the important regional processes which are known to influence rainfall in the Congo Basin, highlighting the dominant role of dynamical, circulation processes in driving spatial and temporal climate variability in the region. In addition, an assessment of previous research into the drivers of climate change across both the tropics and Africa indicates an important role for dynamical processes, as well as highlighting that uncertainties in projections are often related to models' abilities to produce these processes. These findings indicate that process-based approach in the Congo Basin should begin from the perspective of such processes.

Important dynamical processes in the Congo Basin include moisture flux and convergence [*Suzuki*, 2011; *Pokam et al.*, 2012, 2014], atmospheric jets [*Nicholson and Grist*, 2003; *Jackson et al.*, 2009], overturning circulations [*Cook and Vizy*, 2015; *Neupane*, 2016] and SST interactions [*Hirst and Hastenrath*, 1983; *Balas et al.*, 2007; *Dezfuli and Nicholson*, 2013; *Nicholson and Dezfuli*, 2013; *Cook and Vizy*, 2015; *Hua et al.*, 2016]. Regional processes such as these are in many cases better observed and understood than micro-scale processes such as rainfall. In particular, the availability and transport of moisture, as well as the locations of moisture flux convergence, have emerged as prominent processes which relate to rainfall variability in this region, in both reanalyses [*Pokam et al.*, 2012, 2014; *Cook and Vizy*, 2015] and modelling [*Washington et al.*, 2013] studies. This thesis will focus on the representation of the mean state of such features in models, on the recognition that the ability of models to represent temporal variability and trends will ultimately depend on their ability to represent the mean-state. If the process-based methodology developed in this thesis proves fruitful for the Congo Basin, it is expected that such a methodology would be useful for other data scarce regions.

1.5 Summary of aims and objectives

The two overarching objectives of this thesis are to provide insights into the credibility of model rainfall in the historical period and the plausibility of changes in rainfall in the future. The analysis in this thesis falls into in two parts: the first (Chapters 3 and 4) assessing model behaviours in the historical period using a novel model evaluation methodology; and the second (Chapters 5 and 6) applying

this approach to the future period in two complementary ways, to determine whether it can provide insights into the plausibility of climate changes in the Congo Basin. The overall methodological aim of this thesis is thus to develop and test a method for understanding differences between coupled models that can be used in the absence of adequate observations.

Given the limited scientific attention to the climate of the Congo Basin, and even more so to model evaluation in this region, there are a plethora of routes this thesis could have taken. The papers presented in this thesis represent a logical approach to this problem, focusing on the processes which the literature has indicated are most important (for example, moisture flux convergence), as well as the models which are most commonly used for climate projections (GCMs).

The remainder of this section will outline the specific research questions for each results chapter in turn.

Chapter 3: Assessing inter-model differences

Chapter 3 aims to answer the first research question in Section 1.1.2:

> *To what extent can the large-scale processes of water vapour transport, provision and convergence explain in inter-model differences in the representation of rainfall in the Congo Basin?*

Previous research has suggested the relationship between rainfall and low-level moisture flux in models can help to explain model differences. The analysis in Chapter 3 addresses all four seasons, and as such is the first comprehensive

assessment of dry season behaviour in models in the Congo Basin. Specifically, Chapter 3 asks:

- How do CMIP5 coupled models differ in their representation of the magnitude and location of Congo Basin rainfall?
- Are there similarities between models which are wet and models which are dry?
- To what extent does model representation of rainfall relate to model representation of low-level convergence?
    - Does the relationship between rainfall and moisture flux convergence vary across seasons?
    - Are there particular atmospheric levels which are more important for distinguishing between wet and dry models?
- Does moisture inflow across the boundaries of the Congo Basin relate to the amount of rainfall in the basin across models?

Chapter 4: Processes differentiating models in SON

Chapter 4 addresses the second research question:

> *Can we determine the credibility of models based on an assessment of regional processes related to rainfall?*

This chapter focuses on the SON wet season, which displays significant model divergence in the spatial distribution of rainfall in the historical period in Chapter 3. It has also been the focus of several observational and reanalysis studies,

meaning that the processes associated with rainfall in this region are better understood than in other seasons. Following on from the results in Chapter 3, it interrogates to what extent an understanding of the moisture transport processes in the region can be used to establish model credibility. The specific research questions in this chapter are:

- What are the preferred locations of model rainfall in the Congo Basin in SON, and do these differ across coupled models in CMIP5?
- Are model differences in rainfall linked to Atlantic or Indian Ocean SST biases?
- How do these biases relate to the regional circulation, and what other elements of the regional circulation, for example the African easterly jets, help to explain model differences in rainfall?

Chapter 5: Determining whether past capabilities informs future signal

Chapter 5 aims to answer the third research question:

Does model credibility in the historical period give insights into the plausibility of future projections?

This chapter follows directly on from the analysis in Chapter 4. Using the understanding of model credibility in the historical period in SON, it attempts to

determine whether categorising models in such a way results in significantly different future projections. It asks:

- What is the range of Congo Basin rainfall changes across models in SON, both in terms of magnitude and spatial distribution?
- Do models with relatively wet or dry historical climatologies in SON feature significantly different rainfall signals at the end of the 21st century?
- What are the physical processes related to rainfall change in the model wet and dry historical climatologies, and based on previous assessment of the credibility of the model composites, can we determine whether some models produce more plausible future projections than others?

Chapter 6: Identifying processes driving inter-model differences in projections

Finally, Chapter 6 will tackle the fourth research question:

> *What processes contribute to inter-model uncertainty in future climate projections, and can an understanding of these processes help determine the plausibility of projections?*

This chapter uses a process-based understanding to explain the spectrum of projections of rainfall across models. In line with previous research and results from the previous chapters, the representation of circulation features is assessed, and the extent to which changes in these processes is related to rainfall is

determined. The season assessed is the DJF dry season, which exhibits the strongest rainfall signal across models, and for which assessing the likelihood of rainfall changes is particularly important. The specific research questions in Chapter 6 are:

- What is the range of rainfall projections produced by CMIP5 models over the Congo Basin during the SON rainy season?
- What circulation changes are associated with the upper and lower extremes of the range of model rainfall change?
- How do the model projections of rainfall change fit into an understanding of the possible mechanisms of future tropical rainfall change, and can anything be said about the plausibility of these changes?

1.6 Thesis format

This thesis has been submitted via a 'paper route', whereby the results chapters (Chapters 3 – 6) take the form of academic papers that have been submitted to peer-reviewed journals. The minimum requirement is that three papers are submitted. This thesis includes four articles, two of which have been published and two of which have been submitted. The details of the papers are below.

Published

Creese, A. and Washington, R. (2016) Using qflux to constrain modeled Congo Basin rainfall in the CMIP5 ensemble, *Journal of Geophysical Research: Atmospheres*, 121(22), 13415-13442

Creese, A. and Washington, R. (2018) A process-based assessment of CMIP5 rainfall in the Congo Basin: the September-November rainy season, *Journal of Climate*, 31(18), 7417-7439

Submitted

Creese, A., Washington, R. and Munday, C. The plausibility of September-November Congo Basin rainfall change in coupled climate models, *Journal of Geophysical Research: Atmospheres* (submitted 16th October 2018; accepted with minor revisions 22nd December 2018)

Creese, A., Washington, R. and Jones, R. Climate change in the Congo Basin: Processes related to wetting in the December-February dry season, *Journal of Geophysical Research: Atmospheres* (submitted 15th October 2018; accepted with minor revisions 3rd February 2019)

Statements on the authorship of each paper are included at the start of each results chapter. The content of each chapter is the same as appears in the published or submitted version of the paper; however, figure and table numbers have been altered to provide coherency throughout the thesis, and the internal layout of some figures has been adapted to improve readability. Supplementary material for each paper is included at the end of the relevant Chapters.

2 Data and Methods

2.1 Introduction

This section outlines the climate model and observational data used in the analysis in this thesis, as well as the methods used to analyse climate model behaviour. Individual results chapters also include a Data and Methods section which detail the specific data choices and methods employed.

2.2 Data

2.2.1 CMIP5 data

The model data in this thesis is taken from the CMIP5 ensemble [*Taylor et al.*, 2012], a collection of AOGCM models which are freely available via PCMDI (https://pcmdi.llnl.gov/mips/cmip5/). Over 20 modelling centres have contributed to CMIP5, with some providing multiple model versions. Each modelling centre agrees to run the same suite of experiments, using the same set of standardised forcings, in order to provide a fully comparable dataset.

The individual models and their attributes are shown in the relevant results chapters. The whole suite of CMIP5 models was not used in any one chapter; instead, a sample of between 17 and 19 models were used for each portion of analysis. Model selection was based on three considerations:

1. *Variable and experiment availability* – some modelling centres did not produce all output fields, or run all experiments, so these models were excluded from model selection
2. *Representation of range of model behaviours* – models were selected from across the spectrum of mean rainfall values over the basin, to ensure the full range of model behaviours were explored
3. *Model independence* – to try and overcome the issue of model interdependence in multi-model ensembles (Section 1.5.1.1), where possible only one model from each modelling centre was selected, usually the primary GCM model from each modelling group.

In reality, the availability of all variables and experiments needed for each chapter restricted the sample considerably, so criteria 2 and 3 were less significant. One ensemble run (r1i1p1) was used for each model in all analysis.

The analysis in this thesis focussed on both historical and future simulations of the climate. To do this, three experiments were utilised: *historical*, *AMIP* and *RCP8.5* [*Taylor et al.*, 2012] (Table 2.1). The historical (CMIP) experiment simulates the recent past (1850-2005) using known climatic forcings over that period, and is used to calculate the historical climatology of the region in all four chapters for the period 1971-2000 or 1979-2005. The AMIP experiment uses the same atmospheric conditions as the historical experiment, but imposes observed SST data (from 1979 onwards) instead of allowing models to calculate their own SSTs using an oceanic model. It is used in Chapter 4 to analyse the role of SSTs in rainfall patterns. Finally, Chapters 5 and 6 use the RCP8.5 future experiment, a future

climate projection (2006-2100) forced with the most extreme representative concentration pathway (RCP), representing a radiative forcing of 8.5 W m $^{-2}$ by 2100. RCP8.5 is chosen over less extreme scenarios due to both the high vulnerability of the region under such conditions, and to maximise the signal to noise ratio. Both chapters compare the period 2074-2100 in the RCP8.5 experiment to the period 1979-2005 in the historical experiment.

Chapter 3 used data solely from the historical experiment. Chapter 4 used data from the historical experiment and atmosphere-only AMIP experiment. Chapters 5 and 6 used data from both the historical and RCP8.5 experiments.

Table 2.1– CMIP5 model experiments used in this thesis

CMIP5 experiment	Years available (used)	Variables used
Historical	1850-2005 (1971-2005)	Rainfall (*P*), specific humidity (*q*), u-wind (*u*), v-wind (*v*), omega (Ω), sea surface temperature (SST), air temperature (*T*), evaporation (*E*), sea level pressure (SLP), geopotential height (GPH)
AMIP	1979-2005 (1979-2005)	*P*
RCP 8.5	2005-2100 (2005-2100)	*P, q, u, v*, Ω, SST, *T, E*, SLP, GPH

The variables analysed in this thesis are also shown in Table 2.2**.** Monthly and seasonal (MAM, JJA, SON and DJF) long-term means were calculated over the chosen Congo Basin domain for each chapter, shown in Figure 1.3**.** The choice of specific domains is discussed in the Data and Methods sections of individual chapters; however, analysis (not shown) indicates the results are largely insensitive to domain size. All model data was interpolated to a 1.875°x1.875° (Chapter 3) or 1°x1° (Chapters 4 to 6) horizontal resolution to allow for the creation of ensemble means of composites; tests of the metrics in Chapter 3 indicate that interpolation has no substantial effect on the results.

2.2.2 Reanalysis, gauge and satellite data

Reanalysis, gauge and satellite data is used as a point of comparison with models throughout this thesis, although, as the thesis aims to develop a methodology of model evaluation that does not rely on observations, it is not used to calculate errors in model simulations of rainfall. The inconsistencies between different observational datasets in the Congo Basin region are discussed in Section 1.2.5.1.

Two main reanalysis datasets are used in this thesis: the European Centre for Medium Range Weather Forecasts' ERA-Interim dataset [*Dee et al.*, 2011] and the US National Center for Environmental Prediction NCEP/NCAR reanalysis [*Kalnay et al.*, 1996] (Table 2.2). Reanalysis data have been interpolated to the same resolution as models were interpolated to in each chapter.

Table 2.2 - Reanalysis data used in this thesis

Dataset	Native horizontal resolution	Vertical levels	Variables used	Dates used
ERA-Interim (ERA-I)	0.7°×0.7°	37	*u, v, q, P,* Ω, SLP, GPH, SST, *T, E*	1981-2010
NCEP/NCAR (NCEP)	2.5°×2.5°	17	*u, v, q, P,* Ω, SLP, GPH, SST, *T, E*	1971-2000

The observational rainfall data used in this thesis is as follows: gauge data from CRU (Climate Research Unit v3.23) [*Harris et al.*, 2014] and GPCC (Global Precipitation Climatology Centre) [*Schneider et al.*, 2015], both of which include African station data from *Nicholson*'s archive [e.g. *Nicholson*, 1986, 2015; *Nicholson et al.*, 2000]; satellite data from CMAP (Climate Prediction Centre Merged Analysis of Precipitation) [*Xie and Arkin*, 1997] and TAMSAT (Tropical Applications of Meteorology using Satellite data and ground-based observations) [*Maidment et al.*, 2014]; and merged satellite/gauge data from GPCP (Global Precipitation Climatology Project) [*Adler et al.*, 2003] and TRMM (Tropical Rainfall Measuring Mission) [*Huffman et al.*, 2007]. SST data is taken from the HadISST2 satellite dataset (Hadley Centre Sea Ice and Sea Surface Temperature) [*Titchner and Rayner*, 2014]. The details of these products are shown in Table 2.3. All satellite and gauge datasets retain their native resolution in the analysis.

Table 2.3 – Observational data used in this thesis

Dataset	Native horizontal resolution	Type of data	Dates used
CRU	0.5°x0.5°	Gauge	1971-2000
GPCC	0.5°x0.5°	Gauge	1971-2000
CMAP	2.5°×2.5°	Satellite/ gauge-adjusted	1971-2000
GPCP	2.5°×2.5°	Merged satellite and gauge	1981-2010
TAMSAT	0.0375°×0.0375°	Satellite/ gauge-adjusted	1983-2011
TRMM	0.25°×0.25°	Merged gauge and satellite	1998-2014
HadISST2	1°x1°	Satellite and observations	1979-2005

2.3 Methods

This section will first describe the methods used to characterise model climatologies throughout this thesis. It will then explain the primary method of analysis used in this thesis, process-based evaluation, before describing the techniques used within this framework to analyse model outputs, both in the historical and future period.

2.3.1 Characterising the climatology

Model evaluation tends to focus on the capability of models to reproduce either: a) the mean state climatology; b) the interannual variability; or c) the trends over

time in the variable of interest. Given the scale of differences in model climatologies over this region, and the limited understanding of the 'real' climatology due to differences in observational datasets, this thesis will focus on the mean state. This is predicated on the understanding that the processes linked to the higher order statistical moments of variability and trend would likely not be credible if superimposed on a mean state that was deemed implausible.

Metrics are calculated throughout the thesis to establish the mean climatology in the various datasets and experiments. Monthly and seasonal (MAM, JJA, SON and DJF) mean and standard deviation of rainfall, *u* and *v* winds, specific humidity, evaporation, vertical velocity, and sea surface temperature are calculated over a 26-30 year period, depending on the availability of data. Standard statistical techniques are used to conduct the analysis in this thesis. Pearson's product moment correlation coefficient, *r*, is used throughout the thesis to quantify covariance. Significance of *r* is determined from the Student's t-test. In order to compare the mean of variables across the region amongst models, regional area-averages were computed on the interpolated model data.

2.3.2 Process-based evaluation

The concept of process-based evaluation is described in detail in Section 1.4.3; models are assessed on their ability to represent processes that are known to relate to rainfall. Given the limited amount of model evaluation work conducted over the Congo Basin, the analysis in this thesis starts broadly, covering a range of seasons and models, before narrowing to focus on more specific seasons and

model composites. The first results chapter (Chapter 3) presents a broad overview of the atmospheric processes relating to modelled rainfall in all seasons, in particular moisture flux and moisture flux convergence, which have previously been identified as important processes in this region [e.g. *Pokam et al.*, 2012; *Washington et al.*, 2013]. The analysis in Chapter 3 focusses on a wide sample of models selected from CMIP5, as a first step in understanding the reasons behind inter-model differences.

The remainder of the thesis develops a process-based approach for determining which models are most credible, and by extension, which may be producing the most plausible future climatologies. This method is developed to be of particular use in data scarce regions, as it does not rely on observations to make assessments of model capabilities. The methodology is generally deployed as follows:

1. *Categorise models*

The first step in a process-based assessment is to organise the models based on variable of interest. In Chapters 4 and 5, the variable of interest is mean seasonal rainfall in the historical period, so models are ranked by their long term mean rainfall over the Congo Basin domain. The variable of interest in Chapter 6 is rainfall change (ΔP), so models are ranked by the difference between mean rainfall in the historical and future periods.

Once the models are organised, a subset of models at each end of the spectrum are identified which represent the 'extremes' of rainfall climatology or rainfall response in that season. As the goal of the analysis is to determine which models

are most credible, or produce the most plausible projections, analysing the extreme ends of the spectrum is likely to offer the starkest comparison amongst models. The models at each extreme are compared using composite analysis; this is discussed further in Section 2.2.3.1.

2. *Identify processes which are known to be related to rainfall*

Once the models have been categorised, the next step is to identify the processes which likely relate to rainfall. Several of these processes were identified in Section 1.2.3 for the Congo Basin, and include low-level moisture flux and convergence, the African Easterly Jets, Atlantic and Indian Ocean SSTs, local and remote overturning circulations, and winds associated with regional circulations such as the South Atlantic High. Comparing the representation of these processes in different models helps determine whether they are also important for explaining inter-model differences in rainfall,

It is important that there is some prior understanding as to how these processes relate to rainfall, as this will help assess the credibility of models. This understanding is often based on research into the influences on the interannual variability of rainfall, which can then be used as an analogue for model behaviour. For example, *Pokam et al.* [2012] show that wet years in the Congo Basin tend to feature greater low-level moisture flux from the Atlantic Ocean than dry years. Establishing how low-level moisture flux differs between the wet extreme and dry extreme models can give insights into whether models are producing credible moisture flux-rainfall associations, or whether they are related in ways that have not been identified in reanalysis, and thus may be spurious.

3. *Determine the chain of processes which link to rainfall and assess the credibility of the resulting rainfall*

The next step is to determine the chain of physical processes linking the important processes identified in step 2 to rainfall. Figure 2.1 shows a schematic example of a process chain based on results from Chapter 4. It is particularly advantageous if the linking processes are better observed than rainfall, and by extension, if biases in those processes have already been identified. For example, since the late 1970s satellites have provided global coverage of SSTs, meaning that SST biases, such as the prominent warm bias in the southeast tropical Atlantic, are well observed. If biases in processes such as local SSTs can be linked to how models simulate rainfall, this casts doubt on the rainfall climatology produced by that model.

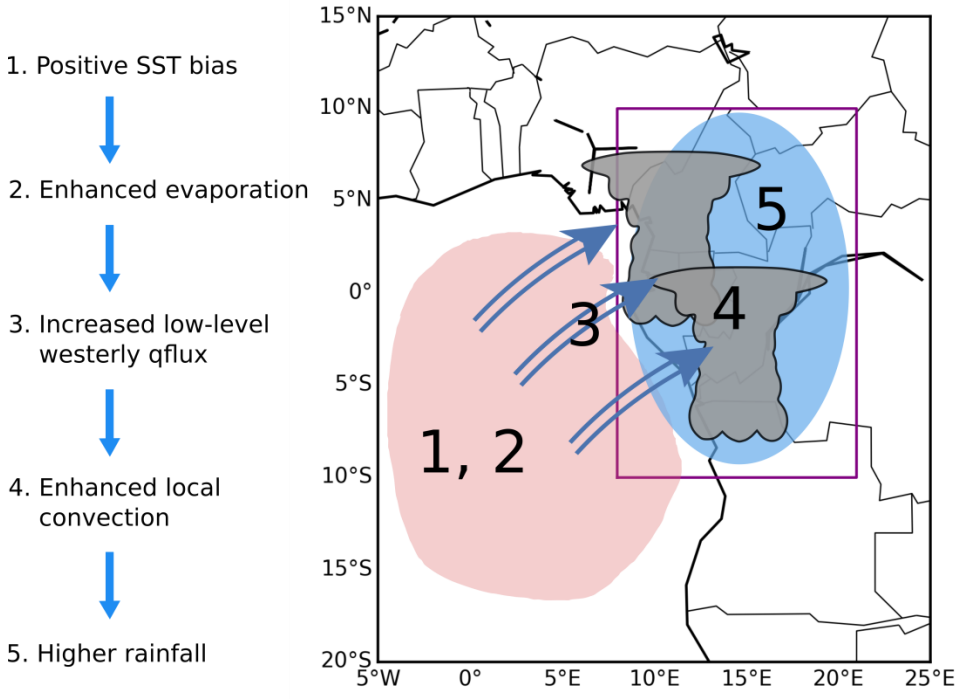

Figure 2.1 - Schematic of the chain of processes related to higher rainfall in the wet composites compared with the dry composites in the west Congo Basin (purple box), as described in Chapter 4.

The ability to determine the reasons models are producing particular rainfall climatologies is a key advantage of process-based assessments. If a model is producing rainfall based on a chain of physical processes that has been identified in previous analyses of the real climate system, we may have reason to trust that model's capabilities in replicating the historical climate. However, it may also be the case that a model is producing what appears to be a sensible rainfall climatology, but it is producing it via an implausible chain of processes, thus casting doubt on that model's capabilities in this region.

2.3.2.1 Composite analysis

Composite analysis is the main type of analysis underpinning the process-based assessment. Composites are simply averages of a field taken across a sample. Selection for the sample is on the basis that an important criterion is fulfilled [*Yarnal*, 1993]; for example, analysis of the circulation patterns associated with heavy rainfall on individual days may be analysed using a composite of days exceeding a certain rainfall threshold. Complex or multiple criteria can be applied, or a number of composites can be created based on a variety of criteria, allowing for comparison across composites.

In this thesis, composites are used in all four results chapters. In Chapters 4 and 5, composites are created for the four wettest and four driest models (upper and lower quartiles of the sample) in both the western and eastern subdomains of the Congo Basin, based on the historical long-term mean climatology (1979-2005). In Chapter 6, composites are made of the four models featuring the largest and

smallest future rainfall change signals. Climatological processes, such as overturning circulations, can then be compared across the two composites. Composites of small samples of models are more useful than analysing individual models, as the averaging process removes some of the noise, while allowing common features amongst the member models to be identified.

There are some limitations to composite analysis, which we have taken into consideration in the thesis. First, averaging across a sample can sometimes create a false impression of the typical conditions in each composite member [*Yarnal*, 1993]. In the context of this thesis, there are some models which exhibit starkly different behaviours to the majority of models, so their inclusion can skew the sample. To guard against this, the climatologies of individual composite member models are inspected in addition to the composite mean, and models which behave in an obviously different manner to the other composite members are excluded from the sample. For example, in Chapter 4, one model (CSIRO-Mk3-6-0) features a cold Atlantic SST bias whereas all other models exhibit a warm bias, so it is not included in the composite analysis. Second, in the analysis in this thesis, there are necessarily a small number of models in each sample, as we are sampling the ends of the distribution. To address this limitation, we have included other checks on model behaviour, including further statistical tests (as recommended by *Boschat et al.* [2016]). For example, the relationship between high rainfall and strong SST biases found in composites in Paper 2 is confirmed with correlation analysis over the whole suite of models. The metric of agreement amongst composites also gives an indication of how distinct the wet and dry composites are; mean differences in grid-boxes without stipples are not considered robust.

2.3.2.2 Representing significant differences between composites

Given the relatively small number of models in the overall sample, and the even smaller number (four) falling into the (approximate) upper and lower quartile of models used in the composites, using a t-test to determine significant differences between the composites is deemed inappropriate. Instead, a multi-level metric of agreement is used to identify regions where the variable under consideration is significantly different between the wet and dry composite. This is indicated by stippling at each grid-box. In Chapter 3, stipples occur at each grid-box under the following conditions:

1. Where all wet model values are greater than all dry model values (large dots)
2. Where all dry model values are greater than all wet model values (crosses)
3. Where all wet model values are greater than the mean of the dry model values (small dots)
4. Where all dry model values are greater than the mean of the wet model values (small crosses)

From Chapter 4 onwards, a refined version of the stippling metric is used. In all composite comparisons, stipples occur under the following conditions:

1. Where all wet model values are larger or smaller than all dry model values (large dots)
2. Where all wet model values are greater or smaller than the dry mean, depending on the direction of difference (squares)

3. Where all dry models are greater or smaller than the wet mean, depending on the direction of difference (crosses)
4. Where both (2) and (3) are true (small dots).

These agreement metrics were developed in order to display as much useful information about model differences as possible.

2.3.3 Projected change

The analysis of future change in Chapters 5 and 6 is conducted predominately by calculating the absolute difference (ΔX) between the future (X_{fut}) and historical (X_{hist}) climatology of a model or models, such that:

$$\Delta X = X_{fut} - X_{hist}$$

The future-minus-historical approach is commonly used in climate change research, particularly as an input to further modelling (e.g. impact modelling). Using only the "delta change" or "factor of change" signal, rather than the full future climatology, can be considered a basic form of bias correction, as the future climatology itself is likely to be highly influenced by underlying biases in the mean state of the model [*Fowler et al.*, 2007; *Lafon et al.*, 2013]. In this way impact or hydrological modellers can attempt to avoid introducing further biases into their model by imposing the delta change signal on top of observed climatological data.

However, given their wide use, it is important to interrogate the plausibility of the delta change signals produced by models. It is likely that biases or differences in the mean state of models will interact with the forcings introduced in the future experiment, and so the delta change signal cannot be assumed to be independent of the model's underlying climatology. The influence of the model climatology on delta change signals is specifically investigated in Chapter 5, and a further process-based analysis of the plausibility of delta change signals is conducted in Chapter 6.

2.3.3.1 Representing dominant climate signals

To represent model agreement in the future climate change signals, this thesis uses metrics based on agreement in the sign (positive or negative) of change in individual variables. When assessing the full ensemble mean of models, stipples are using to represent grid-boxes where more than 15 models agree on the sign of change. When assessing the change within a single composite, stipples are used to signify where all composite members agree on the sign of change. The "sign of change" approach is used widely in climate research, including the IPCC assessment reports [e.g. *Meehl et al.*, 2007]. In addition and where appropriate (i.e. across the full ensemble), statistical tests such as the Student's t-test have been used to identify differences in the range of future climatologies compared to the range of historical climatologies.

3 Using qflux to constrain modelled Congo Basin rainfall in the CMIP5 ensemble

Using qflux to constrain modelled Congo Basin rainfall in the CMIP5 ensemble

A. CREESE[1] and R. WASHINGTON[1]

[1]Climate Research Lab, School of Geography and the Environment,

University of Oxford, South Parks Road, Oxford, OX1 3QY, UK

Journal of Geophysical Research: Atmospheres, **121**(22) 13415-13442,

doi:10.1002/2016JD025596.

Received 29 June 2016

Accepted 7 November 2016

Published online 14 November 2016

Authorship Declaration

I conducted all of the analysis and writing for this paper. Richard Washington contributed to the interpretation of results, discussed the structure of the paper with me, and commented on and edited the manuscript.

Abstract

Coupled models are the tools by which we diagnose and project future climate, yet in certain regions they are critically under-evaluated. The Congo Basin is one such region which has received limited scientific attention, due to the severe scarcity observational data. There is a large difference in the climatology of rainfall in global coupled climate models over the basin. This research attempts to address this research gap by evaluating modelled rainfall magnitude and distribution amongst global coupled models in the Coupled Model Intercomparison Project 5 (CMIP5) ensemble. Mean monthly rainfall between models varies by up to a factor of five in some months and models disagree on the location of maximum rainfall. The ensemble mean, which is usually considered a 'best estimate' of coupled model output, does not agree with any single model, and as such is unlikely to present a possible rainfall state. Moisture flux (qflux) convergence (which is assumed to be better constrained than parameterised rainfall) is found to have a strong relationship with rainfall; strongest correlations occur at 700hPa in March-May (r=0.703) and 850hPa in June-August, September-November and December-February (r=0.662, r=0.707, r=0.809). In the absence of observations, this relationship could be used to constrain the wide spectrum of modelled rainfall and give a better understanding of Congo rainfall climatology. Analysis of moisture transport pathways indicates that modelled rainfall is sensitive to the amount of moisture entering the basin. A targeted observation campaign at key Congo Basin boundaries could therefore help to constrain model rainfall.

3.1 Introduction

Global coupled climate models (GCMs) are crucial to developing climate projections, yet in certain regions they are critically understudied and under-evaluated. Africa is one such region which has historically received little climatic attention; a problem which has begun to be addressed in earnest through the creation of several targeted research projects, for example the NERC/DFID funded Future Climate for Africa. However, glaring omissions remain in the map of African climate research; in particular the Congo Basin, which has been subject to less targeted research that any other African region [*Washington et al.*, 2006]. This is despite the crucial role the Congo plays in both the regional and global climate system.

The importance of the Congo is based upon three key considerations. First, it is one of three global convective hotspots [*Webster*, 1983], experiencing the highest lightning strike frequency of anywhere on the planet [*Jackson et al.*, 2009] and dominating global rainfall totals in the transition seasons [*Xie et al.*, 2003]. Second, the region's forests are a globally significant carbon sink, and thus a crucial element of the climate system via the carbon cycle [*Williams et al.*, 2007]. It is estimated that 60-70 Pg of carbon is stored in above ground vegetation in Africa, second only to the amount stored in Amazonia [*Baccini et al.*, 2012]. During the dry seasons, Congo forests are particularly vulnerable due to their proximity to the rainfall threshold below which rainforest ecosystems transition to savannah [*Malhi et al.*, 2013]. Projections indicate that pronounced warming over Africa could

result in drier and more extended dry seasons, further increasing the region's vulnerability [*James and Washington*, 2013]. Third, the region's population relies heavily on rain-fed agriculture, and has already experienced severe land degradation due to drought in recent years [*Samba and Nganga*, 2012]. Climate prediction is therefore crucial to these populations.

The most significant limitation to climatic research in the Congo Basin is the dearth of observational data, primarily the result of the extreme ratio of size to access of the region, exacerbated by political instability in recent decades. Historical datasets have been compiled for the region [e.g. *Aguilar et al.*, 2009; *Nicholson et al.*, 2012], but the number of maintained rain gauges has been in rapid decline since the 1980s [Figure 3.1; *Harris et al.*, 2014]. Only three meteorological stations in the DRC reported to the Global Telecommunication System in 2013; this compares to over 3000 stations which report to the Met Office in the UK alone (an area 40 times smaller). Nevertheless, the Congo's significance is increasingly being recognised in scientific literature, not least because anthropogenic-induced climatic changes have been brought to the forefront of African environmental policy [*James and Washington*, 2013]. Several recent studies have utilised satellite, gauge and reanalyses data in equatorial Africa to identify controls on both seasonal and interannual rainfall variability, with particular reference to the characteristics of: the African Easterly Jet [*Nicholson and Grist*, 2003; *Dezfuli and Nicholson*, 2011]; low level westerlies [*Dezfuli and Nicholson*, 2011; *Pokam et al.*, 2014]; mesoscale convective systems [*Jackson et al.*, 2009]; SST teleconnections [*Nicholson and Dezfuli*, 2013; *Hirst and Hastenrath*, 1983; *Hansingo and Reason*, 2009]; and zonal overturning circulations across the region [*Cook and Vizy*, 2015].

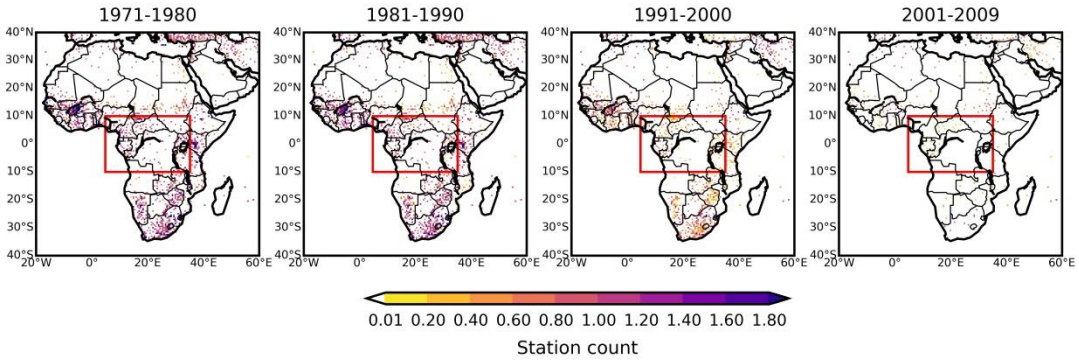

Figure 3.1 - Mean number of stations contributing to the CRU 3.23 gridded precipitation dataset (0.5° horizontal grid spacing). Red box indicates study domain for this research (5°E to 35°E, 10°N to 10°S).

3.1.1 Congo climate regime

The key features of the Congo Basin climate regime are shown in Figure 3.2. The region (here defined as 5°E to 35°E, 10°N to 10°S, shown by the red box in Figure 3.1) is strongly influenced by the latitudinal march of tropical convection, which lags solar heating by roughly a month. Rainfall oscillates meridionally, crossing the equator twice a year during the transition seasons of March to May (MAM) and September to November (SON), with dry seasons in June to August (JJA) and December to February (DJF). MAM events appear to be heavier and more prolonged, whereas SON rains are relatively short and less intense, [*Sandjon et al.*, 2012]; *Jackson et al.'s* [2009] study would suggest this is due to enhanced meso-scale convective system activity. The zone of maximum rainfall occurs broadly over the western central African region, covering almost the entirety of the Congo forest [*Pokam et al.*, 2012], and coinciding with a locus of intensive convective activity [*Sandjon et al.*, 2012].

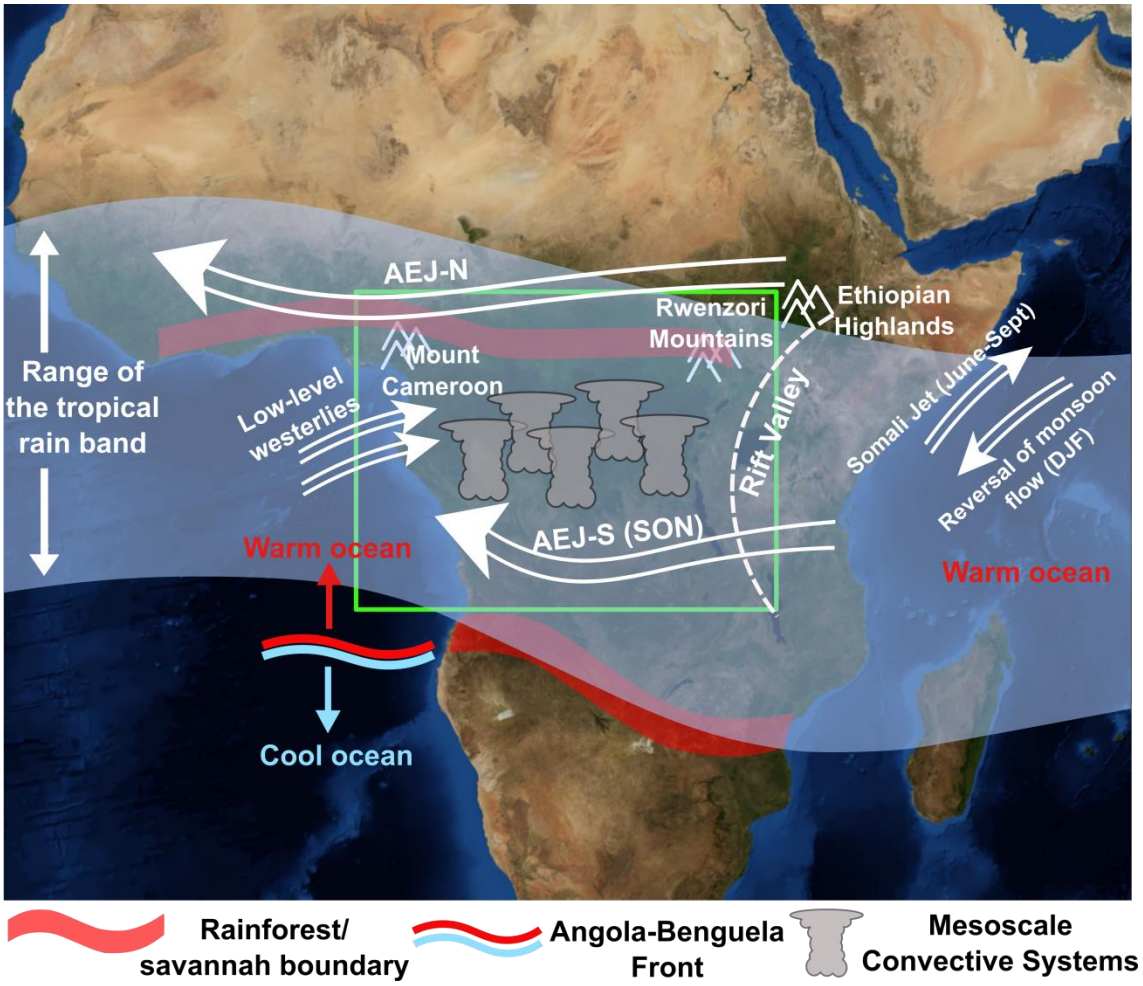

Figure 3.2 - Schematic showing key features of the Congo Basin climate. Locations are approximate. The study area is shown by the green box. AEJ-N= African Easterly Jet – North and AEJ-S = African Easterly Jet South.

One of the key drivers of Congo rainfall variability is the availability, transport and accumulation of moisture in the atmosphere. *Pokam et al.* [2012] suggest there are two maxima of moisture convergence: the first during the MAM wet season, resulting from moisture flux near 700hPa and embedded in the northerly component of the African Easterly Jet (AEJ-N); the second during SON at lower levels (850-1000hPa), dominated by advection from the Atlantic. Such results, in addition to those of *Washington et al.* [2013], indicate that assessment of moisture transport into the region could help constrain coupled model outputs. Moisture

convergence has been utilised similarly in the Amazon by *Yin et al.* [2013]; satellite and ground-based measurements were used to determine the cause of rainfall underestimation in Amazonia in CMIP3 and CMIP5 models. They conclude that models featuring the most realistic moisture convergence and evapotranspiration values also feature the most realistic rainfall magnitudes, particularly in the dry seasons. Models which overestimate moisture divergence feature the strongest rainfall underestimations, pointing to a strong relationship between moisture flux convergence and modelled rainfall.

3.1.2 Coupled models

Coupled models are increasingly being used to diagnose present and future changes in African climate. They have been utilised extensively in the Sahel, the most studied region in Africa due to the multi-decadal drought in the latter half of the twentieth century [*Washington et al.*, 2013] and in some instances have provided a good simulation of Sahelian climate [e.g. *Lau et al.*, 2006]. Multi-model ensembles (MMEs) have also been utilised in West and southern Africa, with some success [*Cook and Vizy*, 2006; *Lau et al.*, 2006; *Kay and Washington*, 2008] Validation of model hindcasts with reference to observations is a frequently used method [*Flato et al.*, 2013]. *Rowell et al.* [2015] ranked 39 coupled models according to their ability to simulate historical observations in a range of metrics over the Sahel and Greater Horn of Africa; and the process-based assessments of *Dieppois et al.* [2015] and *James et al.* [2015] (of southern Africa and the Sahel respectively) rely on the ability of models to reproduce observed patterns of variability. Such methods have also been used over Central Africa; *Aloysius et al.*

[2016] identified a subset of models based on historical performance metrics which could be used to produce projections with smaller uncertainties, and *Haensler et al.* [2013] compared projections from CMIP3, CMIP5 and CORDEX to reanalysis data, concluding that most models have '*substantial skill in representing observed conditions*' (p.16).

However, despite this progress, there remain substantial inconsistencies between models themselves, as well as between models and observations [*Christensen et al.*, 2013]. These differences are starkest in the Congo Basin, where the lack of observational data poses a challenge to traditional model evaluation techniques. Reanalyses data is commonly used in place of 'pure' observations, as it has continuous spatial and temporal coverage. However, for a large region with little or no initialisation, the reanalysis process will be steered significantly more by the model; thus, it cannot be regarded as indicative of observations. Indeed, initial analysis of model, reanalyses and satellite/gauge data suggests that at present there is little agreement between individual models as to the quantity and distribution of rainfall across the basin [*Washington et al.*, 2013], even amongst reanalyses datasets themselves. In addition, satellite and gauge estimates have been found to differ by a factor of 2-3 in this region [*McCollum et al.*, 2000; *Nicholson et al.*, 2003].

3.1.3 Aims

In light of these challenges, this study aims to understand relative differences between models, rather than comparing hindcast output to observations. To do

this, we examine the extent to which large-scale patterns of moisture flux and convergence can explain differences in rainfall amongst models. This broad- scale approach is not only necessary due to the coarse resolution of coupled models but also may contribute to a refined understanding of the wide spectrum of rainfall regimes present across the model suite. This is a first step in understanding the extent to which global models are capable of producing usable outputs for this region. We also aim to understand the relationship between rainfall and moisture transported into the basin; if this can be achieved, addressing the data gap for the Congo becomes a more feasible task.

The following section describes the model, reanalysis, satellite and gauge data used throughout the paper. Section 3.3 outlines the simulated rainfall climatology in all seasons across models, and an assessment of the relationship between rainfall and moisture flux convergence follows in Sections 3.4 and 3.5. Finally, the likely origins of water vapour advected into the basin, and its relationship with rainfall between models, are assessed in Section 3.6. Sections 3.7 and 3.8 discuss the results and conclude.

3.2. Data

The focus of this study is the model output from the Coupled Model Intercomparison Project 5 (CMIP5), the most recent large scale suite of model products from the international community [*Taylor et al.*, 2012]. The experimental design of CMIP5 allows for the creation of multi-model ensembles, which have

been shown to produce some of the most accurate simulations of present climate [*Palmer et al.*, 2005; *Reichler and Kim*, 2008], including in studies of tropical rainfall [*Gulizia and Camilloni*, 2014]. This study focuses on the historical experiment, and one model run is analysed for each model (r1i1p1).

Monthly and seasonal means (MAM, JJA, SON and DJF) of u and v winds, rainfall, specific humidity and sea-surface temperature (SST) from 17 models (Table 3.1; chosen to include dissimilar models) for the period 1971-2000 inclusive were computed from CMIP5 data which had been interpolated to a common grid-spacing of 1.875°x1.875°. Tests of the metrics used in this paper at model native resolution indicate that interpolation does not substantially change the results.

Reanalysis and observational data are also included as a point of comparison (Table 3.2). Reanalysis data has been interpolated to the same resolution as models. Native resolution is retained for the observational datasets. Observed SST data is taken from the HadISST.2 dataset [*Titchner and Rayner*, 2014].

3.3 Rainfall climatology

3.3.1 Annual cycle of rainfall

All observational and reanalyses datasets feature the expected semi-annual cycle of rainfall, with peaks in transition seasons MAM and SON (Figure 3.3). CRU, GPCC,

CMAP, NCEP, GPCP and TRMM feature peak MAM rainfall in April; ERAI is the only dataset to experience peak rainfall in March.

Table 3.1– CMIP5 models used in this study

Model	Institute	Native horizontal resolution	Reference
ACCESS1-3	Commonwealth Scientific and Industrial Research Organization and Bureau of Meteorology Australia (CSIRO-BOM)	1.25° × 1.875°	*Collier and Uhe* [2012]
BNU-ESM	College of Global Change and Earth System Science, Beijing Normal University	2.81° × 2.79°	*Ji et al.* [2014]
CanESM2	Canadian Centre for Climate Modelling and Analysis (CCCma)	2.81° × 2.79°	*Yang and Saenko* [2012]
CESM1-CAM5	National Centre for Atmospheric Research (NCAR)	1.25°x1.0°	*Neale et al.* [2012]
CMCC-CMS	Centro Euro-Mediterraneo per I Cambiamenti Climatici (CMCC)	1.87° × 1.87°	*Scoccimarro et al.* [2011]
CNRM-CM5-2	Centre National de Recherches Météorologiques / Centre Européen de Recherche et Formation Avancée en Calcul Scientifique (CNRM-CERFACS)	1.4° × 1.4°	*Voldoire et al.* [2011]
CSIRO-Mk3-6-0	Commonwealth Scientific and Industrial Research Organization in collaboration with Queensland Climate Change Centre of Excellence (CSIRO-QCCCE)	1.9° × 1.9°	*Jeffrey et al.* [2013]
GFDL-CM3	NOAA Geophysical Fluid Dynamics Laboratory (NOAA GFDL)	2.5° × 2.0°	*Donner et al.* [2011]
GFDL-ESM2G	As above	2.5° × 2.0°	*Dunne et al.* [2013]
GISS-E2-H-CC	NASA Goddard Institute for Space Studies (GISS)	2.5° × 2°	*Schmidt et al.* [2013]
HadGEM2-ES	Met Office Hadley Centre (MOHC)	1. 9° × 1.3°	*Jones et al.* [2011]
IPSL-CM5A-MR	Institut Pierre-Simon Laplace (IPSL)	2.50° × 1.26°	*Dufresne et al.* [2013]
MIROC5	Atmosphere and Ocean Research Institute (The University of Tokyo), National Institute for Environmental Studies, and Japan Agency for Marine-Earth Science and Technology (MIROC)	1.40° × 1.40°	*Watanabe et al.* [2010]
MIROC-ESM	As above	2.81° × 2.79°	*Watanabe et al.* [2011]
MPI-ESM-LR	Max-Planck-Institut für Meteorologie (MPI-M)	1.9° × 1.9°	*Marsland et al.* [2003]
MRI-ESM1	Meteorological Research Institute (MRI)	1.125° × 1.125°	*Yukimoto et al.* [2011]
NorESM1-M	Norwegian Climate Centre (NCC)	2.5° × 1.9°	*Bentsen et al.* [2013]

Table 3.2 – Definition and characteristics of reanalysis and satellite/gauge datasets used in this study

Dataset	Full name and Institute	Native horizontal resolution	Dates used	Reference
ERA-Interim	European Centre for Medium Range Weather Forecasts	0.7°×0.7°	1981-2010	Dee et al. [2011]
NCEP/NCAR	National Centers for Environmental Prediction (NCEP) and the National Center for Atmospheric Research (NCAR)	2.5°×2.5°	1971-2000	Kalnay et al. [1996]
CRU	Climate Research Unit, University of East Anglia (v3.10)	0.5°x0.5°	1971-2000	Harris et al. [2014]
GPCC	Global Precipitation Climatology Centre, Deutscher Wetterdienst, World Meteorological Organisation	0.5°x0.5°	1971-2000	Schneider et al. [2015]
CMAP	Climate Prediction Centre Merged Analysis of Precipitation, NOAA NCEP	2.5°×2.5°	1971-2000	Xie & Arkin [1997]
GPCP	Global Precipitation Climatology Project, World Climate Research Programme (WCRP)	2.5°×2.5°	1981-2010	Adler et al. [2003]
TAMSAT	Tropical Applications of Meteorology using Satellite data and ground-based observations, University of Reading	0.0375°×0.0375°	1983-2011	Maidment et al. [2014]
TRMM	Tropical Rainfall Measuring Mission, NASA Goddard Space Flight Center, Japanese Aerospace Exploration Agency	0.25°×0.25°	1998-2014	Huffman et al. [2007]

All models are able to broadly reproduce the annual distribution of rainfall, with peaks at MAM and SON (Figure 3.3). The majority of models (13/17) exhibit peak MAM rainfall in April; peak SON rainfall is in October (12 models) or November (5 models). All models agree on the month of boreal summer rainfall minimum (July), which is 1-2 months later than all observational and reanalysis datasets (except ERAI). Models place the DJF minimum in January (13/17) or February (4/17). The wettest monthly value features in October (MIROC5, 7.8 mm day^{-1}), with a second rainfall maximum in November (NorESM1-M, 7.8 mm day^{-1}). MAM peak rainfall is seen in April (MIROC5, 7.6 mm day^{-1}). The driest monthly value is in January

(CSIRO-Mk3-6-0, 0.9 mm day^{-1}). July features the lowest JJA value (MRI-ESM1, 2.3 mm day^{-1}).

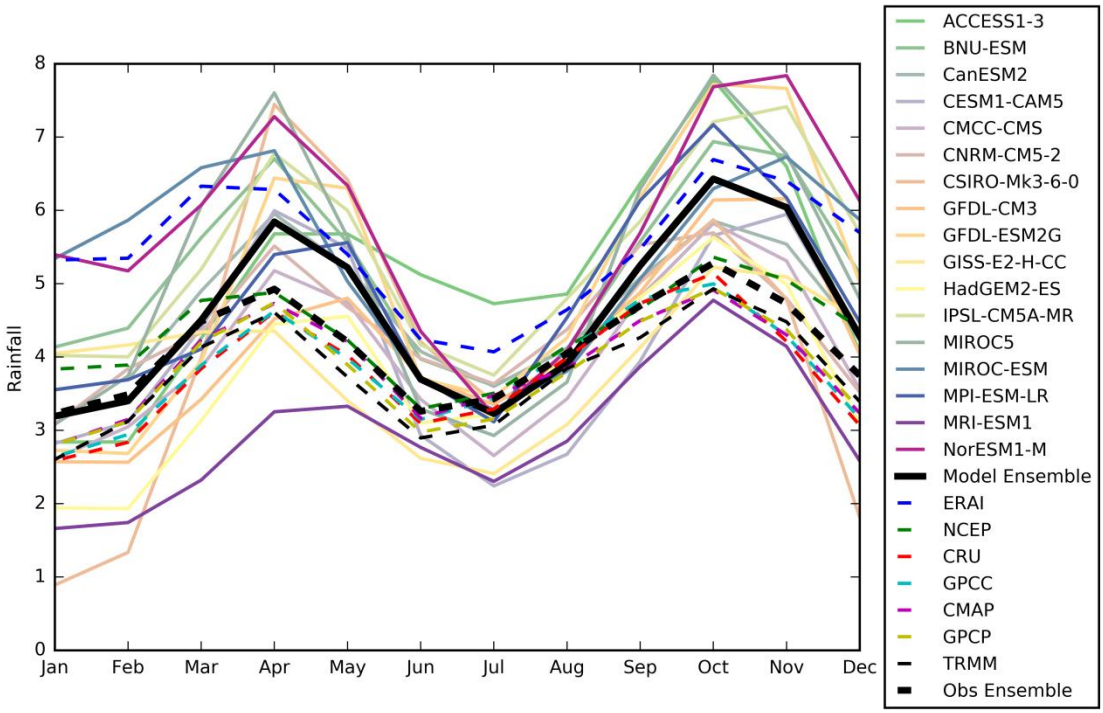

Figure 3.3 - 30 year mean rainfall (mm day^{-1}) for individual CMIP5 models, reanalysis and satellite data 1971-2000. The thick black line shows the ensemble of models; the dashed thick black line shows the ensemble of all observational and reanalysis datasets

Despite all models and datasets reproducing the semi-annual cycle of rainfall, there are large differences amongst annual cycles. The largest spread of absolute values occurs in November, where the difference between the wettest and driest dataset is 6.0 mm day^{-1} (standard deviation = 1.36 mm day^{-1}); this equates to 180 mm difference over the month. The smallest absolute range is seen in August (2.2 mm day^{-1}), and the smallest standard deviation in July (0.6 mm day^{-1}). In several cases, the dry season minimum of some models is wetter than wet season values for other models, and vice versa. For example, the JJA minimum in ACCESS1-3 (July, 4.7mm day^{-1}) is wetter than the MAM maximum in GISS-E2-H-CC (April, 4.4 mm

day^{-1}); NorESM1-M's DJF minimum (January, 5.4 mm day^{-1}) is 0.6 mm day^{-1} wetter than GFDL-CM3's MAM maximum (May, 4.8 mm day^{-1}).

3.3.2 Rainfall distribution

3.3.2.1 Wet seasons

To compare the spatial distribution of rainfall across datasets, long-term (30-year) means are plotted for central Africa across all seasons (Figure 3.4a). Models have been ordered dry to wet (reading left to right across Figure 3.4) based on mean rainfall magnitudes for that season. As expected from the wide variation in rainfall magnitudes, there are large differences in rainfall distribution between models. In MAM, drier models (e.g. MRI-ESM1, HadGEM2-ES, GISS-E2-H-CC) have much less rainfall over land than wetter models in the ensemble (e.g. NorESM1-M, MIROC5). Rainfall is focused on the Atlantic coast and over the Gulf of Guinea, leading to a western position of the rainfall maxima. In contrast, wetter models have much more rainfall in the east of the basin, and relatively less coastal rainfall. To highlight these differences, composites of the five wettest and five driest models are shown in Figure 3.5a, as well as difference plots. To indicate where there is strong agreement that the wet and dry composites differ, stipples occur for the following conditions: where 1) all wet model values are greater than the mean of dry model values and 2) where all wet model values are greater than the maximum value of dry models. Similarly, crosses indicate where 1) all dry model values are less than the mean of wet model values and 2) where all dry model values are less than the minimum value of dry models.

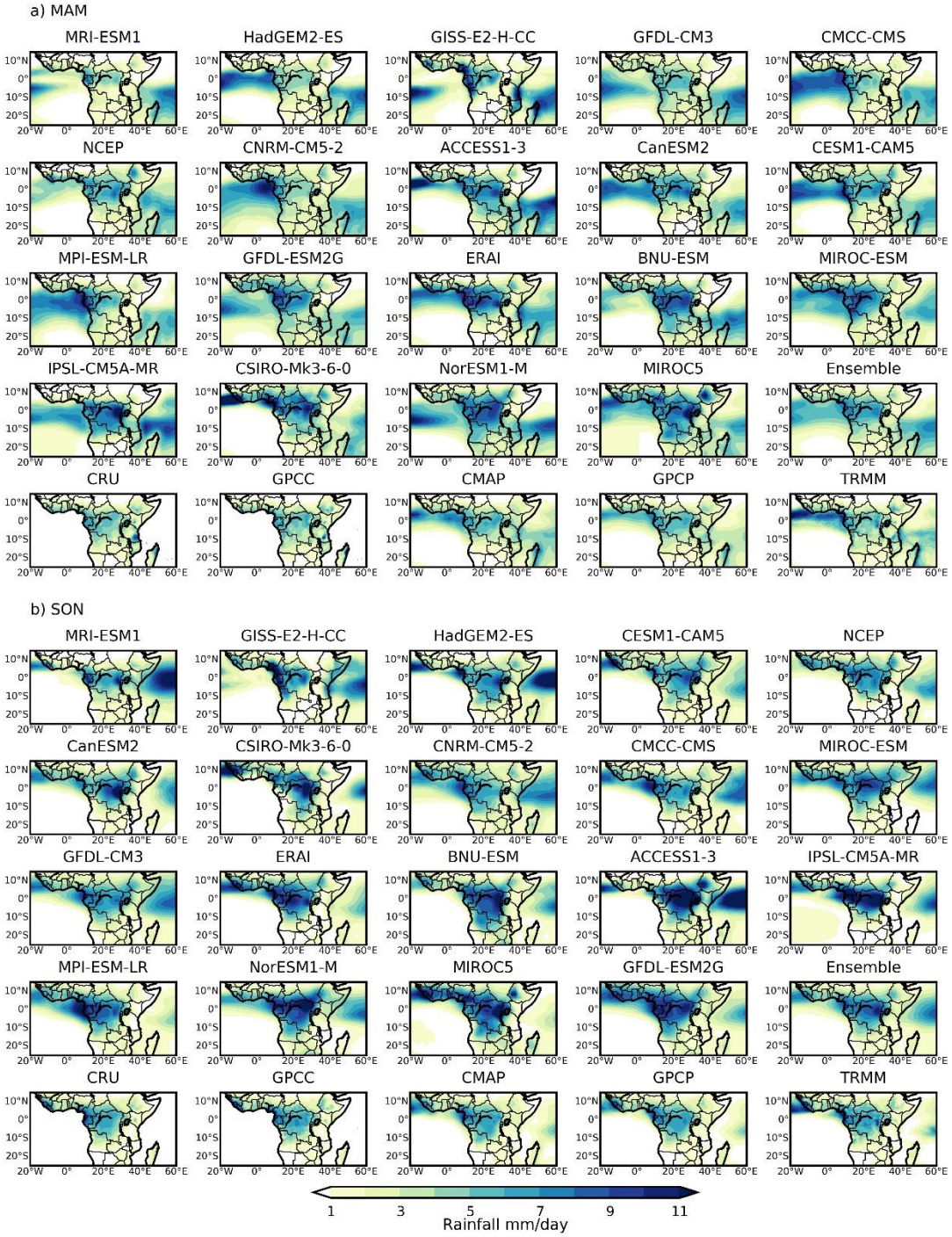

Figure 3.4 - Long term mean (1971-2000) rainfall (mm day-1) for a) MAM and b) SON for 17 CMIP5 models, the ensemble mean, reanalysis, gauge and satellite data sets. Models and reanalyses products are ordered from dry to wet (left to right, top to bottom) based on mean rainfall across the basin.

Figure 3.5a shows that the five wettest models produce an eastern maximum when composited, whereas the five driest show a western maximum (though smaller in magnitude). Wet models are on average 2-3 mm day^{-1} wetter over the whole of the

Congo Basin, with significant differences particularly in the centre and east of the domain (Figure 3.5a). Dry models are significantly drier over a large portion of the domain based on both agreement metrics and the area of agreement extends further north than for wet agreement. This suggests that dry models are more consistently dry than wet models in the wider region. Models in the middle of the distribution do not fall into such obvious distributions; some have more easterly rainfall (BNU-ESM), some more westerly (MIROC-ESM), and some have several, spatially disconnected areas of high rainfall (CSIRO-Mk3-6-0). Reflecting these stark differences amongst models, the ensemble mean features a reasonably uniform distribution across the domain. In addition to differences over land, there are also significant differences in rainfall over the oceans. Wet models are wetter in the north west Indian Ocean, but drier over the south west Indian Ocean and the south west Atlantic. This points to a possible influence of model sea surface temperatures (SSTs) on rainfall in this region; this is discussed further in Section 3.6.

The second wet season SON also features obvious differences amongst models (Figure 3.4b). Dry models tend to feature more of their rainfall along the Atlantic coast, as in MAM, although there is less rain over the ocean than in MAM. The majority of models also feature an area of rainfall maxima in the east; this intensifies along the spectrum of dry to wet models. The wettest models have high rainfall across the whole of the basin. Figure 3.5b shows that the distribution in the composites is quite similar, with higher intensity rainfall in the wet models. Dry models tend to have two, relatively weaker maxima, whereas wet models have one

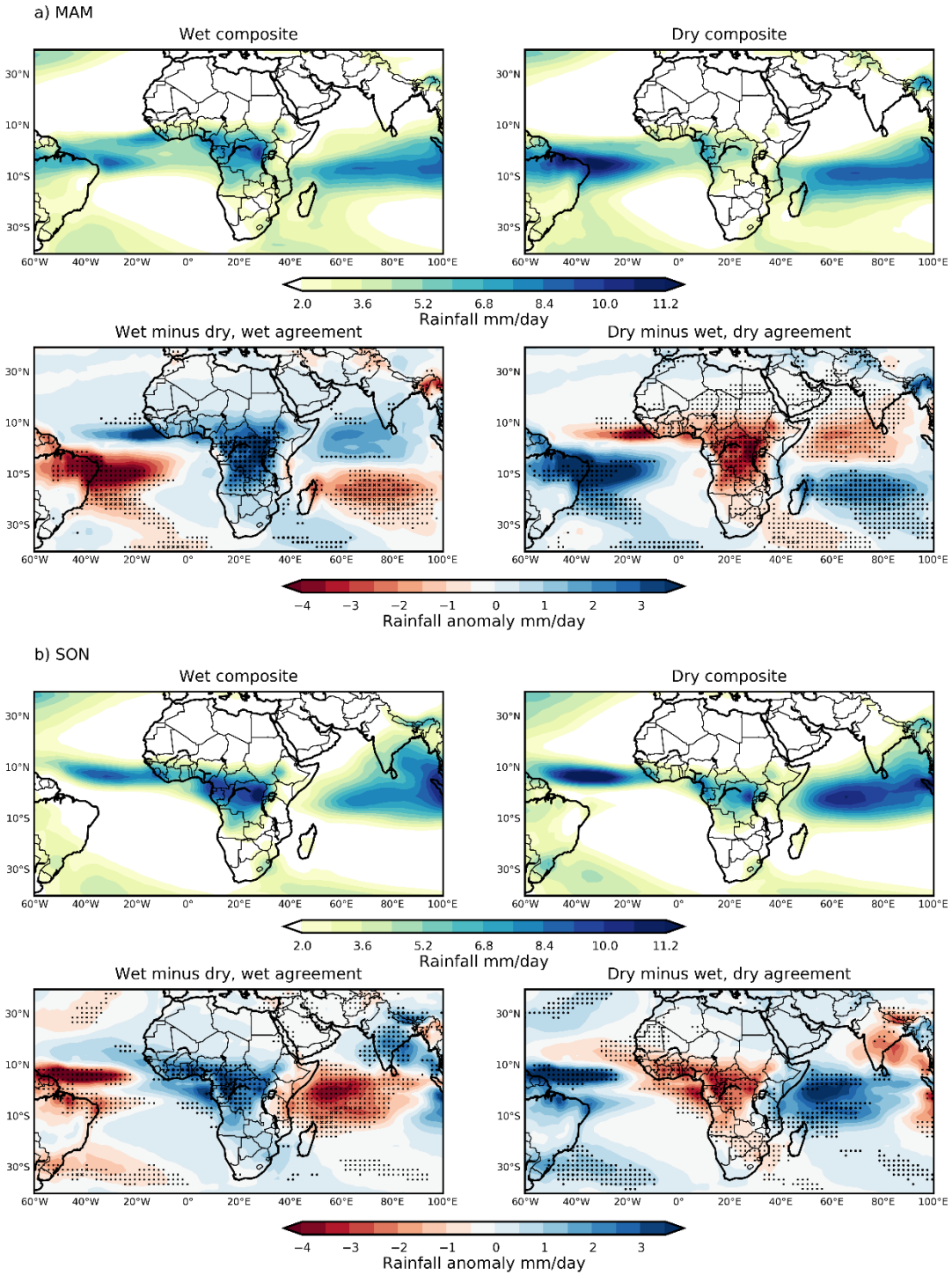

Figure 3.5 - For long-term mean (30-year) rainfall (mm day -1) (a) MAM and (b) SON: composite of five wettest models in Figure 4 (top left); composite of five driest models in Figure 4 (top right); wet composite minus dry composite with stipples for agreement, (bottom left); dry composite minus wet composite, with stipples for agreement (bottom right). Large circles (crosses) indicate that all wet (dry) models are wetter (drier) than the maximum (minimum) of the dry (wet) models at that gridpoint. Small circles (crosses) indicate that all wet (dry) models are wetter (drier) than the mean of the dry (wet) models at that gridpoint.

strong maxima in the east that extends zonally across the basin. The land/ocean precipitation difference is starker than in MAM; wet models (over land) are significantly drier in the western-central Indian Ocean than drier models. Again, this indicates that local SSTs may be one factor influencing model rainfall differences.

3.3.2.2 Dry seasons

The magnitude and distribution of dry season Congo rainfall is important to global and regional processes [*Malhi et al.*, 2013], in particular the climatological regulation of the rainforest. As expected, in JJA the zone of tropical convection shifts northwards from its position in MAM; this is evident in all models (Figure 3.6a). Distributional differences are not as obvious as in the wet seasons; all models show a clear western rainfall maximum in the north-west corner of the domain. Several also feature a second rainfall maximum in the north east corner of the basin; this is stronger in the wettest models, and less evident or non-existent in the drier models (e.g. GISS-E2-H-CC, CESM1-CAM5). Differences between the wet and dry composites are significant over this zonal region (Figure 3.7a). Differences over the adjacent oceans are not as significant as in the wet seasons.

In DJF, the band of tropical convection has shifted southward, and most models feature the majority of their rainfall over land and in the central Indian Ocean (Figure 3.6b). In the wettest models (MIROC-ESM, NorESM1-M) the area of rainfall extends northward beyond the equator; in the dry models, it is limited to the

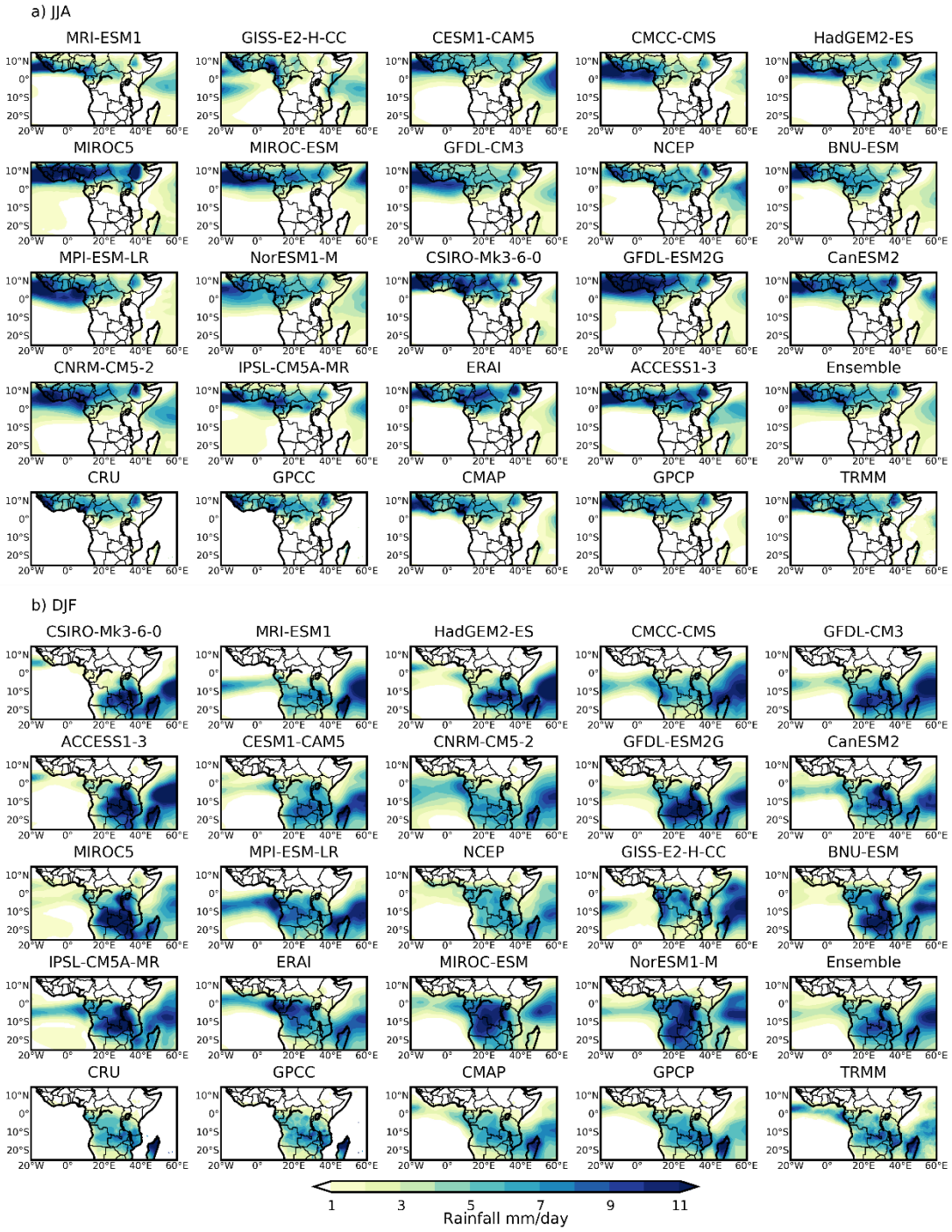

Figure 3.6 - As for Figure 3.4 but for (a) JJA and (b) DJF

region below 5°S, reducing the amount of rainfall in the defined Congo Basin domain. There is not a distinct east/west distinction between wet and dry models (Figure 3.6b); however, some have a more westerly distribution (e.g. CNRM-CM5-

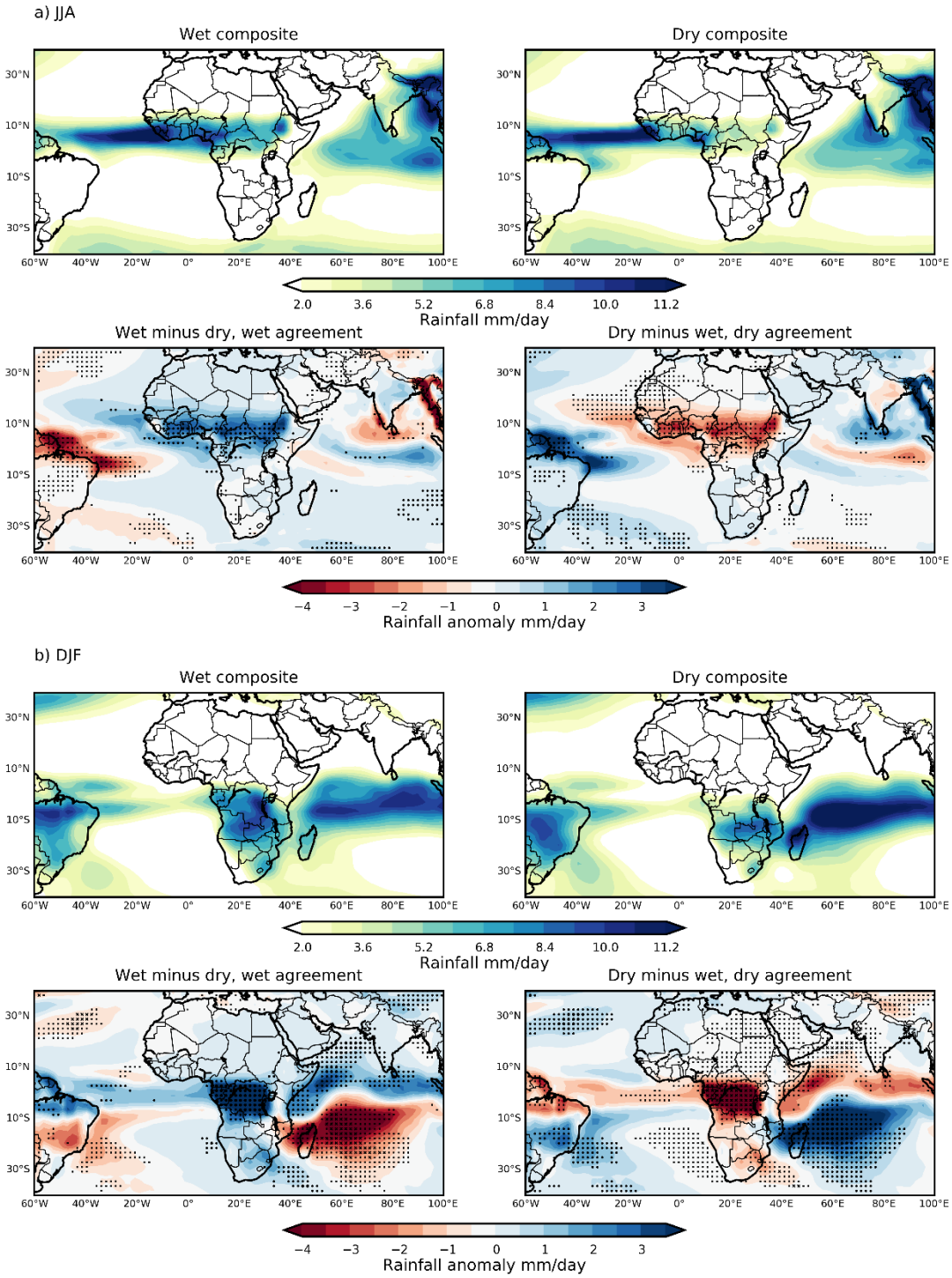

Figure 3.7- As for Figure 3.5 but for (a) JJA and (b) DJF

2, ERAI). The difference in rainfall magnitude between wet and dry models is the largest for any season, exceeding 3mm across the majority of the domain. As in MAM, dry models are more consistently dry across the wider African region, as

noted by the wider expanse of stipples, and there is a dipole in rainfall over the Indian Ocean: wet models are wetter in the north west Indian Ocean and drier in the south west Indian Ocean. As in all seasons, the ensemble mean does not agree with any one model.

3.3.2.3 Seasonal comparisons

Figures 3.4-3.7 indicate some distinct patterns in the organisation of rainfall amongst models. Figure 3.8 quantifies the similarities between models across seasons, showing that models tend to be wet or dry across all seasons (r=0.702). There is also a significant ($p<0.05$) positive relationship between rainfall in MAM and SON (r=0.743), MAM and JJA (r=0.485), MAM and DJF (r=0.561), SON and JJA (r=0.625) and SON and DJF (0.499). The only seasons where the relationship is not significant is between JJA and DJF; this is perhaps expected as rainfall in the northern- and southernmost part of the domain is influenced by different large- and regional-scale systems. Nevertheless, when taken as a whole it is clear that models have a tendency to be generally wetter or drier, regardless of season. This is reinforced by Figure 3.9, which shows the average rank (dry to wet) for each model and the range in ranks that model populates for the wet seasons (3.9a), the dry seasons (3.9b) and all seasons (3.9c). In wet seasons, the three driest models on average (indicated by the order of the models) rank consistently in that position in both MAM and SON. Similarly, three of the four wettest models are consistently wet. The story is somewhat similar in the dry seasons. There is greater spread in ranks across all four seasons, but at the extreme ends the error bars remain

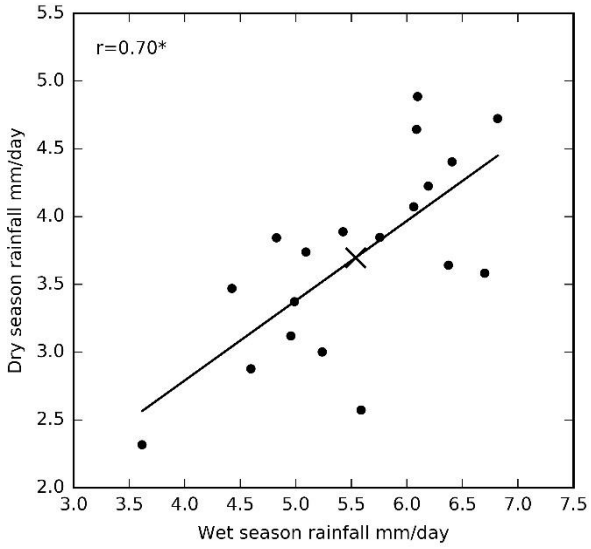

Figure 3.8 - Relationship between the long-term mean (30-year) rainfall (mm day^{-1}) in the wet seasons (MAM and SON mean) and dry seasons (JJA and DJF mean) for individual datasets.

smaller. Of particular note is MRI-ESM1-M, which is consistently ranked the driest or second-driest in all seasons.

3.4 Moisture flux convergence

In light of the disparities in rainfall magnitude and distribution between models, and given the paucity of observed rainfall data with which to confront models, alternative strategies must be adopted to assess model climatology and establish processes of importance for the Congo region. It follows that, given the importance of the CMIP5 dataset in the development of future climate projections, such a process-based analysis may turn out to be crucial in isolating climate projections which are based on realistic representations of the present climate.

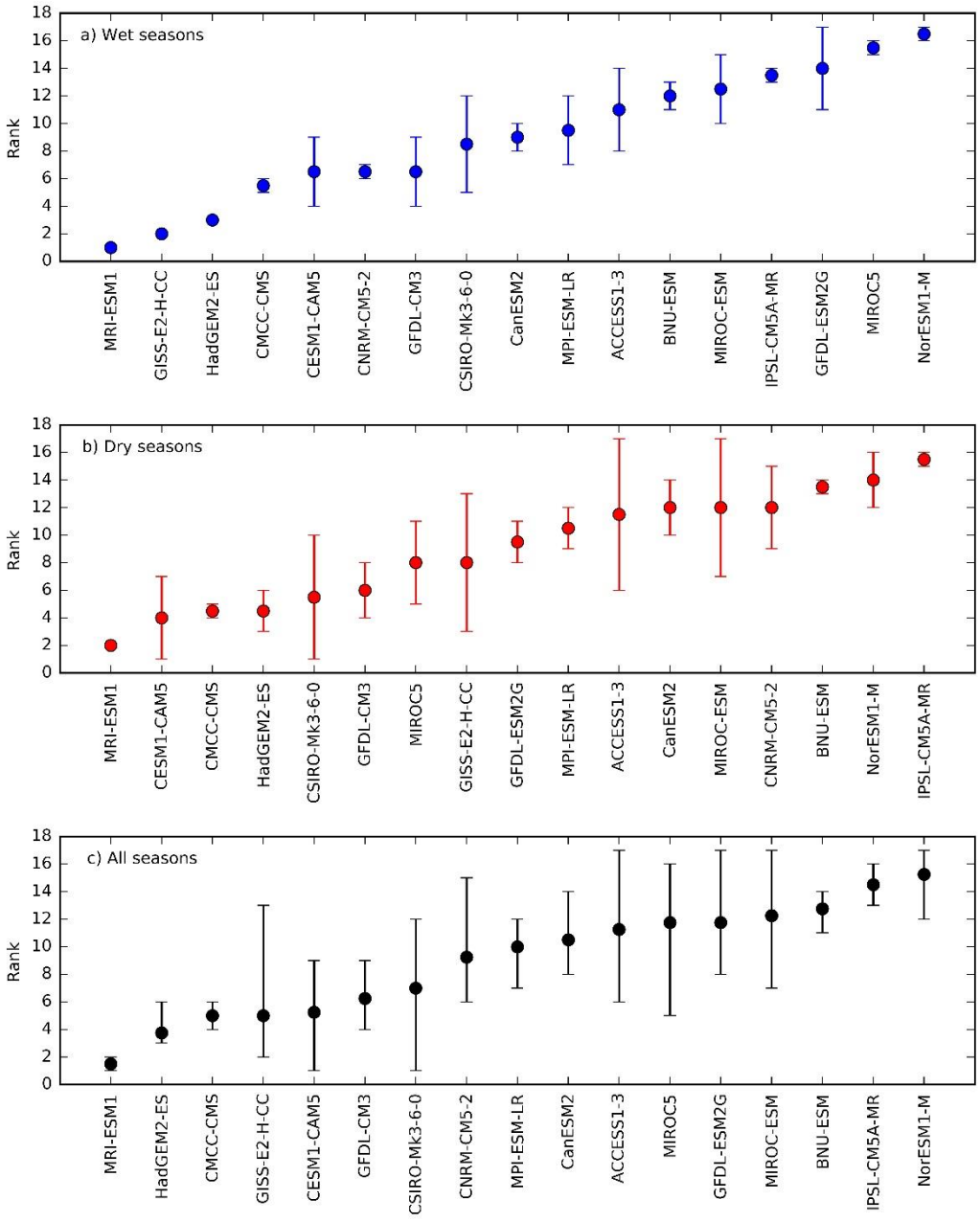

Figure 3.9 - Average long-term mean (1971-2000) rainfall rank of CMIP5 models and reanalysis data sets for (a) wet seasons (MAM and SON), (b) dry seasons (JJA and DJF) and (c) all seasons. Rank 1 is the driest model; rank 17 is the wettest model. Circle denotes the mean rank. Solid lines denote the range in ranks each model occupies for the subset of seasons.

Moisture flux (qflux) convergence is a key aspect of the hydrological cycle in tropical regions [*Burde et al.*, 1996; *Pokam et al.*, 2012]. Previous research

indicates the magnitude, location and height of qflux convergence is related to rainfall [*Washington et al.*, 2013; *Yin et al.*, 2013] and could help establish the credibility of particular models or model groups. These studies suggest that relatively wet (dry) models may experience higher qflux convergence (divergence) than drier (wetter) models at particularly levels, related to branches of the large-scale and regional-scale circulations. If the same can be established for the Congo, the credibility of individual model rainfall could be assessed with reference to moisture flux climatology, which, as a dynamic field rather than a highly parameterised one, is a better constrained variable in the models than rainfall. Thus far research has focussed on this relationship in wet seasons in the Congo in reanalyses. The following section assesses the relationship between rainfall and qflux convergence for all seasons across the CMIP5 ensemble.

3.4.1 Relationship to rainfall

Long term seasonal means were calculated for qflux convergence over the domain 5°E to 35°E and 10°S to 10°N, at 700 hPa and 850 hPa. Individual levels are chosen, as opposed to column-integrated moisture flux convergence, following *Pokam et al.*, [2012], who determined that the wet seasons feature strong moisture flux convergence at these particular levels, and that flux at these levels appears strongly related to branches of both the local- and large-scale circulation. Moisture flux convergence is given by $qconv = -1.\left(\frac{dqu}{dx} + \frac{dqv}{dy}\right)$. Thus positive (negative) values denote qflux convergence (divergence).

The relationship between mean qflux convergence and rainfall at 700 and 850 hPa for the model ensemble is shown in Figure 3.10. Due to large amounts of missing data at 850hPa, CSIRO-Mk3-6-0 is excluded from the analysis at this height. All seasons feature positive correlation with rainfall at both 850hPa and 700hPa such that wetter (drier) models in the ensemble are characterised by higher convergence (divergence); the only season in which it is not a significant relationship is JJA at 700hPa (9b, red). The strongest overall correlation is in DJF at 850hPa (r=0.809), though is it also highly significant at 700hPa (r=0.792). JJA and SON also feature their strongest positive relationship at 850hPa (r=0.662 and r=0.707 respectively); the latter of which concurs with the finding of *Pokam et al.* [2012] that this pressure level is where moisture convergence most influences rainfall in SON. MAM is the only season to have its strongest relationship with

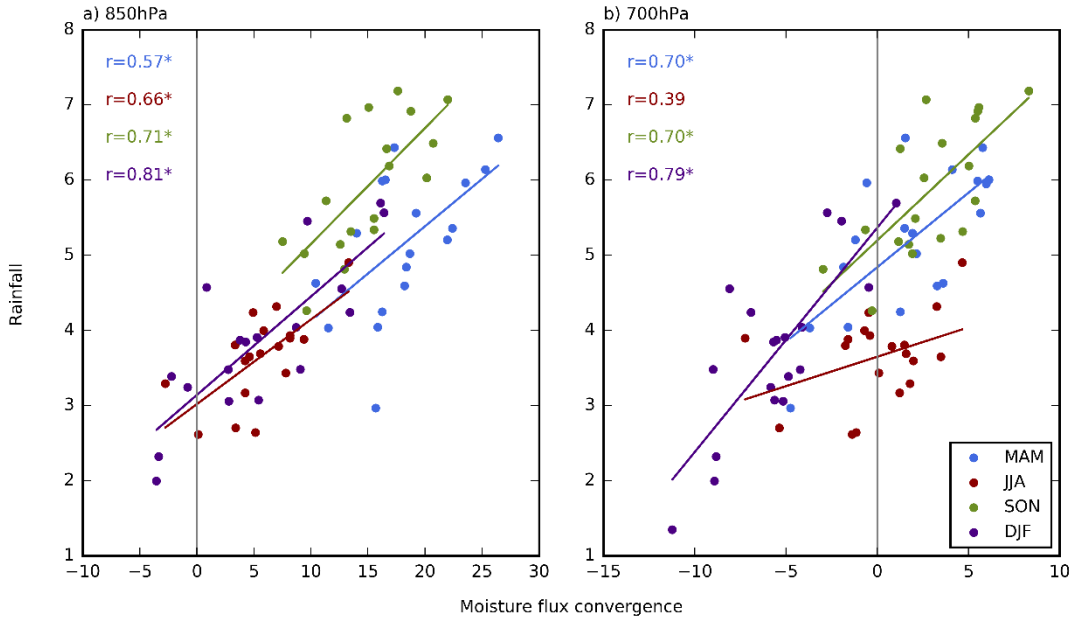

Figure 3.10- Long-term mean (1971-2000) moisture flux divergence (10^8 kg kg^{-1} s^{-1}) and rainfall (mm day^{-1}) at (a) 850hPa and (b) 700hPa for CMIP5 models and reanalyses data

rainfall at 700hPa (r=0.703); also in agreement with *Pokam et al.* [2012]. As expected, models are mostly convergent at 850hPa, whilst at 700hPa the spread of models straddles convergence and divergence. At 700hPa models in SON have slightly higher convergence and rainfall than MAM, which may account for the tendency of SON to be slightly wetter than MAM.

The qflux convergence metric combines wind convergence, in situ specific humidity (q) and moisture advected from surrounding regions [*Pokam et al.*, 2012]. To confirm qflux convergence is more closely linked to rainfall than u, v and q individually, similar correlation analysis is conducted for each constituent component (Table 3.3). At 850hPa the combined role of specific humidity and wind convergence (qflux convergence) exhibits the strongest and most significant relationship with rainfall in all seasons. At 700hPa, MAM, SON and DJF also show the strongest relationship between rainfall and qflux convergence, whilst JJA only features a significant relationship with wind convergence. As a dry season this might be expected, as levels of q are much lower. It should be noted that in SON and DJF the correlation between rainfall and qflux convergence and rainfall and wind convergence are very similar, and thus may not be statistically significant. This may suggest that in these seasons, the dynamical circulation also plays a critical role in determining rainfall. These findings reinforce the importance of analysing both qflux convergence and the wind circulation as potential controls on rainfall at these heights.

Table 3.3 – Correlation (r-value) between model Congo Basin rainfall and a) specific humidity, b) wind convergence and c) qflux convergence at 850hPa and 700hPa, in the long term mean. * denotes significance at 95%. Bold indicates the highest correlation coefficient for each season and pressure level.

	850hPa			700hPa		
	q	**wind conv**	**qflux conv**	**q**	**wind conv**	**qflux conv**
MAM	0.22	0.33	**0.57***	0.33	0.62*	**0.70***
JJA	-0.07	0.58*	**0.66***	0.09	**0.49***	0.38
SON	-0.006	0.69*	**0.71***	-0.07	0.64*	**0.70***
DJF	0.75*	0.68*	**0.81***	0.57*	0.78*	**0.79***

3.4.2 Wet and dry model differences

Figure 3.11 shows the difference in long term (30 year) mean qflux convergence between the five wettest and driest models in each season, overlain with the difference (wet minus dry) vectors of qflux. Only significant vectors (based on the agreement metric) are shown. Comparison with wet and dry model composites (Supplementary materials, Figure 3.S1a) allows an understanding of the direction of difference between the two subsets of models. In MAM at 850hPa (Figure 3.11a), wet models feature more convergence over the majority of the basin than dry models, although dry models experienced greater convergence in the north west corner of the domain (which is the location of maximum rainfall in dry models, as seen in Figure 3.5a). The causes of this difference in overall convergence appear twofold: first, wet models experienced greater qflux from the eastern boundary of the basin (from the Indian Ocean); second, wetter models feature influx on the western boundary of the basin between 0° and 5°N, whereas dry models feature

outward flow at this boundary. In wet models this inward flux is due to the re-curvature of air as it crosses the equator; this does not feature in dry models

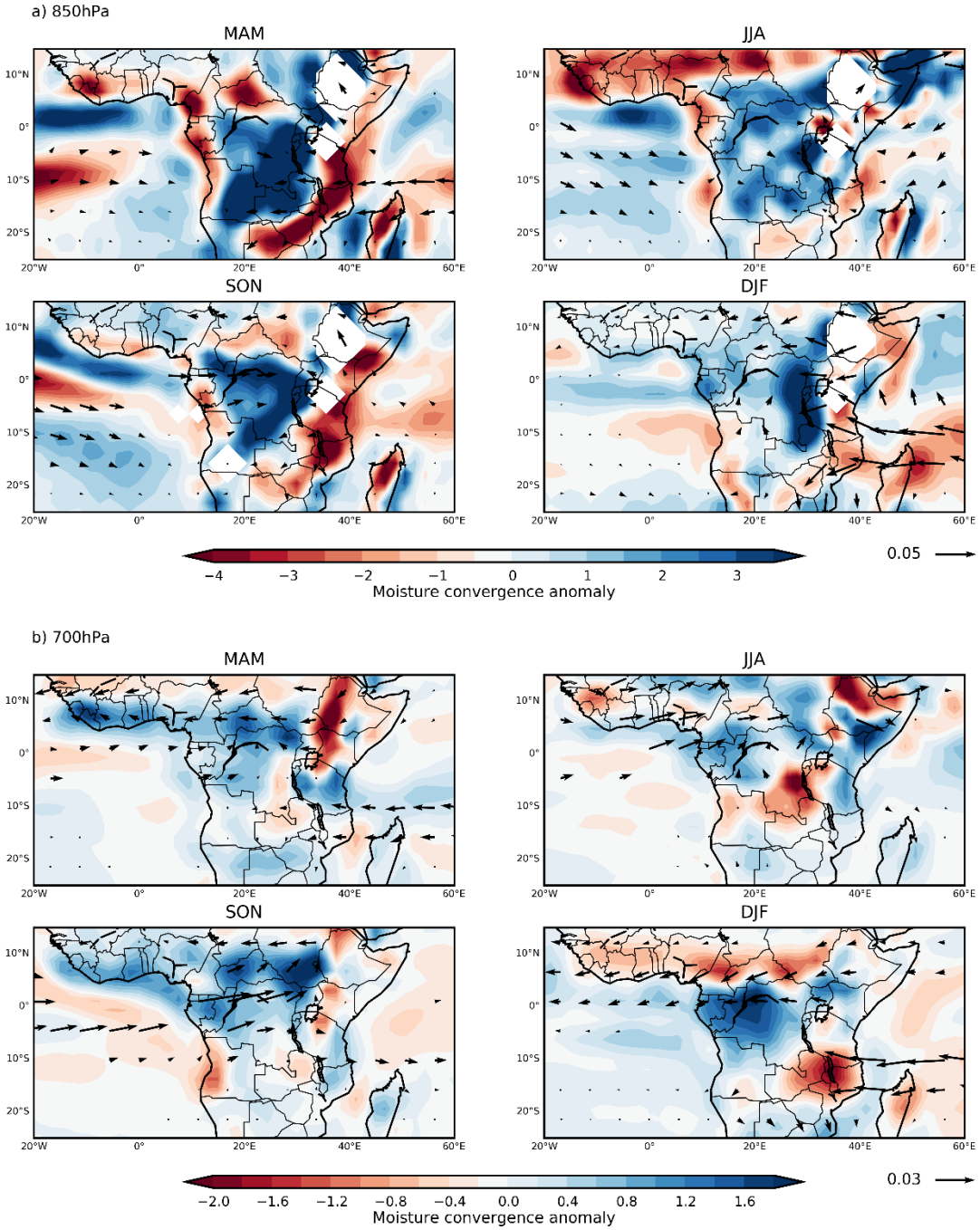

Figure 3.11 - For (a) 850hPa and (b) 700hPa: Difference in moisture flux convergence (shaded; 10^8 kg kg^{-1} s^{-1}) and moisture flux (vectors; kg kg^{-1} m s^{-1}) between composite of five wettest and five driest models in each season. Only vectors which are significantly different between the wet and dry ensembles (using the agreement metric described in Section 3.2.3) are shown

(Supplementary materials, Figure 3.S1a). A similar pattern is evident in SON, where greater influx is evident at the western boundary. In both wet seasons, wet models also feature higher divergence than dry models in the far east of the basin.

At 700hPa strong differences remain between wet and dry models (Figure 3.11b). In MAM, SON and JJA wet models feature anomalous inflow at the western boundary of the basin; the composites show this is due to less moisture-laden air leaving the basin in wet models than dry (Supplementary materials, Figure 3.S1b).

This results in greater convergence over the basin in wet models. In DJF, wet models feature increased influx from the eastern boundary, whereas dry models feature significant outflow towards the south-east of the basin.

3.5 Spatial limits to the convergence-rainfall relationship

3.5.1 Location of convergence maxima

Section 3.3.2 highlights the distinct east versus west rainfall distributions that characterise many models. If local convergence is a controlling factor on the location of rainfall we might expect the rainfall and convergence maxima (at important levels) to co-locate. To this end, Figures 3.12 and 3.13 show the location of the top 20% of rainfall values (blue) and convergence (red), with areas of overlap of the distributions highlighted (pink). The location of the maximum value is designated by a star (rainfall) and a cross (convergence). The pressure level at

which each season featured the highest correlation is shown (850hPa for MAM and SON, 700hPa for JJA and DJF; other heights are shown in Supplementary materials, Figures 3.S2 and 3.S3).

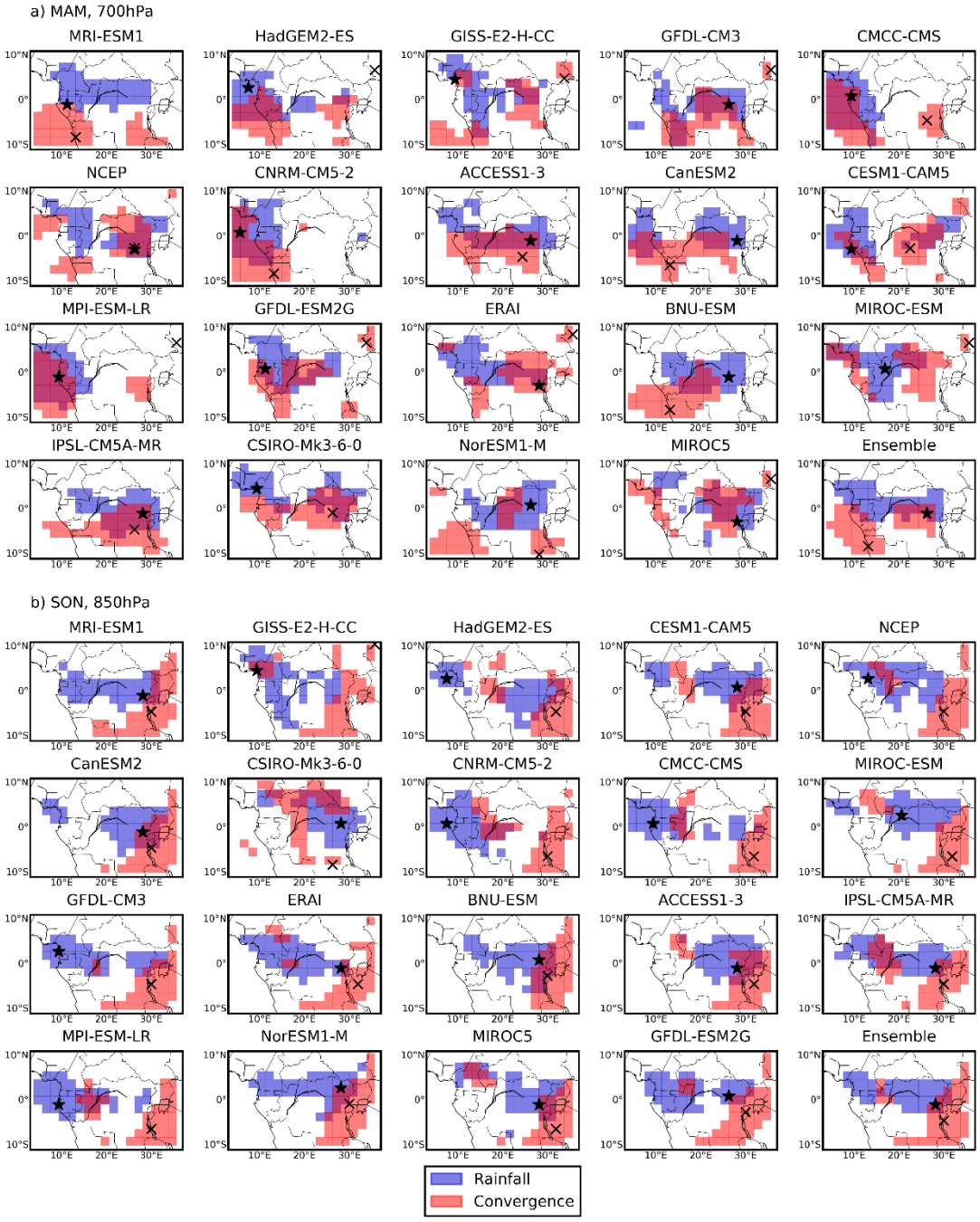

Figure 3.12 - Location of top 20% of rainfall values (blue), moisture flux convergence values (red), and areas of overlap (pink) in (a) MAM at 700hPa and (b) SON at 850hPa. The location of maximum rainfall (convergence) is denoted by a star (cross)

Most models feature some overlap between the location of top 20% of rainfall and convergence. Several datasets in MAM at 700hPa (e.g. MIROC5, ACCESS1-3, NCEP, IPSL-CM5A-MR) (Figure 3.12a) show large areas of overlap on land, and the maximum value of each are very close. Others show less significant overlap, but still co-locate the maxima (e.g. ERAI). There is no distinct pattern however between models which do and do not co-locate. This is affirmed by a correlation analysis on both the latitudinal and longitudinal locations of the maxima, which shows insignificant relationships at both heights for MAM. Nevertheless, five datasets feature very similar locations of rainfall and convergence maxima. In SON (Figure 3.12b) three of the same datasets show co-locating maxima (ACCESS1-3, IPSL-CM5A-MR and ERAI), in addition to MRI-ESM1 and CSIRO-Mk3-6-0. There also appears to be broader agreement in the general location of the top 20% values, with larger areas of overlap than in MAM.

For the dry seasons it must be noted the boundaries of the chosen domain (10°N and 10°S) bisect the zone of tropical convection. This could influence the location of maximum rainfall and convergence, depending on the latitudinal extent of the rainfall band in each model. In JJA at 850hPa (Figure 3.13a), there are two broad zones of rainfall maxima in most models, so a secondary maximum (smaller star) is plotted as well. There is very little agreement between the location of either rainfall maxima, which tend to be in the north-west and north-central zones of the domain respectively, and the convergence maxima, which is in the east-central zone of the domain. These patterns are quite consistent across models and do not seem to be related to the relative wetness or dryness of the model. In DJF at 850hPa (Figure 3.13b) eight models feature near-co-location of maxima, in the

south eastern quarter of the domain. These all span the wetter half of the models; near-co-location does not occur in any of the eight driest models.

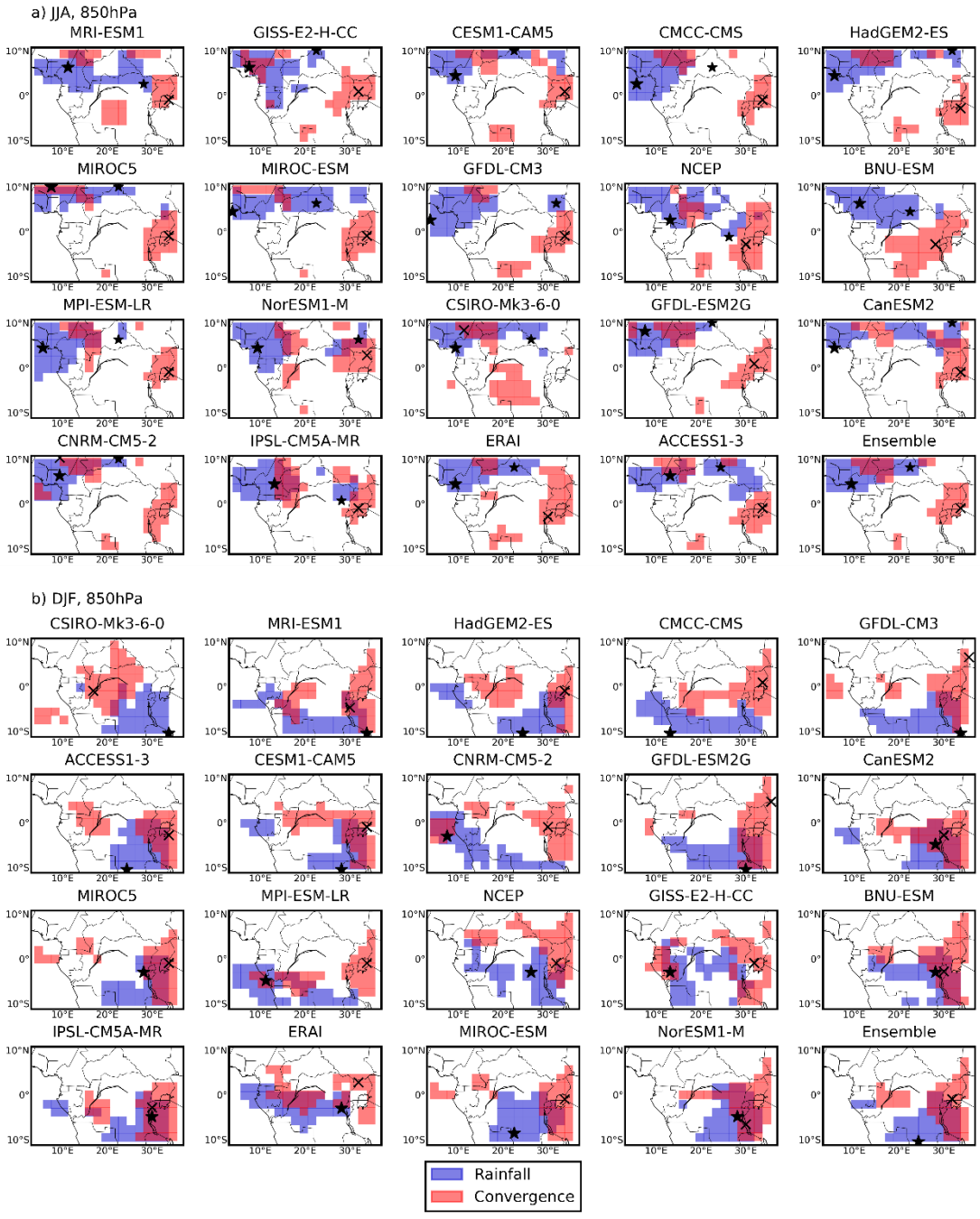

Figure 3.13 - As for Figure 3.12 but for (a) JJA at 850hPa and (b) DJF at 850hPa

3.5.2 Spatial limits at the subdomain scale

Section 3.5.1 indicates that the relationship between rainfall and convergence amongst models is strong at the basin scale. This section further quantifies the spatial limits of this relationship by testing its significance in the four subdomains (north west (5°E, 20°E, 0°, 10°N), north east (20°E, 35°E, 0°, 10°N), south west (5°E, 20°E, 10°S, 0°) and south east (20°E, 35°E, 10°S, 0°)).

3.5.2.1 Wet seasons

At the domain scale, MAM features the strongest positive relationship at 700hPa (r=0.703). This is dominated by relationships in the north east and north west

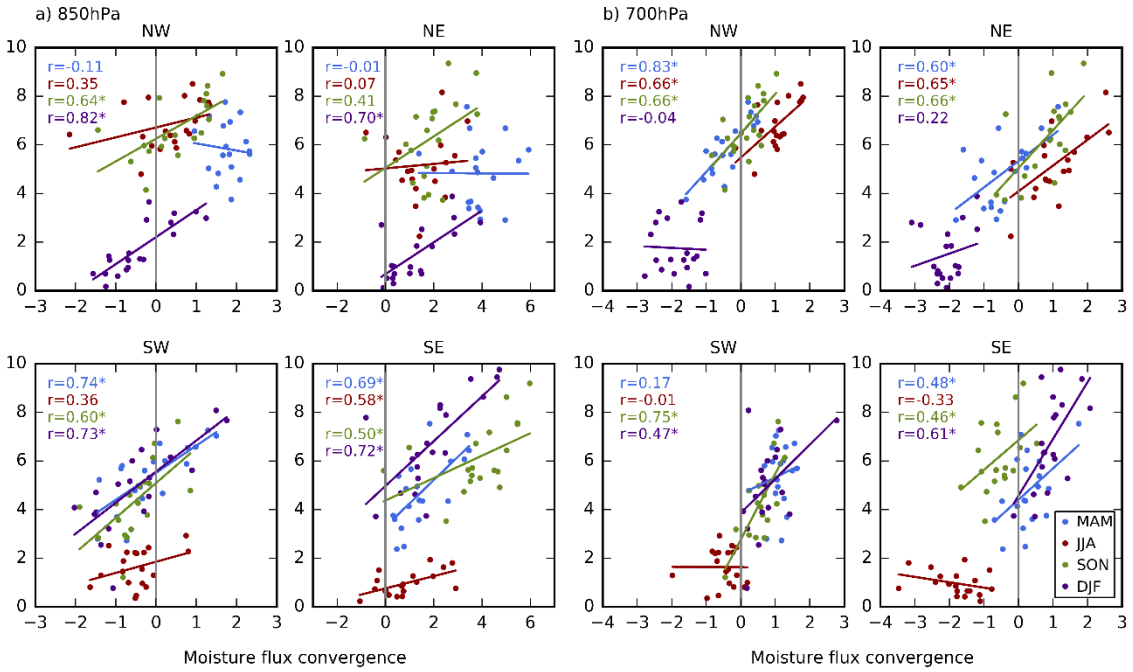

Figure 3.14 - Relationship between long term mean (1971-2000) moisture flux convergence (10^8 kg kg^{-1} s^{-1}) at (a) 850hPa and (b) 700hPa and rainfall (mm day^{-1}) for CMIP5 models, ensemble mean and two reanalysis data sets in: the north west (top left); north east (top right); south west (bottom left); and south east (bottom right)

subdomains, with a smaller but still significant relationship in the south east (Figure 3.14b). Figure 3.14b indicates that the northern half of the domain is dominated by divergence in this season. Thus the overall relationship at 700hPa appears to be dominated by a more divergence/less rainfall relationship. At 850hPa, the domain-scale positive relationship (r=0.573) is dominated by strong correlation in the south west and south east subdomains (Figure 3.14a), the latter of which is dominated by convergence.

At the most significant height (850hPa) in SON, the overall positive relationship (r=0.707) is dominated by the western domains, with a smaller but significant relationship in the south east. The largest r-value, and the greatest gradient of the correlation relationship is in the north west, which overwhelmingly features convergence. This supports the findings in Section 3.4.2, which show that wetter models feature much greater flow into the western half of the basin than dry models (Figure 3.11b), contributing to greater convergence in this region. The south west features divergence in most models; this is a well-defined feature in the south west coast in all individual climatologies at this height (Figure 3.S1). At 700hPa, all subdomains experience a significant relationship between rainfall and qflux convergence (Figure 3.14b). Unlike in MAM, the two northern domains exhibit predominantly convergence, whereas the south east domain, which exhibits the weakest (though still significant) relationship, is dominated by divergence. The largest r-value, and the greatest gradient of the correlation relationship is in the south west of the domain, which overwhelmingly features convergence. This supports the findings in Section 3.4.2, which show that wetter

models feature much greater flow into the western half of the basin than dry models (Figure 3.11b), contributing to greater convergence in this region.

3.5.2.2 Dry seasons

Both dry seasons feature their strongest domain-scale relationship at 850hPa. JJA only features a significant positive relationship in the south east at this height (r=0.582) (Figure 3.14a). Models here are mostly convergent, but weakly so relative to all other seasons and still experiencing very low rainfall totals. At 700hPa, JJA experiences strong positive correlation in the two northern domains, which are the wet, convergent regions in this season. However, it does not feature a significant relationship at 700hPa for the whole domain; this suggests that the relationship is spatially limited to the zone of tropical convection in the northern half. This may mean that the relationship in JJA is less useful when determining differences between models in the southern half of the basin; a region in which rainfall is already marginal in this season.

In DJF at 850hPa, strong positive relationships are found in all subdomains (Figure 3.14a). In the eastern two subdomains these are dominated by convergence. The south east domain is also where several wet models feature their maxima of both rainfall and convergence (Figure 3.13b). In the western domains the models are split between average divergence and convergence. At 700hPa DJF only exhibits significant relationships in the two southern domains, in particular in the south east. This affirms the important role of flux into the basin from the Indian Ocean, as

shown in Figure 3.11b. In the northern domains there is no relationship between qflux and rainfall. This concurs with the pattern seen in JJA; at 700hPa, the relationship is dominated by the region under the band of tropical convection, whereas the dry, divergent regions of the domain do not feature a relationship between the two.

3.6 Origin of Water Vapour Transport

3.6.1 Direction of water vapour transport into the basin

The preceding sections indicate that while the relationship between qflux convergence and rainfall is significant at the domain scale, there are particular regions which contribute most to the total amounts of convergence or divergence in the region. It thus follows that particular branches of the larger regional circulation may be more or less influential depending on the season and height, and, if these can be identified, could be used to further constrain model rainfall values. In the long term, this relationship could lend itself to an observational campaign on the fringes of the Congo. Whilst long-term monitoring of rainfall within the basin itself is difficult, given its remoteness and the political tensions in the region, it remains a possibility that observing dynamical fields such as qflux as it enters the basin may serve as a way of constraining climate models.

To that end, the average gridbox moisture flux into the basin is calculated over all four boundaries: north (10°N); south (10°S); east (35°E); and west (5°E). This is

correlated with rainfall over the basin, and the results are shown schematically in Figure 3.15a (where large arrows indicate significant relationships). Figure 3.15b shows the latitude/longitude-height cross-section of these correlations for significant boundaries.

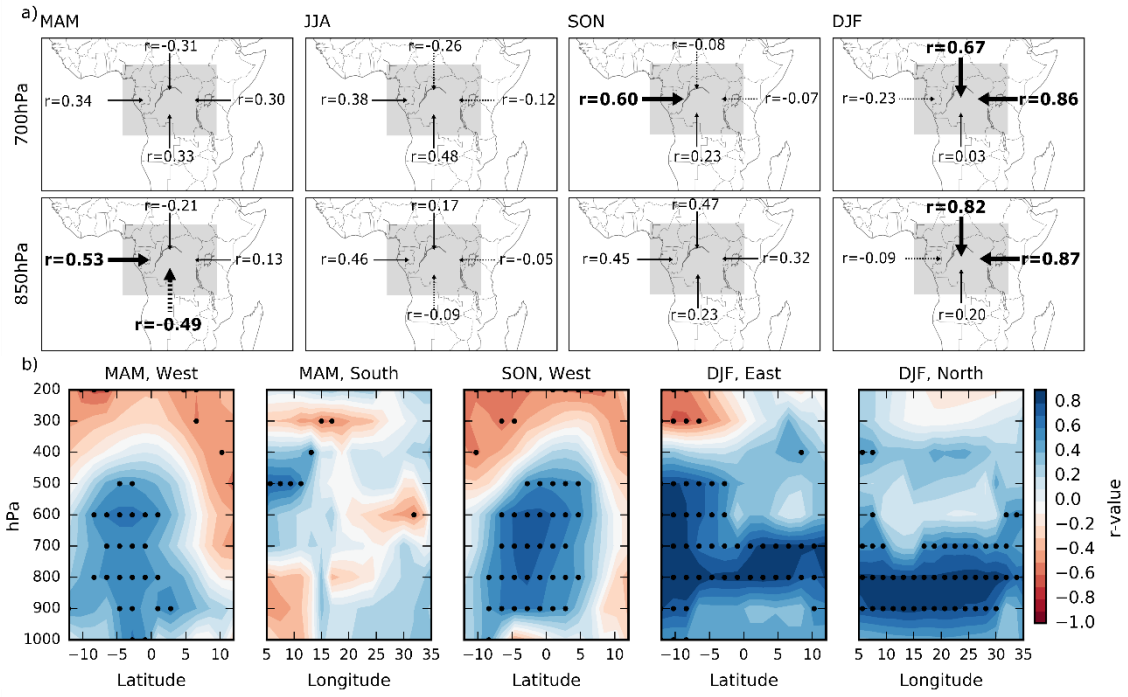

Figure 3.15 – (a) Schematic showing the correlation coefficient between long-term mean rainfall over the basin and moisture (qflux) entering the basin across the northern, eastern, southern and western boundaries at 850hPa and 700hPa. Large arrows and bold text denotes r-values significant at the 95% level. Dashed arrows indicate a negative relationship. (b) Latitude/height and longitude/height cross-sections for flow across boundaries which feature significant correlations. Individual vertical grid locations which feature significant correlations are stippled.

At 850hPa in MAM there is a significant relationship between moisture entering the basin from the west and rainfall. This affirms previous results suggesting that the re-curvature of air at the equator is greater here for wet models than dry models in MAM (Supplementary materials, Figure 3.S1a); therefore, wetter models receive greater inflow across this boundary. Figure 3.15b highlights the dominant

role of low-to-mid level flow. There is also a negative correlation at the southern boundary, whereby models receiving greater flux over this boundary experience less rainfall. This could be a result of stronger southeasterly flux in dry models, which leaves the basin via the eastern boundary and experiences less convergence than in wet models (Figure 3.S1). At 700 hPa, no boundaries feature a significant positive relationship. However, analysis of individual model values (not shown) suggests that there are two extreme outliers that are disproportionately impacting the relationship in MAM. CSIRO-Mk3-6-0 has the lowest qflux value yet the third highest rainfall value. Further investigation indicates that CSIRO-Mk3-6-0 features anomalously low influx from the east between 700 hPa and 500 hPa (compared to other models), but anomalously high influx from the south at 600 hPa and 500 hPa, where most models exhibit net outflow. The height at which this anomaly occurs suggests that the large-scale dynamical circulation (i.e. wind convergence) is dominating the relationship in this model. Analysis of both moisture convergence and wind convergence plots (not shown) confirms the dominant role of large scale circulation in CSIRO-Mk3-6-0's anomalies, in the absence of the role of specific humidity at these heights. The second anomalous model, MRI-ESM1, is consistently dry in all seasons, despite having near-average amounts of convergence. If both models are removed from the analysis, the relationship strengthens considerably more than expected from the removal of two degrees of freedom and becomes significant (r=0.568).

In SON the only significant relationship between rainfall and qflux entering the basin is at 700hPa from the west of the basin. This coincides with the region of greatest difference between wet and dry models (Figure 3.11b), where wet models

show greater inflow over this boundary, as in MAM. This concurs with previous work by *Pokam et al.* [2012; 2014] which suggests low-level westerly flow from the Atlantic is a dominant source of moisture in SON, and Figure 3.15b highlights the dominant role of low-to-mid level flux. At 850hPa, SON exhibits no significant relationships, though it must be noted that at 850hPa several models feature some missing data; in addition, Figure 3.15b shows that for the southern part of the boundary, the relationship remains significant down to 900hPa.

JJA shows no significant correlation between the variables; this may be due to threshold behaviour in JJA, where the total provision of moisture is not consistently high enough to exceed thresholds in thermodynamic instability, resulting in low rainfall across the majority of the basin. DJF exhibits positive, significant relationships between qflux and rainfall over the northern and eastern boundaries at 850hPa, with the most significant flux coming from the east (r=0.85). This strong relationship extends upwards to 700hPa (r=0.86), indicating that the amount of flow at low-mid levels entering the basin from the east is strongly linked to how much rainfall the basin experiences as a whole, and in particular the eastern side (Figure 3.14a). Again, Figure 3.15b highlights the dominance of the low-mid levels in this relationship. This result complements an assessment of individual model climatologies (not shown) which show strong influx into the basin from both the north east and south east from the Indian Ocean. The reversal of the land-sea thermal contrast in northern hemisphere winter, and the associated north easterly flow from the Indian subcontinent, is a likely source for this flow.

3.6.2 Possible influences on water vapour transport at basin boundaries

Figure 3.15 highlights the boundaries and heights at which moisture entering the basin is associated with rainfall. It is likely that these relationships are related to models' representation of the interaction between the regional and large-scale circulations. Figures 3.5 and 3.7 indicate that these circulatory differences may be related to model SST; there are significant differences between basin rainfall and ocean rainfall between wet and dry models. In order to determine the possible role of SST on basin rainfall, correlation analysis was performed between Congo Basin rainfall and SST at each grid box, across the suite of models (Figure 3.16). This indicates that correlations exist between rainfall over the basin and SST in surrounding oceans, and that some of these co-locate with regions of precipitation differences between wet and dry models (Figures 3.5 and 3.7).

SST biases in both the Atlantic and Indian Oceans have been well documented [e.g. *Wang et al.*, 2014]. For example, strong warm biases in the tropical and the south east Atlantic have been a persistent feature of coupled models [*Davey et al.*, 2002; *Richter and Xie*, 2008], and have been attributed to problems in both the atmospheric and oceanic model components, as well as the ocean-atmosphere feedbacks in coupled models (e.g. *Wahl et al.*, 2009; *Richter et al.*, 2012; *Xu et al.*, 2014). It is well established that SSTs in this region influence West and equatorial African rainfall [*Hirst and Hastenrath*, 1983a; *Nicholson and Entekhabi*, 1987; *Camberlin et al.*, 2001; *Todd and Washington*, 2004], and Figure 3.16 shows that

this bias is strongly related to basin rainfall in DJF. Most recently *Cook and Vizy* [2015] have determined that when Gulf of Guinea SSTs are anomalously warm, low level westerly flow into the basin is increased, feeding the lower branch of a Walker circulation over the basin, and resulting in higher rainfall. *Pokam et al.* [2014] have also linked differential heating of land and ocean to the formation of low-level westerlies in reanalysis data. A logical extension of this work is to assess the extent to which SST biases can account for differences in model rainfall via circulation patterns. This is the subject of a follow up paper in preparation by the authors.

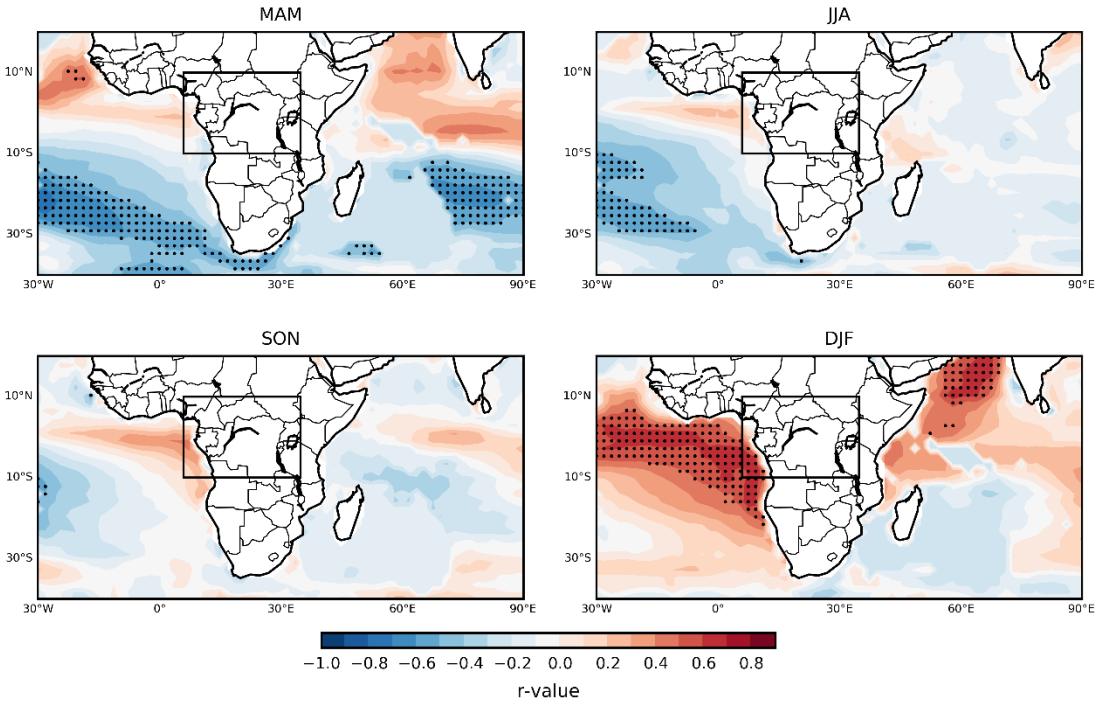

Figure 3.16 - Relationship between basin rainfall (5°E-35°E, 10°S-10°N; mm day-1) and SST bias (°C) at each gridbox, across 17 CMIP5 models

Local-scale factors, such as model representation of topography, may also interact with the large-scale circulation and contribute to some of the differences in moisture flux at the Congo Basin boundaries. A full analysis of the influence of topography will require an experimental set-up of a varying-resolution climate model; however, some insight can be gained from the low-resolution models used here. Figure 3.17a shows the land surface height of a transect across the basin at the equator in 10 models (those in our sample which provided orography data). At the point of maximum difference (0°, 36°E; grey dashed line), a correlation analysis was performed between land surface height and rainfall, for all seasons. Significant negative correlations were returned for MAM (r=-0.65, Figure 3.17b) and SON (r=-0.65, not shown), showing that wetter (drier) models tend to have lower (higher) surface altitude on the eastern boundary of the basin. No significant results were returned for JJA or DJF.

To determine whether qflux totals are also related to topography, a second correlation analysis was conducted between land surface height and qflux into the basin at 700hPa from the east. A significant negative correlation was returned for MAM (Figure 3.17c), suggesting that higher topography in drier models blocks some moisture transport from the east, and may be one cause of model divergence. In SON, the analysis did not return a significant correlation, indicating that for this season the relationship between rainfall and topography is more complex. Further analysis of the role of topography in model rainfall differences is planned for future work.

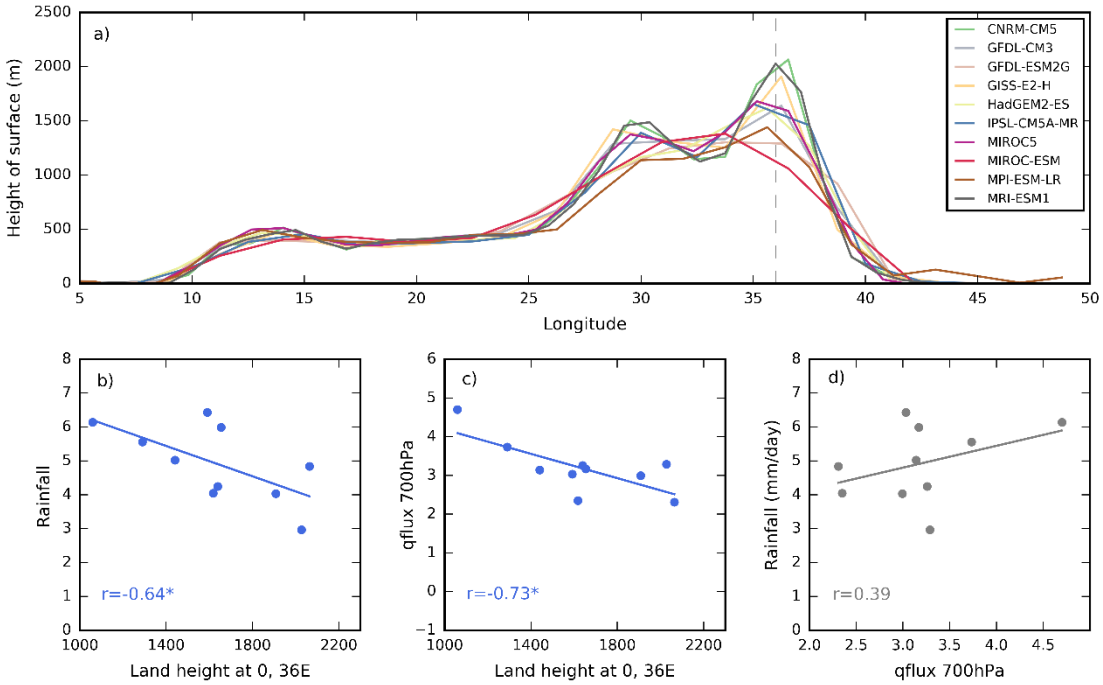

Figure 3.17 - (Top) a) Longitude/height (m) cross section of land surface height for 10 models at the equator. (Bottom) The relationship in MAM only between (b) land surface height (m) at 0°, 36°E and rainfall (mm day^{-1}); (c) land surface height at 0°, 36°E and qflux into the basin at 700hPa at 35°E (10^2 kg kg^{-1} s^{-1}); d) qflux from the east at 700hPa and rainfall.

3.7 Discussion

This study comprises an analysis of CMIP5 rainfall climatologies for the Congo Basin. As expected from the results of *Washington et al.* [2013], there is little agreement amongst model rainfall magnitude, with some monthly totals differing by a factor of five. The spatial distribution of rainfall also varies substantially across models; in some seasons, there is a tendency for either strong eastern or western rainfall maxima which are often consistent within models. Controls on rainfall are likely to be distinct between these two groups, highlighting the importance of inter-model comparison for identifying these differences. This

finding has implications for the use of multi-model ensemble means in climatological analyses. MME means are frequently used as a 'best estimate' of climatology, working on the principle that errors and uncertainties in individual models will be reduced by the averaging process [*Hagedorn et al.*, 2005; *Palmer et al.*, 2005; *Tebaldi and Knutti*, 2007]. However, the strongly opposite distributions between many models (Figures 3.4 and 3.6) cancel out when averaged, resulting in ensemble mean plots that feature homogenous, low magnitude rainfall across large areas of the domain. Unlike the ensemble mean, there are few models in any season which show a central and homogenous rainfall distribution, suggesting that the ensemble mean is not representative of Congo rainfall climatology. If a homogenous area of rainfall *is* representative of the observed, then it is not a distribution captured by any one model.

Recent approaches in model evaluation have encouraged the use of process-based assessments to determine the credibility of individual models. Moisture flux convergence has been established to be a useful metric in constraining rainfall in the tropics and has here been applied to a range of datasets in the Congo. The relationship between qflux convergence and rainfall is positive and significant in all seasons and at both heights, bar JJA at 700hPa. Again excepting JJA at 700hPa, this relationship is stronger than the individual relationships between the components of qflux convergence (specific humidity and wind convergence) and rainfall across the domain, indicating the significance of their combined role on rainfall climatology across models. Previous studies have shown that in the Amazon, another of the three global convective hotspots, coupled models which produce more realistic moisture convergence also simulate more realistic rainfall

amounts and distributions (Yin et al. 2013). A similar relationship was found at the inter-annual scale for reanalysis datasets [*Pokam et al.*, 2012] where wet (dry) years featured stronger (weaker) moisture convergence. This result is therefore promising as a first step in determining the credibility of individual model rainfall climatologies, as the large scale wind component of qflux convergence is better constrained in models than rainfall.

Results in Section 3.3 support previous suggestions that SON is the primary wet season (e.g. Figure 3.3); all models bar four feature higher rainfall in SON than MAM. Whilst differences between the two rainy seasons have been noted (e.g. *Sandjon et al.* [2012] notes that SON rains are shorter and less intense), there is no firm consensus on which season is wetter. It has been noted that rainfall is more intense in equatorial Africa during seasons with African Easterly Jet (AEJ) development both sides of the equator [*Nicholson and Grist*, 2003] as the southern branch of the AEJ only fully develops in the second half of the year. *Haensler et al.* [2013] suggest this might be the reason for higher rainfall in SON. Thus the finding that SON tends to be wetter than MAM is consistent with a shared mechanism, such as the AEJ, acting amongst models. There are some differences in convergence climatologies which further agree with this. For example, whilst all models in both MAM and SON are convergent at 850 hPa, more models in SON are convergent at 700 hPa, and average convergence across models is higher than in MAM (Figure 3.10b). Higher convergence in SON might be accounted for by regional scale circulation, for example the presence of both branches of the AEJ in this season [*Haensler et al.*, 2013b]. Additionally, dry biases in models have been linked to excessive moisture divergence in the tropics, and thus further suppression of

rainfall [*Yin et al.*, 2013]. The relationship between moisture divergence and rainfall may therefore involve positive feedbacks; this warrants further investigation, particularly in the dry seasons where divergence dominates.

These findings build on previous research conducted over the tropics and equatorial Africa on the relationship between thermodynamical mechanisms and rainfall. *Collins et al*. [2013] highlight that thermodynamic feedbacks within individual models may contribute to a 'wet-gets-wetter/dry-gets-drier' mechanism, whereby enhanced water transport creates more convergence (divergence) in convergent (divergent) areas [*Held and Soden*, 2006]. Thus feedbacks in hydrological variables might be the cause of consistent wetness/dryness of models across seasons. This indicates that an assessment of the SST/rainfall relationship in this region might be fruitful. Additionally, analysis of CMIP3 and CMIP5 data suggests that the rainfall response in convection zones is highly sensitive to spatial heterogeneities, which may include local moisture convergence feedbacks or the rate of moisture influx from surrounding regions [*Chou et al.*, 2006; *Neelin et al.*, 2006]. This research reinforces these findings, suggesting that the qflux/rainfall relationship could be used to differentiate models, in the absence of rainfall station data.

Despite a large scale relationship between moisture convergence and rainfall over the basin, the relationship does not appear to have a strong spatial signal. In the wet seasons, there is no obvious relationship between the location of rainfall and convergence maxima. This suggests that while high moisture convergence may set up the conditions for convection, local controls (for example surface heating,

mesoscale convective organisation, orography), most probably have a greater influence on the location of maximum rainfall. Further, the strong positive relationship between rainfall and qflux divergence observed at the domains scale is evident in some subdomains, but not all. In MAM at 700hPa, a significant correlation coefficient is present in subdomains which feature mean divergence and low rainfall (north east and north west). This might indicate that the local relationship is subject to a threshold, below which the relationship between rainfall and qflux convergence does not hold up, or is tempered by another variable. In SON at 700hPa rainfall in all subdomains features a strong, significant relationship with moisture flux convergence; this suggests the presence of a large scale control across the basin. JJA shows the opposite pattern to that in MAM at 700hPa; the only statistically significant relationships are in the northern two domains in JJA, which are the wettest and most convergent. The domain as a whole does not feature significant correlation in JJA at 700hPa, indicating that the relationship rapidly breaks down in the drier, southern half of the domain. DJF features strong positive relationships in all subdomains at 850hPa. As in SON this suggests the region is highly influenced by convergence across the basin in DJF.

Previous work indicates that moisture entering the basin at low levels from the west (SON) and east (MAM) is a key control on rainfall totals and variability in reanalyses [*Pokam et al.*, 2012, 2014]. Figure 3.11 indicates that wetter models tend to experience greater flux across these two boundaries, and Figure 3.15a identifies the relative importance of these boundaries for different seasons. The amount of moisture entering the basin from the west at 700hPa is highly related to rainfall in SON, and Figure 3.15b shows that for some latitudes this relationship

extends in both directions in the atmospheric column. This relationship suggests a possible link to low-level westerlies and Atlantic influences, as found by *Pokam et al*. Additionally, once anomalous models have been removed, MAM features a relationship between low-to-mid level flux across the eastern boundary and rainfall over the basin as a whole (again in agreement with *Pokam et al.* [2012]). Figure 3.17 suggests that for this season, qflux from the east is in part influenced by model representation of topography. However, this relationship is complex or non-existent for the rest of the year, which is perhaps expected as previous studies have found no simple relationship between rainfall and model resolution over this region [*Washington et al.*, 2013; *Moufouma-Okia and Jones*, 2014]. DJF stands out as having the strongest relationships with qflux across several boundaries, in particular the east and across the north-eastern and south-eastern corners of the domain. *Pokam et al.* [2012] suggest this is related to the AEJ-N, which is located in the north of the basin during DJF, and is also likely related to north-easterly flow from the Indian subcontinent in this season.

3.8 Conclusions

This study is the most comprehensive assessment of the causes of model rainfall difference in the Congo. It utilizes the relationship between a dynamical variable and rainfall to determine the likely first-order causes for the relative differences between models. The following conclusions have been reached:

1. There is little agreement amongst CMIP5 model simulations of Congo rainfall. This has implications for the use of multi-model ensemble means for this region.
2. Moisture flux convergence has a strong relationship with rainfall a) in all seasons, and b) at two different levels in the atmosphere
3. The height in the atmosphere at which these relationships are significant differs amongst seasons, and suggests that different circulatory features are more or less important in different seasons
4. The rainfall/moisture convergence relationship is a large-scale feature of the basin; it does not occur at all subdomains in all seasons
5. Model rainfall depends on water vapor transport into the basin across different boundaries and at different heights. A targeted measurement campaign at certain boundaries could help to constrain the spectrum of model rainfall.
6. Model simulations of the large-scale circulation play a significant role in differentiating between model rainfall. Model sea surface temperature biases and topography schemes are possible controls on this relationship; these will be addressed in future work.

The Congo Basin remains a significant challenge for climate modelling due to the dearth of observational data and the unlikelihood of making significant gains in observation in the coming years. Nevertheless, there is scope for a much deeper understanding of the dynamics of individual climate models, and this study comprises a first assessment of the differences between model climatologies for this region. Process-based model evaluation techniques are increasingly being

used to understand why models behave as they do, and whether models can be grouped or ranked by their characteristics. This study also highlights the dangers of using model ensembles as a 'best guess' for current or future climate scenarios in regions with poor observational coverage. For Central Africa, the use of the ensemble mean is misleading and is likely to mask important climate information. Crucially, this paper has outlined the potential utility of processes such as moisture-flux convergence in constraining parameterised outputs, in the absence of high-resolution model datasets which are needed to capture tropical convection processes explicitly. In addition, it highlights the potential utility of long-term field campaigns on the boundaries of the Congo Basin, which fall outside both the physical and practical barriers to access, and may provide important insights into local/regional/global interactions.

A logical next step is to assess the regional circulation for drivers which may be common amongst models or particular subgroups of models. Indian and Atlantic Ocean SST biases are likely to play a role in setting up the moisture dynamics which feed into the basin. The role of convection/convergence feedbacks must also be assessed with respect to the overturning circulation. Topography, and relatedly model resolution, has also emerged as a local factor which may be of significance in particular seasons. Despite the enormity of the challenges still facing Congo climate science, these approaches appear fruitful and provide a possible mechanism for confronting the wide array of future climate trajectories produced by models. This step is vital for providing credible climate products for decision-makers in this region.

Acknowledgements

The GCM data used in this study was made available through the Earth System Grid Federation (ESGF) Peer-to-Peer system (https://pcmdi.llnl.gov/search/cmip5/). We also acknowledge NOAA/OAR/ESRL PSD and ECMWF for making available the NCEP and ERA-I datasets. The first author is fully funded by the National Environmental Research Council via a Doctoral Training Programme (grant number: NE/L002612/1). Richard Washington is partly supported by the NERC funded IMPALA (NE/M017206/1) and UMFULA (NE/M020207/1) programmes. The authors acknowledge the helpful inputs of Dr Sebastian Engelstaedter, Dr Neil Hart and Callum Munday.

Supplementary Material

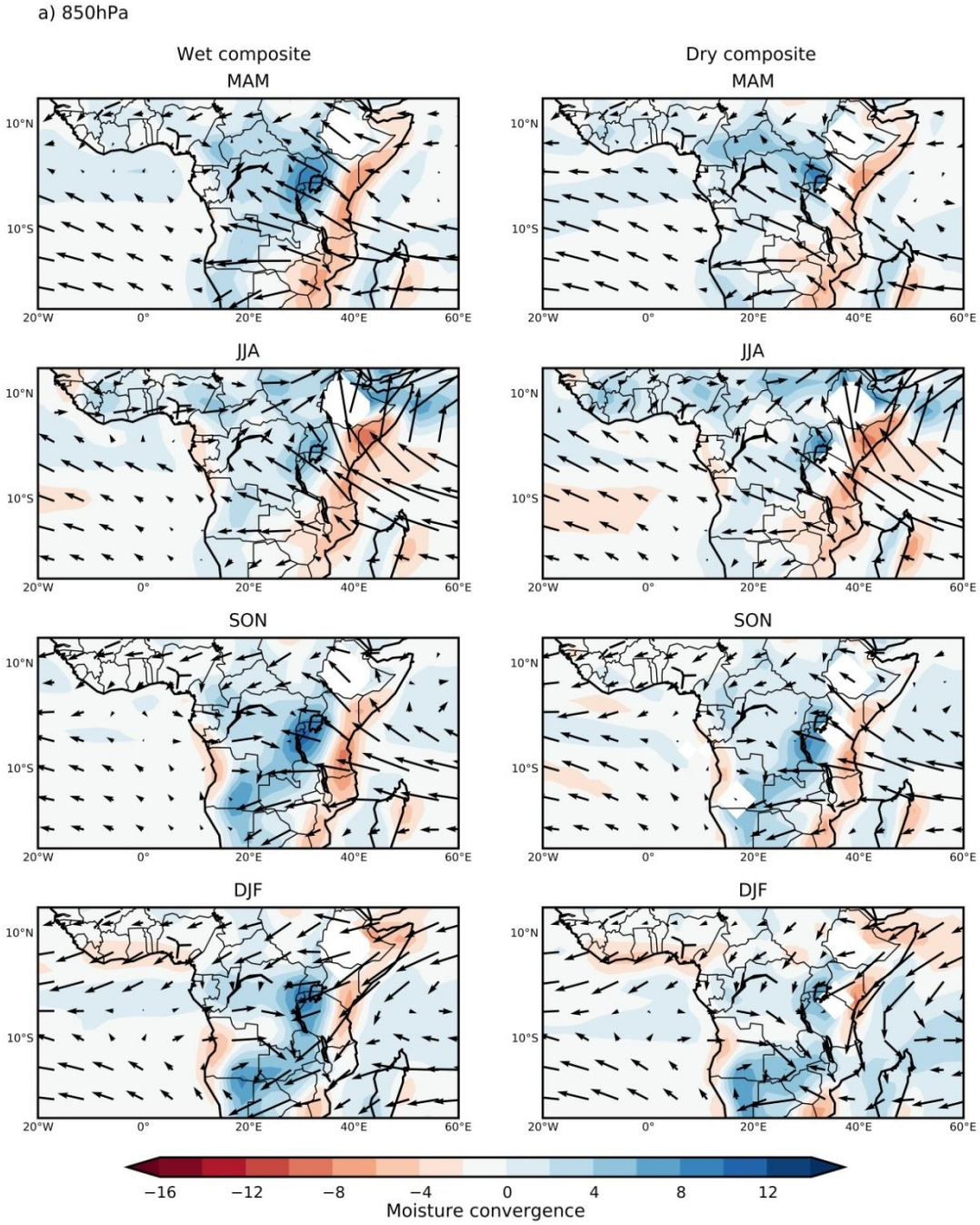

Figure 3.S1 - for (a) 850 hPa and (b) 700 hPa - Composite of moisture flux convergence (shaded) and moisture flux (vectors) in the five wettest models (based on Figure 3.2) (left column) and the five driest models (right column) in each season at 850 hPa

b) 700hPa

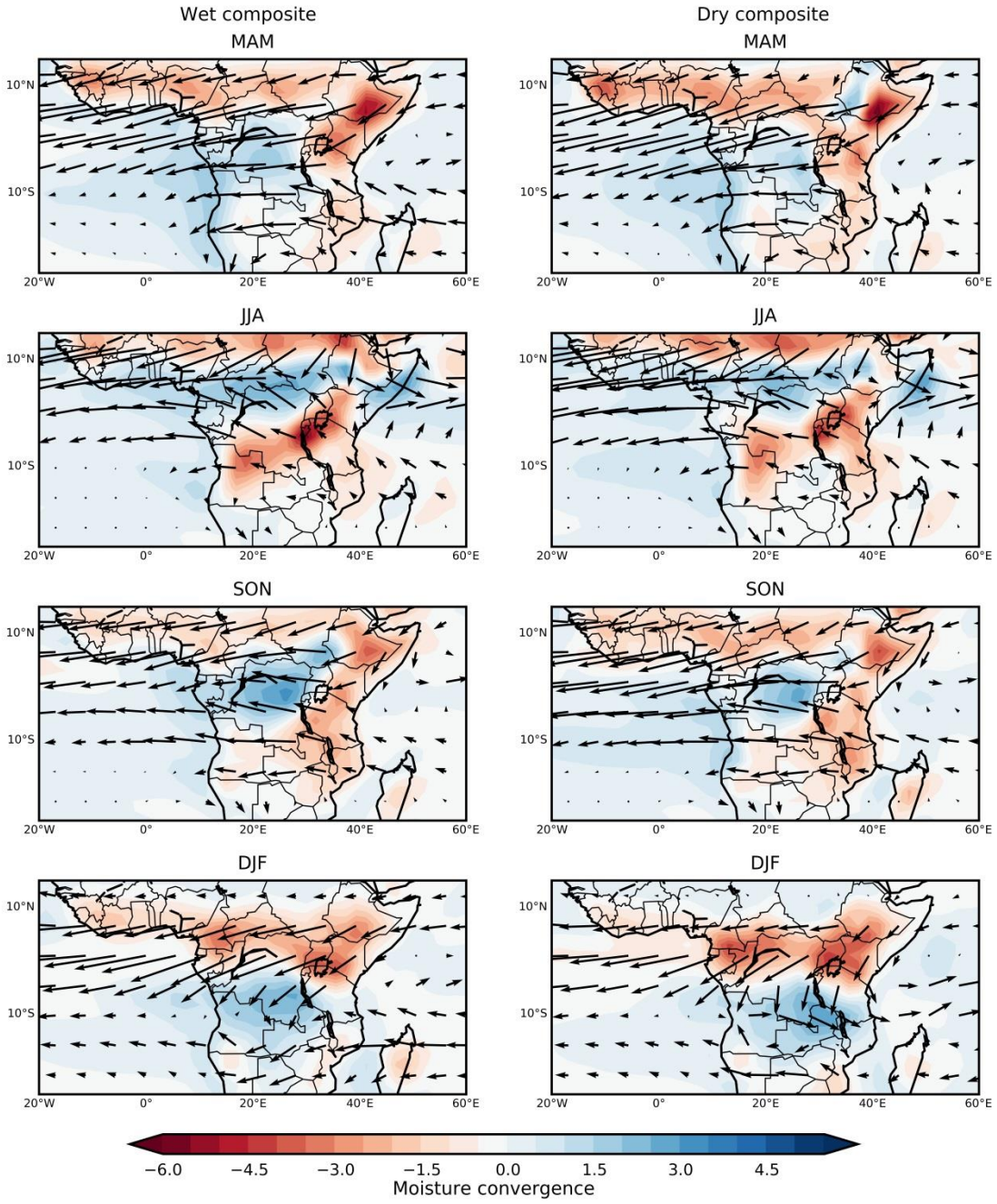
Wet composite
Dry composite
MAM
JJA
SON
DJF
10°N
10°S
20°W
0°
20°E
40°E
60°E
−6.0
−4.5
−3.0
−1.5
0.0
1.5
3.0
4.5
Moisture convergence

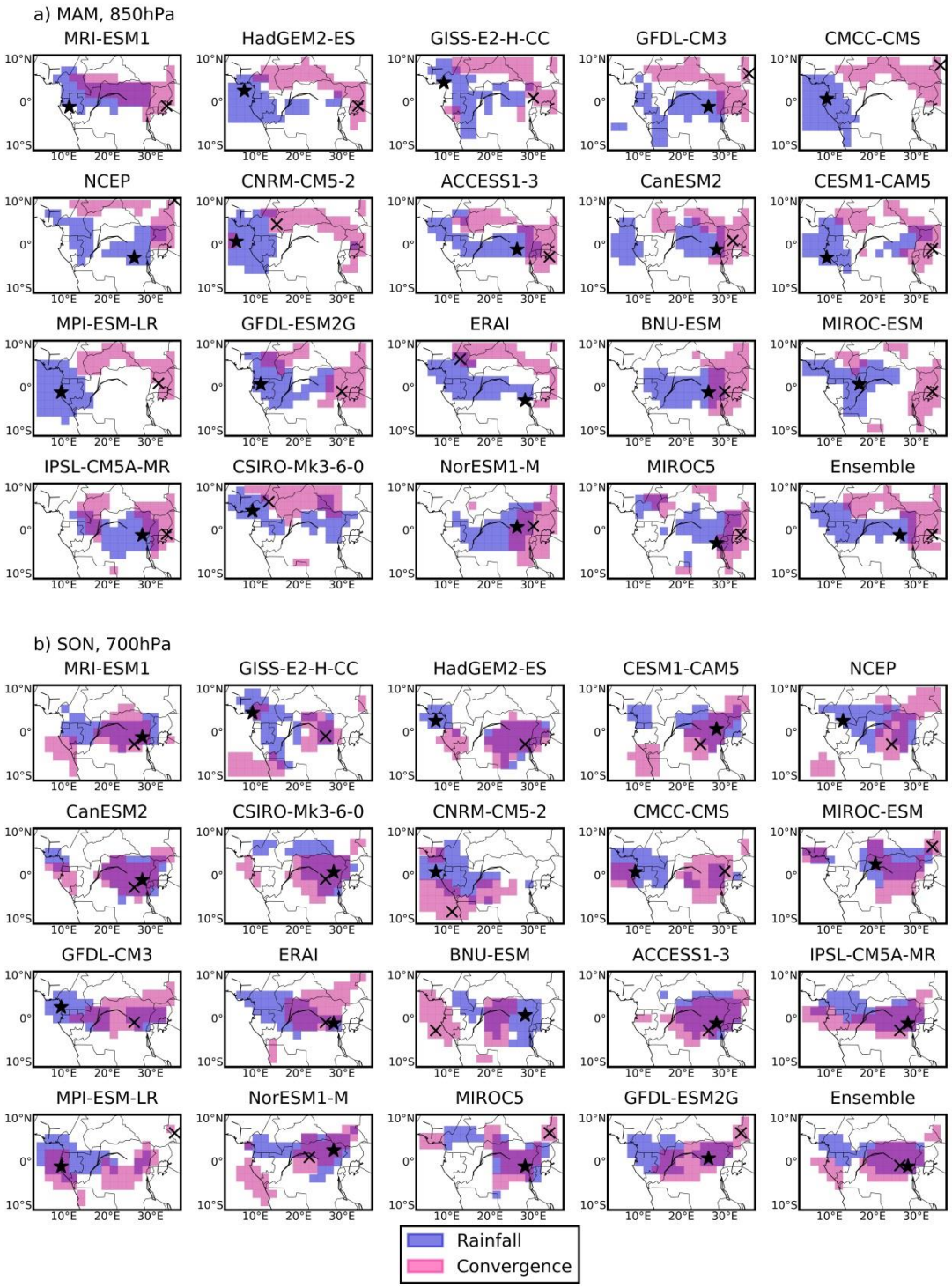

Figure 3.18 - Location of top 20% of rainfall values (blue), moisture flux convergence values (pink), and areas of overlap (purple) in a) MAM at 850hPa and b) SON at 700hPa. The location of maximum rainfall (convergence) is denoted by a star (cross)

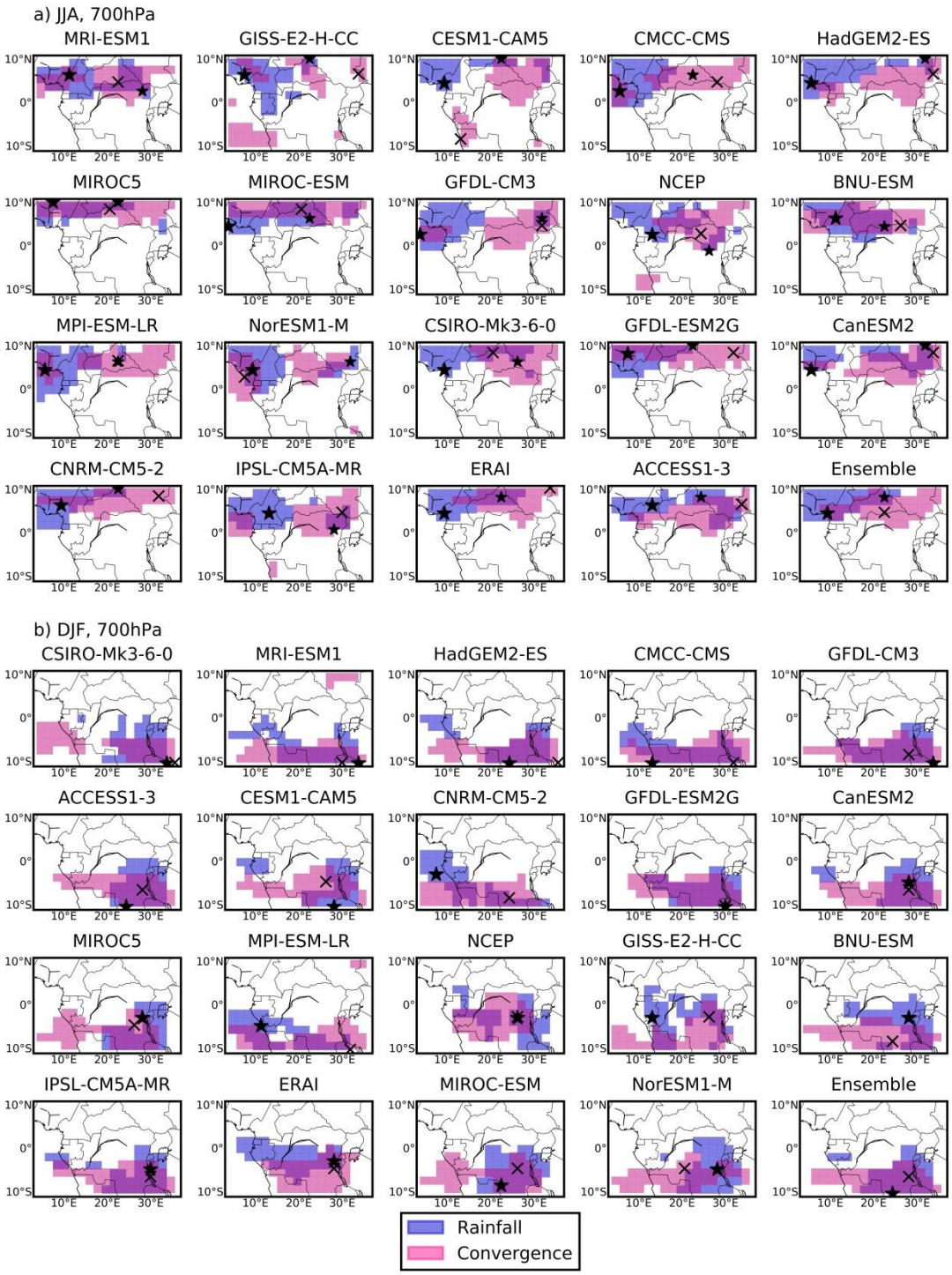

Figure 3.S3 - As for Figure 3.S2 but for a) JJA at 700hPa and b) DJF at 700hPa

4 A process-based assessment of CMIP5 rainfall in the Congo Basin: the September-November rainy season

A process-based assessment of CMIP5 rainfall in the Congo Basin: the September-November rainy season

A. CREESE[1] and R. WASHINGTON[1]

[1]Climate Research Lab, School of Geography and the Environment,

University of Oxford, South Parks Road, Oxford, OX1 3QY, UK

Journal of Climate, **31**(18) 7417-7439,

doi:10.1175/JCLI-D-17-0818.1

Manuscript received 4 December 2017

Accepted 14 May 2018

Published online 3 August 2018

Authorship Declaration

I conducted all of the analysis and writing for this paper. Richard Washington discussed the methodology, results and structure of the paper with me, and edited the manuscript.

Abstract

Congo Basin September-November rainfall varies by up to a factor of three across CMIP5 coupled models. The severe lack of observational data in this region makes model evaluation difficult using standard techniques. This study uses a process-based assessment to evaluate the plausibility of mechanisms related to coupled model rainfall in September-November. Models tend to simulate a rainfall maximum in either the west or east of the basin. In most months west Congo rainfall is positively correlated with east Congo rainfall across models, as relatively wet models are often wetter everywhere; however, in August-November this correlation becomes insignificant, suggesting that processes relating to rainfall differences in each subdomain are distinct. Composite analysis of wet and dry models in each subdomain suggests that the tropical east Atlantic SST bias helps differentiate between models in the west: wetter models tend to have a larger (~1-2°C) and more equatorward SST bias, higher evaporation over the ocean and higher local convection. In the east, rainfall differences between models are related to more remote SST differences, including cold south Atlantic and warm east Indian Ocean SSTs. Wetter models exhibit stronger westerly flow across the tropical east Atlantic, as part of an enhanced equatorial zonal overturning cell. Dry models in the east feature a stronger and more equatorward African Easterly Jet-North, which may contribute to suppressed convection over the domain. This assessment casts doubt on the credibility of models which are very wet in the west of the Congo Basin and have a large Atlantic SST bias.

4.1 Introduction

The climatological importance of the Congo Basin in the large-scale tropical circulation is undisputed. It is the largest hydrological catchment in Africa, and supports the planet's second-largest rainforest, a vast carbon-store [*Williams et al.*, 2007; *Dargie et al.*, 2017]. As such, an understanding of the likely future climatic changes in this region is crucial. Africa as a whole is particularly vulnerable to climate change [*Niang et al.*, 2014], and as a result has been the focus of an increasing number of scientific studies in recent years. However, while the climate systems of West Africa [e.g. *Nicholson*, 1980; *Folland et al.*, 1986; *Cook and Vizy*, 2006; *Pomposi et al.*, 2015], East Africa [e.g. *Camberlin and Okoola*, 2003; *Lyon and Dewitt*, 2012; *Viste et al.*, 2013; *Liebmann et al.*, 2014; *Rowell et al.*, 2015] and southern Africa [e.g. *Reason and Mulenga*, 1999; *Hoerling et al.*, 2006; *Blamey and Reason*, 2012; *Hart et al.*, 2013] have received increasing attention, the Congo Basin has remained critically understudied [*Washington et al.*, 2013; *Creese and Washington*, 2016]. This is due primarily to the lack of recent observational data in the Congo Basin, which is one of the most data sparse continental regions. Fewer than 10 rain gauges over the Congo Basin were included in the CRU 0.5° rainfall dataset in 2010, and problems of access and political insecurity have thus far prohibited targeted observational campaigns [*Washington et al.*, 2013]. Some studies have utilised reanalysis, station data, and gridded-data products to better understand the seasonal climatology [*Nicholson and Grist*, 2003], climate variability [*Todd and Washington*, 2004; *Balas et al.*, 2007; *Jury et al.*, 2009; *Sandjon et al.*, 2012; *Dezfuli and Nicholson*, 2013; *Nicholson and Dezfuli*, 2013] and

dominant climate processes in the region [*Jackson et al.*, 2009; *Pokam et al.*, 2012, 2014]. Despite this progress, there remains a paucity of research on climate model behaviour in the Congo.

4.1.1 Climate model evaluation in the Congo Basin

Climate model evaluation has traditionally relied upon methods of hindcast validation, whereby historical climate simulations are compared to observed data. Whilst some studies have assessed future changes for central Africa across ensembles of coupled models [e.g. *Haensler et al.*, 2013], our understanding of likely future changes is limited by our relatively poor understanding of climatological processes in the region [*Washington et al.*, 2006, 2013]. Reanalysis products can be useful proxies for observations, as they provide global coverage; however, they must be treated with some caution in areas which lack observational data, as in such cases they are mostly controlled by the reanalysis model [*Washington et al.*, 2013]. A recent comprehensive assessment of global rainfall products highlighted large discrepancies between products in terms of interannual and decadal variability in the Congo Basin [*Sun et al.*, 2017], and previous work by the authors has shown that reanalysis, satellite and gauge products disagree on both rainfall magnitude and location; for example, in December-February (DJF) mean rainfall in ERA-Interim (reanalysis) is more than double that in CMAP (satellite and gauge) [*Creese and Washington*, 2016].

Such discrepancies limit the capacity of these datasets to act as a constraint on model hindcasts [*Creese and Washington*, 2016]. Across global coupled climate

models (GCMs) mean Congo Basin rainfall can differ by a factor of five in some months. There is also little consensus between models on the location of maximum rainfall in different seasons; some models simulate a rainfall maximum exclusively in the east of the basin, some in the west (nearly 2,500 km distant), while some exhibit patchy, disconnected regions of rainfall. Without long-term, homogenous observations it is impossible to determine which models are able to reproduce the 'real world' rainfall distribution in the Congo Basin. *Creese and Washington* [2016] showed that use of the ensemble mean is not appropriate for GCMs in the Congo Basin across all seasons, as the combination of models with distinct east and west rainfall maxima produces an ensemble mean with a rainfall distribution which is not evident in any one model.

Considering the challenges imposed by the scarcity of recent observational data on model hindcast validation in the Congo Basin, this paper will instead use a regionally-focused process-based assessment. This framework assesses a model's credibility depending on the mechanisms used to generate weather and climate. Such evaluations tend to focus on the capability of models to reproduce a) the mean state climatology [e.g. *Munday and Washington*, 2017], b) the interannual variability [e.g. *Dieppois et al.*, 2015] and/or c) trends over time in the variable of interest [e.g. *Williams et al.*, 2012]. Given the scale of differences in model rainfall climatologies in this region, this study will focus on the mean state, as the processes linked to the higher order statistical moments of variability and trend would likely be implausible if superimposed on a questionable mean state.

Process-based model evaluation may be of particular use in Africa, which has traditionally not been a focus for model development and where processes may be poorly represented by models [*James et al.*, 2018]. Process-based assessments have proven fruitful in southern Africa [e.g. *Dieppois et al.*, 2015; *Lazenby et al.*, 2016; *Munday and Washington*, 2017], East Africa [e.g. *Tierney et al.*, 2015; *Yang et al.*, 2015; *Hirons and Turner*, 2018], and the Sahel [e.g. *Cook and Vizy*, 2006; *Biasutti et al.*, 2009; *James et al.*, 2015]. *James et al.* [2015], for example, used a process-based assessment to identify the mechanisms by which models produced drying in historically dry years. These mechanisms were found not to be the same as those producing drying in reanalysis data. They argued that future drying in the region may not be credible, as the process by which drying occurs is the same spurious process as that found in historical model years. In essence the models were using the same fictitious overturning circulation to create both historical drought and future drying trends. In the case of the Sahel, the circulation is sufficiently well understood for reanalysis data to be a sensible test of the models. *Munday and Washington* [2017] used a process-based approach to assess a suite of model simulations of southern African rainfall. They found that differences amongst model rainfall estimates are related to their simulation of the strength of the Angola Low pressure system in austral summer. The approach with respect to the Angola Low differs from the Sahel example of *James et al.* [2015], as the dynamics of the Angola Low are poorly understood. If similar approaches can be established for particular seasons or regions in the Congo, then we can begin the process of determining which models are producing plausible rainfall climatologies there too.

4.1.2 The September to November (SON) wet season

The Congo Basin experiences two rainy seasons; one between March and May (MAM) and one between September and November (SON). The timing of the rainy seasons is associated with the meridional movement of tropical convection through the annual cycle. Mean daily rainfall in these seasons is roughly double that experienced in the dry seasons, June-August (JJA) and December-February (DJF), in both model and satellite/gauge datasets [*Creese and Washington*, 2016]. Observational data indicates SON is wetter than MAM over the majority of the Congo Basin, contrasting with East Africa, where MAM constitutes the 'long' and more intense rains [*Dezfuli*, 2017]. *Creese and Washington* [2016] found that SON was the wettest season in over 80% of the CMIP5 coupled models in their sample.

The limited research that has been conducted in the Congo on reanalysis and observations has revealed several processes which are important to SON rainfall. A common theme among studies is the role of moisture transport from the Atlantic Ocean, in particular affecting the west of the Congo Basin. *Pokam et al.* [2012] identified a maximum in low level moisture convergence at around 850 hPa in SON, associated with low-level moisture advected from the Atlantic which *Sorí et al.* [2017], based on a Lagrangian transport model driven by ERA-I reanalysis data, ranks as the most important oceanic source for the Congo Basin in this season. The strength of these low-level westerlies (LLWs) is related to rainfall variability in western equatorial Africa, where wet years exhibit a distinct westerly jet during both wet seasons [*Dezfuli and Nicholson*, 2013; *Nicholson and Dezfuli*, 2013]. *Pokam et al.* [2014] found that the land-ocean heat contrast in this region plays a

crucial role in driving LLW variability in this season. The LLWs form the lower branch of a zonal overturning circulation between June and October, with a subsiding branch over the Gulf of Guinea [*Pokam et al.*, 2014; *Cook and Vizy*, 2015]. The variability of this overturning circulation is linked to sea surface temperature (SST) anomalies in the Atlantic, which have been found to have both direct and indirect effects on Congo rainfall variability [*Balas et al.*, 2007].

The Indian Ocean and associated moisture fluxes are also likely to be a considerable influence on the region [*Black et al.*, 2003; *Ummenhofer et al.*, 2009; *Dyer et al.*, 2017] particularly in the east of the region where interactions with topography also contribute to convection and MCS activity [*Jackson et al.*, 2009; *Van Der Ent et al.*, 2010]. A recent study using water tagging in the CESM model identified the Indian Ocean as a dominant ocean source of moisture into the Congo Basin, with the southwest Indian Ocean contribution roughly 21% of available moisture in both rainy seasons [*Dyer et al.*, 2017]. Studies of East African rainfall have also highlighted the role of the equatorial Indian Ocean zonal overturning cell in determining rainfall variability [*Hastenrath*, 2000], and the Indian Ocean Dipole (IOD) has long been understood to influence East African rainfall, with positive IOD phases linked to increased wetting via enhanced low-level moisture convergence and ascent over East Africa [*Ummenhofer et al.*, 2009; *Nicholson*, 2017b]. Relatedly, it has also been suggested the pressure contrast between the Indian and Atlantic basins could account for zonal differences in rainfall across the Congo Basin [*Dezfuli*, 2017]. Although later in the annual cycle of rainfall than the SON rains, *Dezfuli et al.* [2015] identify a Zonal Asymmetric Pattern (ZAP) in the southern half of central Africa during December to March, where opposite signs in rainfall occur

in the western (10°-30°E) and eastern (30°-40°E) subdomains. Wet periods in eastern central Africa are characterised by enhanced westerlies into the basin, caused by the contrast between low pressure in the southwest Indian Ocean and high pressure over the equatorial Atlantic. These westerlies converge at the East African topography, initiating convection as part of a zonal overturning cell, and intensifying wetting in the east.

Both the northerly and southerly components of the midlevel African Easterly Jet (AEJ-N and AEJ-S respectively) are important circulation features in SON. While the AEJ-N is present throughout the year, the AEJ-S is most clearly defined as a mid-level jet between August and November [*Nicholson and Grist*, 2003]. Both jets are a result of strong meridional surface temperature gradients between the equator and subtropics. Previous research has found that interannual rainfall variability in the West African Sahel appears to be linked to the strength and location of the AEJ-N; wet years tend to feature a weaker and more poleward jet, whereas dry years feature a stronger and more equatorward jet [*Kanamitsu and Krishnamurti*, 1978; *Newell and Kidson*, 1984; *Fontaine et al.*, 1995; *Grist and Nicholson*, 2001]. Links between rainfall variability and zonal wind have also been identified in western equatorial Africa; *Dezfuli and Nicholson* [2013] found that in both the east and western subdomains, wet years feature weaker mid-level easterlies across the basin than in dry years.

Nicholson and Grist [2003] found that the tropical rain band is most intense when both components of the jet are well developed, i.e. between August and November. The presence of the AEJ-S during SON has been linked to strong mesoscale

convective system (MCS) activity during SON. *Jackson et al.* [2009] identified a maximum in MCS activity in a region of strong convergence found to the right of the entrance region of the AEJ-S, as would be expected from the 'jet streak' model [*Uccellini and Johnson*, 1979]. This maximum in midlevel convergence is suggested to enhance upward motion from the surface and contribute to higher MCS activity. As the AEJ-S is only present during SON, they hypothesized that this may be why this season appears to have more intense rainfall than during MAM.

Previous research has begun to assess the relative role that processes such as water vapour flux play in producing rainfall in different coupled models, as SON rainfall can vary by as much as a factor of three amongst CMIP5 models. Following from *Pokam et al.* [2012] work on moisture convergence, *Creese and Washington* [2016] found that rainfall across CMIP5 models in SON is positively correlated with low-level moisture flux from the western boundary of the Congo Basin (the Atlantic coast); i.e. wetter models have greater moisture influx from the Atlantic. In contrast, MAM and DJF experience much stronger positive correlations with moisture inflow at the northern and eastern boundaries of the basin, indicating that fluxes from the north-east and across the Indian Ocean are most important for discriminating between coupled model rainfall in those seasons. These results indicate that the tendency for models to be wet or dry in SON is potentially related to their simulation of the climatology of the Atlantic sector. Given the clear tendency for SON to be wetter than MAM in most models, and the distinct east and west rainfall patterns that models produce, this indicates that the rainfall-producing processes across models in this season are worthy of investigation.

4.1.3 Aims

This paper aims to answer the following questions:

1. What are the preferred locations of model rainfall in the Congo Basin in SON, and do these differ across coupled models in CMIP5?
2. Are model differences in rainfall linked to Atlantic or Indian Ocean SST biases?
3. How do these biases relate to the regional circulation, and what other elements of the regional circulation, for example the African Easterly Jets, help to explain model differences in rainfall?

The paper is structured as follows: Section 2 describes the data and methods used in this study. Sections 3 addresses the characterisation of model rainfall climatology in SON in CMIP5 models, Section 4 explores whether model rainfall is related to known SST biases, and we use composite analysis in Section 5 to determine possible rainfall-producing mechanisms in wet and dry models. We discuss the results and conclude in Sections 6 and 7 respectively.

4.2 Data and Methods

The Congo Basin domain used in this study is 8°E to 35°E, 10°S to 10°N. The western (eastern) subdomain comprises gridboxes between 8°E and 21°E (21°E to 35°E) and 10°S to 10°N. The coupled model data in this study is output from the Coupled Model Intercomparison Project 5 (CMIP5) [*Taylor et al.*, 2012]. A

spectrum of 17 models ranging from wet to dry over the Congo Basin with the required variables (rainfall, SST, specific humidity, *u* and *v* winds, omega, evaporation and mean sea level pressure) were selected (Table 4.1). Data is used from both the historical (coupled) experiments and the AMIP experiments, which use an atmosphere-only model forced with observed SSTs. Monthly and seasonal means for the September-November season were calculated over the period 1979-2005, which is the available period for the AMIP experiments. All CMIP5 data have been interpolated to a common grid of 1°x1° to allow for easy comparison across models; a step to which the results are insensitive.

ERA-Interim (ERA-I) and NCEP/NCAR (NCEP) reanalysis and observational rainfall datasets (Table 4.2) are used as initial points of comparison with coupled models. ERA-I [*Dee et al.*, 2011] is later used as a comparison for processes found in composite analyses. Observed SST data are taken from the HadISST2 dataset [*Titchner and Rayner*, 2014].

Composite analysis is used throughout this study to compare the climatological mean state of models which tend to be wet or dry. Each composite includes the four wettest or driest models defined as the upper and lower quartiles of the samples in each of the western and eastern subdomains (Table 4.3). A metric of difference between the composites is modified from *Creese and Washington* [2016] and is represented by stippling. Stipples occur under the following conditions: (1) where all wet model values are larger or smaller than all dry model values (large dots); (2) where all wet model values are greater or smaller than the dry mean, depending on the direction of difference (squares); (3) where all dry

Table 4.1- CMIP5 models used in this study

Model	Institute	Reference
ACCESS1-3	Commonwealth Scientific and Industrial Research Organization and Bureau of Meteorology Australia (CSIRO-BOM)	*Collier and Uhe* [2012]
bcc-csm1-1	Beijing Climate Centre (BCC)	*Wu et al.* [2013]
CCSM4	National Centre for Atmospheric Research (NCAR)	*Gent et al.* [2011]
CESM1-CAM5	National Centre for Atmospheric Research (NCAR)	*Neale et al.* [2012]
CMCC-CM	Centro Euro-Mediterraneo per I Cambiamenti Climatici (CMCC)	*Scoccimarro et al.* [2011]
CNRM-CM5	Centre National de Recherches Météorologiques / Centre Européen de Recherche et Formation Avancée en Calcul Scientifique (CNRM-CERFACS)	*Voldoire et al.* [2011]
CSIRO-Mk3-6-0	Commonwealth Scientific and Industrial Research Organization in collaboration with Queensland Climate Change Centre of Excellence (CSIRO-QCCCE)	*Jeffrey et al.* [2013]
EC-EARTH	EC-Earth Consortium: European Centre for Medium-Range Weather Forecasts (ECMWF) and other European institutes	*Hazeleger et al.* [2010]
FGOALS-g2	State Key Laboratory of Numerical Modeling for Atmospheric Sciences and Geophysical Fluid Dynamics (LASG) and Institute of Atmospheric Physics (IAP)	*Li et al.* [2013]
GFDL-CM3	NOAA Geophysical Fluid Dynamics Laboratory (NOAA GFDL)	*Donner et al.* [2011]
GISS-E2-R	NASA Goddard Institute for Space Studies (GISS)	*Schmidt et al.* [2014]
HadGEM2-ES	Met Office Hadley Centre (MOHC)	*Jones et al.* [2011]
IPSL-CM5A-MR	Institut Pierre-Simon Laplace (IPSL)	*Dufresne et al.* [2013]
MIROC5	Atmosphere and Ocean Research Institute (The University of Tokyo), National Institute for Environmental Studies, and Japan Agency for Marine-Earth Science and Technology (MIROC)	*Watanabe et al.* [2010]
MPI-ESM-LR	Max-Planck-Institut für Meteorologie (MPI-M)	*Marsland et al.* [2003]
MRI-CGCM3	Meteorological Research Institute (MRI)	*Yukimoto et al.* [2012]
NorESM1-M	Norwegian Climate Centre (NCC)	*Bentsen et al.* [2013]

models are greater or smaller than the wet mean, depending on the direction of difference (crosses); and (4) where both (2) and (3) are true (small dots).

Table 4.2 - Identity and charactertistics of reanalysis and satellite/gauge datasets used in this study

Dataset	Full name and Institute	Native horizontal resolution	Dates used	Reference
ERA-Interim	European Centre for Medium Range Weather Forecasts	0.7°×0.7°	1979-2005	*Dee et al*. [2011]
NCEP/NCAR	National Centers for Environmental Prediction (NCEP) and the National Center for Atmospheric Research (NCAR)	2.5°×2.5°	1971-2000	*Kalnay et al*. [1996]
CRU	Climate Research Unit, University of East Anglia (v3.10)	0.5°x0.5°	1979-2005	*Harris et al.* [2014]
GPCC	Global Precipitation Climatology Centre, Deutscher Wetterdienst, World Meteorological Organisation	0.5°x0.5°	1979-2005	*Schneider et al*. [2015]
CMAP	Climate Prediction Centre Merged Analysis of Precipitation, NOAA NCEP	2.5°×2.5°	1979-2005	*Xie & Arkin* [1997]
TRMM	Tropical Rainfall Measuring Mission, NASA Goddard Space Flight Center, Japanese Aerospace Exploration Agency	0.25°×0.25°	1998-2014	*Huffman et al*. [2007]

Table 4.3 - Models used in wet and dry composites

Models in west composites			
Wet	**mm day^{-1}**	**Dry**	**mm day^{-1}**
MPI-ESM-LR	7.22	MRI-CGCM3	4.16
NorESM1-M	6.88	CESM1-CAM5	4.70
IPSL-CM5A-MR	6.73	HadGEM2-ES	4.75
MIROC5	6.63	CMCC-CM	4.84
Models in east composites			
Wet	**mm day^{-1}**	**Dry**	**mm day^{-1}**
ACCESS1-3	9.0	GISS-E2-R	3.47
MIROC5	7.74	CNRM-CM5	3.69
NorESM1-M	7.51	CMCC-CM	3.99
CCSM4	7.44	MRI-CGCM3	4.40

4.3 Characterising model rainfall

There are distinct zonal differences in the location of SON rainfall across the studied samples of CMIP5 models (Figure 4.1). Many models show distinct western (e.g. CMCC-CM, GISS-E2-R, MPI-ESM-LR) or eastern (e.g. NorESM1-M, ACCESS1-3, CCSM4, CSIRO-Mk3-6-0) rainfall maxima, including some models which show two distinct rainfall maxima (e.g. MRI-CGCM3, HadGEM2-ES). The ensemble mean model (fourth row, centre) smooths much of the spatial variability between individual models, and is not similar to any individual model. This implies that the use of ensemble mean model is misleading, as found in *Creese and Washington* [2016]. Consistent with *Washington et al.* [2013] we find substantial variations between satellite, gauge and reanalysis products.

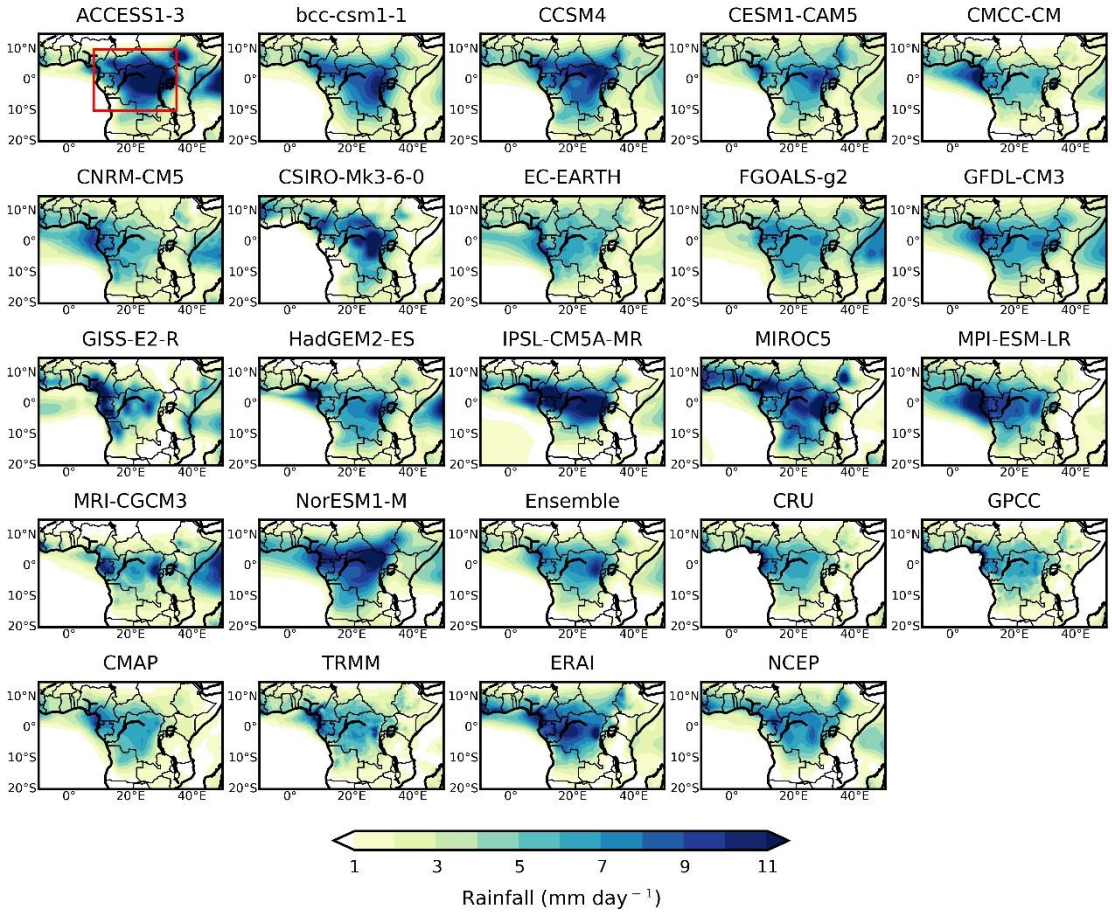

Figure 4.1 - Long term mean (1979-2005) SON rainfall (mm day^{-1}) for 17 CMIP5 models, ensemble mean, reanalysis and satellite-gauge products.

The presence of distinct east and west rainfall maxima raises the possibility that the processes influencing rainfall differ across the basin in coupled models. Figure 4.2 shows the correlation between rainfall in the west of the basin and in the east of the basin, across the suite of models for each of the 12 months. Figure 4.2 highlights that, in the majority of months, rainfall is strongly correlated between both halves of the basin; i.e. models which are wet in the east also tend to be wet in the west. This suggests a common process may be governing model wetness across the basin in these seasons. However, in August-November, rainfall in the east and west are not correlated, suggesting that the processes related to rainfall in each subdomain may be distinct. Studies conducted using reanalysis data on

interannual timescales support this hypothesis, as local processes have been identified which may favour rainfall only in the west of the basin, including the zonal overturning circulation with a downward branch over the Gulf of Guinea [*Cook and Vizy*, 2015] and moisture advection via low-level westerlies from the Atlantic [*Pokam et al.*, 2014].

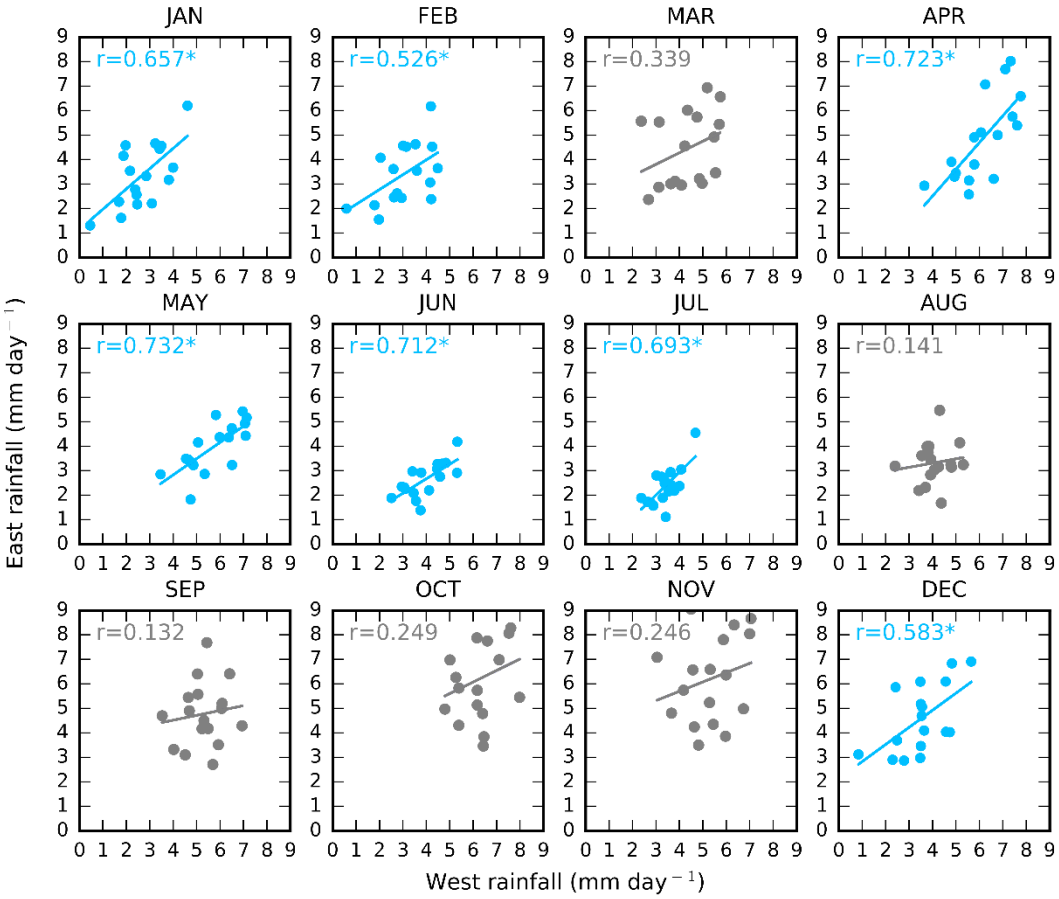

Figure 4.2 - Scatter plots showing relationship between long-term mean (1979-2005) rainfall (mm day^{-1}) in the west (8°E to 21°E, 10°S to 10°N) and in the east (21°E-35°E, 10°S to 10°N) Congo Basin. Blue (grey) plots show relationships that are significant (not significant) at the 95% level.

To help identify the processes associated with differences in rainfall, composites are created of the four wettest and four driest models in each subdomain (based on SON mean rainfall; Table 4.3). Figure 4.3 shows these composites for rainfall. In

addition to showing the magnitude of rainfall differences over the subdomains, Figure 4.3 also highlights significant differences in the surrounding region. For example, in both composites, a wet subdomain is associated with a dry equatorial west Indian Ocean. For the eastern composites, wetness is also associated with drying at the Atlantic coast between north Angola and Gabon. These findings indicate that local SSTs may play a role in determining model wetness or dryness in both subdomains.

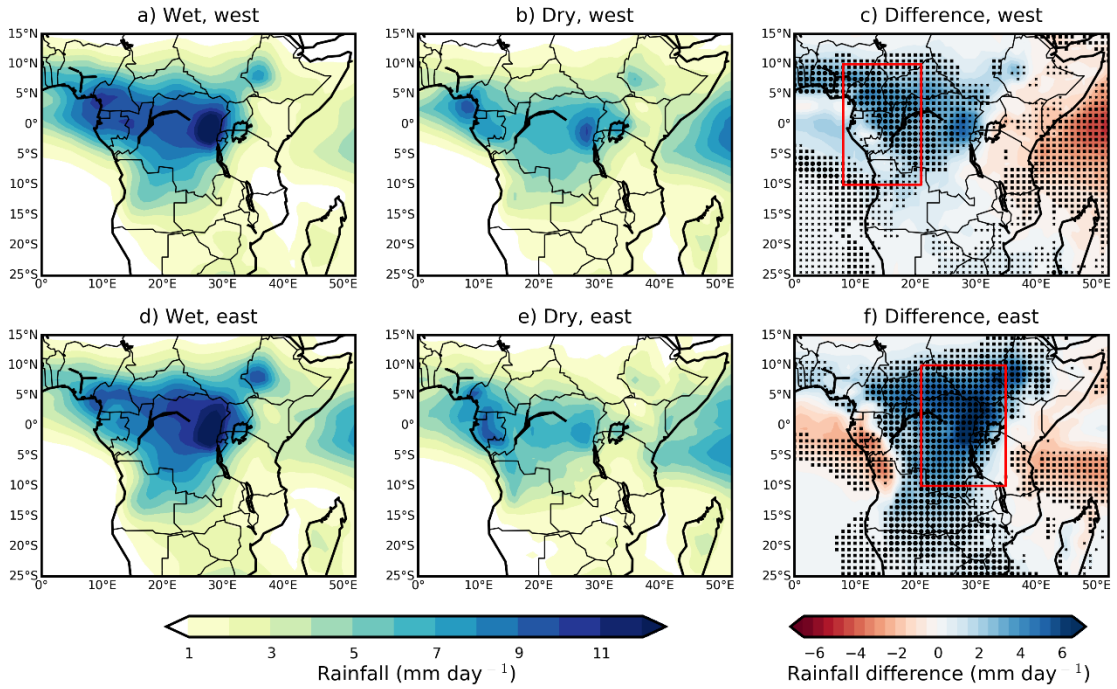

Figure 4.3 - Long term mean (1979-2005) rainfall (mm day^{-1}) composites of (a, d) four wettest models, (b, e) four driest models, and (c, f) the wet-minus-dry difference in the west and east of the basin respectively. The red box shows the location of the subdomain. Stipples occur under the following conditions: (1) where all wet model values are larger or smaller than all dry model values (large dots); (2) where all wet model values are greater or smaller than the dry mean, depending on the direction of difference (squares); (3) where all dry models are greater or smaller than the wet mean, depending on the direction of difference (crosses); and (4) where both (2) and (3) are true (small dots).

4.4 Influence of Tropical Atlantic and Indian Ocean Sea Surface Temperatures

SST biases are well-documented in coupled models and many studies have linked them to biases in the hydrological cycle [*Large and Danabasoglu*, 2006; *Joseph et al.*, 2012; *Bollasina and Ming*, 2013; *Prodhomme et al.*, 2014; *Wang et al.*, 2014; *Eichhorn and Bader*, 2016; *Richter et al.*, 2016]. The Congo Basin is adjacent to two ocean basins, and previous research has linked moisture advected from the Atlantic and Indian Oceans to rainfall variability [e.g. *Pokam et al.*, 2012; *Dyer et al.*, 2017]. Therefore, an evaluation of SST biases in relation to model rainfall biases is a useful first-order assessment.

All CMIP5 models in this study, apart from CSIRO-Mk3-6-0, have a well-documented [e.g. *Wang et al.*, 2014] strong warm bias in the tropical eastern Atlantic (Figure 4.4). This is a common feature of eastern tropical ocean basins in coupled models [*Richter*, 2015; *Zuidema et al.*, 2016]. While the cause of the bias is not fully understood, it likely relates to the location of the Angola-Benguela Frontal Zone (ABFZ), and the inability of models to produce adequate stratocumulus cloud coverage in the south east Atlantic [*Richter et al.*, 2012; *Xu et al.*, 2014]. The proximity of the bias to the western Congo Basin invokes the possibility that it may impact the provision and transport of water vapour in this region. Biases in the Indian Ocean are of much smaller magnitude than in the Atlantic. These are generally much less consistent between models, with some showing slight warm

biases (e.g. CCSM4, bcc-csm1-1) and others slight cold biases (e.g. GFDL-CM3, MIROC5).

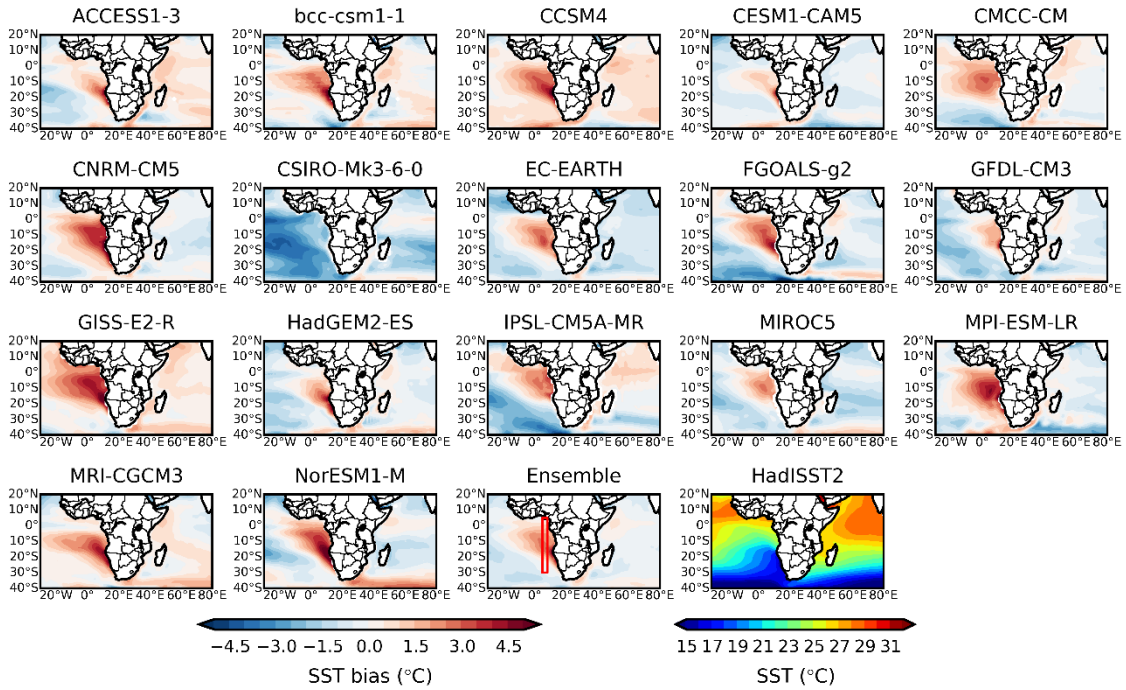

Figure 4.4 - Long term mean (1979-2005) SST bias (°C; model minus HadISST2) in SON, for all CMIP models, and HadISST2 observed SST (°C). Red box shows location of Atlantic SST mean bias in Figure 4.8.

As a first-order assessment of how rainfall may be influenced by SSTs, atmosphere-only (AMIP) versions of the CMIP5 models are assessed. In AMIP experiments, the atmosphere model is forced with observed SSTs, and so comparisons between CMIP and AMIP runs are a useful indicator of model biases which may be produced by ocean-atmosphere coupling in coupled models. Figure 4.5 shows the difference in long-term mean rainfall between 17 CMIP and AMIP model experiments. It indicates that the largest differences between CMIP and AMIP tend to be in the western half of the Congo Basin and over the Gulf of Guinea (~2-4 mm day^{-1}). In

the east, the difference between CMIP and AMIP is smaller in most models. It is also interesting to note that CSIRO-Mk3-6-0, the only model to have a mean cold bias (-1.9°C) in the tropical Atlantic, is also the only model where AMIP is wetter than CMIP in the west. Despite it clearly having a different coupling error to most models, this indicates that it may respond to SST biases in a similar way, i.e. warm (cold) biases are related to more (less) rainfall near the Atlantic coast.

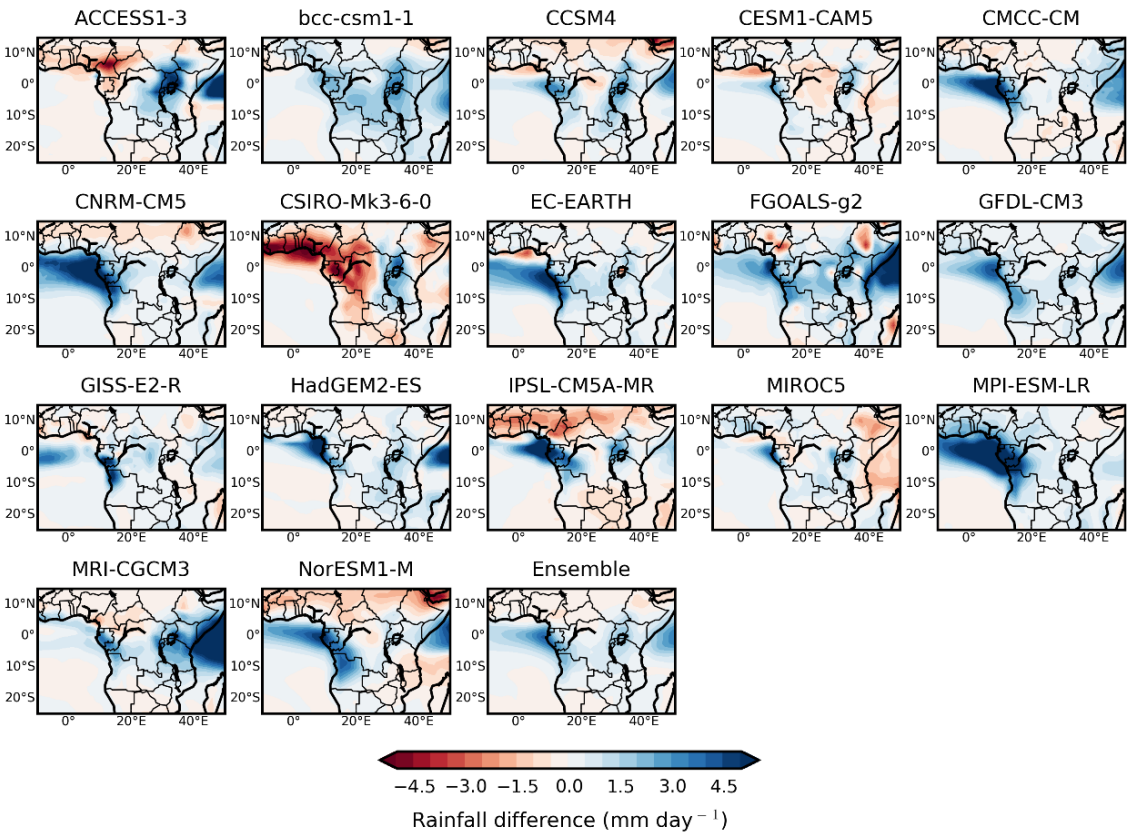

Figure 4.5 - Long term mean (1979-2005) CMIP minus AMIP rainfall (mm day^{-1}) in SON, for all CMIP5 models and the ensemble mean

Figure 4.6 quantifies the differences between CMIP and AMIP in the annual cycle and compares it to the annual cycle of the Atlantic warm bias, the largest and most persistent bias in the region. Boxplots represent the CMIP-minus-AMIP values in

the a) west and b) east of the Congo, for all models in each month. Figure 4.6 highlights that the difference between CMIP and AMIP in the west Congo closely follows the annual cycle of the Atlantic SST bias, particularly in July to October where high median CMIP-AMIP differences (0.99 - 1.58 mm day^{-1}) correspond to the largest SST biases (1.90 - 2.47°C). Between January and April, small SST biases correspond with much smaller differences between AMIP and CMIP. The boxplot for the east Congo (Figure 4.6b) suggests that SST biases in general are less important for differentiating between wet and dry models in this region, as CMIP and AMIP values are much more similar. In addition, throughout the SON period, CMIP-AMIP differences in the east do not as obviously track the cycle of Atlantic SST biases, suggesting that this particular bias has limited effect on relative model wetness in the east Congo.

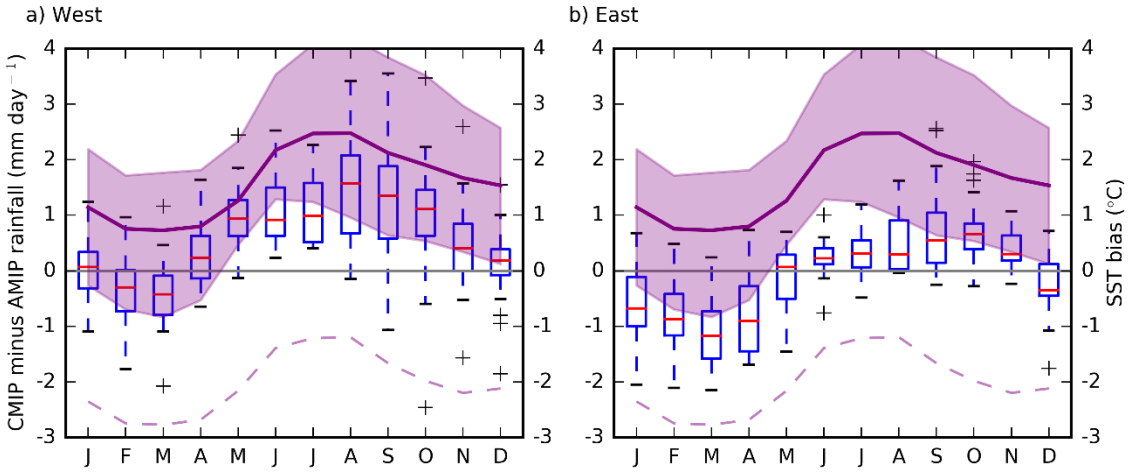

Figure 4.6 - Annual cycle of long term mean (1979-2005): CMIP minus AMIP rainfall (mm day^{-1}) for all models (boxplot); the mean model Atlantic SST bias between 5°W to 8°E, 12°S to 3°N (°C ; purple line); and intermodel spread of Atlantic SST biases (purple shaded area; excluding CSIRO-Mk3-6-0). The dashed line shows the SST bias in CSIRO-Mk3-6-0, the only model to have a consistent cold bias.

Whilst AMIP experiments are a useful comparison point, they must be treated with some caution for two reasons. First, they do not allow for interaction between the atmosphere and ocean, so atmospheric processes which would induce a feedback from the ocean in the real world are not represented. Second, they represent a "correction" of SSTs on a global scale, and so AMIP simulations do not to isolate the effects of correcting a specific bias such as the one in the south east Atlantic. Nevertheless, CMIP/AMIP comparisons give a good first indication of the impact of SST biases.

4.5 Identifying processes related to rainfall differences

The results so far highlight that:

a) Rainfall in the west is not correlated with rainfall in the east across CMIP5 models, so different processes may be dominant in maintaining rainfall in the east and the west subdomains.
b) CMIP-AMIP differences are larger in the west Congo than in the east, suggesting a larger influence of SSTs in this subdomain.

The following section attempts to identify a chain of processes which explain rainfall differences in each subdomain in turn. ERA-I is included in the following plots to give a sense of whether wet or dry composites are closest to an observational 'best-guess'; however, comparison with reanalysis is not the dominant method for assessing model credibility.

4.5.1 Processes in the west

To help identify how model rainfall may be related to the Atlantic SST bias, wet and dry west Congo composites are shown in Figure 4.7. The largest bias in both wet and dry models is in the tropical east Atlantic, where models feature large (>2°C) warm biases. The bias is consistently warmer (approximately 1-2°C) and more equatorward in the wet composite. In addition, wet models also feature a cold anomaly, relative to dry models, in the west Atlantic, near the South American coast. A similar warm-cold pattern is evident in the Indian Ocean, though the magnitudes of both the bias and difference between wet and dry models are much weaker.

Given its proximity to the west Congo, it is hypothesised that the warm Atlantic SST bias is one of the dominant influences on model wetness. To further understand the Atlantic warm bias in this season in particular, Figure 4.8 shows the annual cycle of the Atlantic coast SST bias (5°E to 8°E, 25°S to 2°N; see ensemble plot of Figure 4.4) in the west composites. For wet models in the west of the basin (Figure 4.4a), the Atlantic SST warm bias is present in all months between 0° and 15°S, but is strongest from June to October between 0° and 5°S. In the dry models, the northerly bias is much weaker, and the strongest bias is further south, centred on 15°S. The wet-minus-dry difference shows that the largest amplitude and most consistent difference is centred over August and the SON rainy season; stipples indicate that all wet models have a bias larger than the dry model mean. Correlation analysis across all models between mean rainfall in the west

Congo Basin and mean SST bias in the studied box along the tropical Atlantic coast shows that this relationship holds across the suite of models (r=0.67, p<0.007).

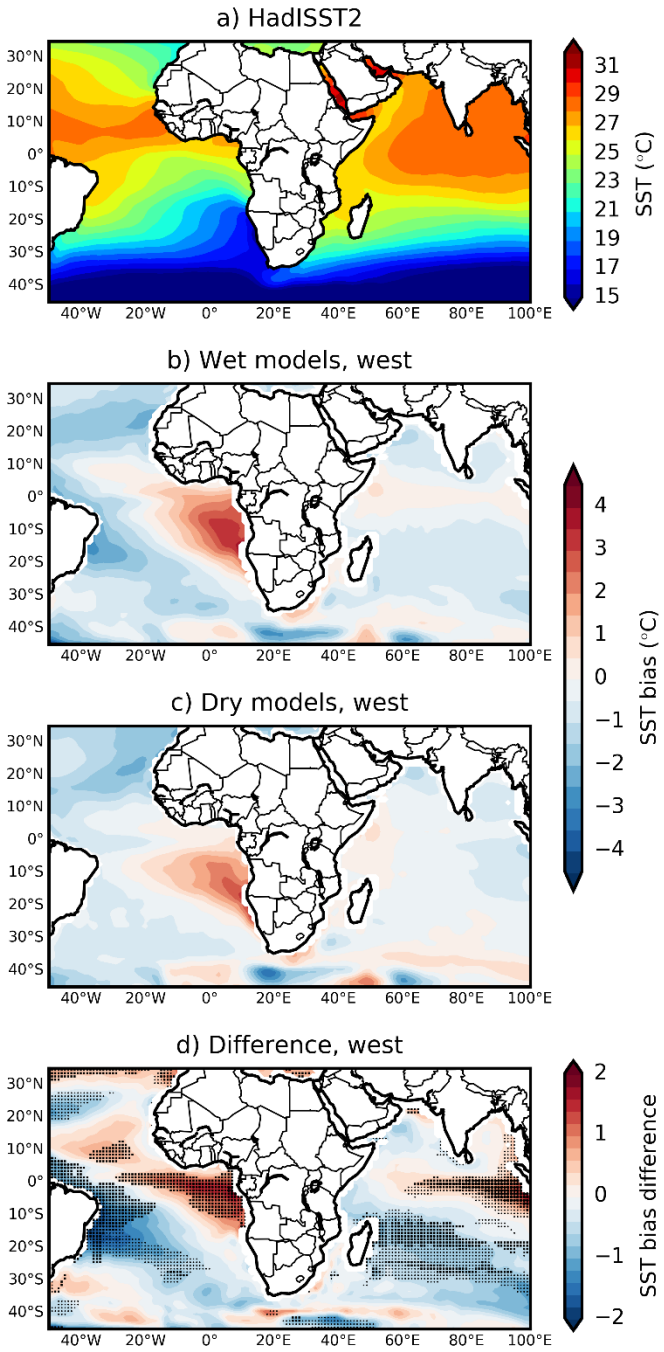

Figure 4.7 - Long term mean (1979-2005) SST bias (°C) in SON in (a) HadISST2 (observed), (b) west Congo wet composite, (c) west Congo dry composite, and (d) wet-minus-dry difference between wet and dry composite.

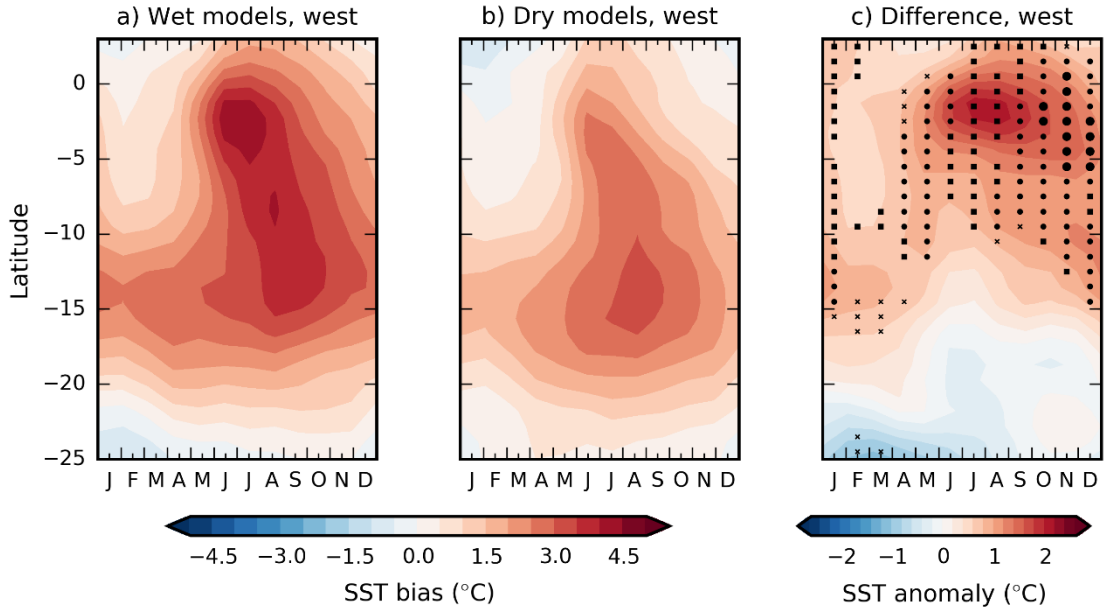

Figure 4.8 - Annual cycle of long term mean (1979-2005) SST bias (°C; model minus HadISST2) between 5°E and 8°E for the (a) west Congo wet composite, (b) west Congo dry composite, and (c) the wet-minus-dry difference.

One way in which a warm SST bias could affect Congo rainfall is by enhancing available moisture via increased evaporation. Composites of evaporation in the Gulf of Guinea in wet and dry models are shown in Figure 4.9. For most of the Gulf of Guinea region and the central African coast, evaporation is significantly higher in wet models across most of the central east Atlantic. A comparison with ERA-I shows that the dry models are much closer to the reanalysis estimate than wet models, further suggesting that the stronger SST bias in wet models may be causing enhanced evaporation.

Higher evaporation rates in wet models is hypothesized to be related to enhanced moisture advection through the western boundary of the Congo. This is based on both observational studies [*Pokam et al.*, 2012, 2014; *Cook and Vizy*, 2015] and

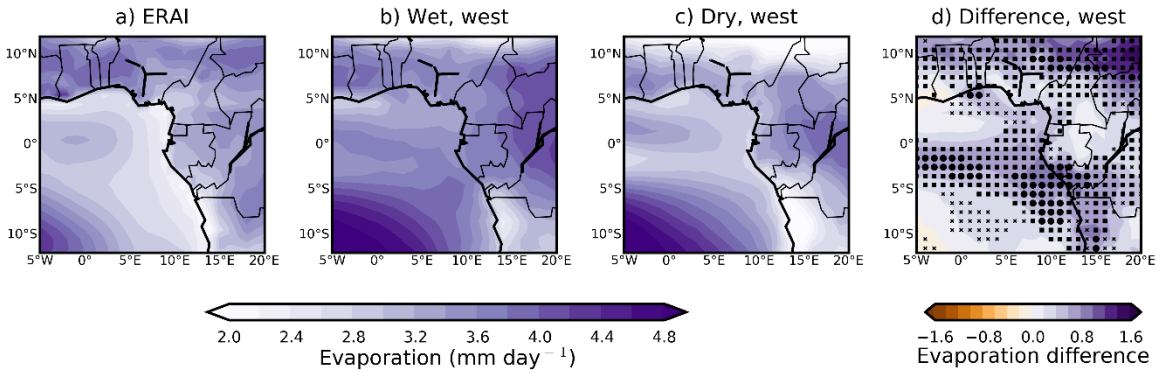

Figure 4.9 - Long term mean (1979-2005) evaporation (mm day^{-1}) in SON in (a) ERA-I, (b) west Congo wet composite, (c) west Congo dry composite and (d) wet-minus-dry difference. Stipples are as described in Figure 4.3 caption.

model analysis [*Creese and Washington*, 2016]. The long-term mean 925 hPa moisture flux (qflux) and qflux convergence for the composites and ERA-I is shown in Figure 4.10. ERA-I is a useful comparison point for wind-related processes, as dynamical components such as wind are much better constrained than heavily parameterised processes such as rainfall. Both wet and dry models show some similarity to ERA-I; north-easterly flow over the south-east Atlantic, which re-curves into north-westerly flow at the equator. This is promising as it suggests that models are producing credible circulation features; it also indicates that wet/dry differences in the west are the result of differences in the amplitude of the same mechanism, rather than distinct mechanisms. The wet-minus-dry difference plot shows that wet models have enhanced wind convergence over the western subdomain, and stronger westerlies in the central tropical Atlantic and at the central African coast. In conjunction with Figures 4.8 and 4.9, this suggests that a combination of local convective and circulatory processes is a key driver of rainfall differences in the west Congo.

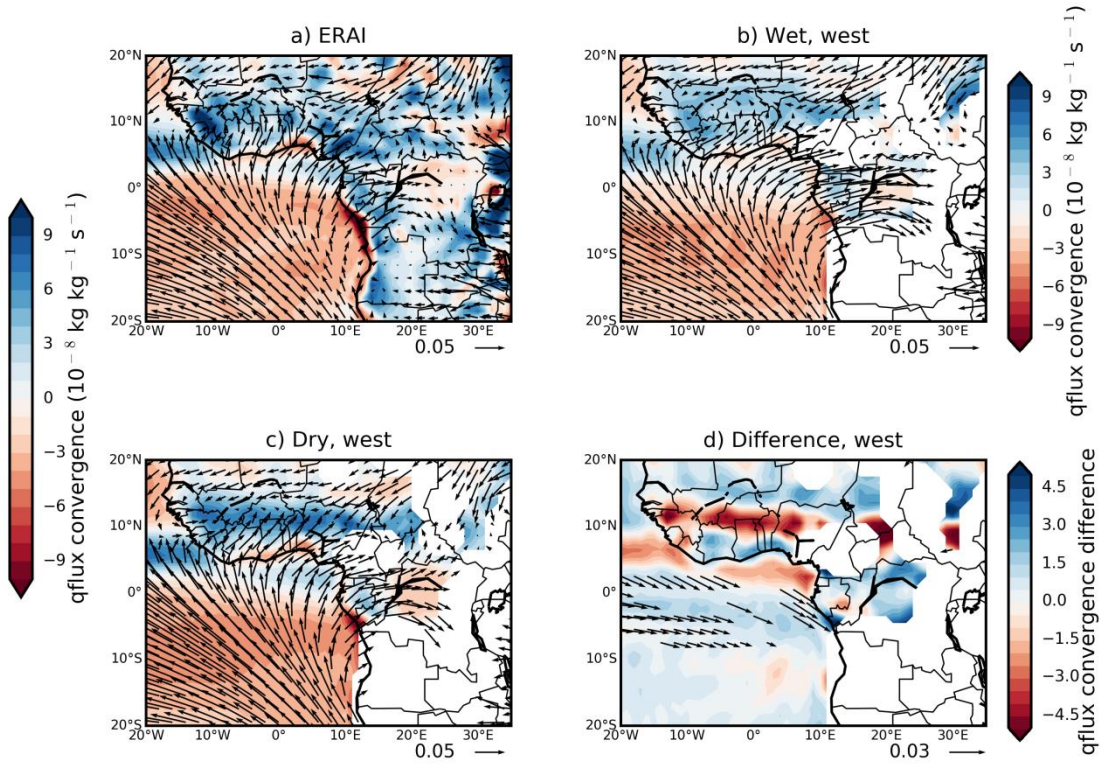

Figure 4.10 - Long term mean (1979-2005) SON qflux convergence (10^{-8} kg kg^{-1} s^{-1}; shaded) and qflux (kg kg^{-1} m s^{-1}; vectors) at 925 hPa in (a) ERA-I, (b) west Congo wet composite, (c) west Congo dry composite and (d) wet-minus-dry difference. Vectors are only shown at gridboxes in (d) when the values in all wet models are greater than the values in all dry models, or all the values in all dry models are greater than the values in all wet models.

Studies of interannual variability in reanalysis data find that low-level westerly flow into the Congo Basin in SON forms the lower branch of an Atlantic-Congo zonal overturning circulation with uplift over the continent [*Pokam et al.*, 2014; *Cook and Vizy*, 2015]. Figure 4.11 shows the vertical profile of omega, averaged between 3°S and 3°N, as a cross-section by longitude, for the composites and ERA-I (the purple box shows the longitudinal extent of the western subdomain). Overlain are streamlines of the divergent component of zonal wind and omega. The divergent component of zonal wind has been used as it is the component that is coupled with omega [*Cook and Vizy*, 2015]. Over the Atlantic and the west Congo

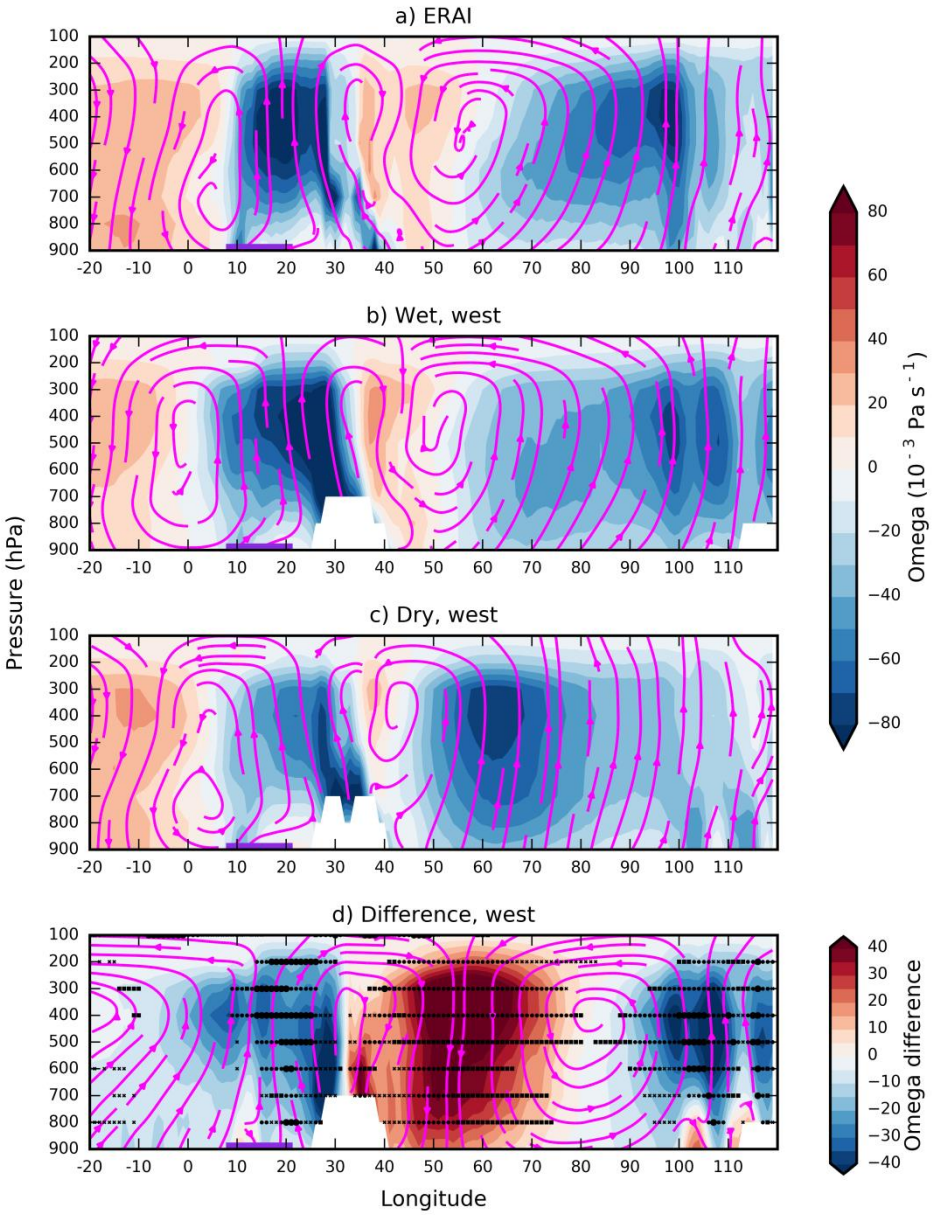

Figure 4.11 - Long term mean (1979-2005) SON omega between 3°S and 3°N (10^{-3} Pa s^{-1}; shaded) and divergent component of zonal wind (m s^{-1}) and omega (streamlines) in (a) ERAI, (b) west Congo wet composite, (c) west Congo dry composite, and (d) wet-minus-dry difference. Stipples are as described in Figure 3 caption. A bilinear interpolation scheme was used to fill missing values to calculate the divergent component of u-wind. Areas with high topography in models are masked (white); values below 900hPa are not shown due to large amounts of topography-related missing data. The purple box shows the extent of the west Congo domain.

the circulation in both wet and dry models takes the same general form as in ERA-I; a large region of convection over land, and subsidence over the ocean; the streamlines show that this is a connected zonally overturning circulation. Previous

studies have identified the zonal overturning circulation as a mechanism for advecting moisture into the basin, and *Cook and Vizy* [2015] study suggests that in years with above average SSTs, the zonal overturning circulation is strengthened due to enhanced evaporation and increased westerly moisture flux. However, Figure 4.11d shows that whilst wet models do have enhanced upward motion over the Congo, they do not have correspondingly stronger subsidence over the Atlantic Ocean. Therefore, wet models cannot be said to have a stronger Atlantic-Congo overturning circulation. Instead it appears that warmer SSTs and the associated increased in evaporation drive a local enhancement of convection, leading to greater rainfall over the coastal region.

The Atlantic-Congo cell is one aspect of the equatorial zonal cell; Figure 4.11 shows that there are also differences between wet and dry models in the Indian Ocean cell(s). The wet composite features enhanced convection in the east Indian Ocean (90-120°E), coincident with the warm anomaly compared to the dry composite (Figure 4.7d). This is connected via an overturning cell to enhanced subsidence over the east Indian Ocean and the East African coast, which in turn is connected to outflow from the Atlantic-Congo cell. This may explain why the wet composite features anomalous drying at the East African coast (Figure 4.3). In contrast, dry models feature significantly weaker convection in the east Indian Ocean, and greater convection in the west Indian Ocean (50-80°E). This has two implications. First, as the location of this cell much further westward, there is enhanced rainfall in the west Indian Ocean (Figure 4.3) compared with wet models. Second, the region of subsidence over the East African coast, present in the wet composite and ERA-I, occupies a much smaller longitudinal region, as the two up-branches are

closer together. This may also contribute to dampening of convection over the Congo, and subsidence from the Indian cell interacts with convection from the Atlantic cell.

4.5.2 Processes in the east

Figures 4.5 and 4.6 indicate that differences in model rainfall in the east Congo are less sensitive to SST biases as in the west. Nevertheless, given the scale of SST biases in coupled models, there could still be SST influences of opposite signs which work to partially cancel each other out, and which still represent implausible processes in the models. Figure 4.12 shows SST differences between the wet and dry composites. There is no significant difference in the warm bias in the tropical Atlantic coastal region between wet and dry models in the east, and additionally no significant difference in evaporation in this region (not shown), again suggesting that the influence of the tropical Atlantic SST bias in enhancing evaporation only manifests locally, and does not extend further eastward into the basin. Instead, Figure 4.12 suggests that east Congo model rainfall is connected to more remote SST biases in models. Wet models feature colder central and west Atlantic SSTs, and a small area of consistently warmer SSTs in the tropical east Indian Ocean. The west Indian Ocean does not appear to be a significant factor in differentiating between wet and dry models in the east Congo Basin. In this section we attempt to identify processes which may be driving the differences between models in the east.

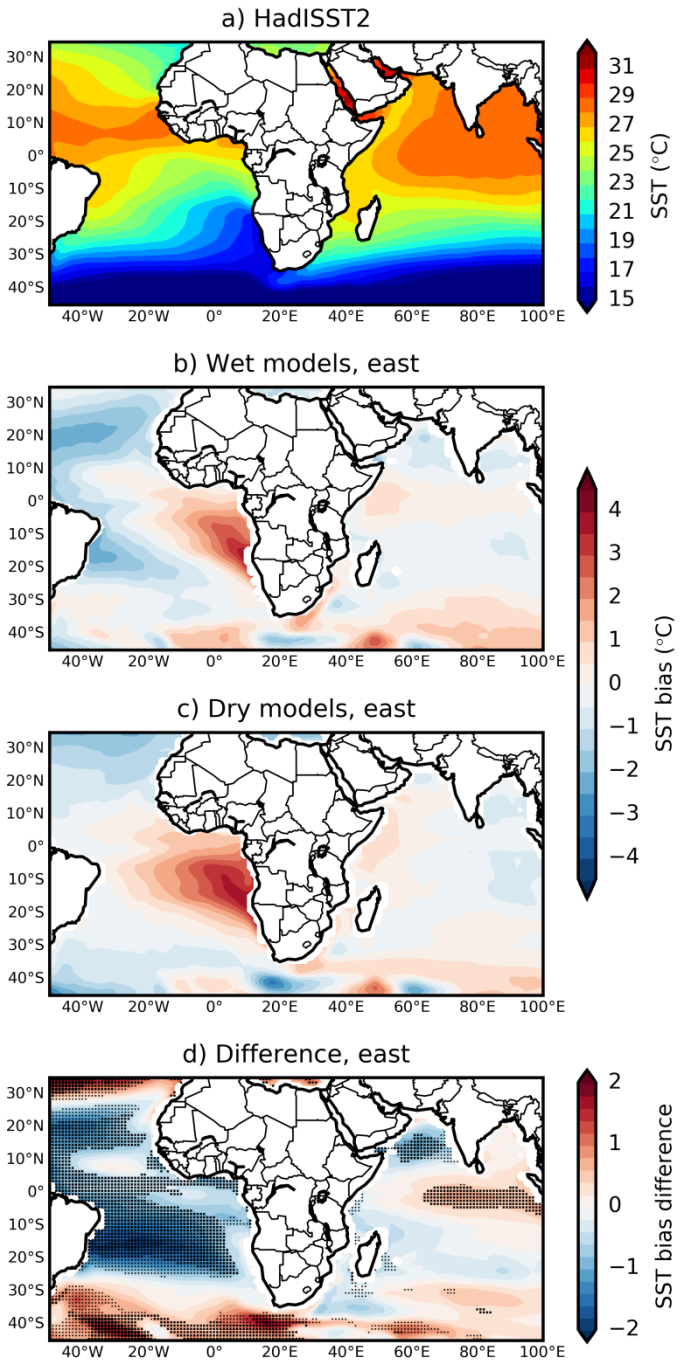

Figure 4.12 - As in Figure 4.7 but for the east Congo composites

As well as influencing rainfall via enhanced moisture availability, as appears to be the dominant effect in the west Congo, SSTs can also influence the dynamical circulation, including wind direction and intensity, particularly at low levels. Figure 4.13 shows the low-level (925 hPa) and mid-level (700 hPa) qflux and qflux

convergence climatologies in the composites and ERA-I. At both levels the models broadly capture the patterns seen in reanalysis. At 925 hPa (Figure 4.13a), the key differences between wet and dry models are an enhanced westerly flow from the Atlantic. The enhanced westerly flow from the Atlantic is due to greater recurvature of the south-easterlies, which are also stronger in the wet composite. This resembles that seen in Figure 4.10 for the wet/west models. There are two key differences, however. In wet/west models, the flux was more convergent at the coast, whereas in wet/east models the flow is more divergent. In addition, the westerlies in wet/east models extend much further into the basin. This suggests that greater acceleration (i.e. divergence) of the westerly flow at the Atlantic coast is allowing moisture to penetrate further inland to the east of the basin in wet models. Wet models also feature enhanced south easterly flow in the south Indian Ocean, emulating that in the south east Atlantic.

At 700 hPa (Figure 4.13b), the direction of the zonal flux is reversed; both wet and dry models show mean easterly flow, associated with the African Easterly Jets. However, the wet-minus-dry difference shows that wet models have anomalous westerlies at the equator. This suggests that one or both components of the AEJ are weaker in wet models. At upper-levels (200hPa; not shown), wet models feature stronger easterlies, particularly to the west of 35°E, which is consistent with a stronger upper branch of the zonal overturning circulation. This finding is also analogous to *Dezfuli and Nicholson* [2013] finding that wetter years in observations feature enhanced (reduced) upper-level (mid-level) easterly flow. The role of both low- and mid-level processes, and their connections to the overturning circulation and upper-level flow, is assessed below.

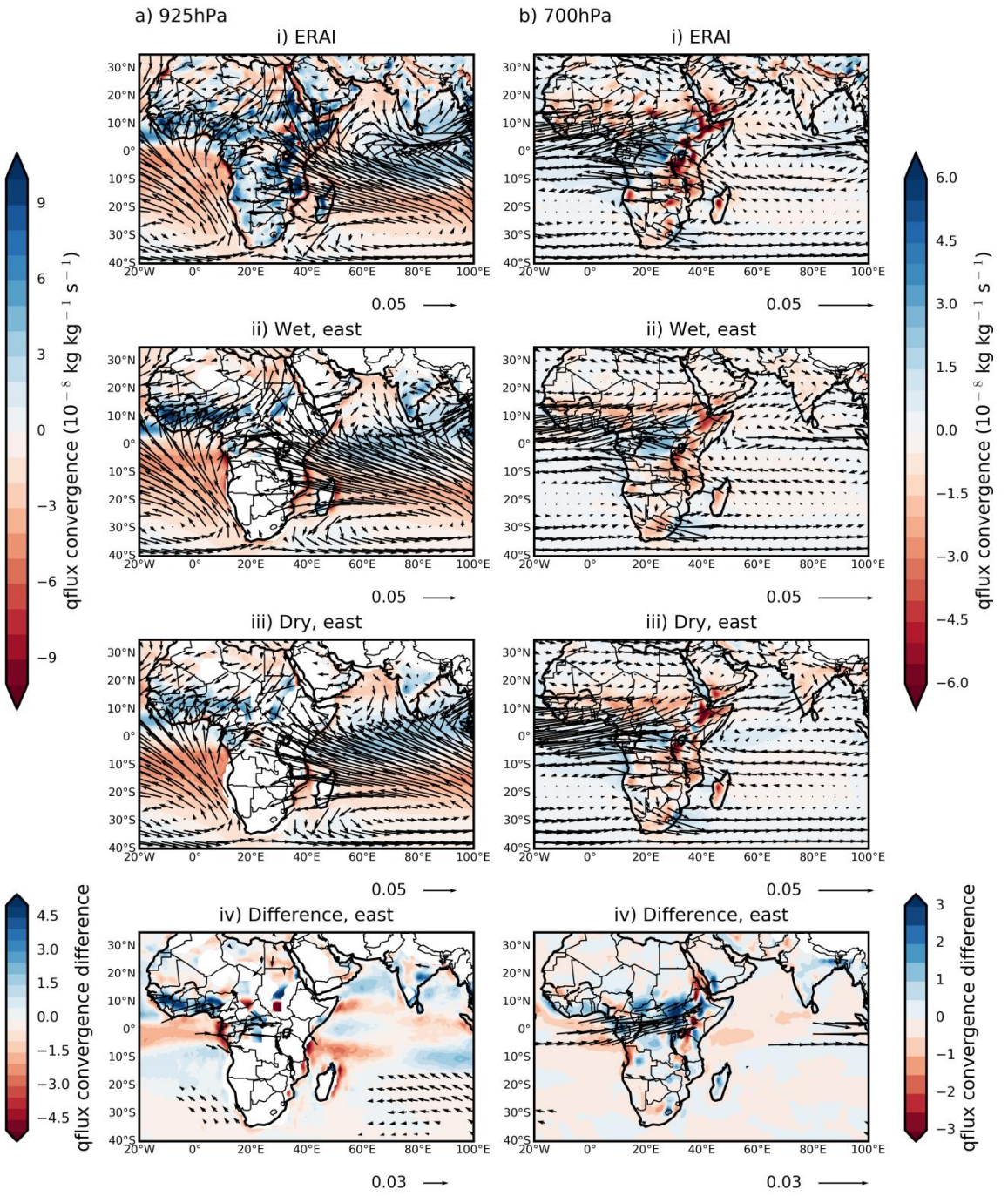

Figure 4.13 - Long term mean (1979-2005) SON qflux convergence (10^{-8} kg kg^{-1} s^{-1}; shaded) and qflux (kg kg^{-1} m s^{-1}; vectors) at (i) 925 hPa and (ii) 700 hPa in (i) ERA-I, (ii) east Congo wet composite, (iii) east Congo dry composite and (iv) wet-minus-dry difference. Vectors in (iv) are as described in Figure 4.10 caption.

4.5.2.1 Low-level circulation differences

Enhanced recurvature of low-level south-easterlies into south-westerlies in the south Atlantic has previously been linked to the South Atlantic high pressure system (SAH) [*Nicholson and Grist*, 2003]. The strength of the subtropical highs can also influence (or be influenced by) SSTs, which Figure 4.12 highlights are anomalously cold here in wet models. Figure 4.14 shows the mean sea level pressure (shading) overlain with 925 hPa qflux vectors in the two ocean basins, for ERA-I, wet and dry models in the east, and the wet-minus-dry difference. Wet models have an enhanced and south-shifted SAH compared to dry models; this is significant across the whole suite of models, where correlation between mean sea level pressure in the SAH region and rainfall is strong and positive ($r=0.81$, $p=<0.0003$). Wet models also have a stronger Mascarene High, though the difference in strength is smaller than the SAH. In both oceans the enhanced high coincides with enhanced south-easterlies to the north east of the high. In the Atlantic, these recurve into enhanced westerlies at the equator near the African coast. There is a strong, positive correlation between the mean strength of the SAH (averaged between 40°S and 15°S, 40°W to 10°E) and the mean westerlies (averaged between 5°S to 5°N, 0° to 20°E) ($r=0.70$, $p<0.004$).

Given the known link between equatorial westerlies and the zonal overturning circulation in this region, the overturning circulation over the wider region is shown in Figure 4.15. While both wet and dry models feature low-level westerly flow, in the wet composite this is part of a well-defined Atlantic-Congo zonally overturning circulation up to 200 hPa. Dry models feature a much weaker and less

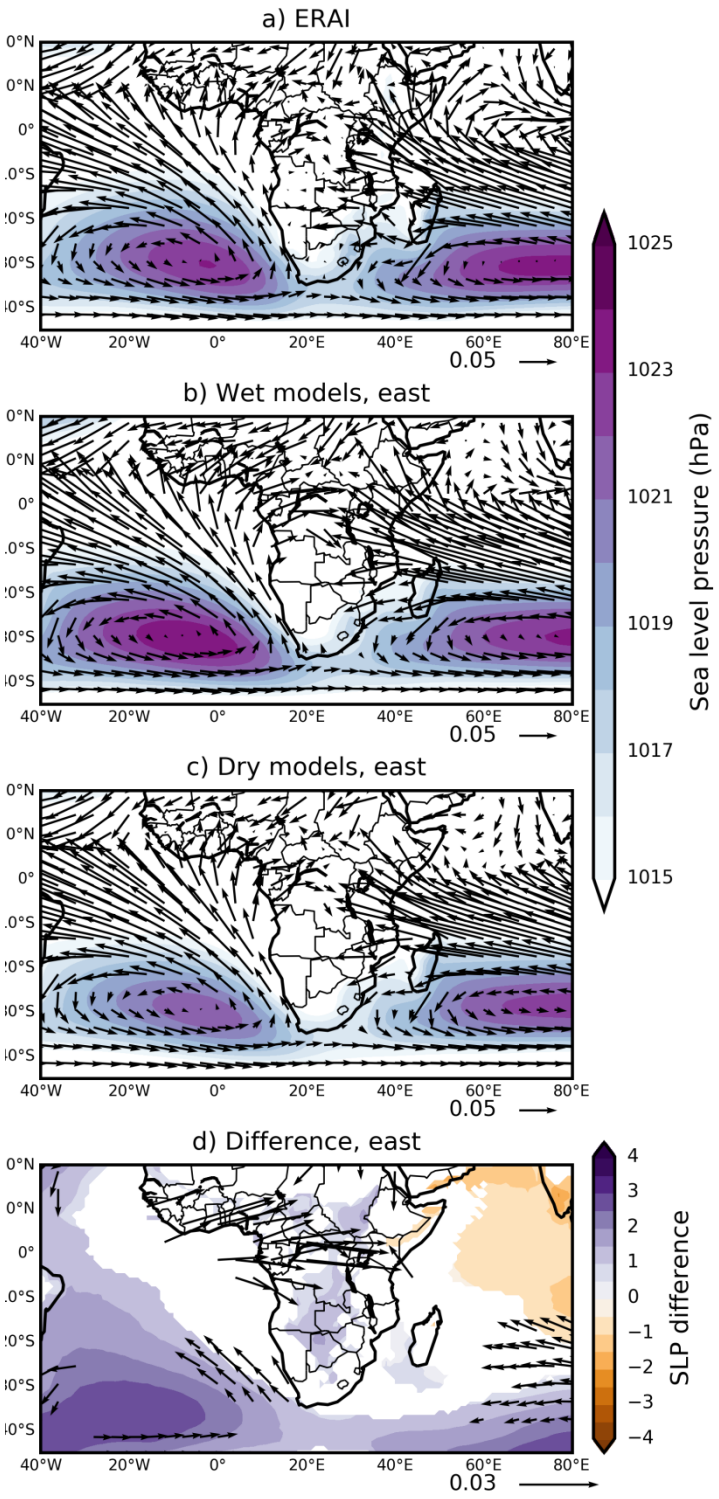

Figure 4.14 - Mean sea level pressure (hPa; shaded) and 925 hPa qflux (kg kg^{-1} ms^{-1}; vectors), in (a) ERA-I, (b) east Congo wet composite, (c) east Congo dry composite and (d) wet-minus-dry difference. Vectors and MSLP shading are only shown at gridboxes in (d) when the values in all wet models are greater than the values in all dry models, or all the values in all dry models are greater than the values in all wet models.

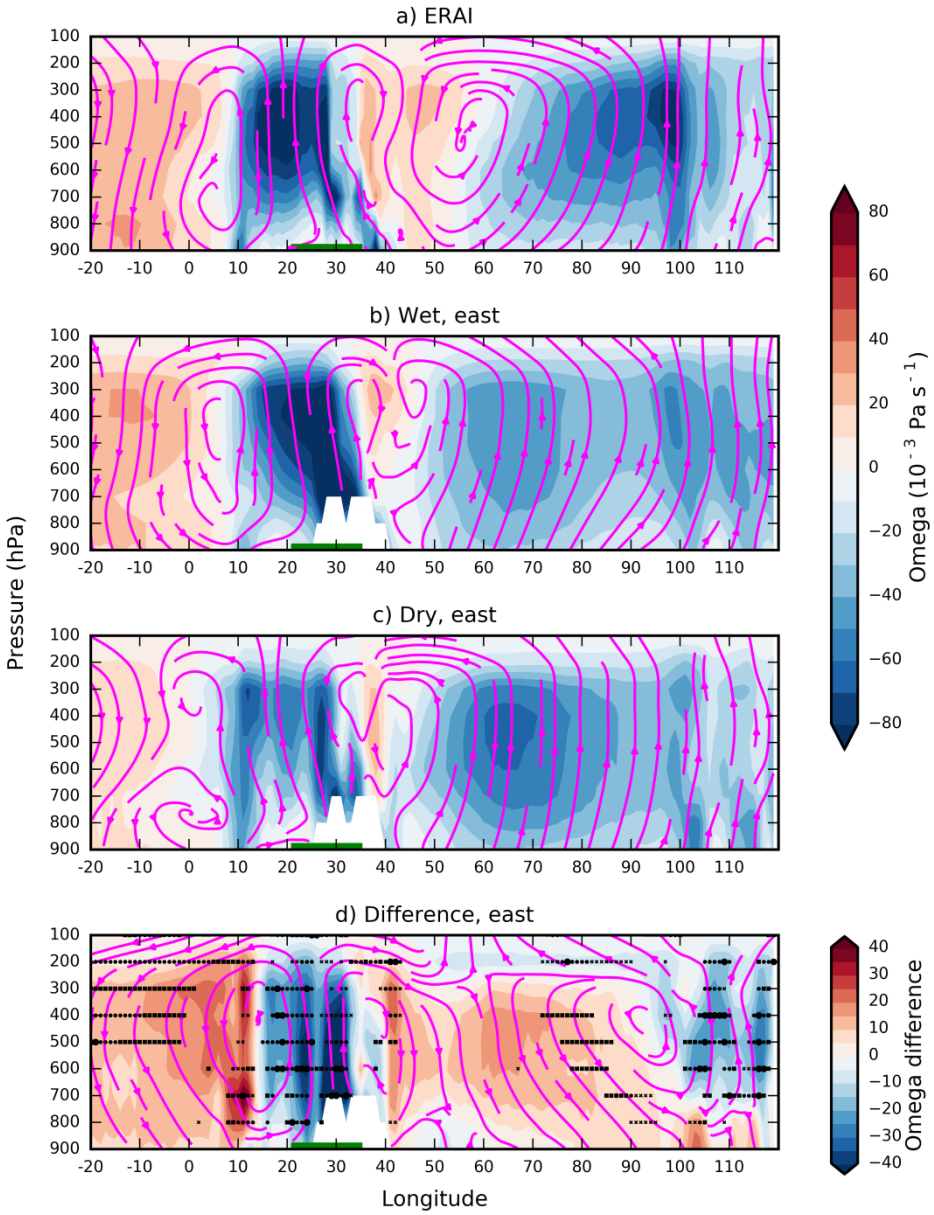

Figure 4.15 - As in Figure 4.11 but for east Congo composites. The green box shows the extent of the east Congo Basin domain.

well defined overturning circulation. The wet-minus-dry difference plot confirms that the wet composite features both much stronger uplift and subsidence, over the majority of the circulation. Given the lack of significant differences in SST across these composites, this suggests that the driving force for the formation of

the overturning circulation is not related to differences in moisture availability, but instead differences in the strength of the dynamical circulation.

Over the Indian Ocean, the differences between wet and dry models are similar to the west composites, though weaker in magnitude. Wet models feature slightly enhanced convection in the east Indian Ocean (co-located with a warm SST anomaly), whereas dry models feature stronger convection in the west-central Indian Ocean. Again, this means that the region of subsidence over the East African coast is much less developed in dry models, leading to relative wetting there (Figure 4.3).

4.5.2.2 Mid-level circulation differences

Figure 4.13b suggests that wet and dry models also differ in their representation of the mid-level easterly winds. Wet models show weaker easterlies over the majority of the basin, as well as over the Atlantic. These differences may be due to how the models simulate both the AEJ-N and AEJ-S. Figure 4.16 shows the latitude-height section of zonal wind in two longitudinal locations; one over the eastern Congo, and one over the western Congo. In the east Congo, ERA-I features both a northerly and southerly jet at around 700 hPa, with the AEJ-S slightly stronger than the AEJ-N. The wet models also feature a two-jet structure, although the AEJ-S is much weaker. However, dry models do not feature two distinct jets in the mean climatology. Instead they simulate one region of easterly flow centred slightly north of the equator. This structure is also seen in the individual months of September-November (not shown) and extends further west with increasing

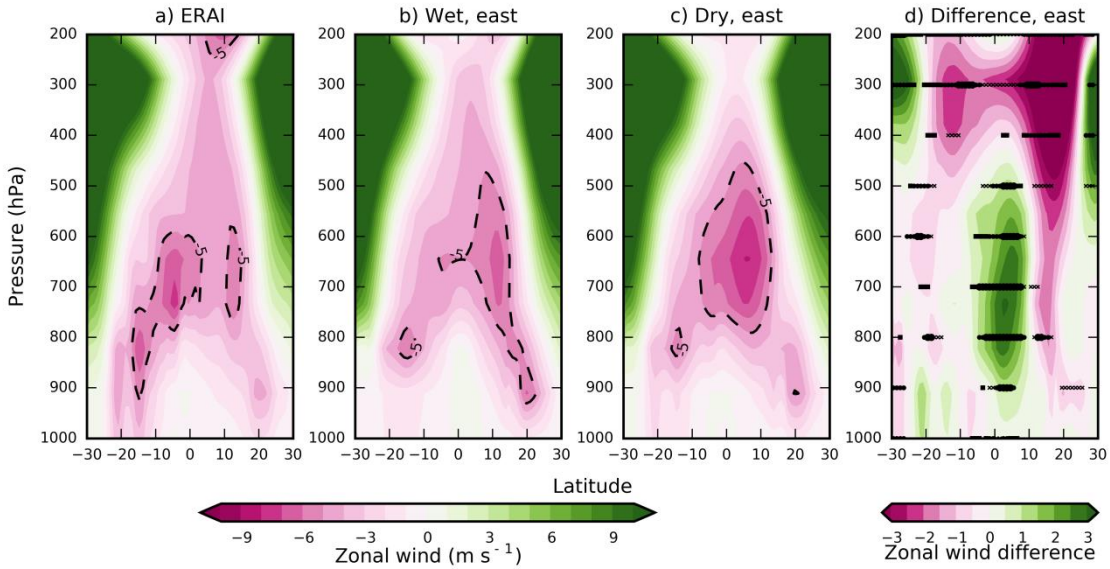

Figure 4.16 - Latitude-height cross section of zonal wind averaged across 26°E-30°E (m s^{-1}; shaded) and location of -5 m s^{-1} contour in (a) ERA-I, (b) east Congo wet composite, (c) east Congo dry composite and (d) wet-minus-dry difference. Stipples in (d) are as described in Figure 4.3 caption.

difference between wet and dry models (not shown). The anomalously strong easterlies in dry models are up to 3 ms^{-1} stronger than wet models and ERA-I at the equator.

The difference between wet and dry model jet strength and location can be explained with reference to the meridional gradient in potential temperature (Figure 4.17). Dry models feature a stronger and more equatorward peak in meridional potential temperature gradient than in wet models. This co-locates well with a more equatorward maximum easterly wind speed at 700 hPa.

Differences in jet strength across the basin suggest that in dry models the anomalously strong AEJ may be suppressing rainfall in the region of the upward branch of the overturning circulation seen in Figure 4.15. This is discussed in the following section.

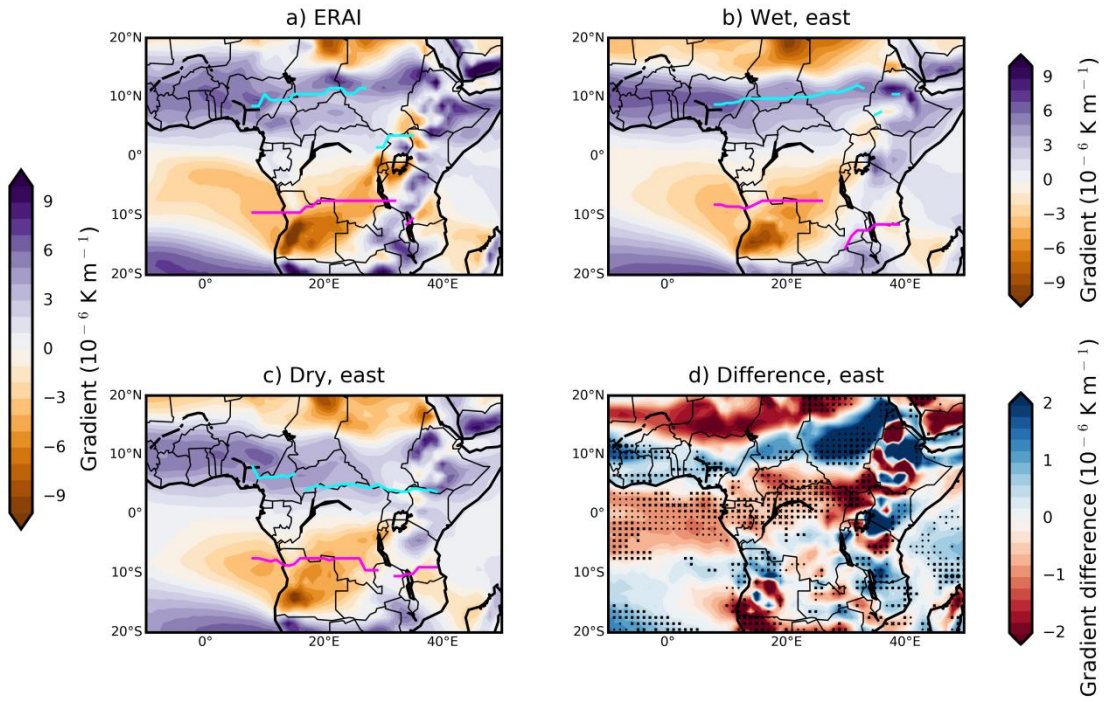

Figure 4.17 - Long term mean (1979-2005) meridional potential temperature gradient (10^{-6} K m^{-1}; shaded) at 850 hPa in (a) ERA-I, (b) east Congo wet composite, (c) east Congo dry composite and (d) wet-minus-dry difference. Lines show latitudinal location of maximum easterly wind speed (≤ -5 m s^{-1}) at 700 hPa in region of AEJ-N (cyan) and AEJ-S (magenta). Stipples in (d) are as described in Figure 4.3 caption.

4.6 Discussion

4.6.1 Rainfall differences between east and west

There is large variation in mean Congo Basin rainfall across models in SON, with some models simulating twice as much rainfall as others. There are also large spatial variations between models, with models tending to feature rainfall maxima in the eastern and western subdomains. These spatial differences have been noted previously [*Creese and Washington*, 2016] but as Figure 4.2 shows, they are of particular interest in SON because models with a wet (or dry) west of the basin do

not necessarily have a correspondingly wet (or dry) east in this season. This mirrors *Dezfuli and Nicholson*'s [2013] finding that different processes relate to interannual rainfall variability in the east and west of the basin in observational data, and suggests that processes relating to model rainfall in each subdomain could be distinct. Our analysis further supports the conclusion that the use of ensemble means as a 'best estimate' of the climatology is misleading in the Congo Basin [*Creese and Washington*, 2016], as the ensemble shows a rainfall magnitude and distribution not captured by any single model.

Figure 4.3 also shows that the distinct wet/dry differences in the west and east Congo are associated with other nearby rainfall differences. Models which are wetter in the west tend to be drier over the west Indian Ocean and the East African coast than models which are dry in the west. Models which are wetter in the east Congo also have slightly drier west Indian Oceans, as well as being drier on the Atlantic coast between north Angola and Gabon. This suggests that factors influencing rainfall in the Congo often have opposite impacts in these adjacent regions.

4.6.2 Influence of SSTs on the west of the basin

It has long been established that regional climates within Africa are coupled to variations in SSTs in both adjacent and remote oceans. For example, Nicholson and Entekhabi (1987) identified that coastal rainfall in equatorial and southern Africa is suppressed in years with low SST anomalies (SSTAs), and enhanced in years with warm SSTAs, as a result of both direct local forcings and indirect atmospheric

mechanisms. *Balas et al.* [2007] found that rainfall variability is associated with ENSO and the west Indian Ocean in the early part of the year, whilst in the summer and early fall the Atlantic becomes more important. Previous studies on coupled models have shown that low level moisture flux across the Atlantic coast is found to be related to model rainfall [*Creese and Washington*, 2016], concurring with studies which show this to be a key region of moisture advection into the Congo in reanalyses [*Pokam et al.*, 2012, 2014]. It is also well-established that coupled models consistently produce a persistent warm bias in the eastern tropical oceanic regions [*Wang et al.*, 2014].

As a first order assessment, Atlantic SST biases appear to be one key differentiator between wet and dry models in the west of the basin. Wet models in the west tend to feature a stronger, more northerly, and more persistent bias in the annual cycle than dry models; this is significant in SON across the suite of models ($r=0.67$, $p<0.007$). The largest difference in west Congo rainfall between AMIP and CMIP models in the annual cycle also co-locates with the peak in the Atlantic SST bias. However, in the east, tropical Atlantic SSTs do not emerge as a significant differentiating factor between the wet and dry composites. Combined with the western subdomain's proximity to the warm bias, this indicates a local process related to SSTs which affects the west, but not the east of the basin. Given that we have good SST observations, we can say with certainty there is a misrepresentation of this process in the mean state of these models. This casts doubt on models which are wet in the west of the basin and have a large Atlantic SST bias, as this rainfall can be related to a spurious chain of processes resulting from a known bias in the mean state.

It is interesting to note that the warm/wet relationship found across models is not due to the same 'chain' of processes as found in wet and dry year comparisons in reanalysis data. *Pokam et al.* [2014] and *Cook and Vizy* [2015] find that years with warm SSTAs are related to enhanced rainfall via a zonal overturning circulation. *Cook and Vizy* [2015] additionally find that the Atlantic cold-tongue and associated land-sea thermal contrast (approximately 2-4K) is necessary to initially set up the overturning circulation. This is not analogous to the relationship found across models in the west, whereby warm SSTAs are associated with enhanced convection over the west Congo Basin coast but not corresponding subsidence over the ocean. This is most likely due to the much larger magnitude of coupled model warm biases compared to year-on-year SSTAs in this season. The largest yearly observed SSTA from the mean in the study period is 0.7°C; positive model biases are on average 1.9°C warmer than the observed. This suggests that while the direction of the relationship between Atlantic SSTs and rainfall is the same in both interannual studies and across models, the chain of processes is not, casting further doubt on the credibility of very wet models in the west Congo with large SST biases.

Analysis of the wider region indicates that wet and dry models can also be differentiated by their representation of the Indian Ocean zonal cell. In contrast to the Atlantic cell, wet models are more similar to ERA-I in the Indian Ocean than dry models. Dry models convect much further westward, away from the warm pool region, and thus feature wetting in the west Indian Ocean where ERA-I and wet models are dry. The down-branch of this circulation is also further westward, possibly contributing to dampened convection over the west Congo. However, SST

biases in the tropical Indian Ocean are relatively small in both composites, and so it is more difficult to determine whether biases are causing the rainfall differences. Further work is needed to assess the plausibility of the link between the Indian Ocean and rainfall in dry models. It may be the case that neither wet or dry models represent a plausible future due to different sets of processes, or that either set of models is producing the correct climatology but for the wrong reasons.

4.6.3 Dynamical processes affecting the east of the basin

The processes which are most important for differentiating between wet and dry models in the east of the Congo Basin appear to be different to those in the west. Tropical Atlantic SST biases are not found to be a differentiator between wet and dry models in the east Congo Basin. Instead, the two dominant processes which are identified relate more to the dynamical circulation of the region. These are discussed below.

First, wet models exhibit enhanced low-level westerly flow from the Atlantic, which is positively related to the strength of the south-easterly flow along the north-east flank of the SAH. These south-easterlies then recurve into westerlies at the equator. This flow is divergent (i.e. accelerates) over the Atlantic coast, where wet/east models are drier (Figure 4.3), and penetrates far into the continent to the east of the basin. This low-level westerly flow constitutes the lower branch of an Atlantic-Congo overturning circulation, which is stronger in wet models than dry models, and which has an enhanced upward branch over the east and central Congo. This cell is also linked to an overturning cell in the Indian Ocean, which has

greater subsidence at the East African coast in wet models. The enhanced SAH may also be linked to the relatively cold SSTs in the south Atlantic in wet models compared to dry models. It is important to note that this analysis cannot determine cause and effect; the enhanced convection over the Congo is itself likely to contribute to stronger subtropical highs via an enhanced Hadley circulation.

In addition to the likely local influence of the SAH on the strength of the westerlies, and thus convection over the east Congo, Figure 4.14 suggests the contrast between relatively high pressures in the subtropical south Atlantic, and low pressures in the Indian Ocean could also play a role in enhancing westerly flow, via an enhanced pressure gradient. *Dezfuli et al.* [2015] identified a similar mechanism that differentiates between wet and dry years in the south east Congo, between December and March. In their analysis, wet years featured anomalously high pressure over the tropical Atlantic and anomalously low pressure over the south west Indian Ocean, contributing to enhanced flow into the eastern part of south equatorial Africa.

The second process identified as important for differentiating between wet and dry models is model representation of the mid-level AEJs. Dry models have much stronger and more equatorward AEJs, which may contribute to suppressed rainfall in the region of the upward branch of the overturning circulation over the central Congo Basin. *Jackson et al.*'s [2009] analysis suggests that a stronger AEJ-S may actually enhance rainfall, as low-level convergence is encouraged at the right-side of the jet entrance which lies over the basin. However, the dry models' tendency to merge the two jets with a core near the equator may suppress this activity, as the

Coriolis influence is small in proximity to the equator. Indeed, at both 700hPa (Figure 4.13b) and 600hPa (not shown), dry models feature anomalous divergence across the basin compare to wet models. The negative relationship between rainfall and AEJ strength has also been found in observational data in this region, whereby dry years feature stronger mid-level easterlies than wet years, associated with anomalous subsidence throughout the column [*Dezfuli and Nicholson*, 2013]. This analysis suggests that the combination of stronger low-level westerlies and weaker mid-level easterlies allows for the formation of a stronger overturning circulation in wet models, enhancing convection over the eastern subdomain of the Congo.

As before, it is interesting to note that the chain of processes relating to rainfall are not the same across models as between years in interannual data. First, the strength of the low-level westerlies appears to be dominated by different processes in models and observations. While some studies have suggested that the formation of equatorial westerlies is associated predominantly with the surface pressure gradient associated with the SAH [e.g. *Nicholson and Grist*, 2003], *Pokam et al.* [2014] suggest that when they recurve into south-westerlies, their strength is driven by the land-sea thermal contrast near the equator. However, in models the land-sea contrast is significantly weakened due to the large SST biases in the equatorial Atlantic, and the difference in strength of both the south easterlies and westerlies appears to be related to the strength of the South Atlantic High. Second, whilst both wet models and wet years in reanalysis feature enhanced overturning circulations, the mechanisms responsible for setting up and driving this circulation are not the same. *Cook and Vizy* [2015] analysis found that a strong overturning

circulation, and associated increase in rainfall, is related to anomalously warm SST biases, as they contribute to enhanced moisture flux into the region. This study instead finds that an anomalously strong low-level westerly flow in wet models is the main differentiating factor, as SST differences are negligible. Therefore, whilst observational studies of interannual variability are a good starting point for determining the processes likely to influence relative rainfall in models, in this instance they are not a complete analogue for how models behave.

4.7 Summary

This study uses a process-based methodology to try and determine some of the processes related to model rainfall in SON in the Congo Basin. Mean rainfall in SON can differ by as much as a factor of three amongst CMIP5 models, and models feature large differences in rainfall distribution. Rainfall in the west and east of the basin is not correlated across models in SON; i.e. models which are wet in the west are not necessarily wet in the east, whereas in most months, western and eastern rainfall are positively correlated. This suggests that distinct processes may be the dominant influences on rainfall in each half of the basin in SON.

Wet models in the west of the basin tend to have a stronger warm SST bias in the tropical eastern Atlantic than dry models. A proposed chain of processes in the west is as follows:

a) Wet models tend to have higher SST biases in the Gulf of Guinea.
b) This enhances evaporation at the coast.

c) Enhanced evaporation contributes to a local enhancement of convection and thus rainfall on the western Congo coast.

Enhanced rainfall in the west is also linked to a stronger Indian Ocean overturning cell, which may in turn be related to anomalously warm SSTs in the east Indian Ocean. However, this SST link is less obvious than in the tropical Atlantic, and more work is needed to establish the plausibility of this mechanism.

Model wetness in the east of the basin is unrelated to the strength of Atlantic SST biases, and appears to be more related to dynamical processes. A proposed chain of processes in the east is as follows:

a) Wet models have significantly stronger low-level westerlies across the tropical eastern Atlantic, related to the strength of the South Atlantic High.
b) This flow is more divergent at the Atlantic coast in wet models and penetrates further inland to the east Congo Basin.
c) The stronger LLWs form the lower branch of an enhanced zonally overturning circulation, which contributes to greater moisture advection into and greater uplift over the east Congo Basin.
d) A stronger Indian Ocean overturning cell may also contribute to greater subsidence over the west Indian Ocean and greater convection over the east Congo.
e) Wet models have a weaker and more poleward AEJ-N, whereas the stronger and more equatorward AEJ-N in dry models may contribute to disrupting the overturning circulation and suppress rainfall.

This assessment questions the credibility of models which are very wet in the west of the Congo where they are associated with a large Atlantic SST bias. However, this does not necessarily mean that dry models are more plausible; this analysis suggests that dry models feature a significant different Indian Ocean overturning cell, and further work is needed to establish the plausibility of this. Further work is needed to assess the credibility of rainfall-producing processes in coupled models in the east Congo, due to the presence of several processes with combined effects.

Acknowledgements

The GCM data used in this study was made available through the Earth System Grid Federation (ESGF) Peer-to-Peer system (https://pcmdi.llnl.gov/search/cmip5/). We also acknowledge NOAA/OAR/ESRL PSD and ECMWF for making available the NCEP and ERA-I datasets. The first author is fully funded by the UK Natural Environmental Research Council (NERC) via a Doctoral Training Programme (grant number: NE/L002612/1), and partly funded by a UK Met Office CASE studentship. Richard Washington is partly supported by NERC and the U.K. Government's Department for International Development (DfID) UMFULA project (NE/M020207/1). The authors acknowledge the helpful inputs of Callum Munday, Dr Rachel James and Dr Neil Hart, and thank the two reviewers for their constructive comments on the manuscript.

5 The plausibility of September-November Congo Basin rainfall change in coupled climate models

The plausibility of September-November Congo Basin rainfall change in coupled climate models

A. CREESE[1], R. WASHINGTON[1] and C. MUNDAY[1]

[1]Climate Research Lab, School of Geography and the Environment,

University of Oxford, South Parks Road, Oxford, OX1 3QY, UK

Submitted to *Journal of Geophysical Research: Atmospheres*

16th October 2018

Accepted for publication

20th March 2019

Key points:

- The magnitude and distribution of Congo Basin rainfall change varies across coupled models in the future
- Process-bases model evaluation can help identify the plausibility of rainfall projections in the absence of observational data
- Low magnitude wetting in the east Congo Basin seems implausible as it builds on underlying biases in the African Easterly Jets

Authorship Declaration

I conducted all of the analysis and writing for this paper. Richard Washington and Callum Munday both discussed the methodology with me, contributed to the interpretation of the results, and provided comments on the manuscript.

Abstract

As one of three hotspots of tropical convection, potential future changes to the Congo Basin climate system will have regional and tropics-wide implications. However, the latest generation of climate models from the Coupled Model Intercomparison Project 5 (CMIP5) disagree on the sign and magnitude of future change and diverge in their estimation of the historical rainfall climatology, in some months by a factor of five. This study assesses the plausibility of different signals of future rainfall change in the Congo Basin by examining the processes relating to rainfall projections in samples of historically wet or dry models during the September-November (SON) rainy season. In the west Congo Basin, there are no significant differences in the projections of rainfall change in models which are historically wet or dry. Both model samples feature wetting in the north of up to 1.8 mm day $^{-1}$ and drying in the south, associated with enhanced tropical Atlantic sea surface temperatures, increased evaporation and enhanced low level moisture flux into the basin. In the east Congo Basin, historically wet models project significant wetting in the north-east (1.19 mm day^{-1}) associated with a weakened northern component of the African Easterly Jet (AEJ) and enhanced moisture convergence at mid-levels. Dry models do not capture the latitudinal structure of the AEJs in the historical period, and so changes to the AEJs under warming do not produce the same wetting pattern. The analysis therefore casts doubt on the plausibility of the driest rainfall change signals in the east Congo Basin.

5.1 Introduction

The continent of Africa is particularly vulnerable to climate change [*Niang et al.*, 2014]. Temperatures over Africa have been increasing at more than double that of global mean increases [*Engelbrecht et al.*, 2015], and future warming over the African tropics exceeds the global average (greater than 1.4K per 1K of global mean warming) in projections from multiple climate model datasets [*James et al.*, 2013]. Combined with the region's low adaptive capacity and reliance on rain-fed agriculture, such changes may amplify existing stressors [*Niang et al.*, 2014]. In recent years there has been increased scientific interest in both the physical mechanisms and the impacts of climate change over Africa, a region which has historically received limited scientific attention [*Washington et al.*, 2006; *Farnsworth et al.*, 2011; *James et al.*, 2018]. Research into climate change in the continent has focused predominantly on the sub-regions of West Africa and the Sahel [e.g. *Cook and Vizy*, 2006; *Hoerling et al.*, 2006; *Biasutti and Sobel*, 2009; *Vizy et al.*, 2013; *James et al.*, 2015], East Africa [e.g. *Shongwe et al.*, 2011; *Kent et al.*, 2015; *Hirons and Turner*, 2018], and southern Africa [e.g. *Kay and Washington*, 2008; *Shongwe et al.*, 2009; *Lazenby et al.*, 2018], and has led to an improved understanding of the climate systems and projections in these areas.

Despite this progress, there remains a dearth of scientific research into the historical and future climate in the Congo Basin [*Washington et al.*, 2006; *James and Washington*, 2013], the convective core of the continent and one of the three wettest places on Earth [*Webster*, 1983]. This is likely due to the scarcity of recent

observational data in this region, which has severely limited our understanding of the Congo Basin's climatology and climate variability [*Washington et al.*, 2006, 2013]. Data scarcity has severe implications for the evaluation of climate models, the tools used to predict and diagnose future climate changes. Without temporally and spatially homogenous observational data it is difficult to test models' capabilities, and this may be one reason different models diverge significantly in their representation of historical climatology. A consequence of this is that the response of rainfall to warming across models is superimposed on vastly different basic states [*Washington et al.*, 2013; *Creese and Washington*, 2016]. Unsurprisingly, there is uncertainty into both the sign and magnitude of future change in rainfall in the Congo Basin across various global and regional climate models [*Haensler et al.*, 2013a; *Aloysius et al.*, 2016; *Pokam et al.*, 2018]. Changes to rainfall amounts and seasonality have the potential to impact agricultural output and hydroelectricity, both of which are important for local and national economies in Congo Basin countries [*Hamududu and Killingtveit*, 2012; *CKDN*, 2014; *Pereira*, 2017]. In addition, changes in rainfall have the potential to affect the boundaries of the Congo rainforest, the second largest above-ground carbon-store in the world after the Amazon rainforest [*Baccini et al.*, 2012; *Malhi et al.*, 2013]. It is therefore imperative that uncertainty in the climate response in this region is reduced, so that decision-makers have the most robust evidence available for policy decisions.

5.1.1 Regionally-focussed process-based assessments

Regionally-focussed process-based assessments have emerged as a method for characterising and differentiating amongst climate models, particularly where

there is disagreement amongst models, or between models and observations [e.g. *Cook and Vizy*, 2006; *Seth et al.*, 2013; *James et al.*, 2015; *Pinto et al.*, 2018]. Models are assessed on their ability to represent processes which relate to rainfall; for example, low-level winds, jets and overturning cells. This can be used to help determine the credibility of models in the absence of observational data. For example, *James et al.* [2015] assess the plausibility of model projections of change in West Africa via a comparison with known processes which drive rainfall variability in the historical period. They find that the processes associated with a strong drying signal in the future are not observed in the reanalysis data, casting doubt on the credibility of the drying signal.

Such approaches have also been used previously to assess modelled historical climatology in the Congo Basin. *Creese and Washington* [2016] analyse a sample of CMIP5 models and find that model rainfall is strongly related to the strength and pattern of low-level circulation, in particular the amount of water vapour entering the basin through specific boundaries. *Creese and Washington* [2018] further this analysis in the September-November rainy season, finding that models which are extremely wet in the west Congo Basin tend to have larger tropical Atlantic sea surface temperature (SST) biases than drier models. The study links the enhanced SSTs to higher rainfall via a set of processes. Warmer SSTs lead to enhanced evaporation in the Gulf of Guinea and associated enhanced low-level westerlies, which lead to enhanced local convection over the west Congo Basin, and thus enhanced rainfall. Given that the SST bias is well established in observed data, identifying this link to rainfall casts doubt on extremely wet models, as their high rainfall appears to be in part caused by a spurious set of processes. In the east

Congo Basin, the study finds that tropical Atlantic SST biases are not a significant differentiator between wet and dry models. Instead, wetter models feature stronger 925 hPa westerly moisture flux and more poleward African Easterly Jets (AEJs) than dry models.

The process-based assessment conducted by *Creese and Washington* [2018] led to a better understanding of why model climatologies diverge in the Congo Basin, and questioned the credibility of models which have large Atlantic SST biases and are wet in the west of the basin. In this paper, we extend the process-based analysis to future rainfall changes within the same groups of models in order to establish whether categorising models by their historical climatology results in different future rainfall signals. This may provide important insights into the plausibility of different rainfall change signals in the Congo Basin.

5.1.2 Climate change in the Congo Basin

There are a small number of studies which have investigated the range of model projections of rainfall change in the Congo Basin across multi-model ensembles (MMEs). Analyses of multiple projections from CMIP3, CMIP5 and CORDEX has found that the annual multi-model mean of these datasets projects a slight wetting over the basin in the future, though these changes are not large [*Haensler et al.*, 2013a]. Similarly, *Aloysius et al.* [2016] find precipitation increases in CMIP5 models of only 2.4% and 2.8% by the end of the century under the RCP4.5 and RCP8.5 forcing pathways respectively. However, the range of precipitation change amongst models varies between -9% and 27%. It is interesting to note that

analysis of rainfall and hydrological data over recent decades has identified a drying trend over the Congo Basin [e.g. *Malhi and Wright*, 2004; *Yin and Gruber*, 2010; *Diem et al.*, 2014], which contrasts with mean projections of wetting in model ensembles.

There may also be differences in the projected signal between global (GCMs) and regional models (RCMs; analysis of projected rainfall changes under 1.5°C and 2°C warming suggests that while GCMs tend to show increases in rainfall in this region, RCMs show an equal number of positive and negative changes [*Pokam et al.*, 2018]. In addition, all three studies find spatial patterns of rainfall change much less consistent amongst models, with *Aloysius et al.* [2016] noting in particular large variations in projected changes in the north and eastern parts of the region.

A process-based assessment has also been used in this region; *James et al.* [2013] evaluate rainfall changes in the Congo Basin in CMIP3 and two perturbed physics ensembles (PPEs), before examining the atmospheric dynamics associated with different rainfall signals. They find the majority of models project drying in the west of the basin, which is associated with enhanced subsidence and a shift in the zonal circulation. They highlight that differences in models' preindustrial climatologies may influence their response to warming and conclude that further work is required to assess the plausibility of such changes.

5.1.3 Tropical rainfall change

As one of three core convective hotspots on the planet, changes in the Congo Basin will occur within the context of tropics-wide change. A number of mechanisms have been proposed which, in combination, could help to explain rainfall changes across the tropics. Global atmospheric water content will increase under warming, in line with Clausius-Clapeyron scaling (~7% K^{-1}) which could result in a 'wet-gets-wetter' pattern of rainfall change, where convection, and thus rainfall, increases in areas of climatologically high rainfall, and decreases in climatologically dry regions [*Chou and Neelin*, 2004; *Held and Soden*, 2006; *Chou et al.*, 2009]. This is likely to be offset at least in part by a weakening of the tropical overturning circulation [*Held and Soden*, 2006; *Vecchi et al.*, 2006; *Ma et al.*, 2012; *Chadwick et al.*, 2013; *Ma and Xie*, 2013] , but can explain some of the changes observed and modelled at large spatial scales [*Allan et al.*, 2010; *Allan*, 2012; *Durack et al.*, 2012]. *Chadwick et al.*'s [2013] analysis finds that the wet-gets-wetter mechanism does not explain most of the rainfall change in the tropics, and they suggest that dynamical mechanisms of change may play a larger role, including shifts in the location of convection and alterations to the circulation. Patterns of sea surface temperature (SST) change are also likely to influence the rainfall increases and decreases ('warm-gets-wetter'). This has been found to be particularly influential over tropical oceans [*Xie et al.*, 2010; *Huang et al.*, 2013], but may also influence land areas via teleconnections [e.g. *Biasutti and Sobel*, 2009; *Brown et al.*, 2016; *Rowell and Chadwick*, 2018]. In East Africa, for example, *Rowell and Chadwick* [2018] find that differences in rainfall in CMIP5 models in part relate to their representation of SST pattern

change, and in southern Africa, *Lazenby et al.* [2018] find that the pattern of rainfall change in the region may be related to changes in the Indian Ocean SST-gradient.

5.1.4 Aims

The aim of the paper is to ascertain whether we can establish the plausibility of future climate projections in the Congo Basin based on their past performance. We will do this by investigating whether the processes linked to the extremely wet or dry rainfall climatologies in models in the present day have a bearing on the magnitude or sign of future rainfall change in those models. The paper focuses on the September-November (SON) rainy season, which has some of the largest historical differences in mean rainfall amongst models. The authors have previously linked model differences in SON rainfall to the representation of important regional processes such as the African easterly jets and the tropical Atlantic SST bias [*Creese and Washington*, 2018]. This understanding will therefore underpin the analysis of the future projections in this paper.

The paper proceeds through answering three key questions:

1) What is the range of Congo Basin rainfall changes across models in SON, both in terms of magnitude and spatial distribution?
2) Do models with relatively wet or dry historical climatologies in SON feature significantly different rainfall signals at the end of the 21st century?
3) What are the physical processes related to rainfall change in the model wet and dry historical climatologies, and based on previous assessment of the

credibility of the model composites, can we determine whether some models produce more plausible future projections than others?

This paper is structured as follows. The data and methods used are outlined in Section 5.2. Section 5.3 will assess the broad-scale rainfall changes that occur across models in the SON season, including the magnitude and distribution of rainfall change. Section 5.4 will then identify the processes associated with rainfall change in the west Congo Basin composites defined above. The analysis is repeated in Section 5.5 for the east Congo Basin composites. Section 5.6 will discuss the results and summarise.

5.2 Data and Methods

Coupled model data is taken from the latest Coupled Model Intercomparison Project (CMIP5), which comprises models from different modelling centres which have committed to running the same suite of experiments [*Taylor et al.*, 2012]. As this study builds on the analysis of coupled model climatology by *Creese and Washington* [2018], the same sample of 17 models is used for analysis (Table 5.1). These models represent the full spectrum of wet to dry over the Congo Basin, and contain the required variables for analysis. Data is used from the historical (coupled) experiment and the RCP8.5 future experiment, which represents 8.5 Wm^{-2} of global net radiative forcing by 2100 [*van Vuuren et al.*, 2011]. This level of forcing is consistent with a 'business-as-usual' approach to climate mitigation.

Analysis is conducted separately on the eastern (22°E to 35°E, 10°S to 10°N) and western (8°E and 21°E, 10°S to 10°N) subdomains, following *Creese and Washington* [2018]. Long term means of the historical (1979-2005) and future (2074-2100) periods are calculated over the above domains. The future-minus-present rainfall signal is denoted throughout as ΔP. The four wettest and four driest models in each subdomain are selected for use in composite analysis and are indicated in Figure 5.1. These are the same models used by *Creese and Washington* [2018] as one aim of this paper is to understand if categorising models in this way, with an understanding of the plausibility of their climatologies, can give insights into their rainfall change signal and pattern. Long term means of the historical (1979-2005) and future (2074-2100) periods are calculated over the above domains. The future-minus-present rainfall in the wet and dry composites is denoted as ΔP_{wet} and ΔP_{dry} respectively.

5.3 Rainfall changes in SON

Figure 5.1 shows that in both the east and west Congo Basin subdomains, models which are currently relatively wet compared to the suite of models remain so in the future, as do models which are currently dry. Historical and future mean basin rainfall are strongly positively correlated across models in both the west ($r=0.96$, $p<0.000001$) and east ($r=0.97$, $p=<0.000001$) of the basin during SON, and indeed in all other seasons. This suggests that some of the processes controlling rainfall magnitude and distribution in the historical period may continue to play a role in the future and may account for any differences in the rainfall change (ΔP) signal

Table 5.1 – CMIP5 models used in this study

Model	Institute	Reference
ACCESS1-3	Commonwealth Scientific and Industrial Research Organization and Bureau of Meteorology Australia (CSIRO-BOM)	Collier & Uhe (2012)
bcc-csm1-1	Beijing Climate Centre (BCC)	Wu et al. (2013)
CCSM4	National Centre for Atmospheric Research (NCAR)	Gent et al. (2011)
CESM1-CAM5	National Centre for Atmospheric Research (NCAR)	Neale et al. (2012)
CMCC-CM	Centro Euro-Mediterraneo per I Cambiamenti Climatici (CMCC)	Scoccimarro et al. (2011)
CNRM-CM5	Centre National de Recherches Météorologiques / Centre Européen de Recherche et Formation Avancée en Calcul Scientifique (CNRM-CERFACS)	Voldoire et al. (2011)
CSIRO-Mk3-6-0	Commonwealth Scientific and Industrial Research Organization in collaboration with Queensland Climate Change Centre of Excellence (CSIRO-QCCCE)	Jeffrey et al. (2013)
EC-EARTH	EC-Earth Consortium: European Centre for Medium-Range Weather Forecasts (ECMWF) and other European institutes	Hazeleger et al. (2010)
FGOALS-g2	State Key Laboratory of Numerical Modeling for Atmospheric Sciences and Geophysical Fluid Dynamics (LASG) and Institute of Atmospheric Physics (IAP)	Li et al. (2013)
GFDL-CM3	NOAA Geophysical Fluid Dynamics Laboratory (NOAA GFDL)	Donner et al. (2011)
GISS-E2-R	NASA Goddard Institute for Space Studies (GISS)	Schmidt et al. (2014)
HadGEM2-ES	Met Office Hadley Centre (MOHC)	Jones et al. (2011)
IPSL-CM5A-MR	Institut Pierre-Simon Laplace (IPSL)	Dufresne et al. (2013)
MIROC5	Atmosphere and Ocean Research Institute (The University of Tokyo), National Institute for Environmental Studies, and Japan Agency for Marine-Earth Science and Technology (MIROC)	Watanabe et al. (2010)
MPI-ESM-LR	Max-Planck-Institut für Meteorologie (MPI-M)	Marsland, Haak, Jungclaus, Latif, & Roske (2003)
MRI-CGCM3	Meteorological Research Institute (MRI)	Yukimoto et al. (2012)
NorESM1-M	Norwegian Climate Centre (NCC)	[*Bentsen et al.*, 2013]

found amongst the wet and dry composites. This hypothesis will be explored in Sections 5.4 and 5.5. Understanding the role of the underlying determining future change will be particularly important, as the differences between model climatological rainfall are much greater than the values of ΔP that are being projected in this region (Figure 5.1, dark blue bars). Figure 5.1 also shows that historical rainfall is not correlated with the change in rainfall in either subdomain across the suite of models; that is, there is no evidence that wet models get wetter or that dry models get drier.

Spatial patterns of ΔP in individual models and the ensemble mean in SON are shown in Figure 5.2. Across the annual cycle (not shown) there is some evidence of a north-south pattern of future-minus-present rainfall (ΔP) over Africa, where northern areas get wetter and southern areas get drier under RCP8.5 forcing. In SON the north-south pattern of ΔP is most clear, and the majority of models agree on the direction of changes broadly between 0° and 10°N and 10°S and 25°S. However, in the south Congo Basin (between 0 and 10°S) there is little agreement on the sign of change. This suggests that models disagree on the precise location of the change between the wetting and drying zones. While some show distinct north/south divisions (e.g. GFDL-CM3, MPI-ESM-LR), others exhibit less regular distributions of rainfall change (e.g. CSIRO-Mk3-6-0, IPSL-CM5A-MR). It is also evident that even amongst models with a clear north-south divide, the location of the change from wetting to drying varies; for example, in GFDL-CM3 this change occurs near the equator, whereas in MPI-ESM-LR, it occurs closer to 10°S. This implies that whilst the overall north-south pattern across Africa is consistent

across models, processes controlling rainfall change at more local scales within the basin may not be consistent amongst models.

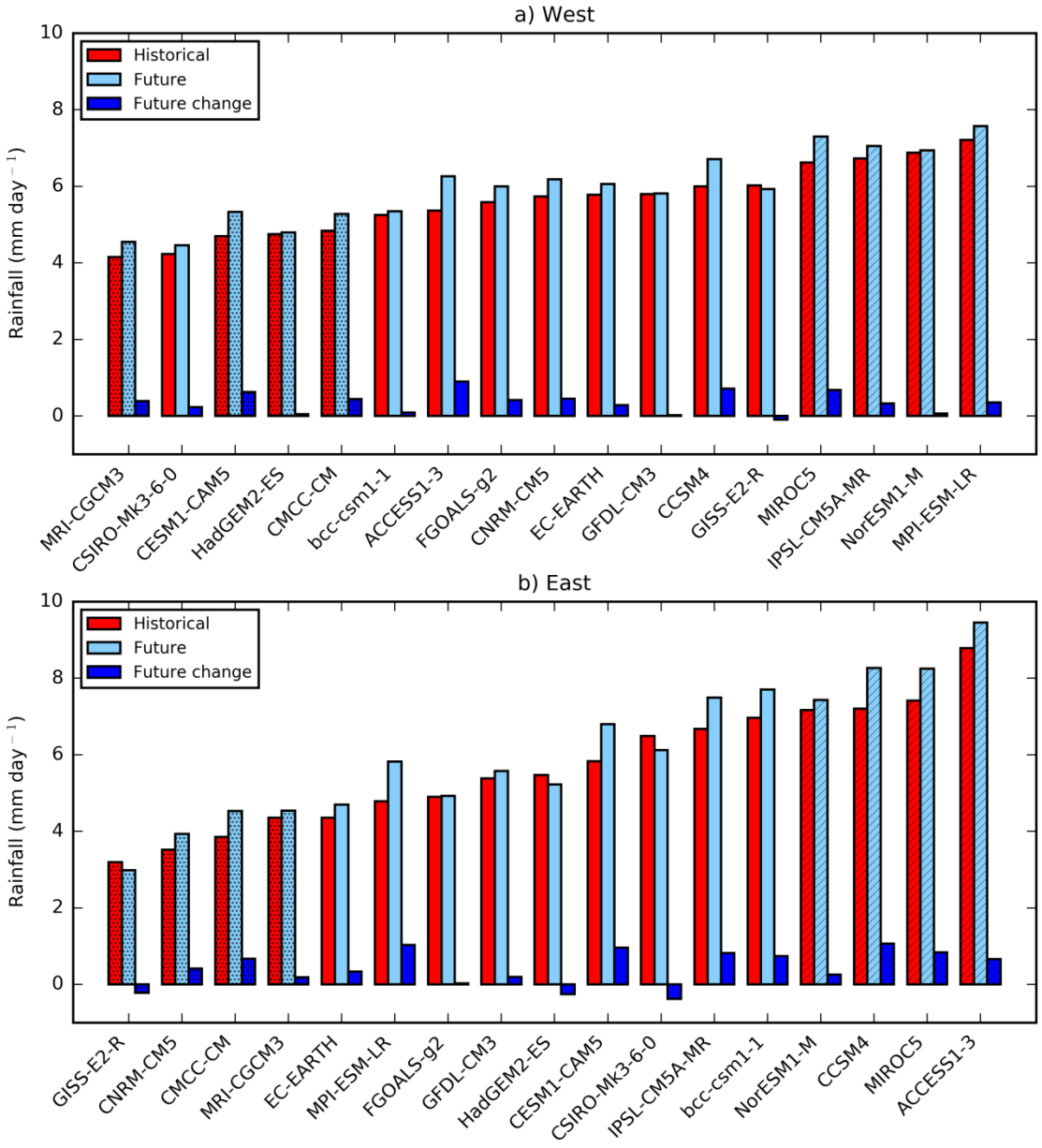

Figure 5.1 - Long term mean SON rainfall (mm day^{-1}) in individual CMIP5 models in (a) the west Congo Basin (8°E to 21°E, 10°S to 10°N) and (b) east Congo Basin (22°E to 35°E, 10°S to 10°N), in: the historical period (1979-2005; red); the future period (2074-2100; light blue); and the 2074-2100 minus 1979-2005 (ΔP; dark blue). Ordered by mean historical rainfall (low to high). Models used in the wet (dry) composites are denoted by hatching (stipples). CSIRO-Mk3-6-0 is excluded from the dry composite (as in Creese and Washington 2018) due to the opposite signal of the historical SST bias

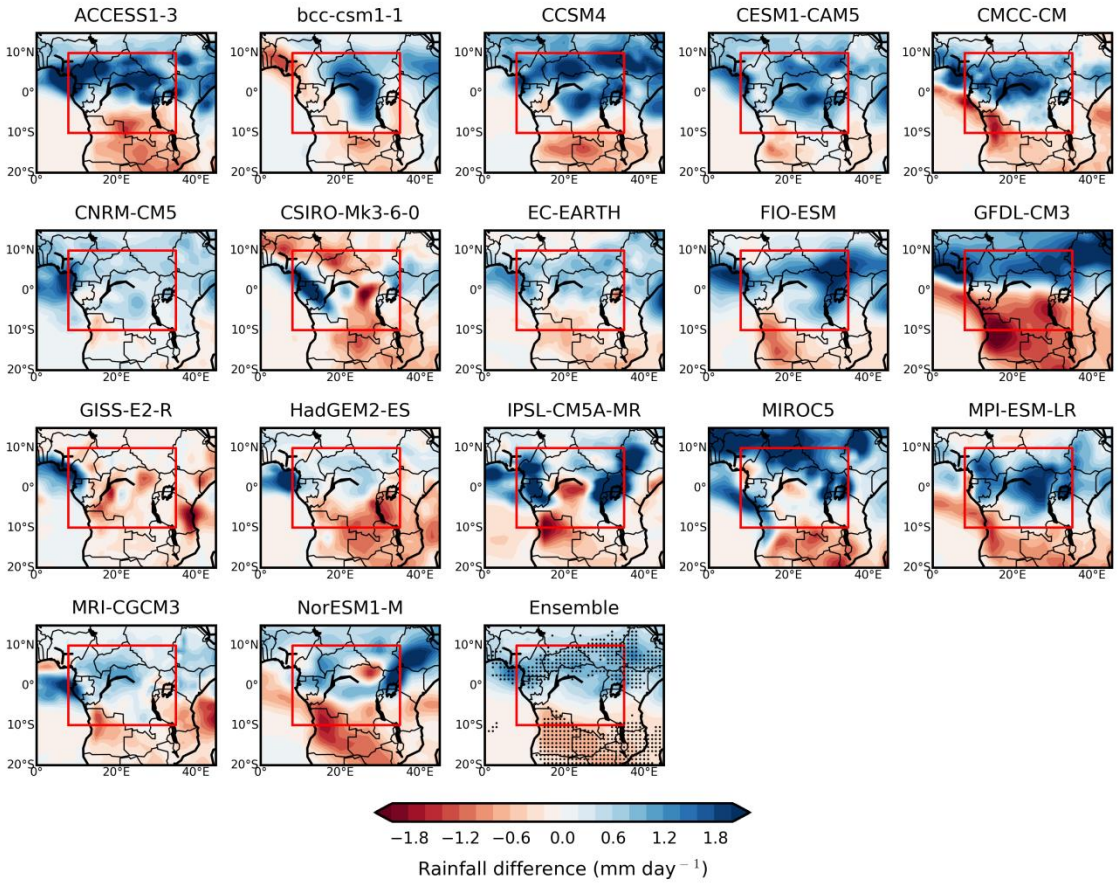

Figure 5.2 - Future (2074-2100) minus historical (1979-2005) long-term mean rainfall (ΔP; mm day^{-1}) in individual CMIP5 models. Stipples in the ensemble mean plot show gridboxes where 14 out of 17 models agree on the sign of change.

5.4 Rainfall change mechanisms in the west Congo Basin

The aim of this paper is to determine whether categorising models as climatologically wet or dry in the east and west Congo Basin (as in *Creese and Washington* [2018]) provides insight into the processes controlling rainfall change over the Congo Basin in such models, and, by extension, the plausibility of such rainfall changes. This section will undertake this assessment for the west Congo

Basin; Section 5.5 assesses processes of change in the east Congo Basin composites.

5.4.1 Rainfall change

The rainfall distribution in the historical and future period, for both wet and dry composites, is shown in Figure 5.3. In the historical period, wet models are on average 2.2 mm day^{-1} wetter than dry models over the west Congo Basin domain (Figure 5.3h). The wet-minus-dry difference of future simulations of the composites is also very similar (Figure 5.3g), showing that the broad patterns of rainfall in each model remain similar in the future. For example, in the historical period in the west wet composite, there are two regions of high rainfall; one in the east of the basin, and one near the Atlantic coast. This pattern does not change significantly in the future period. This is also the case in individual models; the rainfall distribution (which *Creese and Washington* [2016, 2018] found varied significantly amongst models) does not change significantly in the future simulation of that model (not shown).

Of interest to this paper is the pattern of ΔP in the wet composite (ΔP_{wet}, Figure 5.3c) and dry composite (ΔP_{dry}, Figure 5.3f), and the difference between the two (ΔP_{wet} minus ΔP_{dry}, Figure 5.3i). Both wet and dry models show similar patterns of rainfall change; as in the ensemble mean, there is a north-south pattern of wetting and drying. In both composites, the wetting is north of the equator, but in dry models, the region of wetting covers a larger area. Both composites also feature

drying to the south of the Congo Basin domain, with a small incursion of robust drying into the domain along the Atlantic coast.

The first aim of this paper is to determine whether categorising models based on their historical climatology has an impact on the ΔP signal across the Congo Basin. Figure 5.3i shows that there are some differences between ΔP_{wet} and ΔP_{dry}. Wet models feature greater wetting in the centre of the west Congo Basin domain,

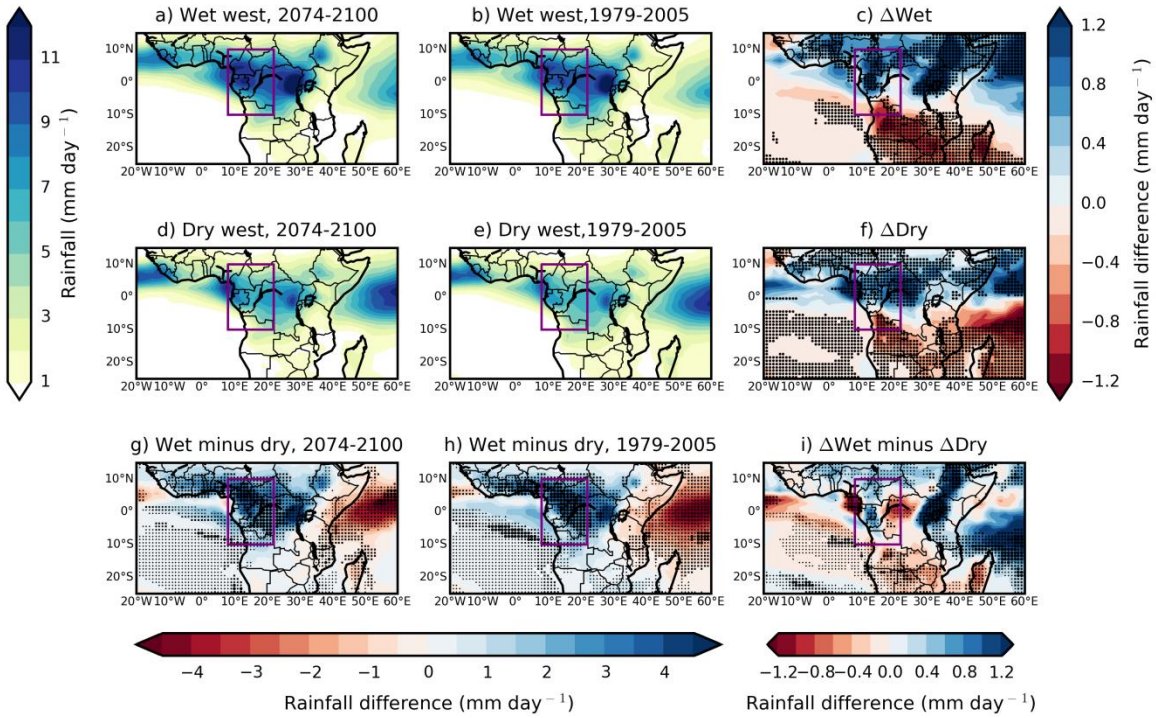

Figure 5.3 - Long term mean SON rainfall (mm day^{-1}) in the west Congo Basin wet composite (top row) and dry composite (middle row) in (a), (d) 2074-2100, (b), (e) 1979-2005; and (c), (f) 2074-2100 minus 1979-2005 (ΔP); (g) 2074-2100 wet minus dry composite; (h) 1979-2005 wet minus dry composite; and (i) wet ΔP minus dry ΔP. Stipples in (c) and (f) indicate where all four models in the composite agree on the sign of change. Stipples in (g-i) occur at gridboxes where: 1) all wettest composite values are larger or smaller than all driest composite values (large dots); 2) all wettest composite values are greater or smaller than the driest composite mean (squares); 3) driest composite values are greater or smaller than the wettest composite mean (crosses); and 4) both (2) and (3) are true (small dots). The purple box indicates the location of the west Congo Basin domain.

whereas dry models feature greater wetting at the western and eastern boundaries of the domain. However, for a large portion of the domain, there is no clear difference between ΔP_{wet} and ΔP_{dry}. This suggests that in thus subdomain during SON, whether or not a model is historically extremely wet or dry does not have a large impact on the ΔP signal for parts of the basin.

The second aim of this paper is to try and understand the plausibility of projected changes in rainfall, based on previous assessments of processes related to rainfall in coupled models [*Creese and Washington*, 2016, 2018]. As the wet and dry composites feature in many ways similar patterns of ΔP, a process-based assessment can be used to try and determine whether the change in rainfall is related to plausible or implausible processes in the region.

5.4.2 Processes associated with rainfall change

Creese and Washington [2018] identified the following processes which help to explain the differences between historically wet and dry models in the west Congo Basin:

a) Models which are wetter tend to have higher SST biases in the tropical east Atlantic Ocean
b) This leads to higher evaporation and low-level westerlies in wet models than dry models
c) The combination of enhanced evaporation and low-level wind transports moisture onto the west Congo Basin coast and contributes to a local enhancement of convection and rainfall in wet models.

Given the important role these processes play in determining rainfall amounts and patterns in the Congo Basin in the historical period, assessing how these processes change in models in the future is considered next.

5.4.2.1 SST

Most coupled models feature a large and persistent warm SST bias in the tropical east Atlantic Ocean [*Wang et al.*, 2014], and this has been found to be generally stronger in wet west Congo Basin models in the historical period [*Creese and Washington*, 2018] (Figure 5.4h). Both wet and dry models feature positive SST change (ΔSST) across both the Atlantic and Indian Oceans (Figure 5.4c and 5.4f). Both composites feature particularly strong warming over the tropical east Atlantic, in the region of the historical SST bias. The pattern of ΔSST is broadly similar between the wet and dry composite; the only robust region of difference is a small area in the tropical east Atlantic where dry models warm slightly more than wet models (Figure 5.4i). As in the processes identified in the historical period, warmer SSTs in both composites are also associated with enhanced evaporation over this region; this is also slightly greater in dry models than wet model, fitting with the greater ΔSST (Supplementary Figure 5.S1).

The enhanced SST and evaporation in the future could therefore explain some of the wetting in this region in both composites, and may explain the enhanced wetting in dry models compared to wet models along the coasts of Gabon and

Cameroon. It does not however explain the greater wetting wet models experience in the centre of the western subdomain. It is also noteworthy that the positive ΔSST signal is in a region of historically large positive SST biases (of more than 4K in some models), and so changes in SST build on this bias.

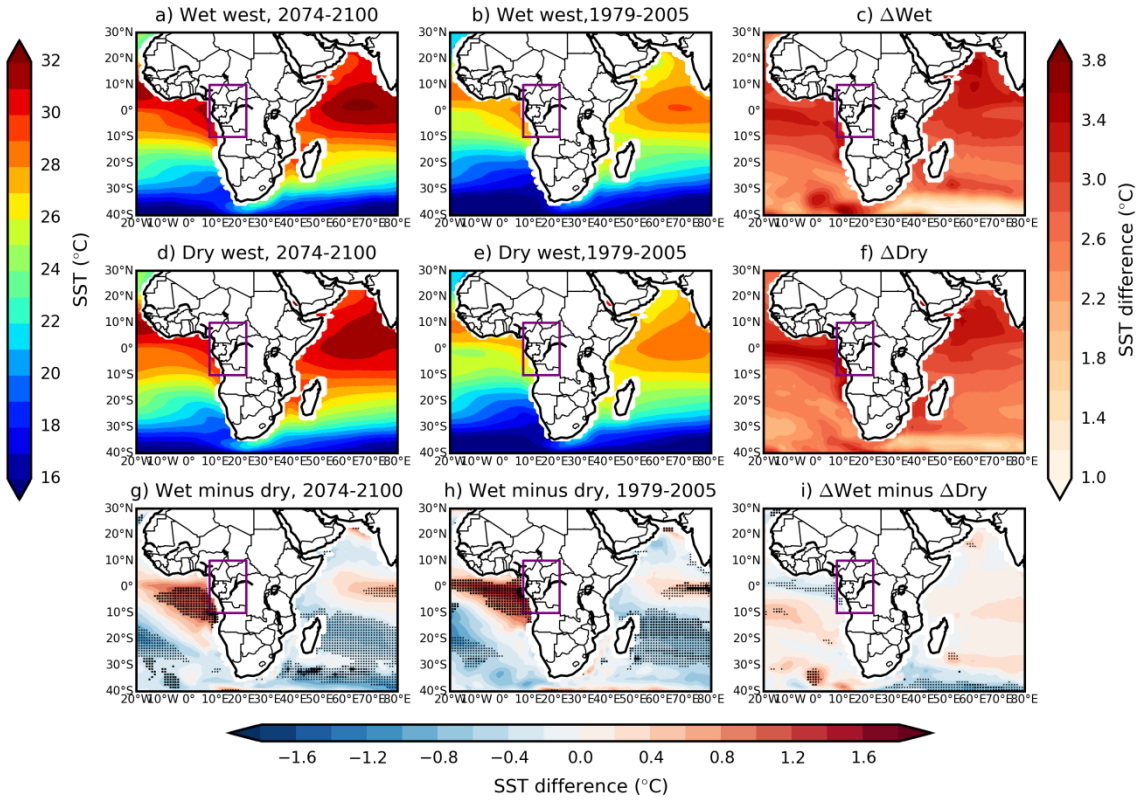

Figure 5.4 - Long term mean SON SST (°C) in the west Congo Basin wet composite (top row) and dry composite (middle row) in (a), (d) 2074-2100, (b), (e) 1979-2005; and (c), (f) 2074-2100 minus 1979-2005 (ΔSST); (g) 2074-2100 wet minus dry composite; (h) 1979-2005 wet minus dry composite; and (i) wet ΔSST minus dry ΔSST. Stipples as in Figure 5.3. The purple box indicates the location of the west Congo Basin domain.

5.4.2.2 Low-level moisture flux

Previous work has identified low-level moisture flux (qflux) as an important influence on model wetness, particularly in the form of low-level westerlies during SON. Both wet and dry models feature increases in low-level (925 hPa) westerly

qflux into the basin in the future (Figure 5.5), with no significant difference in the pattern of qflux change (Δqflux) between the two composites (Figure 5.5i). Both composites feature generally enhanced convergence to the north of the domain, co-located with the broad region of wetting in all models. Despite broad-scale similarities, there are some differences in the pattern of qflux convergence over the western subdomain between the two composites. Wet models feature an enhancement of moisture flux convergence in the west of the subdomain (over Gabon) in the future, whereas dry models feature a weakening. This co-locates with the region of enhanced wetting in wet models compared to dry models (Figure 5.3i). Both composites also feature enhanced divergence in the east of the subdomain in the future. This is weaker in dry models, coinciding with where dry models feature greater wetting than wet models. These findings suggest that local patterns of low-level convergence may relate to spatial differences in ΔP between the composites, but that the overall low-level circulation is not significantly different between wet and dry models.

5.4.2.3 Overturning circulation

In the historical period during SON, stronger low-level moisture flux and enhanced evaporation are associated with enhanced convection in wet models in the west Congo Basin. It is hypothesized that the wetting signal in both composites may therefore be linked to increased local uplift. Figure 5.6 shows the zonal cross section of omega (Ω) near the equator, where a zonal overturning circulation is present in the climatology of both composites, and the change in omega (ΔΩ)

signal. Somewhat surprisingly, in wet models, uplift weakens in the future in the wet composite, though the sign of change across composite members is not consistent throughout the column (Figure 5.6c). In dry models, there is some weakening of uplift between 800 and 600 hPa, but less so than in the wet models (Figure 5.6f). In both wet and dry models, there is a decrease in subsidence above 600 hPa between 35° and 40°E, over East Africa. The pattern of decreased uplift

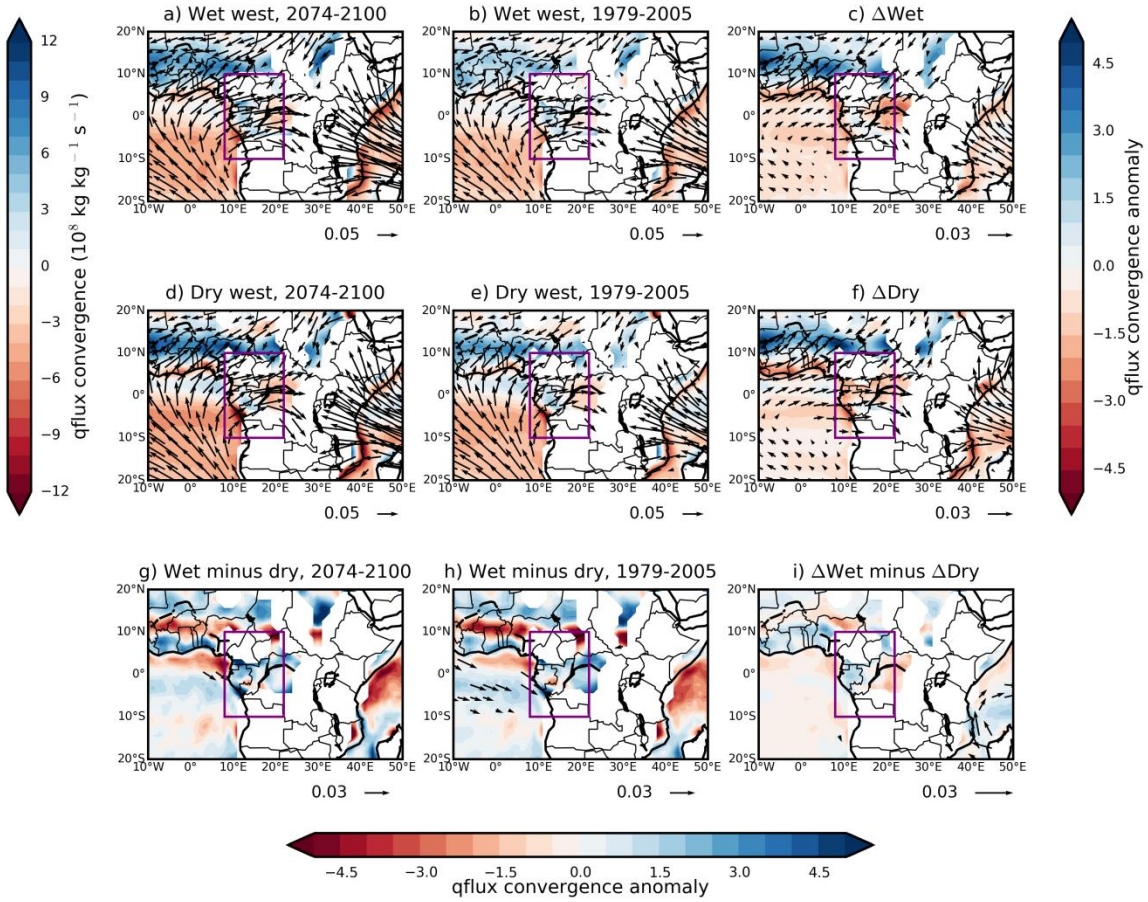

Figure 5.5 - Long term mean SON qflux convergence (10^{-8} kg kg^{-1} s^{-1}; shaded) and qflux (kg kg^{-1} m s^{-1}; vectors) at 925 hPa in the west Congo Basin wet composite (top row) and dry composite (middle row) in (a), (d) 2074-2100, (b), (e) 1979-2005; and (c), (f) 2074-2100 minus 1979-2005; (g) 2074-2100 wet minus dry composite; (h) 1979-2005 wet minus dry composite; and (i) wet change minus dry change. Vectors in (c) and (f) indicate where all four models in the composite agree on the sign of change. Vectors in (g), (h) and (i) occur at gridboxes where all wettest composite values are larger or smaller than all driest composite values. The red box indicates the location of the west Congo Basin domain.

over the west Congo Basin is reduced slightly in the north of the domain (0°-10°N; Supplementary materials, Figure 5.S2), which features mean wetting, and increases in the south (5°-10°S), where both composites feature mean drying over land. In the south, the decrease in uplift co-occurs with reductions in subsidence over the coastline and tropical Atlantic (Supplementary materials, Figure 5.S3) indicating that the zonal overturning circulation weakens in the future in both composites.

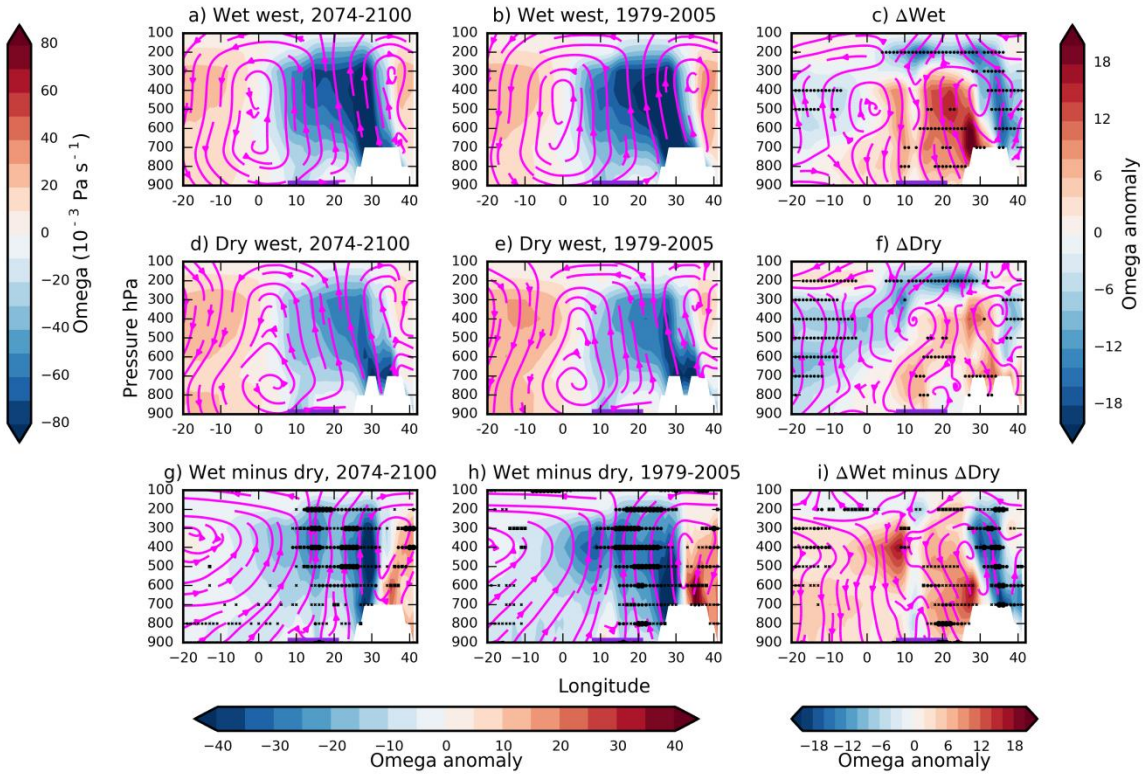

Figure 5.6 - Long term mean SON omega (10^{-3} Pa s^{-1}; shaded) averaged between 3°S and 3°N and divergent component of zonal wind (m s^{-1}) and omega (10^{-3} Pa s^{-1} streamlines), in the west Congo Basin wet composite (top row) and dry composite (middle row) in (a), (d) 2074-2100, (b), (e) 1979-2005; and (c), (f) 2074-2100 minus 1979-2005; (g) 2074-2100 wet minus dry composite; (h) 1979-2005 wet minus dry composite; and (i) wet change minus dry change. Areas with high topography in models are masked (white). The purple box shows the extent of the west Congo Basin domain (8°E to 21°E). Stipples as in Figure 5.4 and refer to omega values.

The general overturning circulation is expected to weaken under warming, and these results suggest that, particularly in the historically-wet models, a local weakening of the overturning circulation is present despite wetting. Figure 5.7 shows how the changes in Ω at 500 hPa map on to changes in rainfall across the annual cycle in the composites. In both the future and historical climatology, the region of rainfall throughout the annual cycle maps reasonably well onto the region of negative omega. However, when comparing the ΔΩ and ΔP patterns, it is clear there is some displacement of the two variables in the future (Figure 5.7c, 5.7f). In both composites, there is a clear pattern of positive ΔΩ (i.e. reduced uplift) though out the annual cycle, following approximately the north-south trajectory of the rain band. Changes in rainfall, however, are displaced from this band; wetting tends to occur on the northern flank of the region of positive ΔΩ and drying occurs on the southern flank. This pattern is strongest between July and December in both composites.

Wetting in the northwest of the domain despite a weakening of uplift may be related to changes in the frequency distribution of daily rainfall, as shown in Figure 5.8. In the future in the wet composites, which feature greater reductions in uplift, the distribution of daily rainfall is flatter and wider, showing an increase in both wet and dry days in the future. This is despite a clear shift towards less negative daily omega values in the future in the wet composite (Supplementary materials, Figure 5.S4). The increase in rainfall over the north west domain is thus likely to be the result of increases in q which are sufficient to overcome the slight decreases in uplift. Increased q could in turn be a result of either dynamical (e.g. enhanced flux

into the basin, as shown in Figure 5.5) or thermodynamic (e.g. increased q as the atmosphere warms) mechanisms.

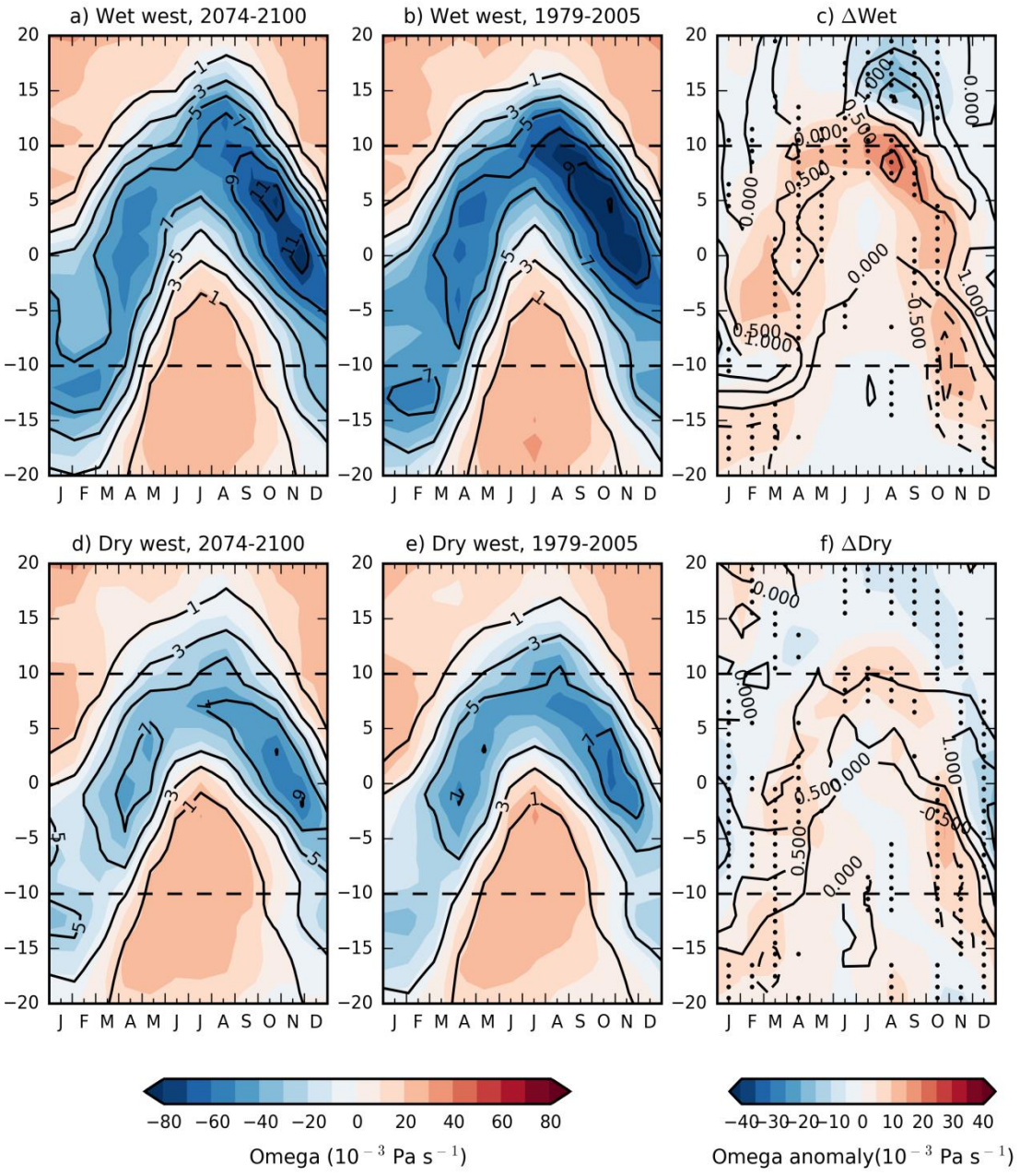

Figure 5.7 - Annual cycle of long term mean omega at 500hPa (10^{-3} Pa s^{-1}; shaded) and rainfall (mm day^{-1}; contours), averaged between 8°E and 21°E in the west Congo Basin wet composite (top row) and dry composite (bottom row) in (a), (d) 2074-2100, (b), (e) 1979-2005; and (c), (f) 2074-2100 minus 1979-2005. Stipples as in Figure 5.4 and refer to omega values. Dashed lines indicate the northern and southern boundaries of the domain.

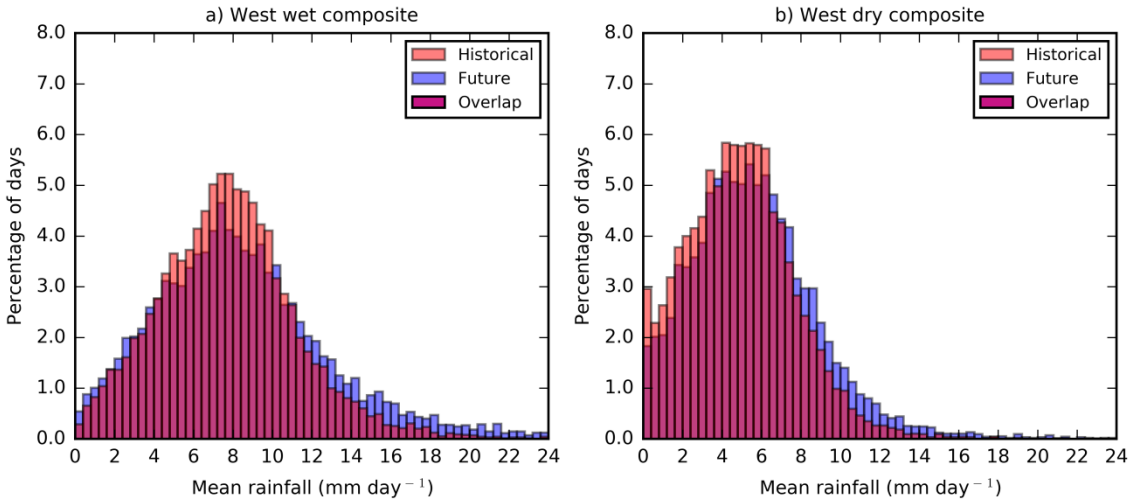

Figure 5.8 - Frequency distribution of daily rainfall (mm day^{-1}) in all SON days in the northwest of the basin (8°E to 21°E, 0° to 10°N) in all composite member models in (a) the west Congo Basin wet composite and (b) the dry composite, between 2074 and 2100 (blue) and 1979-2005 (orange). Pink denotes overlap between the orange and blue distributions.

5.5 Rainfall change mechanisms in the east Congo Basin

5.5.1 Rainfall change

Rainfall changes over the east Congo Basin for the wet and dry composites are shown in Figure 5.9. In the historical period, models in the wet composite are on average more than twice as wet as those in the dry composite, with the largest differences in the interior of the continent. The difference between wet and dry models increases in the future climatology, particularly in the north of the domain (Figure 5.9g). Wet models feature a robust and positive ΔP signal in the future (Figure 5.9c), while the dry models feature weak wetting over this domain, with very little agreement on the sign of change (Figure 5.9f). Figure 5.9i quantifies the difference in ΔP between the composites, showing that wet models experience significantly higher wetting than dry models in the east near the equator, and in

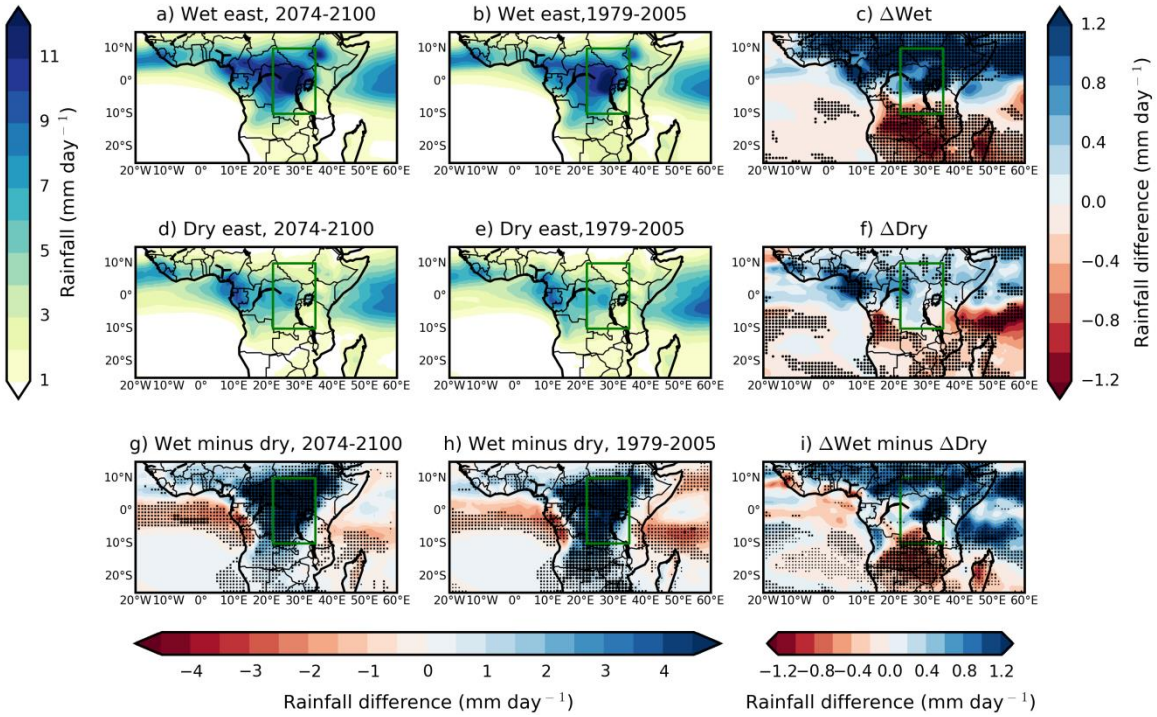

Figure 5.9 - As in Figure 5.3 but for the east Congo Basin composites. The green box indicates the location of the east Congo Basin domain.

the north of the subdomain. This indicates a 'wettest-models-get-wetter' response across models, whereby rainfall increases most in models with historically high rainfall, and suggests that the magnitude of a model's historical rainfall climatology is related to the magnitude of future rainfall change in this region. The following section will therefore examine future changes in the processes known to relate to model wetness in the historical period, to determine whether they relate to model differences in the ΔP signal in this region.

5.5.2 Processes associated with rainfall change

The following processes have previously been found to be related to climatological rainfall differences across models in the east Congo Basin [*Creese and Washington*, 2018]:

a) Models which are wetter tend to have stronger low-level westerlies from the tropical Atlantic, associated with a stronger South Atlantic High (SAH)
b) The LLWs form the lower branch of a stronger zonally overturning circulation between the Atlantic and Congo Basin, such that wet models have enhanced convection over land and subsidence over the ocean
c) Wet models also have a weaker and more poleward African Easterly Jet-North (AEJ-N), whilst dry models have a stronger and more equatorward jet. The stronger jet in dry models may act to export moisture out of the basin through the western boundary and suppress rainfall.

Given that historical model rainfall appears to be associated with the magnitude and distribution of the ΔP signal, it is hypothesized that these mechanisms may also play a role in determining ΔP. The extent to which these processes relate to rainfall changes in the east Congo Basin is assessed below.

5.5.2.1 Low level westerlies and South Atlantic High

As in the west composites, low-level westerly qflux into the basin increases in the future in both the wet and dry composites (Figure 5.10). There is also an increase

in south easterly flow in the south tropical Atlantic, along the north-eastern flank of the SAH. Sea-level pressure (SLP) increases slightly across the Atlantic in the future, with the largest increases south of 30°S, suggesting a southward expansion of the high-pressure cell, which is consistent with the observed and theorised poleward expansion of the Hadley cell under warming [*Held and Hou*, 1980; *Hu and Fu*, 2007]. However, there are few significant differences in both fields between

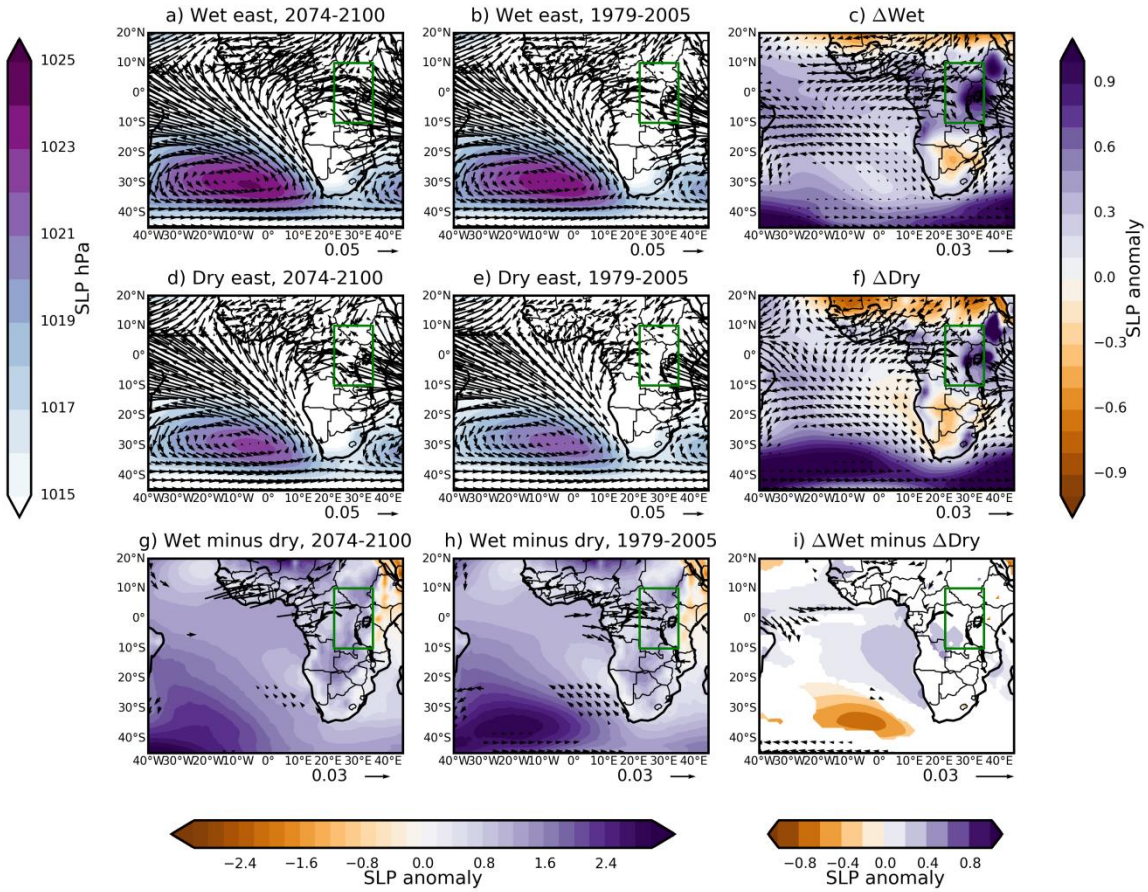

Figure 5.10 - Long term mean SON sea level pressure (hPa; shaded) and qflux at 925 hPa (kg kg^{-1} m s^{-1}; vectors) in the west Congo Basin wet composite (top row) and dry composite (middle row) in (a), (d) 2074-2100, (b), (e) 1979-2005; and (c), (f) 2074-2100 minus 1979-2005; (g) 2074-2100 wet minus dry composite; (h) 1979-2005 wet minus dry composite; and (i) wet change minus dry change. Vectors as in Figure 5.5. SLP shading is only shown at grid boxes in (i) when the values in all wet models are greater than the values in all dry models, or all the values in all dry models are greater than the values in all wet models.

the wet and dry models. The strength of the increase in 925 hPa westerly qflux is not significantly different between the two composites, nor are there other low-level circulation differences (Figure 5.10i). The dry models do feature a greater increase in the strength of the southern flank of the SAH than wet models; however, this does not co-occur with greater westerly qflux, or greater wetting in the east Congo Basin domain. Thus, while changes in both variables may contribute to wetting in both composites, they are not the dominant processes differentiating between the ΔP_{wet} and ΔP_{dry} signals.

5.5.2.2 Overturning circulation

In the historical period, wet models had a stronger zonal overturning circulation near the equator between the Atlantic and the Congo Basin (Figure 5.11h), as well as enhanced uplift over the Maritime continent and subsidence over the East African coast. This wet-minus-dry pattern is very similar in the future (Figure 5.11g), suggesting that this process is still important for maintaining relatively wet or dry future climatologies. However, as in the west composites, both wet and dry composites feature a decrease in uplift in the future over a large part of the east Congo Basin domain. In wet models, this decrease is confined to a narrower portion of the column (~15°E-30°E); to the east of 30°E, there is an increase in convection above 600 hPa. This is also evident in the north of the domain (0°-10°N, Supplementary materials, Figure 5.S5). Conversely, dry models feature decreased uplift across the whole of the domain and throughout the column. There is therefore anomalous uplift wet composite compared to the dry in the east of the

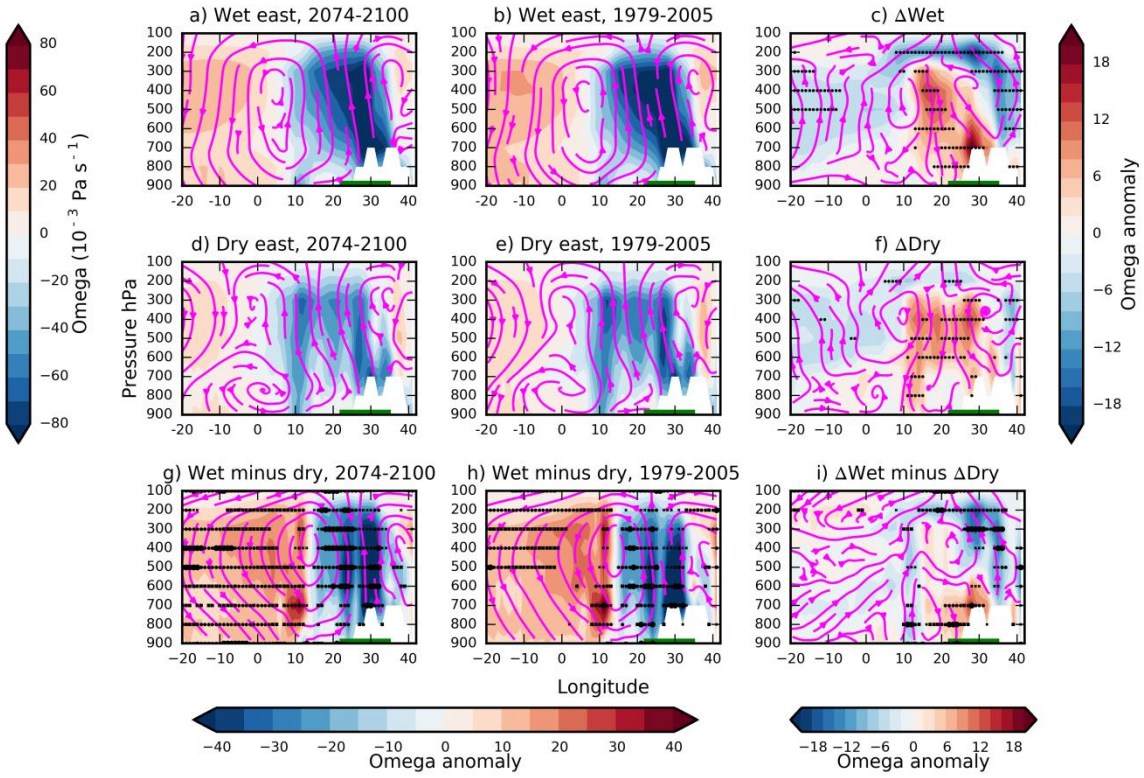

Figure 5.11 - As in Figure 5.6 but for the east Congo Basin composites. The green box indicates the location of the east Congo Basin domain.

domain above 500 hPa. This may explain some of the difference in wetting signals between the composites; the forcing in the future period may be sufficient to suppress convection in the dry models more easily than in the wet models.

The annual cycle of Ω at 500 hPa and rainfall are shown in Figure 5.12. As in the west composites, the rainfall changes are shifted meridionally to the northern and southern flanks of the decrease in omega (wetting and drying respectively), although it appears that the regions of positive Δ*P* falls more in the region of negative ΔΩ than positive ΔΩ. Alongside Figure 5.12 this suggests that rainfall increases are occurring in a region with uncertain changes in omega, both throughout the atmospheric column and latitudinally.

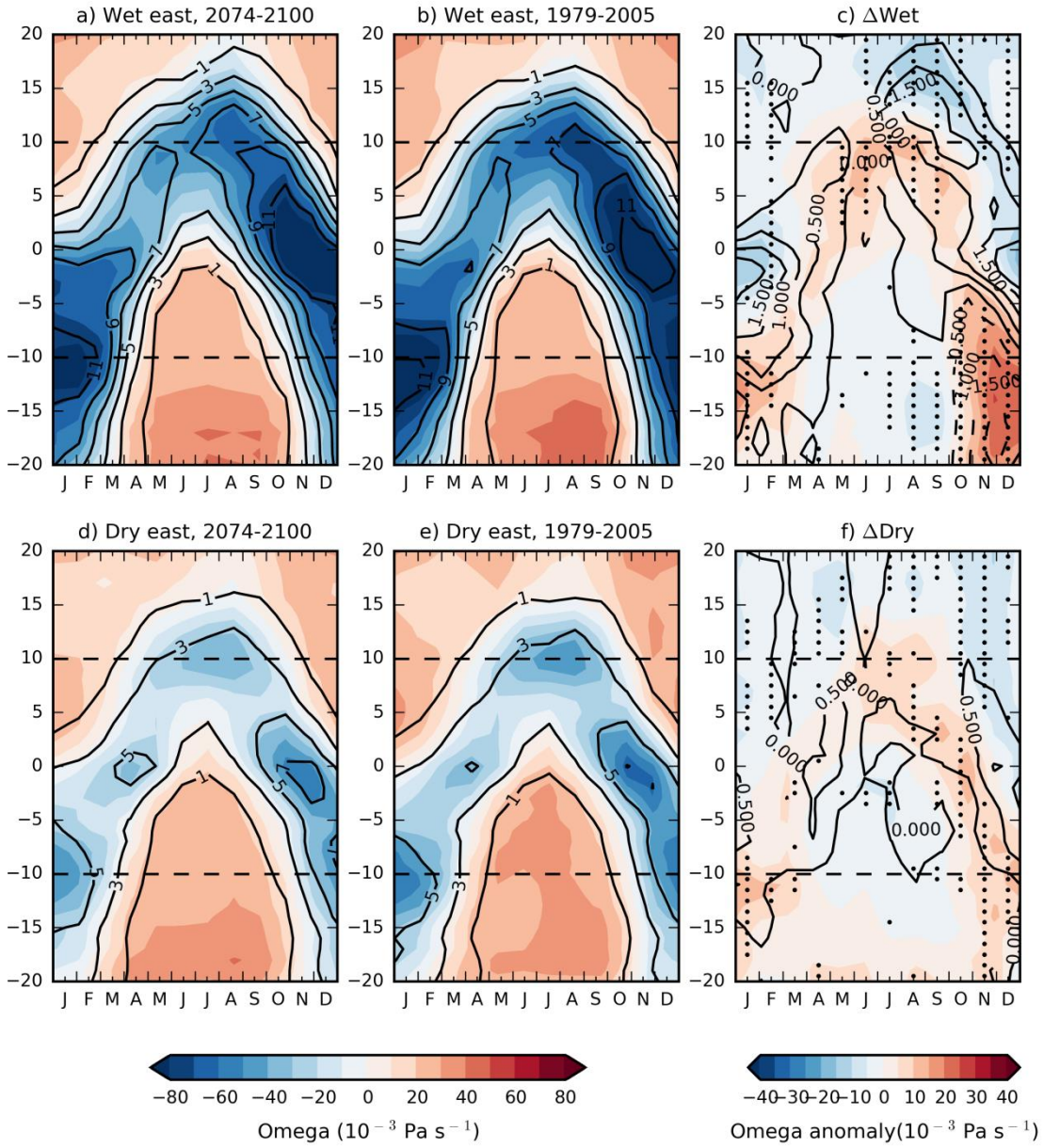

Figure 5.12 - As in Figure 5.7 but for the east Congo Basin composites. Dashed lines indicate the northern and southern boundaries of the domain.

These results suggest that while the weakening overturning circulation under warming is manifesting locally in both composites, there may be other processes in wet models which are able to contribute to increases in rainfall despite weakened uplift, for example, increased moisture supply or convergence. In dry models, there

is a greater reduction in uplift in wet models above 500 hPa in the east of the domain, which may contribute to suppression of increased rainfall. It may also suggest that the processes which contribute to enhanced rainfall in spite of weakened uplift are not present in the dry models.

5.5.2.3 700hPa qflux and the African Easterly Jets

Creese and Washington [2018] found that 700hPa wind and qflux were important differentiators between historically wet and dry models in the east Congo Basin. Figure 5.13 shows the 700hPa qflux and qflux convergence fields for the wet and dry composites. Both wet and dry models feature an increase in qflux divergence in the south of the subdomain, possibly associated with enhanced south-easterly qflux from the Indian Ocean, which becomes more meridional in future. The increase in strength of the south-easterly qflux is not significantly different between the wet composite and dry composite (Figure 5.13i). Near the equator, where wet models feature anomalous wetting in the future compare to dry models, wet models also feature anomalously enhanced qflux convergence. Dry models feature enhanced qflux convergence further north, at the top of the subdomain, and enhanced north-easterly qflux into the basin across the northern border. Increased north-easterly qflux in dry models (Figure 5.13f) is not present in the wet models (Figure 5.13c), and thus is the dominant difference between wet and dry models in their future change signal.

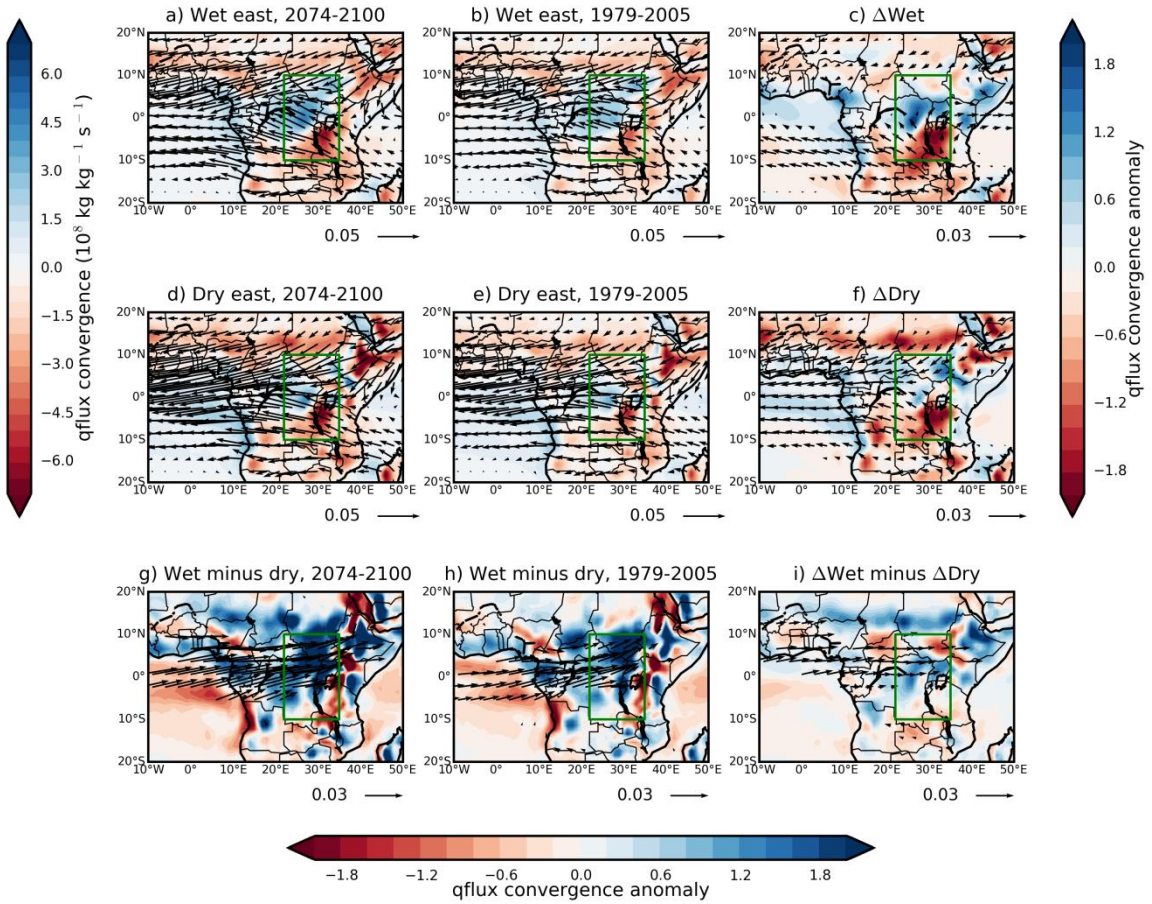

Figure 5.13 - As in Figure 5.5, but for the east Congo Basin composites at 700 hPa. The green box indicates the location of the east Congo Basin domain.

Changes in the strength and location of the north-easterly and south-easterly qflux into the basin are suggestive of changes in the strength and structure of the AEJs. *Creese and Washington* [2018] found that historically wet models feature two distinct AEJs during SON, with a clear separation between them near the equator. Conversely, dry models feature one, strong jet, centred just north of the equator. Figure 5.14 shows the latitudinal structure of the zonal wind (u) and future changes (Δu) between composites. In wet models, there is a weakening of the AEJ-N in the future, while easterly winds south of the equator increase, particularly above 700hPa. Combined with the more meridional direction of the 700 hPa south-easterlies (Figure 5.13c), these changes may account for some of the increases in

convergence in the north of the subdomain, which may contribute to increased wetting. In the dry composites, changes in the zonal wind field are much smaller; the AEJ-N weakens slightly, and there are few significant changes south of the equator.

The difference in Δu between the wet and dry composites (Figure 5.14i) is very similar to the historical wet-minus-dry difference (Figure 5.14h). This suggests that the process causing differential wetting between the composites is similar to that causing wetness/dryness in the historical period; namely, a relatively stronger and more equatorward AEJ-N in dry models compared to wet models. Despite the fact that dry models feature some weakening of the AEJ-N, it is of much smaller magnitude than in the wet models and does not correct for the equatorward bias of the jets. This indicates that the future changes experienced by models may be influenced by their underlying base climatology. In the case of the dry models, this means that the equatorward location and enhanced strength of the jet in the mean–state of the climatology dominates over mechanisms which may contribute to wetting in the future, such as enhanced moisture supply. The equatorward jet structure instead continues to remove moisture from the basin through the western boundary, resulting in only a weak wetting signal in dry models. As the structure of the AEJs in dry models is inconsistent with reanalysis estimates of the circulation, there is cause to question the plausibility of the weak wetting signal in the dry composite.

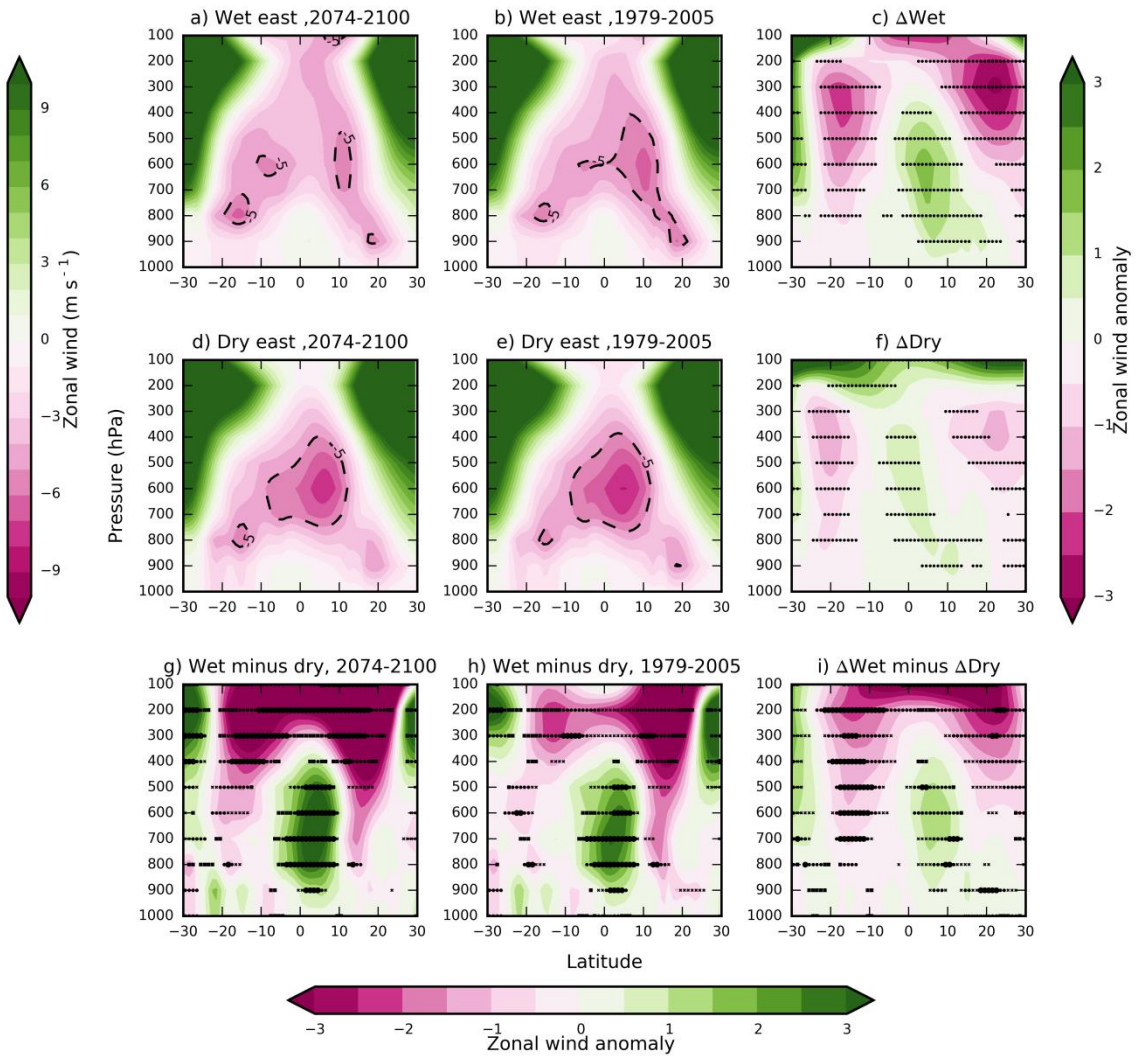

Figure 5.14 - Latitude-height cross section of zonal wind averaged across 26°E-30°E (m s^{-1}; shaded) and location of -5 m s^{-1} contour in the east Congo Basin wet composite (top row) and dry composite (middle row) in (a), (d) 2074-2100, (b), (e) 1979-2005; and (c), (f) 2074-2100 minus 1979-2005; (g) 2074-2100 wet minus dry composite; (h) 1979-2005 wet minus dry composite; and (i) wet change minus dry change. Stipples as in Figure 5.4.

5.6 Discussion

While previous research has indicated that ensemble mean changes in Congo Basin rainfall are relatively small [*Haensler et al.*, 2013a; *Aloysius et al.*, 2016], there remain differences in both the sign and magnitude of rainfall changes across

coupled models. There has been little research to date on the plausibility of these varying signals, especially in terms of the spatial patterns of change. This paper used a process-based framework to identify the mechanisms associated with rainfall change in subsets of models which have historically wet or dry climatologies, in order to assess the credibility of these rainfall signals.

5.6.1 Magnitude and patterns of rainfall change across models

Under a high emissions experiment (RCP8.5), the majority of coupled models in our sample feature slight wetting in the future, in both the east (average wetting 0.43 mm day^{-1}) and west (average wetting 0.35 mm day^{-1}) Congo Basin (Figure 5.1). These changes are generally low magnitude compared to the mean historical rainfall in individual models. Nevertheless, there are still differences amongst models in both the sign and magnitude of the change. In the east of the basin, three models feature mean drying in the future, whilst the remaining models feature wetting. The model with the most wetting in this subdomain (CCSM4) features over 30 times more wetting than the model featuring the least (FGOALS-g2). Given that ΔP is relatively small, models which are relatively wet or dry in the historical period remain so in the future period (Figure 5.1). In addition, the distribution of rainfall in individual models remains similar in the future climatology; models which have rainfall maxima in the east or west continue to do so in the future. *Creese and Washington* [2018] used a process-based assessment to identify chains of processes, predominantly related to moisture flux and low-level circulation, which differentiate between the extremely wet and dry models in the historical period. This paper hypothesizes that differences in model representation of these

processes in the historical period may translate into differences in the rainfall change pattern and signal simulated by that model.

In terms of the spatial distribution of Δ*P*, models all simulate a broadly similar pattern of wetting in the north Congo Basin and beyond and drying to the south of the basin (Figure 5.3). This has been identified in coupled models over the broader African region by *Lazenby et al.* [2018], and is hypothesized to relate to shifts in the location of convection under warming as a result of patterns of tropical SST warming and changes in circulation. Despite agreement in the broad pattern, the latitude at which wetting switches to drying is not consistent amongst all models, resulting in disagreement in the signal of change in the south of the basin (Figure 5.2). Further, the magnitude of the northern wetting and southern drying can differ by several millimetres per day between models.

There is some evidence that the north-south divide is related to shifts in the latitudinal location of the tropical rain-belt across the annual cycle. The northern region of wetting reaches its southernmost position in DJF and northernmost position in JJA, mapping broadly onto the north-south oscillation of the climatological rain-belt. The north-south pattern is therefore suggestive of either a delay in the southward movement of the rain-belt, or a cessation of the movement of the rainfall band further north compared with the historical period. Figures 7 and 12 indicate that it is the latter; during SON positive Δ*P* values are anomalously northwards in the future compared to the historical period, and during DJF there is enhanced drying over southern Africa as the rain-belt does not traverse as far south. The potential regional processes which may relate to this shift, including

changes in vertical motion, are discussed further below, with reference to the west and east composites.

5.6.2 Rainfall change in the west composites

Coupled models in the Congo Basin produce a wide spectrum of historical rainfall climatologies, which are related to different models' representations of circulation processes in the wider region [*Creese and Washington*, 2016, 2018]. Previous research by the authors has also indicated that the processes most strongly related to the inter-model spread in rainfall differ between the west and east of the basin. The aims of the latter part of this paper were thus two-fold. First, does the categorisation of models by the magnitude of their historical rainfall climatologies result in a different magnitude of future rainfall change? Given that some of the historical differences in climatology are related to known biases (for example, the tropical Atlantic SST bias), it is possible that changes in the future period build on these biases, resulting in different future rainfall signals across models. Second, are the future rainfall changes projected by models plausible based on our understanding of the processes related to those changes? This question is applicable whether the wet and dry model ΔP signals differ significantly or not.

In the west Congo Basin, both the wet and dry composites feature similar patterns and magnitudes of rainfall change in the future. Both feature some wetting in the north and drying in the south of the domain. Wet models tend to feature greater wetting over land in the west of the domain, and dry models feature more wetting over the Gulf of Guinea, but these differences are small compared to the overall

signal. This analysis suggests that, despite the significant differences in the rainfall climatology in the historical period between the extreme wet and dry models, these do not translate into large differences in the ΔP signal projected by those models. Figure 5.15 shows that excluding the spurious (wet) models from the total ensemble has little impact on the spread of ΔP values in the future. In the north west domain, where wetting is more consistent, the spread of the inter-quartile range and the median value reduce slightly, but the range remains large. The results for the west Congo Basin, therefore, suggest that there is not a simple relationship between the strength of present day model biases and the magnitude of future change. However, comparison of the processes underlying the signal of change with those which drive present day climatological differences in models could tell us something about the plausibility of the rainfall change signals across the suite of models.

In the future-minus-present analysis, both wet and dry composites feature an increase in SST generally across the tropics, with above-average increases in the tropical east Atlantic (>3 °C). This is the region where models feature present-day biases of up to 4°C, and so any warming here is superimposed on top of an already too-warm base-state. The SST warming is slightly higher in the dry composite than the wet composite, though only significantly so over a small area. Both composites also feature increased evaporation over this region; again, this is slightly greater in the dry models, coinciding with the relatively higher SSTs. Further, both wet and dry composites feature enhanced low-level westerly qflux into the basin from this region. This was also found to be a differentiating process between extremely wet and dry historical climatologies.

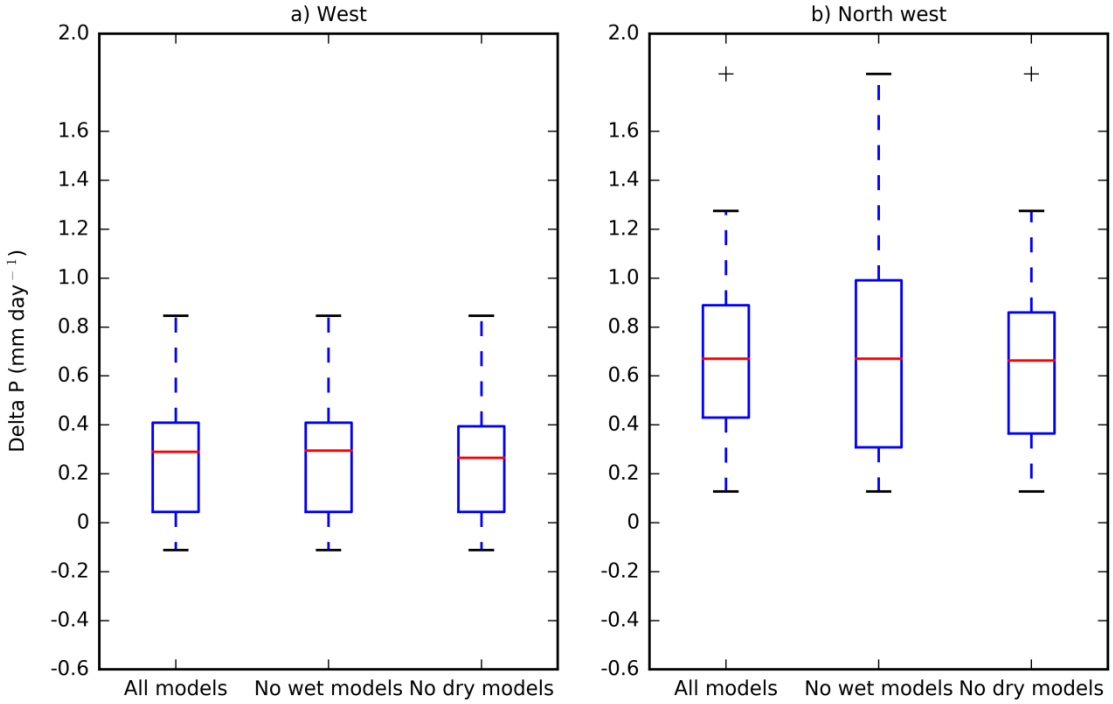

Figure 5.15 - Box plot of 2074-2100 minus 1979-2005 long-term mean rainfall (mm day^{-1}; ΔP) averaged over (a) the west Congo Basin domain (8°E to 21°E, 10°S to 10°N) and (b) the north west Congo Basin domain (8°E to 21°E, 0° to 10°N). The first boxplot includes all models, the second excludes the wet composite models, and the third excludes the dry composite models.

That some of the same processes related to extreme model wetness in the historical period may be related to the future wetting signal in both composites is a cause for concern. While the 'rich-gets-richer' mechanism of tropical rainfall change posits that the low-level moisture transport into already-convective regions will increase, this analysis also indicates that enhanced tropical Atlantic SSTs, and associated increases in evaporation, may also contribute to enhanced moisture transport within the low-level westerlies in the future. This potentially casts doubt on the magnitude of the positive ΔP signal in all models in the north west Congo Basin domain, as the processes related to wetting are building on known SST biases in the region. The Gulf of Guinea warm SST bias is present in all but one model in the sample, not just the historically wet models.

There is one element of the historical process chain which does not manifest in relation to the positive Δ*P* signal. In the historical period, enhanced model wetness is associated with a local enhancement of convection at the Atlantic coast, and it was hypothesized that the enhanced moisture from too-warm Gulf of Guinea SSTs was contributing to a local enhancement of convection in this region. However, in the future experiment uplift decreases in both wet and dry models. This may be a local manifestation of the weakening of the overturning circulation under warming [*Held and Soden*, 2006; *Vecchi and Soden*, 2007]. One explanation for wetting in the future despite decreased uplift is that the frequency distribution of daily rainfall changes in the future. As Figure 5.8 shows, the distribution of daily rainfall flattens in the future, and in the wet composite there are a greater number of both very wet and very dry days in the future. Further, the wetting in the north west co-locates with the northern edge of the area of decrease in upward motion (Figure 5.7), whereas the south of the domain, which features drying, is located within the core of the decrease in uplift. This indicates that in the north, the increased moisture supply into the basin is enough to counteract the slight decrease in uplift, resulting in a positive Δ*P* signal.

These results suggest that enhanced moisture from the tropical east Atlantic may be contributing to wetting in the west Congo Basin, despite decreases in subsidence. Given that this process builds on dubious historical SST biases, which are present in both composites, there is reason to be cautious about accepting the magnitude of the wet signal displayed in both composites. Analysis of the processes related to the long-term drying trend over equatorial Africa may support this hypothesis. *Hua et al.* [2016] analyse the circulation features associated with

drying over Central Africa in reanalysis data between April and June, and suggest that it may reflect the response of the large-scale circulation to relatively greater warming of west Pacific SSTs compared to the central Pacific SSTs. This differential SST warming has resulted in a westward extension of the tropical Walker circulation, and may have resulted in anomalous subsidence over equatorial Africa in recent decades. Whilst in a different season, and highlighting SST anomalies in a different basin, these results indicate that observed patterns of SST change are likely to induce drying, rather than wetting, over the Congo Basin. A dedicated coupled model experiment with varying baseline SSTs upon which to apply the emissions forcings would be necessary to test this hypothesis.

5.6.3 Rainfall change in the east composites

In the east composites, categorising models as historically wet or dry does result in significantly different patterns of ΔP, particularly in the north east of the basin, where wet models feature an average rainfall increase 1.19 mm day^{-1}; more than twice the amount of wetting in dry models (0.43 mm day^{-1}). This 'wettest-models-get-wetter' response amongst models is investigated with reference to the processes which differentiate wet and dry model climatologies in the historical period.

In the historical period, wet models feature a stronger SAH, which is related to stronger low-level south-easterlies in the south tropical Atlantic, and stronger westerlies near the equator. This enhanced westerly flux constitutes the lower branch of a zonal overturning cell, bringing moisture into the east of the basin and

contributing to greater convection. In the future-minus-present analysis, both wet and dry models feature enhanced south-easterly and south-westerly qflux in the Atlantic, alongside a strengthening of the southern flank of the SAH. However, there is no significant difference in this signal between wet and dry models, indicating that changes in these processes are not the dominant cause of differences in the composites' Δ*P* signals.

Further, as in the west composite models, models in the east feature a slight decrease in uplift in the future, despite wetting, particularly in the historically wet models. Again, this could be explained by differences in the distribution of daily rainfall in the two periods; in the future, the distribution of rainfall on individual days flattens, with more very wet days in the future compared to the present (not shown). In terms of differences between the two composites, the decrease in upward motion is stronger in wet models near the surface, but stronger in dry models above 500 hPa, the core of convective activity, which could be related to enhanced wetting in wet models. Overall, the decrease in uplift in wet models despite significant wetting indicates that , like in the west composites, increases in *q* may be sufficient to enhanced rainfall despite reduced convection.

While there are few differences between composites in the 925 hPa circulation and vertical motion, there are greater differences in the mid-level (700 hPa) moisture circulation (Figure 5.13). At 700hPa, both composites feature enhanced qflux into the basin from the south-east. In wet models, this is more meridional in the future than in the historical period. In addition, dry models feature greater qflux from the north-east, whereas this flux does not change significantly in wet models. In both

composites, these changes appear related to increase qflux convergence in the north east of the basin and divergence in the south of the basin; this pattern is strongest in the wet models, possibly due to the more meridional orientation of the south-easterly feed contributing to enhanced convergence. The wet-minus-dry Δqflux pattern (Figure 5.13i) is similar to the historical wet-minus-dry pattern; wet models have weaker easterly qflux in the north of the basin than dry models. This suggests that the cause of the different Δ*P* signals in the composites is related to similar processes that produce relative wetness or dryness in the historical period.

In addition to the horizontal circulation, there are significant differences between the wet and dry composites' simulations of the latitudinal structure of the zonal wind, in particular the African Easterly Jets (Figure 5.14). In the historical period, this is a key differentiator between wet and dry models, with wet models featuring a weaker and more equatorward AEJ-N, while dry models feature a stronger and more poleward AEJ-N. Analysis of ERA-Interim reanalysis data suggests that wet models are closer to observations, as they produce two distinct AEJs, and therefore are possibly more plausible [*Creese and Washington*, 2018]. In the future, the AEJ-N weakens in both composites; however, this weakening is stronger in the wet models (Figure 5.14i). In addition, in the wet models, the AEJ-S strengthens slightly, whereas in the dry models there is not a distinct AEJ-S between 0° and 10°S, and so it does not strengthen.

As in the 700 hPa horizontal circulation, the wet minus dry Δ*u* pattern (Figure 5.14i) is very similar to the historical wet minus dry pattern (Figure 5.14h). This suggests that differences in the Δ*P* signal between composites may be related to

the same process differences in AEJ structure identified in the historical period. In wet models, the presence of two distinct and relatively weaker jets is hypothesized to contribute to convergence, and hence rainfall, where they meet. As the northern component weakens in the future and becomes more meridional, this convergence increases, resulting in wetting in the north east Congo Basin. Conversely, in dry models, the strong, equatorward jet acts to remove moisture from the basin in the historical climatology, and the lack of distinction between the two jets reduces convergence between the two. In the future, despite some weakening of the equatorward AEJ, there is not an increase in convergence, and the enhanced easterly flow acts to remove moisture from the basin. This finding indicates that

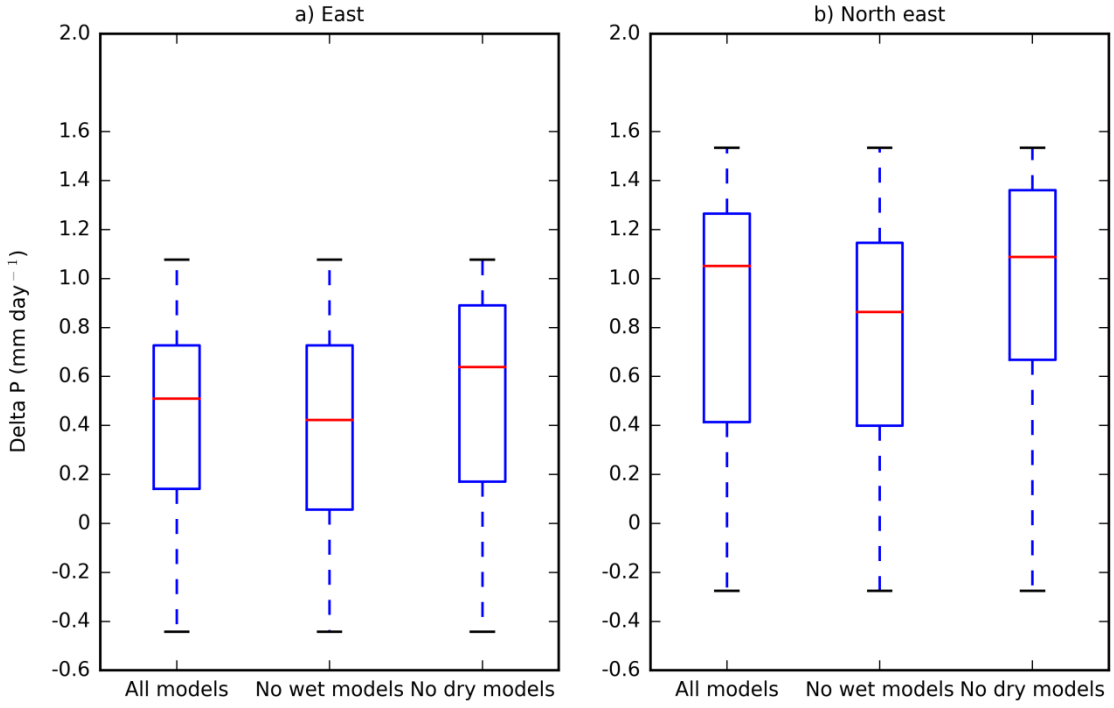

Figure 5.16 - Box plot of 2074-2100 minus 1979-2005 long-term mean rainfall (mm day^{-1}; ΔP) averaged over (a) the east Congo Basin domain (22°E to 35°E, 10°S to 10°N) and (b) the north east Congo Basin domain (22°E to 35°E, 0° to 10°N). The first boxplot includes all models, the second excludes the wet composite models, and the third excludes the dry composite models.

the influence of the climatological AEJ structure in dry models dominates over any changes in the circulation in the future, and acts to suppress significant rainfall change in this region.

This analysis suggests that biases in the historical period may influence the Δ*P* signal projected by models in the east of the basin, and that removing models with such historical extremes could help reduce the range of uncertainty in the Δ*P* signal. Figure 5.16 quantifies the removal of both extremely wet and dry models on the ensemble spread. In the north east of the domain, where wetting is most consistent across models, excluding extremely dry models does increase the upper quartile, median and lower quartile values, as well as reducing the interquartile range. The overall range is significantly reduced (from 1.813 mm day $^{-1}$ to 1.244 mm day $^{-1}$) if the CSIRO-Mk3-6-0 model is excluded from the analysis. This is the only model to exhibit mean drying in the north east of the basin, and has previously been identified as an outlier in the historical period [*Creese and Washington*, 2018]. If we consider dry models to be untrustworthy due to their dubious representation of the AEJs, then this analysis indicates that greater wetting is a more likely response to warming. However, the overall range still includes both positive and negative Δ*P* signals, and so further work is needed to elucidate the plausibility of this response.

5.7 Summary

This study used a process-based analysis to attempt to elucidate the influence of extreme historical climatologies on rainfall change in the future period, and to identify the processes driving rainfall changes. In terms of changes in the Congo Basin, this study finds that:

1. Rainfall changes in the Congo Basin across CMIP5 models are small compared to historical rainfall differences amongst models
2. Rainfall increases in the north and decreases in the south of the Congo Basin across all models in SON; however, there are differences in the latitude of where the rainfall change signal switches from positive to negative.
3. The rainfall change signal in the west of the Congo Basin is not significantly different between wet and dry composites, suggesting that the rainfall response to forcing dominates over differences in the present day mean-state.
4. In both wet and dry models in the west Congo Basin, the low-level circulation intensifies, which may be part of a rich-gets-richer response.
5. In both composites SSTs increase in the tropical east Atlantic, a region which features positive SST biases in all composite members. There is also enhanced evaporation over the Gulf of Guinea and qflux into the basin.
6. As the SST increases build on a region of historical biases, the enhanced evaporation and qflux in the future may contribute to higher magnitude

wetting than would be the case without the underlying bias in all models investigated. Further investigation is needed to test this hypothesis.

7. There are significant differences in the rainfall change signals between historically wet and dry models in the east Congo Basin. Wet models feature greater wetting than dry models, particularly in the north east of the domain.
8. The differences in rainfall change between wet and dry composites in the east are related to changes in the AEJs. In the wet models, the AEJ-N weakens, contributing to enhanced convergence and rainfall. In dry models, the underlying equatorward AEJ structure dominates over changes to the circulation, continuing to export moisture away from the east Congo Basin and resulting in reduced wetting.
9. Given that the climatological structure of the AEJs in dry models is not reflected in reanalysis data, this casts doubt on the low magnitude wetting/drying signal projected in the dry composite models.

In addition to understanding the processes related to rainfall change in the Congo Basin, this study also tested the hypothesis that a model's representation of processes in the historical period may impact its rainfall change signal in the future. The results in this regard were mixed. In the east Congo Basin, where the two composites (representing differing historical rainfall) feature different climatological structures of the same feature (the African Easterly Jets), the method was useful since the underlying differences related to the amplitude of the rainfall change signal. However, in the west Congo Basin, where all models share a similar bias (the tropical Atlantic SST bias), the approach was less successful. This

suggests that a process-based approach may be most useful in cases where there are clear differences in the representation of the process between composites, or where some feature biases and others do not. In cases where a similar bias exists in all models, sampling models across the rainfall spectrum is not helpful in constraining the range of rainfall change values.

In regions where biases are present across all models, such as the west Congo Basin, a different approach to process-based evaluation may therefore be required. This study sampled models from the extreme ends of the spectrum of historical rainfall; another approach is to sample instead on the representation of climatological processes in models. In the case of the west Congo Basin, this could involve examining models with the largest and smallest Atlantic SST biases, or strongest and weakest westerly moisture flux, to determine whether they produce different rainfall change signals. Another option is to sample based on rainfall change itself, and identify the processes controlling rainfall change at the extreme ends of the rainfall change spectrum. Assessing the plausibility of changes in regionally-important processes (and by extension rainfall) will require an understanding of which processes are important for controlling inter-model differences, and so the historical process-based assessments, as developed in *Creese and Washington* [2018], will remain a useful step in this method.

Acknowledgements

The GCM data used in this study was made available through the Earth System Grid Federation (ESGF) Peer-to-Peer system (https://pcmdi.llnl.gov/search/cmip5/). Amy Creese and Callum Munday are fully funded by the UK Natural Environment Research Council (NERC) via a Doctoral Training Programme (NE/L002612/1), and partly funded by a UK Met Office CASE studentship. Richard Washington is partly supported by NERC and the U.K. Government's Department for International Development (DfID) UMFULA project (NE/M020207/1). The authors acknowledge the helpful inputs of Emma Howard, Rachel James and Neil Hart.

Supplementary material

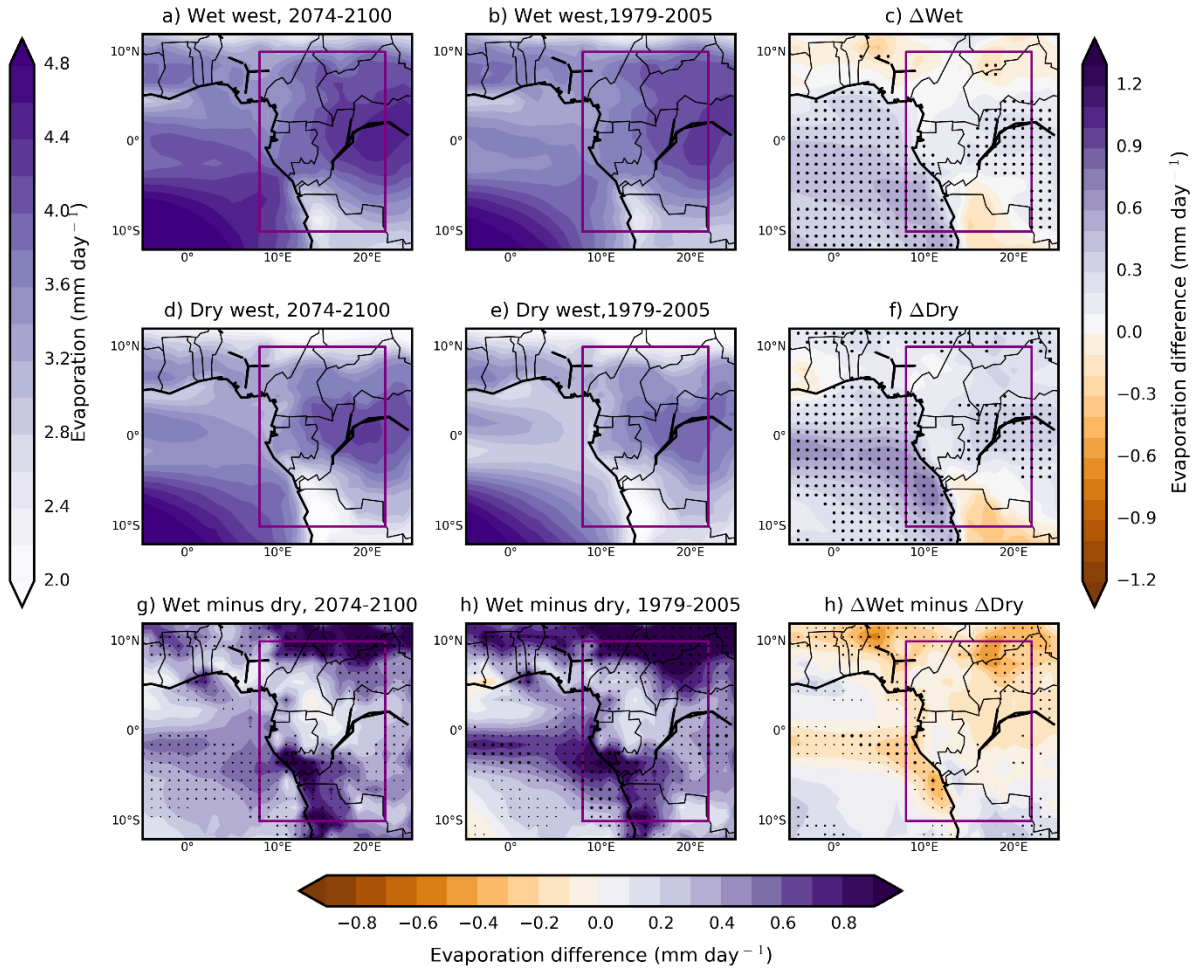

Figure 5.S1 - Long term mean SON evaporation (mm day^{-1}) in the west Congo Basin wet composite (top row) and dry composite (middle row) in (a), (d) 2074-2100, (b), (e) 1979-2005; and (c), (f) 2074-2100 minus 1979-2005 (ΔE); (g) 2074-2100 wet minus dry composite; (h) 1979-2005 wet minus dry composite; and (i) wet ΔE minus dry ΔE. Stipples in (c) and (f) indicate where all four models in the composite agree on the sign of change. Stipples in (g-i) occur at gridboxes where: 1) all wettest composite values are larger or smaller than all driest composite values (large dots); 2) all wettest composite values are greater or smaller than the driest composite mean (squares); 3) driest composite values are greater or smaller than the wettest composite mean (crosses); and 4) both (2) and (3) are true (small dots). The purple box indicates the location of the west Congo Basin domain.

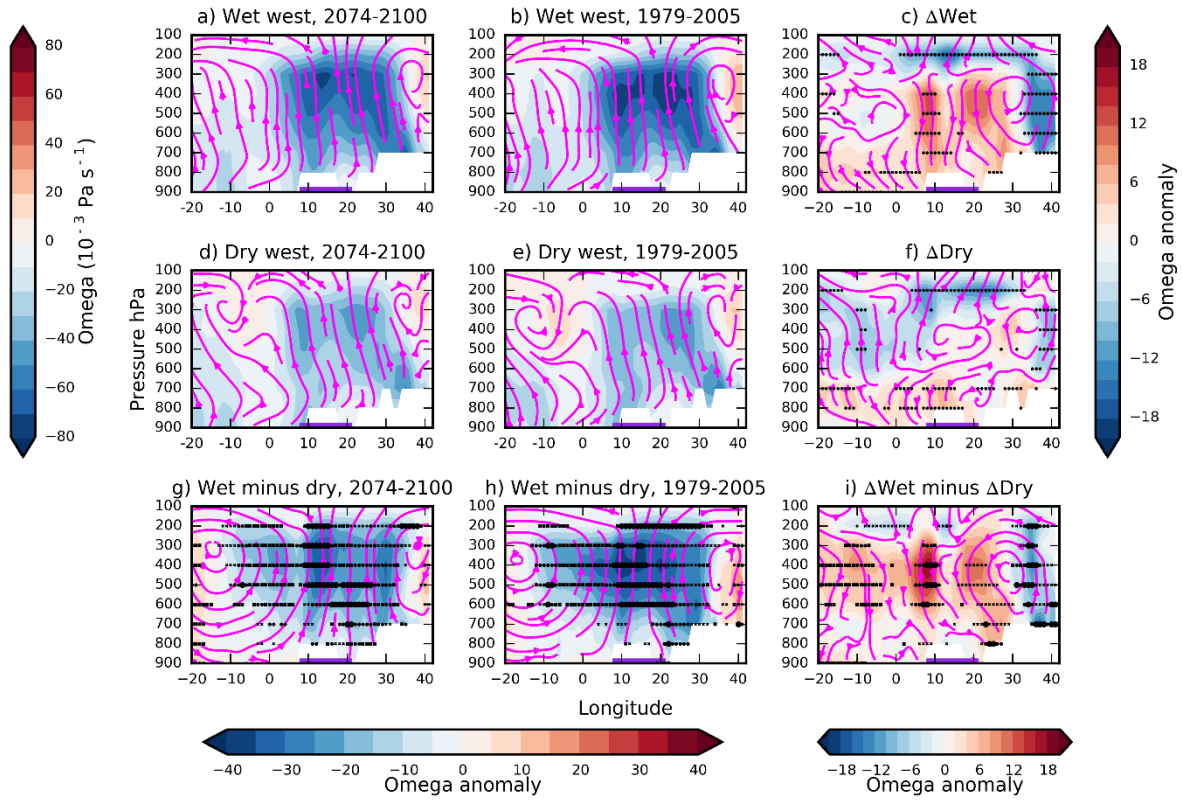

Figure 5.S2 - Long term mean SON omega (10^{-3} Pa s^{-1}; shaded) averaged between 0° and 10°N and divergent component of zonal wind (m s-1) and omega (10^{-3} Pa s^{-1} streamlines), in the west Congo Basin wet composite (top row) and dry composite (middle row) in (a), (d) 2074-2100, (b), (e) 1979-2005; and (c), (f) 2074-2100 minus 1979-2005; (g) 2074-2100 wet minus dry composite; (h) 1979-2005 wet minus dry composite; and (i) wet change minus dry change. Areas with high topography in models are masked (white). The purple box shows the extent of the west Congo Basin domain (8°E to 21°E). Stipples as in 5.S1 and refer to omega values.

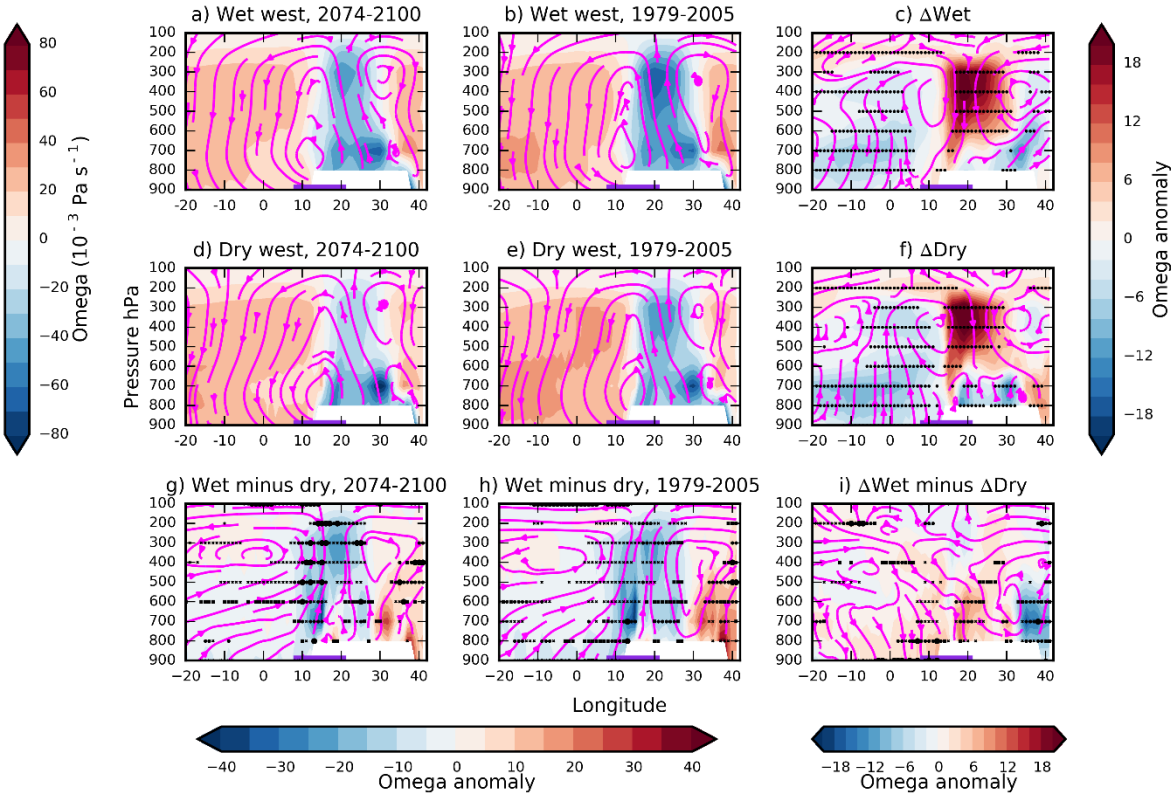

Figure 5.S3 - As in Figure 5.S2 but averaged between 5°S and 10°S

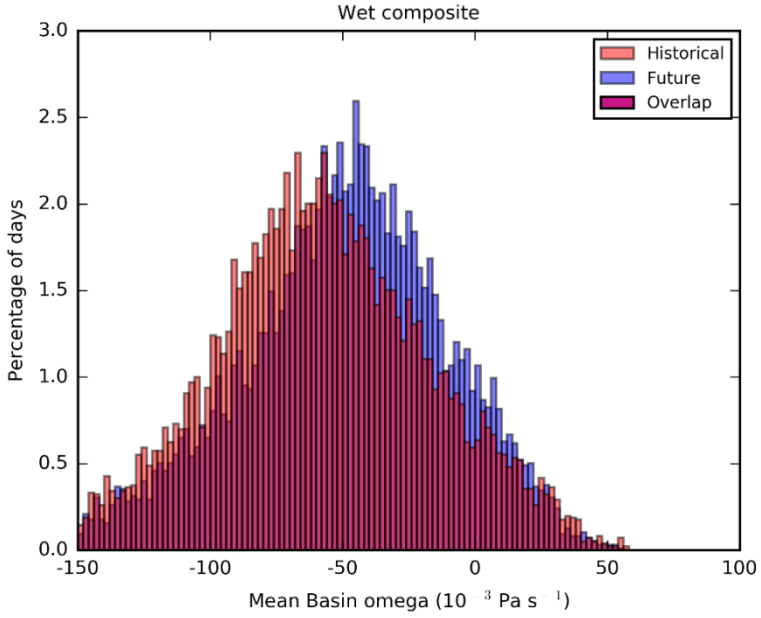

Figure 5.S4 - Frequency distribution of daily omega (10^{-3} Pa s^{-1}) in the northwest of the basin (8°E to 21°E, 0° to 10°N) in all SON days in all composite member models in the west wet composite, in 2074-2100 (blue) and 1979-2005 (orange). Pink denotes overlap between the orange and blue distributions. The dry composite is not shown as daily omega data is unavailable for two composite member models.

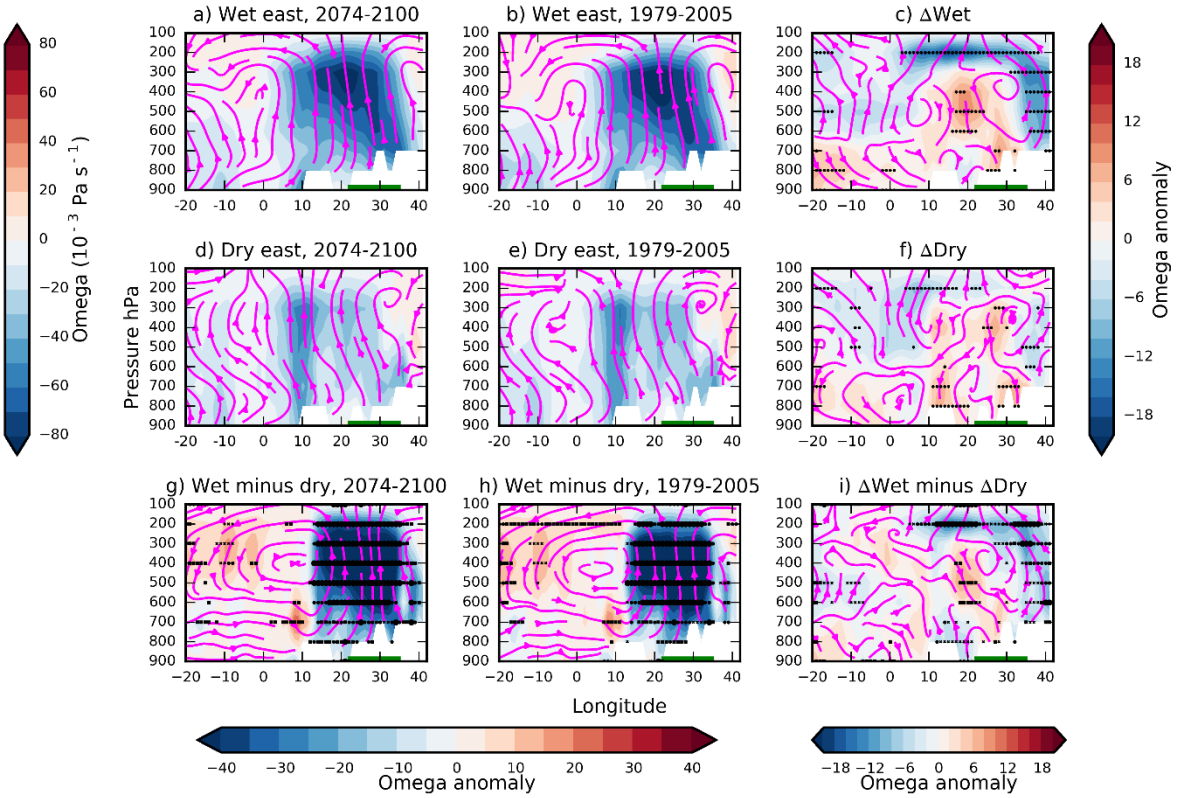

Figure 5.S5 - As in Figure 5.S2 but for the east Congo Basin composites. The green box shows the extent of the east Congo Basin domain

6 Climate change in the Congo Basin: Processes related to wetting in the December-February dry season

Climate change in the Congo Basin: Processes related to wetting in the December-February dry season

A. CREESE[1], R. WASHINGTON[1] and R. JONES[1,2]

[1]Climate Research Lab, School of Geography and the Environment,

University of Oxford, South Parks Road, Oxford, OX1 3QY, UK

[2] Met Office Hadley Centre, FitzRoy Road, Exeter EX1 3PB, UK

Submitted to *Climate Dynamics*

15th October 2018

Accepted for publication

10th March 2019

Authorship Declaration

I conducted all of the analysis and writing for this paper. Richard Washington discussed the methodology, results and structure of the paper with me, and edited the manuscript. Richard Jones discussed the methodology and results with me and edited the manuscript.

Abstract

The Congo Basin is one of three key areas of tropical convection and contains the planet's second largest rainforest. Understanding how global warming might change its climate is crucial, particularly during the dry seasons, when rainfall amounts currently bring the rainforests close to the threshold of viability. There is considerable uncertainty in projections of future rainfall change from the Coupled Model Intercomparison Project (CMIP5) under the high-emissions experiment (RCP8.5). Whilst there is a general trend towards wetting in most months, its magnitude varies considerably. In the December to February dry season, the projected change in seasonal rainfall varies from 2 to 160 mm across models. This study uses a regionally-focused process-based assessment to understand inter-model differences in rainfall projections, as a first step to assessing their plausibility. Models which produce the most wetting by the end of the century feature enhanced convection over the Congo Basin region, enhanced subsidence in the African subtropics, and decreased uplift over the Maritime Continent. In contrast, models with a small wetting response feature reduced convection over the Congo Basin. This indicates that wetting over the Congo Basin is related to a weakening of the Indian Ocean Walker circulation, reminiscent of a positive Indian Ocean Dipole state. Models with the highest magnitude wetting also feature greater low-to-mid-level moisture flux from the north and the east compared to models with less wetting. These results indicate that the future degree of wetting over the Congo Basin will be linked to changes in convection over the Maritime Continent.

6.1 Introduction

The Congo Basin hosts the planet's second largest rainforest, a vital global carbon store and significant element of the global carbon cycle. However, changes in regional precipitation under climate change have the potential to influence rainforest composition and distribution [*Malhi and Wright*, 2004]. The Congo rainforest boundaries already exists close to the hydrological limits which support a closed-canopy forest, and there is evidence of rainforest contraction and changes to forest composition during drier periods in the past three thousand years [*Brncic et al.*, 2007; *Ngomanda et al.*, 2007; *Lewis et al.*, 2009; *Malhi et al.*, 2013]. It is therefore crucial that possible climatic changes in the region are understood, in order to provide decision-makers with the most credible information for mitigation and adaptation planning.

However, despite its climatic importance, the Congo Basin is critically understudied, particularly in terms of the likely effects of anthropogenic climate change. A lack of homogenous and widespread rainfall records has meant traditional methods of model evaluation are limited, and the lack of data with which to test models is likely to have contributed to extreme model divergence in this region [*Washington et al.*, 2006, 2013]. As models are our only tool for diagnosing and assessing future climate change, this has contributed to considerable uncertainty in the likely changes in this region. Recent work analysing models in the Coupled Model Intercomparison Project (CMIP5) over the Congo Basin has found that coupled global climate models (GCMs) can differ in

their climatological mean rainfall by up to a factor of five in some months, with the largest differences found in December, during the December-February (DJF) dry season [*Creese and Washington*, 2016]. Recent efforts have concentrated on understanding model uncertainties in the wet seasons [*James et al.*, 2013; *Washington et al.*, 2013; *Creese and Washington*, 2016, 2018], whereas the dry seasons have been largely overlooked. However the effects of climate change on the rainforests are likely to be felt most keenly during the dry seasons during which rainforest boundaries already exist close to the rainforest-savannah rainfall threshold [*Malhi et al.*, 2013]. A shift in the location or intensity of rainfall in the dry seasons in the future is likely to have implications for the rainforest extent, which in turn is likely to influence the carbon storage capacities of the region [*James et al.*, 2013; *Malhi et al.*, 2013].

This paper aims to help address these knowledge gaps by conducting an assessment of the plausibility of signals of rainfall change in the Congo Basin in the December to February (DJF) dry season. Where previous work has focused on determining the credibility of models in the historical period [*Creese and Washington*, 2016, 2018], this paper will add to these insights by examining processes which are related to model simulations of future rainfall change. This approach will be a vital first step towards providing reliable projections of future change in the region.

6.1.1 Congo Basin rainfall change

There have been few attempts to understand the mechanisms of rainfall change and uncertainties in the range of future projections across models in the Congo Basin. Studies have thus far focused on rainfall changes in the region simulated in large model ensembles. *Haensler et al.* [2013] analyse changes in rainfall across 77 climate change projections, including models from the CMIP3, CMIP5 and CORDEX projects. They found that the multi-model ensemble (MME) does not indicate severe rainfall changes across the region by the end of the century, even under the highest emissions scenarios. Across the whole ensemble, they find a large range of mean simulated rainfall change; in one region during DJF, the range spans from -50% to +150%. Using a skill scores-based approach to choose a subset of models based on their realism in representing the historical rainfall climatology compared to observations, *Aloysius et al.* [2016] find that large heterogeneities also exist in spatial patterns of annual mean rainfall change in CMIP5, contributing to overall uncertainty in projections for this region. This model subset projects slightly higher magnitude rainfall change than in the full MME, and features a smaller range in the signal.

James et al. [2013] analysed the rainfall projections over the Congo Basin in the CMIP3 ensemble and two Hadley Centre perturbed physics ensembles (PPEs), finding substantial variation amongst models. However, some patterns emerged; the majority of models featured some wetting in the east of the domain and drying in the west of the domain during the September-November rainy season. An analysis of the dynamics associated with this change indicated shifts in the zonal

circulation may be related to rainfall changes, and this understanding could be used in further work to assess the plausibility of such changes.

There has also been some work on rainfall projections from regional models (RCMs). *Pokam et al.* [2018] analyse the rainfall changes in the region at 1.5°C and 2°C of warming in the Coordinated Regional Climate Downscaling Experiment (CORDEX) models. They find that in the parent GCMs, there is a tendency for wetting across the basin in the future, whereas in the RCMs there is greater uncertainty in the sign of change across the basin, with roughly half of models projecting negative changes and half projecting positive changes. This is the case at both temperature thresholds, as well as across different forcing pathways (Representative Concentration Pathways; RCPs). The models in the sample also show little agreement in the magnitude or spatial pattern of rainfall change across the basin. *Saeed et al.* [2013] compare rainfall projections in the regional climate model REMO to its driving GCM MPI-ESM, finding that the former projects rainfall decreases while the latter projects rainfall increases. By assessing the land surface processes associated with rainfall, they find that the RCM's tendency to simulate more extreme rainfall events led to higher surface runoff and less soil moisture, resulting in a less intense hydrological cycle and lower rainfall overall. Given that the number of extreme events in the RCM better matches the observational data, they suggest the RCM's projection may be more reliable than the GCM.

6.1.2 Mechanisms of tropical rainfall change under warming

The processes relating to model rainfall change in the Congo Basin will be embedded within larger structures of change in tropical rainfall. The response of tropical rainfall to warming is complex, and involves several interlinked and sometimes opposing mechanisms of change. The thermodynamic increase in atmospheric moisture content (q) under warming may result in enhanced moisture transport, and thus enhanced moisture convergence (divergence) in regions which are already feature convergence (divergence) [*Chou and Neelin*, 2004; *Held and Soden*, 2006]. This 'wet-gets-wetter' mechanism and has been found to occur in model simulations at very large spatial scales, as well as in recent observational data [*Allan et al.*, 2010; *Allan*, 2012; *Durack et al.*, 2012]. To some extent the wet-gets-wetter response will be opposed by the dynamical weakening of the tropical overturning circulation, resulting from the differential rate of increase in q and rainfall [*Allen and Ingram*, 2002; *Held and Soden*, 2006; *Vecchi and Soden*, 2007; *Ma et al.*, 2012; *Chadwick et al.*, 2013]. This weakening of the circulation has been found to occur more robustly zonally, in the Walker cell, than meridionally, in the Hadley cell [*Vecchi and Soden*, 2007].

Other dynamical mechanisms of rainfall change include: the 'warmer-gets-wetter' mechanism [*Xie et al.*, 2010], whereby the spatial pattern of sea-surface temperature (SST) change is important in inducing changes in convection over oceans; changes in atmospheric circulation [*Shepherd*, 2014]; land-sea temperature contrasts [*Dong et al.*, 2009]; and the direct and indirect effects of aerosols [*Hansen et al.*, 1997; *Lohmann and Feichter*, 2004; *Huang et al.*, 2007].

Recent studies have also identified connections between dynamical and thermodynamical mechanisms; *Huang et al.* [2013] find that annual mean rainfall in the tropics is dominated by the warm-gets-wetter response near the equator, while seasonal anomalies of rainfall change follow the wet-gets-wetter response.

The warm-gets-wetter and wet-gets-wetter mechanisms are useful for explaining patterns of change over large spatial scales and across oceans. However there are still uncertainties regarding the balance of these mechanisms at regional scales and over land [*Chadwick et al.*, 2013], reflected in the fact that at a regional-scale there is much less agreement amongst models in the patterns and behaviours of rainfall change [e.g. *Meehl et al.*, 2007; *Rowell*, 2012]. In their assessment of spatial changes in tropical precipitation, *Chadwick et al.* [2013] showed that when rainfall change in CMIP5 models is decomposed into its constituent parts, the spatial patterns of the wet-gets-wetter component and the dynamically-driven weakened large-scale circulation component largely cancel one another out, leaving the pattern of rainfall change to be dominated by other, regional dynamical mechanisms, primarily relating to shifts in the location of convection. Similar results have been found over Africa. *Lazenby et al.* [2018] note that model uncertainty over southern Africa and the south west Indian Ocean is related most strongly to shifts in the location of convection, associated with SST-gradients over the Indian Ocean. *Giannini et al.* [2018] use a different decomposition metric to understand the contribution of thermodynamic and dynamic mechanisms to rainfall change in East Africa during the wet seasons, finding that the wetting signal in the CMIP5 multi-model mean (MMM) can be explained by circulation changes including the advection of moisture away from the Congo Basin to the East

African margin. *Rowell and Chadwick* [2018] also find that uncertainties in the East Africa response to warming primarily derive from uncertainties in regional dynamics across the CMIP5 ensemble, related to spatial shifts in convection due to SST warming.

Dynamical mechanisms are also likely to be a particularly important consideration for understanding model diversity in the Congo Basin. Rainfall in the region is governed not only by the north-south movement of the tropical rain band, but also a complex set of regional factors, including topography, mid-level jets, local overturning cells, monsoon winds, land-sea interactions, and mesoscale convective systems [e.g. *Nicholson and Grist*, 2003; *Balas et al.*, 2007; *Jackson et al.*, 2009; *Pokam et al.*, 2012; *Cook and Vizy*, 2015; *Dezfuli et al.*, 2015; *Dezfuli*, 2017; *Nicholson*, 2017]. All of these processes will exhibit responses to greenhouse gas-induced warming, which will complicate the large-scale picture of tropical rainfall change in this region.

6.1.3 A process-based assessment of change

The studies described above give useful insights into the range of projections in this region, and the possible tropics-wide mechanisms that may cause them. A regionally-focused process-based investigation will help further determine the plausibility of model projections via an examination of the processes behind such changes. Such assessments examine the processes associated with rainfall in models, with the aim of determining the credibility of the simulated rainfall, either

in the historical or future periods. For example, *James et al.* [2015] determined the processes associated with drying in historically dry years in the Sahel from reanalysis data, and found them to differ from the processes causing dry years simulated in the current climate of a model ensemble. On finding that the same spurious processes were responsible for the drying in the future, they concluded that we could not trust projections of extreme drying in this region in the sample of models analysed. In the Congo Basin, *Creese and Washington* [2018] identified a chain of processes leading to extremely wet or dry mean climatologies in the Congo Basin in CMIP5 models. They found that models with extremely wet western subdomains also featured larger and more persistent Atlantic SST biases, casting doubt on the credibility of those models' climatologies.

Process-based assessments can help to overcome some of the issues of using large ensembles of models. While MMMs are sometimes found to give the 'best estimate' of climates, with the suggestion that the averaging process cancels out errors in individual models and highlights similarities [*Hagedorn et al.*, 2005; *Palmer et al.*, 2005; *Reichler and Kim*, 2008], there is reason to be cautious about their use in the Congo Basin. Previous analysis indicates that in the Congo Basin, large model disparities in both rainfall magnitude and distribution result in MMMs that are not representative of any individual models [*Creese and Washington*, 2016]; in addition, there are many inter-related models in inter-comparison projects such as CMIP, which can skew the MMM. Further, the scarcity of recent observational data in the region, and non-trivial differences between observational products, limits the strength of approaches based on skill in replicating historical climatology [*Washington et al.*, 2013; *Creese and Washington*, 2016]. As *Aloysius et al.* [2016]

highlight, an analysis of how well models represent causal mechanisms of change is also required to determine model plausibility, and the authors highlight some mechanisms which may be of particular importance (e.g. SST departures, sources and fluxes of atmospheric moisture). This paper will thus undertake a more in-depth analysis of such processes involved in rainfall change across individual models.

6.1.4 Aims

The focus of this study is to explain the spectrum of model projections of rainfall. We hypothesize that both the low-level and overturning circulations will help to differentiate between modelled rainfall changes, given their importance in describing both interannual variability in observations, and inter-model differences in rainfall [e.g. *Pokam et al.*, 2012, 2014; *Cook and Vizy*, 2015; *Creese and Washington*, 2016, 2018]. Understanding such processes will be an important starting point for future work investigating the plausibility of projected changes.

Specifically, this study aims to:

1. Quantify and characterise the spectrum of rainfall changes in the Congo Basin between the end of the 20th and end of 21st century across CMIP5 models. The focus will be the season with the strongest rainfall change signal, DJF.

2. Identify the large-scale circulation changes associated with the inter-model spread in projections of rainfall change in DJF
3. Assess different model rainfall projections in the Congo Basin in the context of proposed mechanisms of tropics-wide rainfall change

6.2 Data and Methods

This study uses two domains for its assessment of the Congo Basin; the first, used in Section 6.3, is 8°E to 35°E, 10°S to 10°N (red box, Figure 6.4), following *Creese and Washington* [2018]. From Section 6.4 (Figure 6.3) onwards, the smaller domain 10°E to 35°E, 10°S to 5°N is used (green box, Figure 6.4), to reflect the more southward location of the tropical rain belt during the December-February season.

The Coupled Model Intercomparison Project (CMIP5) provides the coupled model data analysed in this study [*Taylor et al.*, 2012]. A sample of 19 models (shown in Figure 6.3) was chosen based on the availability of required variables: rainfall, surface temperature, sea surface temperature (SST), specific humidity, surface pressure, geopotential height, *u* and *v* winds and omega. Where there are multiple models from the same modelling group, only one version is used. All variables in all models are interpolated to a common grid of 1° x 1°, for ease of comparison; this does not affect the results. Data are taken from both the historical experiment and the future experiment with the highest emission forcings (and thus largest

temperature increases), RCP8.5, which represents a global net radiative forcing of 8.5 Wm^{-2} by 2100 (roughly a 'business as usual' scenario) [*van Vuuren et al.*, 2011].

Rainfall change in models is calculated by subtracting the historical end of 20th century mean (1979-2005) from the RCP8.5 end of 21st century mean (2074-2100) for any given variable. Composite analysis is used to identify the processes of importance in the extreme ends of the ensemble rainfall response. Composites are created of the four models at each end of the spectrum of rainfall responses; in DJF, this is the four models which show the most wetting ('wettest' composites) and the least wetting ('driest' composites).

Two methods are used to identify the robustness of signals in the figures. First, stipples are used when comparing the historical and RCP8.5 fields in a single composite and indicate where all models in the composite agree on the sign of change of the variable. This method is widely used, including in the IPCC assessment reports, and is a useful initial assessment of model agreement. Second, stipples are used when comparing two different composites, to signify areas where the values of the variable are distinct between the composites. This gives an indication of the robustness of the differences between composites. This metric, from *Creese and Washington* [2018] is more appropriate than using a t-test, given the small sample size.

The paper is structured as follows. Section 6.3 will provide an overview of the spectrum of rainfall changes in the Congo Basin across all seasons. Section 6.4 examines the spatial patterns of rainfall change across models, focusing on the dry

season DJF, which shows the strongest wetting signal across the majority of the basin. In Section 6.5, we assess model differences in the large-scale vertical circulation, and in Section 6.6 we examine differences in low-level horizontal circulation between models. We discuss the results and summarise in Section 6.7.

6.3 Rainfall change across the annual cycle

Rainfall in the Congo Basin is distributed bi-modally in the annual cycle, with two wet seasons (March-May (MAM) and September-November (SON)) and two dry seasons (June-August (JJA) and December-February (DJF)). Coupled models are able to broadly capture this distribution in the historical simulation (1979-2005), with peak SON (MAM) rainfall occurring in October (April) (Figure 6.1). This pattern is largely similar in the future simulations (2074-2100), although peak median rainfall in the SON rainy season shifts to November. There is a general pattern of future wetting: in ten out of 12 months, the median model value in the future simulation is greater than that in the present. In addition, in seven out of 12 months, both the upper and lower limits of the range increase in the future compared to the historical simulation. These results fit with previous research based on MMEs of coupled GCMs, which have indicated that the Congo Basin will get slightly wetter in the future [*Haensler et al.*, 2013a; *Aloysius et al.*, 2016].

The positive shift in the median values of rainfall is small compared to the large spread of model mean rainfall values in each month, which, in some months, can vary by a factor of five [*Creese and Washington*, 2016]. This inter-model spread of

simulated rainfall persists in the future simulations, and in nine out of 12 months, the inter-quartile range of the future values exceeds that of the historical values, indicating increasing divergence amongst the coupled models mean rainfall in the future. Nevertheless, between October and May the two historical and future samples show significant differences using a paired Students t-test ($p<0.05$) with the largest and most significant differences between November and April ($p<0.001$). In all of these months, the median, inter-quartile range, and upper and lower limits are shifted positively in the future simulations. Differences between the two simulations are insignificant at 95% in the JJA dry season and September. In addition, Figure 6.2 shows that while model rainfall values tend to be shifted towards wetter values in most seasons, especially DJF, model wetness is strongly correlated between the historical and future periods.

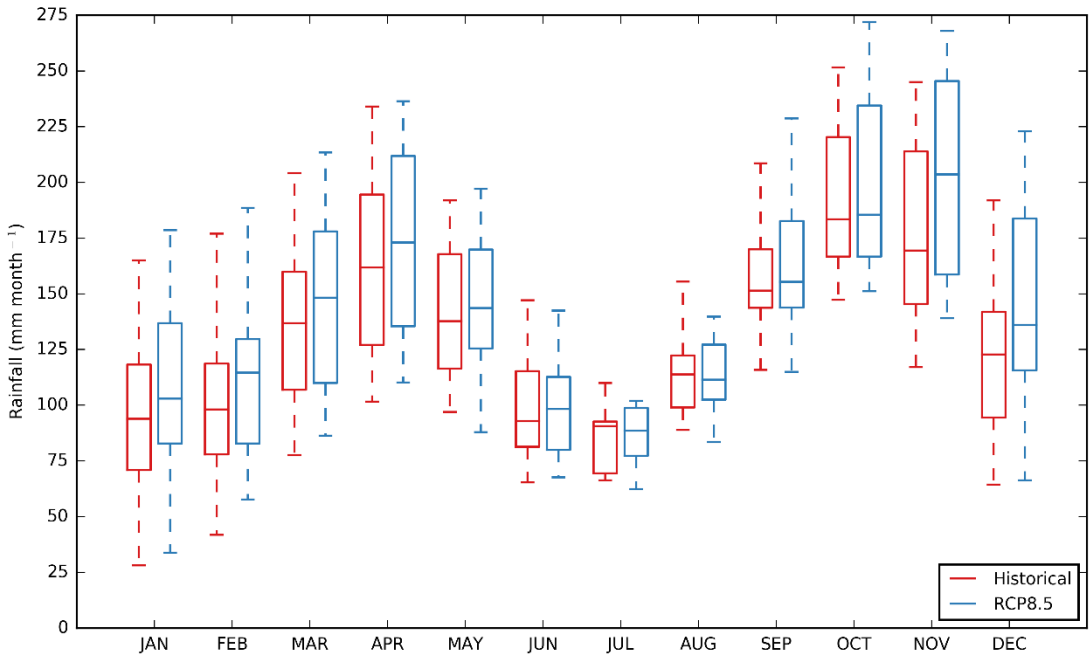

Figure 6.1 - Box plot of long term mean rainfall (mm month $^{-1}$) across CMIP5 models in the historical (1979-2005; red) and future (2074-2100; blue) periods for each month, averaged over 8°E to 35°E, 10°S to 10°N

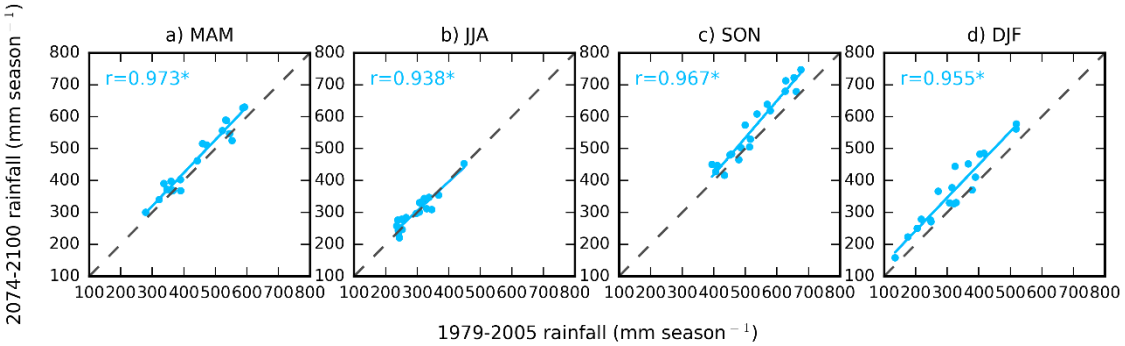

Figure 6.2 - Scatterplots of long term mean rainfall (mm season^{-1}) in the future (2074-2100, RCP8.5) and historical (1979-2005) periods, averaged over 8°E to 35°E, 10°S to 10°N. Asterisks indicate r-values significant at the 99.9% level.

6.4 Rainfall change in DJF

Given that DJF features the largest and most consistent signal of any season, and given the importance of the dry seasons in this region, we focus on this signal to demonstrate a general process-based methodology for examining inter-model differences of rainfall change. To assess the likely rainfall changes in this season, we focus on a smaller domain than in previous figures (10°E-35°E, 10°S to 5°N, green box in Figure 6.4), which comprises the core of the tropical rain-belt over the Congo Basin during this season.

6.4.1 All models

All but one model features mean wetting in DJF across the smaller domain (Figure 6.3). However, there are relatively large differences in the mean Δ*P* values in each model; inmcm4 exhibits only 2.3 mm season^{-1} wetting, whereas ACCESS1-3 features 160.4 mm season^{-1}. Figure 6.3 also highlights the lack of correlation between Δ*P* (blue bars) and historical model rainfall (red bars); i.e. the historically wet (drier) models do not get wetter (less wet/dry) (r=0.107, p=0.66). This is interesting to note as a predominantly thermodynamic understanding of rainfall change would suggest that models with high rainfall already will get relatively wetter in future. This implies that other mechanisms may better describe the spectrum of model rainfall responses.

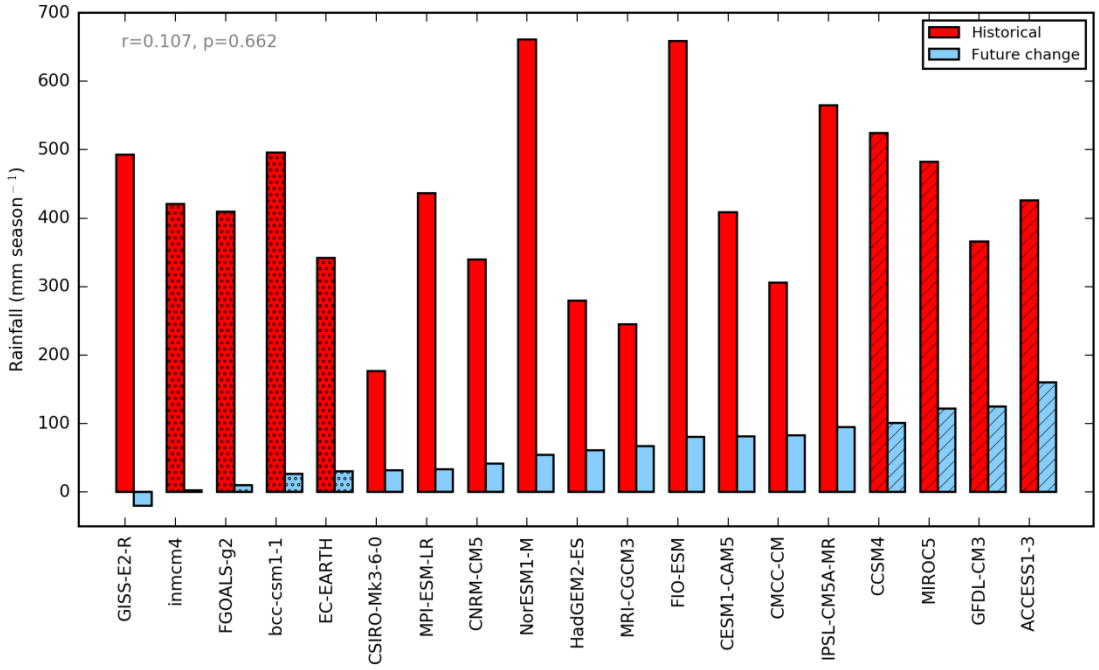

Figure 6.3 - Long term mean DJF rainfall (mm season^{-1}) in the historical period (1979-2005; red) and future (2074-2100) minus historical rainfall change (Δ*P*; blue) in individual CMIP5 models, averaged over 10°E to 35°E, 10°S to 5°N. Models are displayed in order of Δ*P* values (low to high). Models used in the wettest (driest) composites in Section 6.4 are denoted by hatching (stipples).

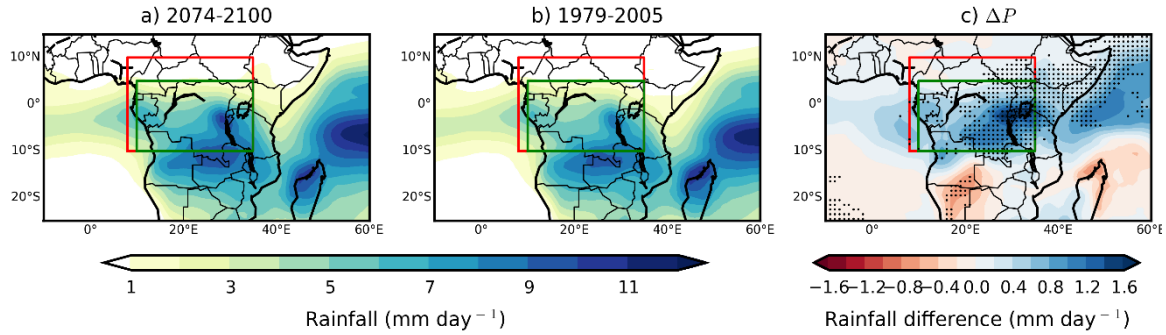

Figure 6.4 - Long term mean DJF rainfall (mm day^{-1}) in (a) 2074-2100, (b) 1979-2005 and (c) Δ*P*. The red (green) box is the location of the 8°E to 35°E, 10°S to 10°N (10°E to 35°E, 10°S to 5°N) domain. Stipples in (c) indicate where 15 out of 19 models agree on the sign of change.

Figure 6.3 also highlights that the values of Δ*P* are small compared to the mean historical rainfall in all models; the magnitude of Δ*P* accounts for between 0.54% (inmcm4) and 37.67% (ACCESS1-3) of historical rainfall across individual models. In addition, the differences in historical rainfall between models are in many cases larger than any Δ*P* values; for example, in the historical mean NorESM1-M (660.7 mm season^{-1}) is almost 500 mm season^{-1} wetter than CSIRO-Mk3-6-0 (177.0 mm season^{-1}), which is more than double even the largest Δ*P* value (ACCESS-1-3, 160.4 mm season^{-1}).

Figure 6.4 shows the spatial distribution of rainfall in the future and historical simulations, and the future-minus-present difference. Despite heterogeneity in the future rainfall change for each season, the spatial pattern and quantity of rainfall is similar between the ensemble means of future and historical rainfall. Both simulations show two regions of climatological rainfall maxima: one at the DRC-Tanzania border near the equator, and the other at the southern boundary of the

domain (10°S). Previous work has indicated there are large disparities between models on the location of maximum rainfall, with some models showing rainfall predominantly in the east or west of the basin, particularly in the wet seasons [*Creese and Washington*, 2016, 2018]. The similarities between future and historical rainfall distributions are also evident in individual models; e.g. models which feature their rainfall maximum in the east in the historical simulation also do so in the future (not shown). Alongside the strong correlations in Figure 6.2, this further suggests that a model's historical climatology is important for the future rainfall magnitude and distribution in this region, meaning that present-day biases could affect the location or magnitude of rainfall change.

There is some consistency in the spatial pattern of the rainfall change signal across models (Figure 6.5). Most models show wetting across the majority of the domain (green box), in particular in the east, where ΔP is largest. Some models show areas of negative ΔP in the north (e.g. MPI-ESM-LR) and west (e.g. inmcm4, FGOALS-g2, bcc-csm1-1). Most models also feature some drying to the south of the domain and wetting to the east of the domain and over the WIO. However, there are large inconsistencies in the magnitude of ΔP across models, even where the signal remains the same. For example, wetting in the east Congo Basin reaches 8.15 mm day^{-1} in IPSL-CM5A-LR, whereas the maximum in inmcm4 is only reaches 0.68 mm day^{-1}.

The one model that features mean drying, GISS-E2-R, has previously been found to have an anomalous climatology in this region, both in terms of rainfall magnitude and distribution. Whilst the majority of models broadly feature maximum rainfall

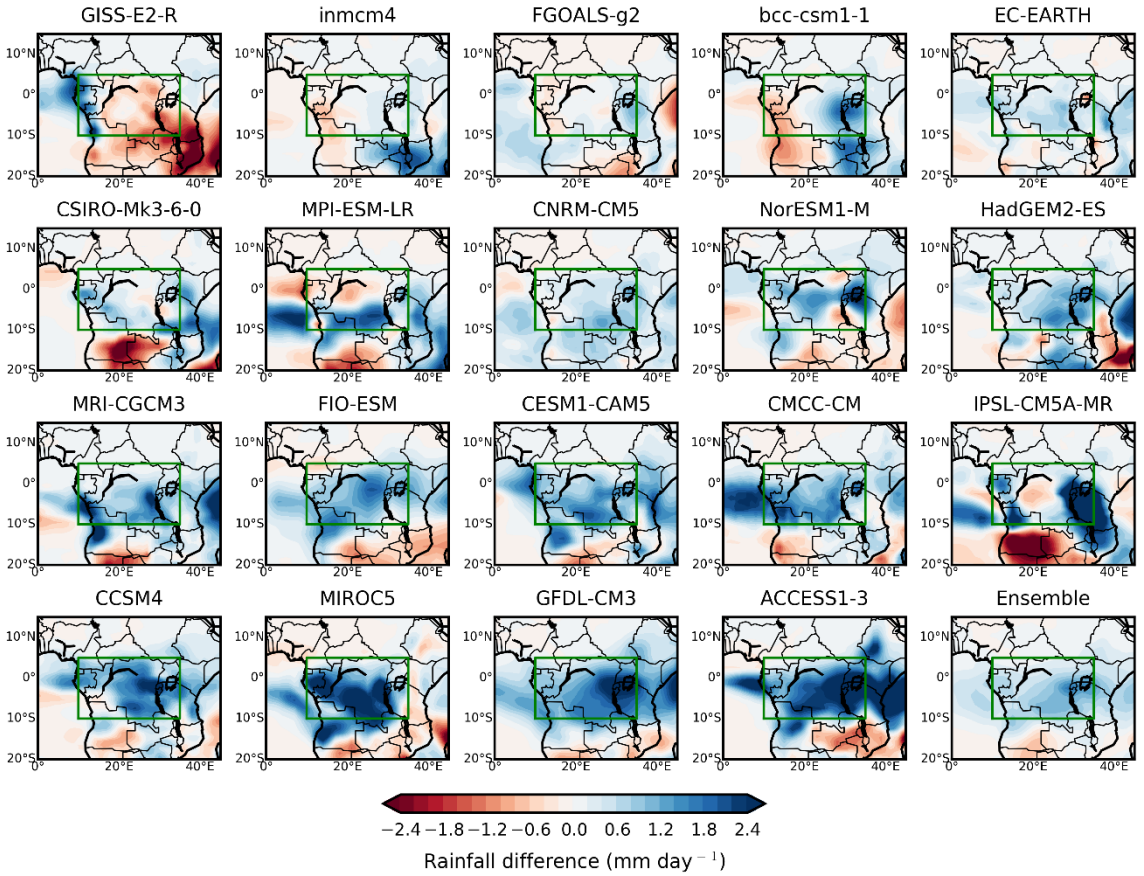

Figure 6.5 - DJF ΔP (mm day^{-1}) in individual CMIP5 models, ordered by mean ΔP (low to high) calculated over the domain 10°E to 35°E, 10°S to 5°N (green box).

in the south-east Congo Basin in this season, matching reanalysis and satellite datasets, in GISS-E2-R rainfall hugs the Atlantic coast in all seasons, rarely extending into the continent. Because of its vastly different historically climatology and Δ*P* signal, GISS-E2-R has been excluded from the composite analysis in the following figures.

Figure 6.6 shows how the patterns of changing rainfall fit into the latitudinal annual cycle of rainfall in the ensemble mean. A north-wetting, south-drying pattern is evident between October and December (as anticipated from Figure 6.4). Enhanced wetting is present in the ensemble mean of models beginning in July at

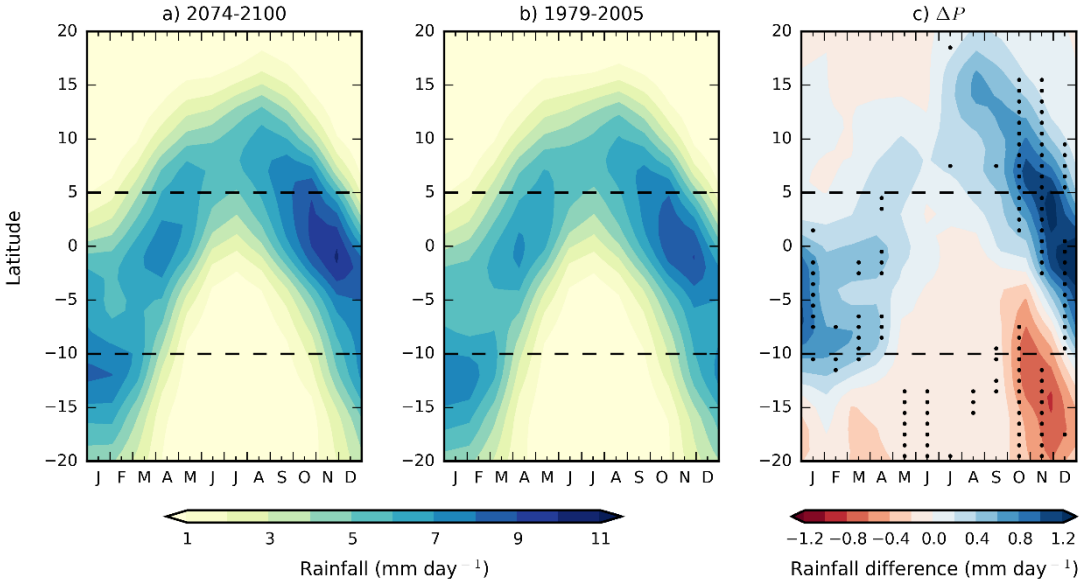

Figure 6.6 - Annual cycle of long term mean rainfall (mm day^{-1}) averaged between 10°E and 35°E, in (a) 2074-2100, (b) 1979-2005 and (c) ΔP. Dashed lines denote the northern and southern boundaries of the domain. Stipples as in Figure 6.4 caption.

around 15°N, and continues through the annual cycle until April in the south of the Congo Basin domain. Further south, there is future drying throughout much of the annual cycle, which is strongest between October and January. Figure 6.6 indicates that the wetting over the Congo Basin during DJF cannot be properly described as a delay in the southward movement of the rain band, as Figure 6.4 may have suggested, as there is not a subsequent wetting over southern Africa from February onwards, as would be expected with such a delay. Instead, there is concurrent wetting over the Congo Basin and drying over southern Africa between October and December, suggesting that the rain band stops further north than in the historical period, and is more intense over the Congo Basin.

6.4.2 Composites

To understand how patterns of Δ*P* differ across the spectrum of models, Figure 6.7 shows model future rainfall, historical rainfall and Δ*P* in the wettest and driest composites (as defined in Section 6.2). Both the wettest and driest composites have reasonably similar rainfall climatologies in both the future and historical simulations (column one and two); rainfall is highest in the south and east of the

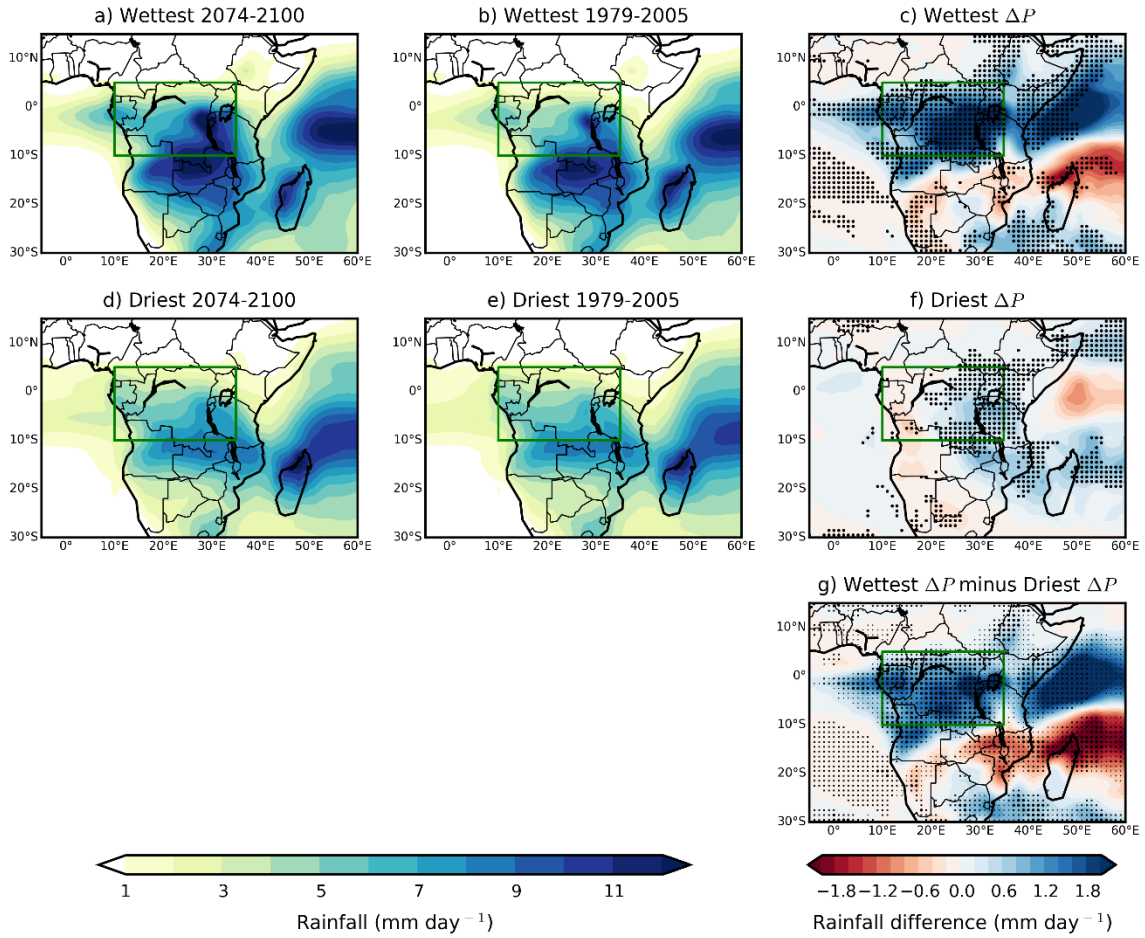

Figure 6.7 - Long term mean DJF rainfall (mm day^{-1}) in the wettest composite (top row) and the driest composite (middle row) in: (a), (d) 2074-2100; (b), (e) 1979-2005); and (c), (f) ΔP; (g) wettest composite ΔP minus driest composite ΔP. Stipples in (c) and (f) indicate where all four models in the composite agree on the sign of change. Stipples in (g) occur at gridboxes where: 1) all wettest composite values are larger or smaller than all driest composite values (large dots); 2) all wettest composite values are greater or smaller than the driest composite mean (squares); 3) driest composite values are greater or smaller than the wettest composite mean (crosses); and 4) both (2) and (3) are true (small dots).

domain, with the rainfall band extending into southern Africa. Both composites also feature areas of high rainfall over the WIO and north Madagascar, though this region is further south and east in the driest composite.

However, the distribution of ΔP is quite different between the two composites (column three). In the wettest models, rainfall increases across almost the entire domain, in some places exceeding 2 mm day^{-1} in the composite mean. Models within the wettest composite agree on the sign of change across the whole domain, except for a small area in the south west over north Angola. In addition to wetting over the Congo Basin, these models also show robust wetting over the East African coast and coastal WIO and drying over the northern tip of Madagascar. This is suggestive of a northward shift and change in intensity of the WIO wet region.

In contrast, in the driest composite there is less consistency in the response over the Congo Basin. All models feature low magnitude wetting in the east and south of the basin, but in the west of the basin models don't all agree on the sign of change. From Figure 6.5 we can see that three out of four of the driest models show slight drying in the west, whilst EC-EARTH shows weak wetting. However, the magnitudes of these changes are very low (<1 mm day^{-1}). In contrast to the wettest composite, the driest composite doesn't feature consistent wetting over the WIO, and features some wetting near northern Madagascar. Over the Congo Basin, the most consistent differences between the two composites are in the central and eastern portions of the Congo Basin domain (Figure 6.7g, larger stipples). Figure 6.7g also highlights an anomalous north-south pattern between the two composites, whereby the wettest models show enhanced wetting over the Congo

Basin and the WIO, and the driest models feature greater wetting over Mozambique and northern Madagascar.

6.5 Changes in large-scale vertical circulation

To better understand the large-scale tropical context in which these changes occur, in this section we examine the changes in vertical circulation that occur in the two composites. Wetting over the Congo Basin, a convective hotspot, will require changes in uplift and subsidence elsewhere, and examining this will help our understanding of how Congo Basin rainfall change is a part of the wider global warming signal.

In the meridional cross-section, the wettest and driest composites feature quite different patterns of future-minus-present change in omega ($\Delta\Omega$) (Figure 6.8). In the wettest, uplift increases throughout the column between roughly 10°S and 5°N, with the largest mean increase at the equator at 500 hPa (Figure 6.8c). Further south, at around 15°S, there is a decrease in uplift in the future (anomalous subsidence), further indicating that the tropical rain-belt does not traverse as far south over Africa in the future. The wettest composite also features enhanced subsidence in the subtropics, particularly north of 30°N. Comparing Figure 6.8a and 6.8b shows that this enhancement is not in the core region of climatological subsidence (20°N -30°N), but to the north of this, suggesting a poleward expansion of the downward branch of the Hadley cell, consistent with recent observations

and theoretical predictions [*Frierson et al.*, 2007; *Hu and Fu*, 2007; *Lu et al.*, 2007; *Johanson and Fu*, 2009].

The driest composite shows the opposite pattern ΔΩ over the domain, with models generally agreeing on a decrease in uplift between 10°S and 5°N, particularly above 600 hPa. Further north there is increased low-level uplift and decreased upper level subsidence at 10°N, though as this is not a region of deep convection it is unlikely to be related to co-located rainfall changes. This composite also features an increase in subsidence north of 30°N, though much weaker in

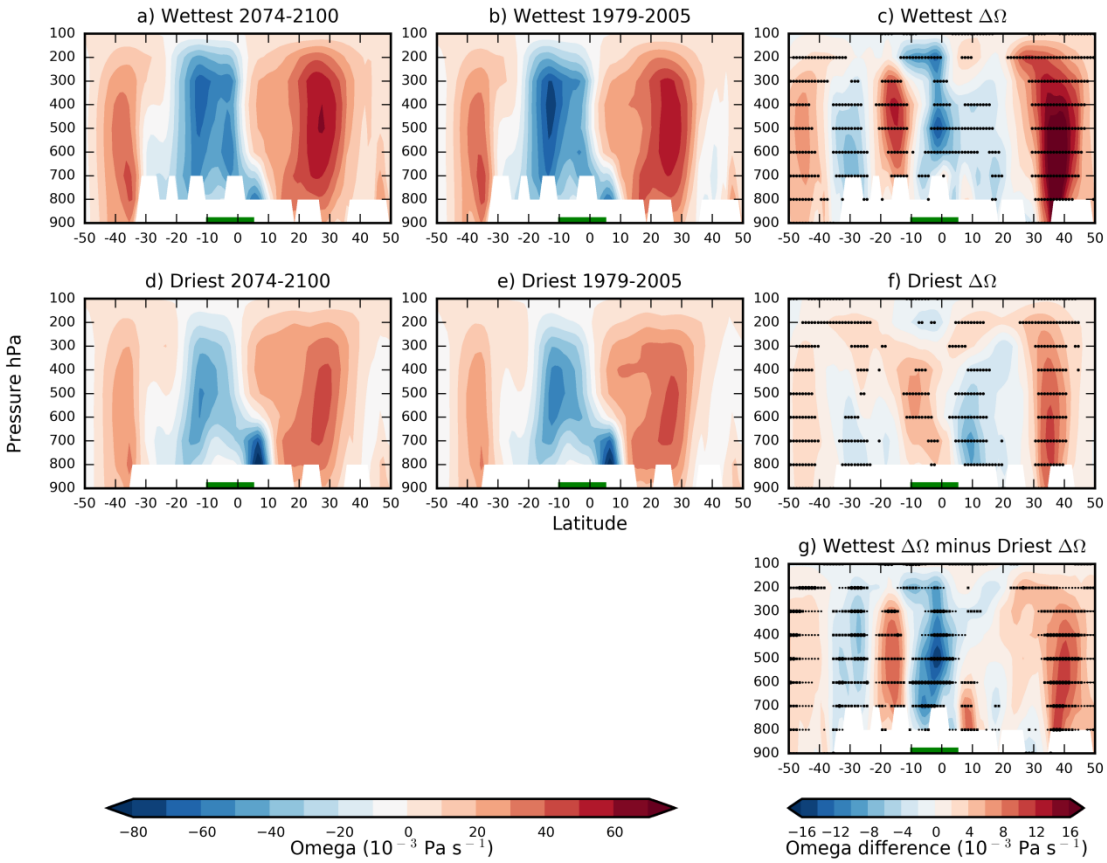

Figure 6.8 - Long term mean DJF omega (Ω, 10^{-3} Pa s^{-1}) averaged between 10°E and 35°E, in the wettest composite (top row) and the driest composite (middle row) in: (a), (d) 2074-2100; (b), (e) 1979-2005); and (c), (f) ΔΩ; (g) wettest composite ΔΩ minus driest composite ΔΩ. Areas with high topography in models are masked (white). The green box shows the extent of the Congo Basin domain (10°E to 35°E). Stipples are as described in Figure 6.7 caption.

magnitude than in the wettest models. Overall, the difference in ΔP between the two composites is well supported by the difference in $\Delta\Omega$ (Figure 6.8g), which shows models with the wettest (driest) change feature anomalously stronger uplift (subsidence) across the entire Congo Basin domain.

In the zonal cross-section, as in the meridional cross-section, $\Delta\Omega$ is negative (more uplift) over the Congo Basin in the wettest composite and positive (less uplift) in the driest composite (Figure 6.9). In the wettest composite, there is a narrow gap at around 35°E between enhanced uplift over the Congo Basin and enhanced

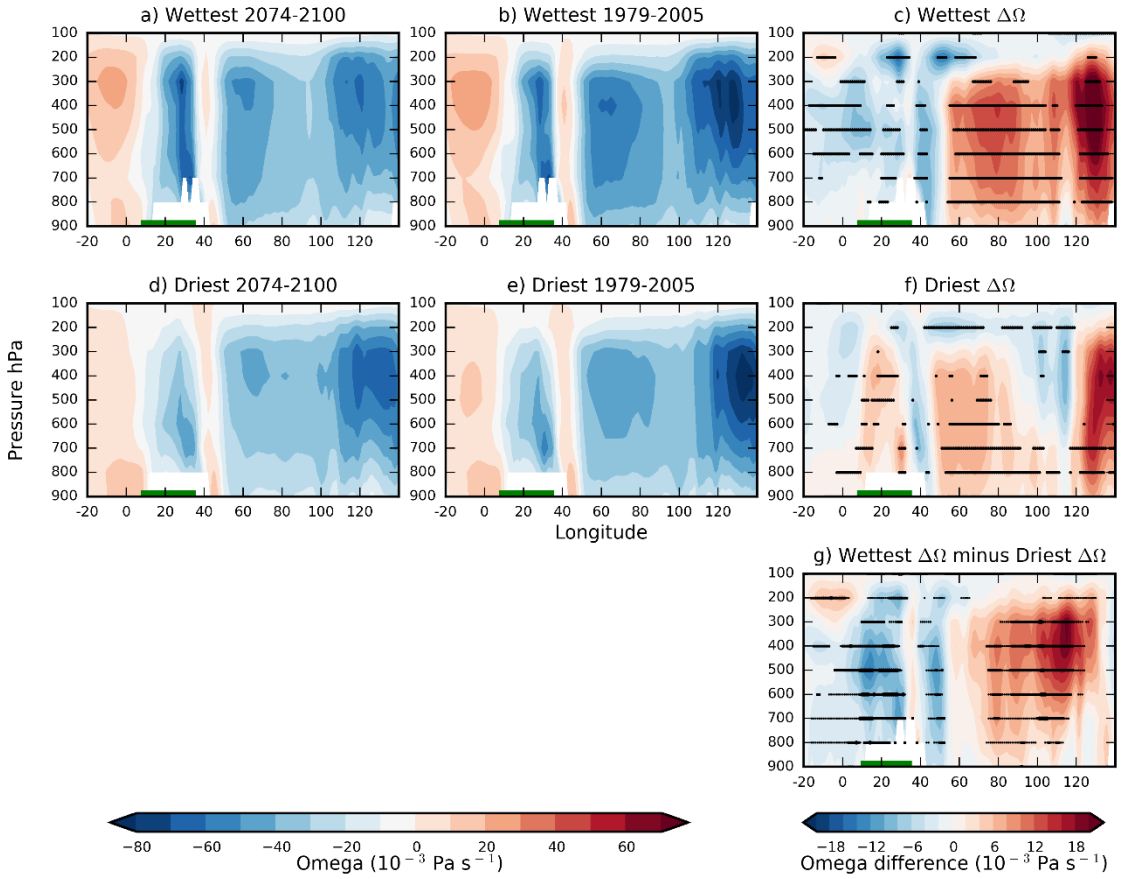

Figure 6.9 - Long term mean DJF omega (10^{-3} Pa s^{-1}) averaged between 10°S and 5°N, in the wettest composite (top row) and the driest composite (middle row) in: (a), (d) 2074-2100; (b), (e) 1979-2005); and (c), (f) ΔΩ; (g) wettest composite ΔΩ minus driest composite ΔΩ. Areas with high topography in models are masked (white). The green box shows the extent of the Congo Basin domain (10°S to 5°N). Stipples are as described in Figure 6.7 caption.

uplift/decreased subsidence over the East African coast at 40°E, mapping onto a similar gap in positive Δ*P* in Figure 6.7). There is a significant decrease in uplift in the east Indian Ocean in the warm pool region, as well a reduction in upward motion in the central Indian Ocean. In the driest composite, the patterns over the Indian Ocean are similar but much weaker in magnitude. The anomalous convection in the west and anomalous subsidence in the east is reminiscent of the atmospheric response to a positive Indian Ocean Dipole (IOD) event, where warmer-than average SSTs in the WIO contribute to enhanced convection and thus rainfall. A weakening of the zonal overturning cell has been identified in many previous studies as a consequence of warming. As this pattern is larger in wettest composite (Figure 6.9g), it suggests that these models may show a greater dynamical response to warming; this will be discussed further in Section 6.7.

6.6 Low-level moisture flux changes

In this section we assess the role of low-level circulation in explaining model differences in Δ*P*. Low-level moisture flux (qflux) has previously been found to differentiate between wet and dry models in this region in the historical period. *Creese and Washington* [2016] found that low-to-mid level qflux from the north and east is much stronger in wet models than dry models during DJF, suggesting that understanding the mechanisms behind these fluxes is important for establishing which models have a more realistic climatology. Similarly, *Creese and Washington* [2018] found that low-level westerlies into the Congo Basin from the tropical Atlantic are enhanced in models with larger SST biases there, resulting in

increased oceanic evaporation and convection over the west Congo Basin during the wet season. Given the importance of qflux in the historical climatologies therefore, it is a sensible place to begin understanding why ΔP differs across models. The qflux field at both 850hPa and 700hPa is analysed below.

6.6.1 Moisture flux at 850 hPa

Climatological qflux and qflux convergence at 850hPa in the historical period is broadly similar for both the wettest and driest composites (Figure 6.10b, e). Water vapour flux into the basin is predominantly from the north east, with some low-level westerly flow from the south west, and moisture outflow in the south east corner of the domain. Both composites show convergence in the north and east of the domain, and divergence in the south west of the domain. The similarities between composite climatologies is in line with previous results from *Creese and Washington* [2016], who found that differences in rainfall across models were more associated with the intensity of such circulation features, rather than distinct differences in the pattern of the qflux.

Both composites feature a similar distribution of qflux and qflux convergence in the future (Figure 6.10a, d), and both feature an enhancement of the continent-wide pattern of convergence and divergence. Future-minus-present qflux convergence (Δqconv) is positive in the north east-to-south west band across the continent, and negative (i.e. increased divergence) in along much of the east and west coasts.

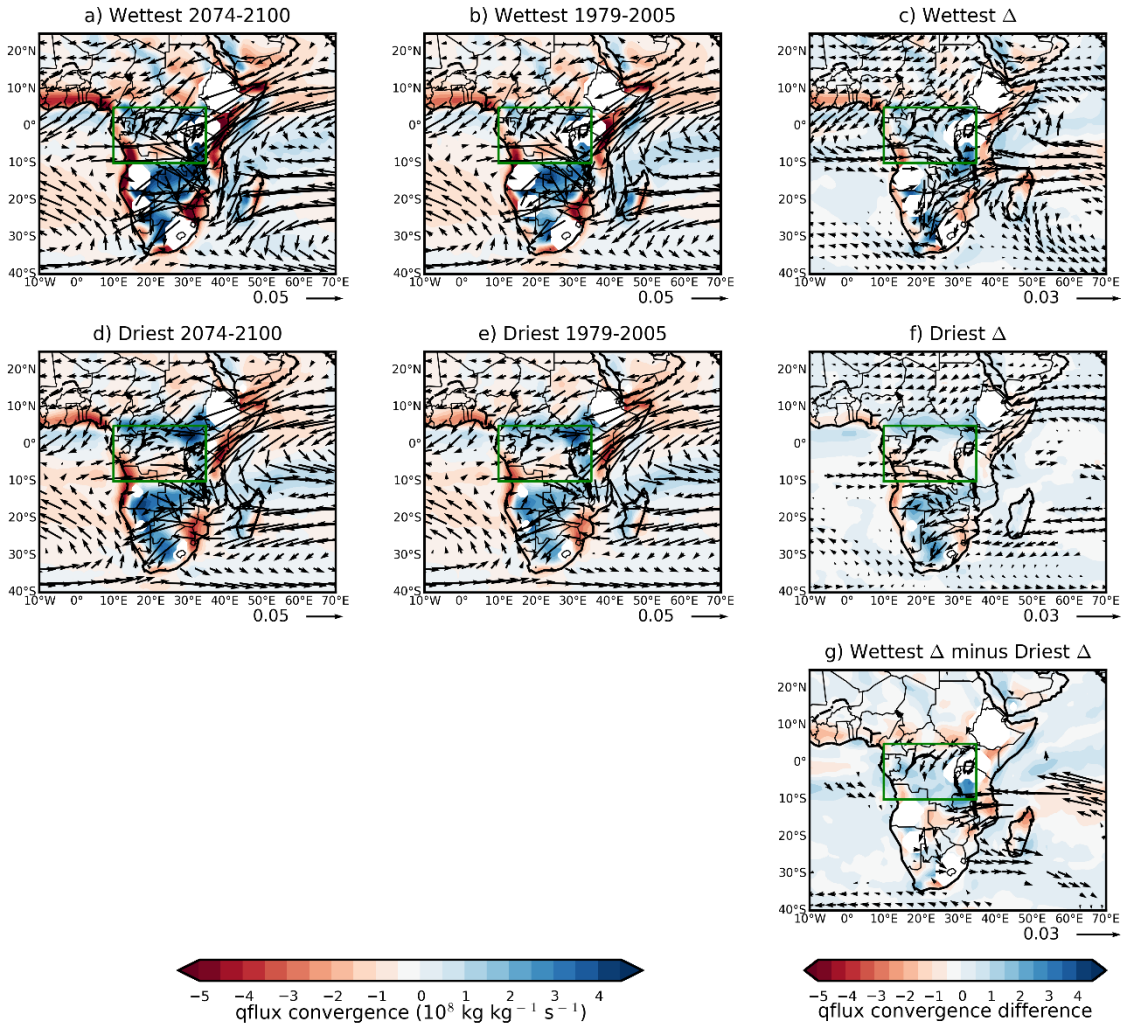

Figure 6.10 - Long term mean DJF qflux convergence (10^{-8} kg kg^{-1} s^{-1}; shaded) and qflux (kg kg^{-1} m s^{-1}; vectors) at 850 hPa in the wettest composite (top row) and the driest composite (middle row) in: (a, d) 2074-2100; (b, e) 1979-2005); and (c, f) Δqflux and Δqflux convergence; (g) wettest composite minus driest composite Δqflux and qflux convergence. Vectors in (c) and (f) are only present where all four models in the composite agree on the sign of change. Vectors in (g) are only present at gridboxes where all wettest composite values of qu or qv are larger or smaller than all driest composite values. The green box indicates the location of the 10°E to 35°E, 10°S to 5°N domain.

However, within and around the Congo Basin there are some key differences between the composites. While the wettest composite features increased convergence across the majority of the Congo Basin domain in the future, the driest composite features slightly enhanced divergence/weakened convergence over the south Congo Basin. The positive relationship between Δqconv and Δ*P*

holds across the whole suite of models; the correlation between mean Δqconv and Δ*P* returns an r-value of 0.71 (p=0.0009). The wettest composite also features enhanced divergence over northern Madagascar and Mozambique, whereas the driest features enhanced convergence here.

In terms of the origin of the qflux, there are also differences between the composites. Models in the wettest composite experience an increase in the northeasterly and westerly fluxes into the basin in the future. They also feature anomalous easterlies at the south-eastern edge of the domain, which are the result of strengthened easterlies and weakened southerlies over the WIO and Mozambique Channel, respectively. In contrast, while models in the driest composite also show some enhanced north easterly flow, this is less intense and less penetrating than the wettest models (Figure 6.10g). In addition, there is some evidence of the driest models featuring enhanced westerlies over the equatorial WIO, potentially diverting moisture away from the Congo Basin. Models in the driest composite also feature enhanced westerlies from the Atlantic, as in the wettest composite; however, these are associated with divergence which penetrates much further into the basin than in the wettest models. This again suggests that moisture is increasingly diverted from the core region of rainfall in the models with the driest changes.

6.6.2 Moisture flux at 700 hPa

Moisture flux at 700hPa includes the role of the African Easterly Jets. The north jet in particular is present in the circulation field throughout the year, peaking in the wet seasons, while the southern jet is only present during the September to November rainy season [*Nicholson and Grist*, 2003; *Jackson et al.*, 2009]. As at 850 hPa, the overall spatial patterns of qflux and qflux convergence at 700 hPa are similar in both composites in the historical period (Figure 6.11b, e). Convergence is strongly zonally banded, with convergence to the south of ~2°N, and divergence to the north. This pattern is similar in the future but with changes in intensity. In the wettest composite, convergence increases over the majority of the domain, while divergence intensifies at the northern boundary. There is also evidence of a northward shift both convergence and divergence, as Figure 6.11c shows anomalous convergence between ~2°N and 5°N. The driest composite shows an intensification of both convergence and divergence, though increases in convergence are smaller than in the wettest composite.

There are some stark differences between 700 hPa Δqflux in the two composites. In the wettest composite, models feature enhanced north easterlies across the northern and north eastern boundary of the domain, and enhanced easterlies at the southern boundary. In the driest composite, models also feature enhanced north easterlies, but they are much more meridionally oriented, and south of the equator deflect eastward, diverting moisture out of the basin. This leads to anomalous westerlies across the south of the domain and into the Indian Ocean which is not a robust signal in the wettest models. In the region to the south east of

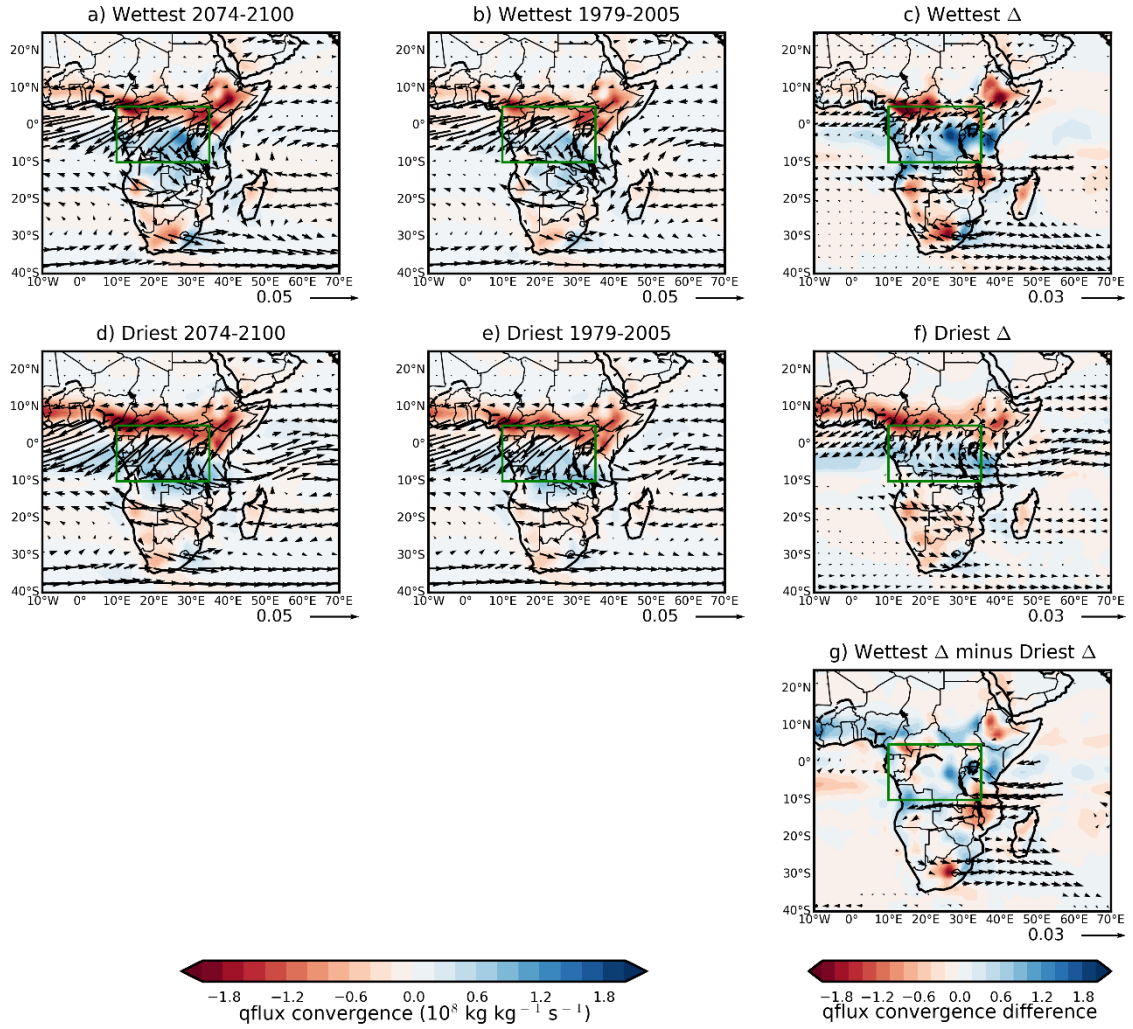

Figure 6.11 - As in Figure 6.10 but for 700 hPa.

the domain, the two composites show zonal winds of opposite direction. As at 850 hPa, there is a significant positive relationship between Δqconv and Δ*P* across all models (r=0.67, p=0.0016).

6.6.3 Flux across domain boundaries

Figures 6.10g and 6.11g highlight regions where the Δqflux and Δqconv signals in the two composites differ most significantly, and show that fluxes across the

boundaries of the domain are often significant differentiators between models with the wettest and driest changes. Figure 6.12 shows the relationship between Δqflux and Δ*P* across the suite of models at each boundary to the Congo Basin, throughout the atmospheric column. It confirms that Δqflux from the north and east is positively and significantly correlated with Δ*P* over the basin; it also shows that the relationship between Δqflux from the east and Δ*P* extends up to 400hPa, whilst the northerly relationship is only significant at low levels. Figure 6.12a also shows that while enhanced westerly qflux from the Atlantic is quite prominent in the composite maps, it is only significant across the whole suite of models over a small number of gridboxes. Finally, there is evidence that enhanced qflux into the basin at low levels is related to enhanced flux out of the basin at upper levels, as seen across the western, northern and southern boundaries.

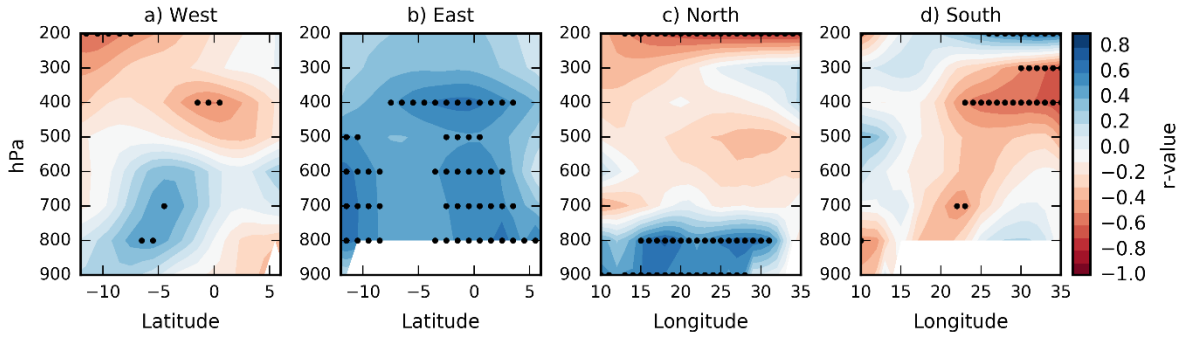

Figure 6.12 - Latitude/height and longitude/height cross-sections showing the correlation (r-values) across CMIP5 models between long term mean ΔP over the Congo Basin and long term mean Δqconv across the: (a) western; (b) eastern; (c) northern; and (d) southern boundaries of the Congo Basin. Stipples indicate vertical grid locations which feature significant correlations at the 95% level.

6.7 Discussion and summary

Previous research has indicated that mean rainfall amounts in the Congo Basin are unlikely to change significantly by the end of the 21st century, based on analysis of ensembles of coupled models [*Haensler et al.*, 2013a; *Aloysius et al.*, 2016]. This may be the case when considering large ensembles of equally-weighted members, but such a conclusion masks the complex spectrum of rainfall changes in this region, across different seasons and different models. In this paper we have focused on the DJF dry season and show that the amount of wetting projected in models is related to the strength of the enhancement of the low-level *qflux* circulation, and the increased amount of moisture entering the basin.

6.7.1 Changes in rainfall magnitude and distribution

The most consistent pattern to emerge across models is a slight wetting in the future, concurring with *Aloysius et al.* [2016] findings in CMIP5. In ten months out of 12 median rainfall in the ensemble increases, and in seven months, the whole spectrum of model values shifts positively. However, in five months, the spread of rainfall values increases in the future, with more models featuring drying. Even where seemingly robust changes occur in rainfall magnitude, such as in DJF where models generally agree on wetting across the domain, these changes are small compared to the range of climatological mean values of rainfall in individual models. For example, on average, in January the mean monthly ΔP (14.8 mm month^{-1}) is only 15.8% of the median historical rainfall mean (94.0 mm month^{-1}).

In addition, values of Δ*P* are small compared to the large range of model climatological values; in January, for example, the mean historical rainfall in models ranges from 28.1 mm to 165.0 mm month^{-1}, whereas the Δ*P* values only range from -4.0 to 43.5 mm month^{-1}. Nevertheless, between October and May the means of the historical and future distributions in Figure 6.1 are significantly different at the 95% threshold, indicating that mean wetting across the basin is robust across the model spectrum.

Spatially, the distribution of rainfall in the future period is similar to that in the historical period, so the location of rainfall maxima in the historical period tends to persist into the future for all seasons. However, this does not necessarily translate into a spatial wet-gets-wetter pattern over the domain. Inspection of individual model historical rainfall (not shown) and Δ*P* (Figure 6.5) shows that increases in rainfall do not necessarily map onto already-wet regions, and spatial correlation analysis confirms that across models, there are only small areas which exhibit a significant positive relationship between historical rainfall and Δ*P*.

6.7.2 Circulation changes associated with rainfall change

Model rainfall changes under warming in the Congo Basin are more complex than a simple wet-get-wetter response, and there is disagreement amongst models in both the magnitude and spatial pattern of rainfall changes. Previous work on mechanisms of tropical rainfall change [e.g. *Chadwick et al.*, 2013; *Kent et al.*, 2015; *Lazenby et al.*, 2018] suggests that inter-model uncertainty derives predominantly

from uncertainty in the dynamical response to warming. Such a dynamical response can include changes in both vertical and horizontal motion.

Models with the wettest and driest changes exhibit pronounced differences in the structure of vertical motion, both in the meridional mean over the Congo Basin longitudes and the zonal mean near about the equator. Wettest models feature increases in uplift over the core of the continent, and decreases over areas including the northern subtropics and the Maritime Continent. Conversely, models which feature limited wetting on average exhibit less uplift over the continent, and comparatively weaker changes elsewhere. This helps explain the large differences in rainfall between the two composites. It is also indicative of wider changes in the tropical circulation alongside changes in the Congo Basin. Figure 6.9 indicates that models with the wettest change over the Congo Basin experience may also experience drying over the Maritime continent and wetting over East Africa, indicative of a weakening of the Walker circulation and switch to a more positive IOD-like state, which has previously been identified as a possible response to warming in CMIP3 and CMIP5 models [*Vecchi and Soden*, 2007; *Shongwe et al.*, 2011; *DiNezio et al.*, 2013]. However, the wetting response across models is at odds with evidence of a drying trend over the Congo Basin in recent decades [*Sanga-Ngoie and Fukuyama*, 1996; *Laraque et al.*, 2001; *Malhi and Wright*, 2004], which recent studies have linked to an enhancement of the tropical Walker circulation [*Hua et al.*, 2016, 2018]. Further work is needed therefore to establish the plausibility of simulated changes to zonal circulation and, by extension, Congo Basin rainfall.

Changes in the patterns of vertical motion in the composites will also be associated with changes in the horizontal circulation, as patterns of wind and convergence respond and provide feedbacks to enhanced uplift and subsidence. In DJF, there are some obvious differences in the qflux and qflux convergence fields between the models with the wettest and driest changes, with the former featuring a much greater enhancement of both fields at 850 hPa and 700 hPa. There is also a significant positive correlation between increased wetting and enhanced qflux from the north and east of the Congo Basin, indicating that increases in moisture advection and its convergence over the basin contribute towards enhanced wetting.

Increases in qflux convergence (*qconv*) are also found to correlate significantly with increases in rainfall, just as high *qflux* convergence is correlated with model rainfall in the historical period [*Creese and Washington*, 2016]. As qflux convergence combines both wind and moisture components, it is possible that one of these is more dominant in explaining model differences in rainfall. If the wind component is dominant, this suggests that changes in the circulation may dominate rainfall change; if the *q* component dominates, it could indicate either in situ (i.e. thermodynamic) increases in *q*, or greater *q* transported into the basin (dynamical), or a combination of both. To help quantify the influence of the *q* and wind components of qflux convergence, we have performed some simple calculations, whereby mean q from the driest models (q_D) is swapped with mean q from the wettest models (q_W) in the calculation of qflux, and vice versa, such that:

$$\Delta q_W \text{ conv} = \Delta (\text{d } q_W u_D/\text{dx} + \text{d } q_W v_D/\text{dy})$$

and:

$$\Delta q_D \text{ conv} = \Delta (\text{d } q_D u_W/\text{dx} + \text{d } q_D v_W/\text{dy})$$

This gives an indication as to whether changes in winds (Δu, Δv) or changes in q (Δq) play a greater role in rainfall differences between the two composites. These results are shown in Table 6.1. As described above, at 850hPa models in the wettest composite feature an increase in qflux convergence while those in the driest feature a decrease. When q_D is paired with winds from the wettest composite, there is still an increase in qflux convergence, though of weaker magnitude. However, when q_W is paired with winds from the driest models, the percentage decrease in qflux convergence is similar to the decrease when q_D is used. This suggests that in the wettest composite, changes in both q and wind are important, whereas in the driest, changes in the winds dominate the change in qconv. This is supported by analysis of the circulation fields of the swapped values at the eastern boundary of the basin (Supplementary material, Figure 6.S1). In the wettest composite, 850 hPa and 700hPa circulation changes include an enhanced flux into the basin, meaning that changes in q can influence moisture availability in the basin (Supplementary material, Figures 6.S1 and 6.S2). However, in the driest composite there is outflow over much of the eastern boundary, meaning that differences in q are less important, as the moisture is being diverted away from the basin regardless of its magnitude.

Table 6.1 – Calculations of qflux convergence (10^{-8} kg kg^{-1} s^{-1}) using different combinations of mean q and mean winds from the driest and wettest composites

	Δ(*qconv*), 850hPa		Δ(*qconv*), 700hPa	
	Wettest winds	Driest winds	Wettest winds	Driest winds
q_W	0.466419 (127.05%)	-0.123061 (-24.35%)	0.373057 (317.14%)	0.277326 (80.28%)
q_D	0.371642 (74.27%)	-0.192186 (-23.54%)	0.274558 (115.67%)	0.195421 (48.14%)

This analysis suggests that both the moisture and wind component of qflux convergence are important for understanding the different model responses to warming. This ties in with previous work which has found that qflux convergence exhibits stronger correlations with historical rainfall across models than wind convergence or *q* alone [*Creese and Washington*, 2016]. Studies of both models and observations have identified qflux and qflux convergence as key factors differentiating between wet and dry models [*Creese and Washington*, 2016, 2018], and wet and dry years [*Pokam et al.*, 2012, 2014], as well as their role as branches of local overturning cells [*Cook and Vizy*, 2015]. In DJF, low-level *qflux* across the north and east boundaries of the Congo Basin, embedded within the reversed Asian monsoon flow, has been strongly related to model wetness within the basin, with higher r-values than in any other season [*Creese and Washington*, 2016]. These boundaries are also found to be important in the future; models which get wetter during DJF in the Congo Basin exhibit greater low-level *qflux* from the north, and low-to-mid-level qflux from the east.

Changes in qflux and qflux convergence could be related to both thermodynamic and dynamic mechanisms of rainfall change. Enhanced winds could be related to a 'rich-get-richer' dynamical feedback on increased q under warming, where reduced gross moist stability in wet regions drives uplift and greater convergence at low levels [e.g. *Chou et al.*, 2009]. They could also be a consequence of a dynamical shift in the locations of convection under warming, which in turn influence patterns of low-level circulation. While increased q could be purely a result of "in situ" thermodynamic increases in moisture under warming, it may also be exacerbated by strengthened wind convergence, or an increase in the advection of q from elsewhere.

It is not possible to disentangle the precise influence of each component across a suite of models without dedicated experiments; however, there is some evidence supporting the latter hypothesis (enhanced q transported into the basin from elsewhere) as playing some role in inter-model differences in rainfall changes. First, as Figure 6.12 shows, the wettest composite features enhanced qflux from the north and east, and the analysis above of swapped values shows enhanced winds and q are important. As Figure 6.7 shows, models which wet most over the Congo Basin also tend to get relatively wetter over the WIO at the East African coast. Analysis of SSTs between the composites (Supplementary material, Figure 6.S3) shows that SST warming is much higher in this region in the wettest composites. Under a warmest-gets-wetter mechanism of rainfall change [*Xie et al.*, 2010] we might expect this warming to drive enhanced evaporation, and thus enhanced q, over the WIO at the East African coast (Supplementary material,

Figure 6.S4). This would provide a greater moisture source for the easterly winds crossing into the Congo Basin in the wettest models.

The next steps in this research are to elucidate which magnitude and pattern of rainfall change is most plausible in this region. This will involve establishing whether the processes by which models produce future change are plausible processes in this region. Given that the observed drying trend in recent years has been linked to changes in the zonal circulation [*Hua et al.*, 2016], an assessment of the ability of models to capture the processes associated with historical dry periods, similar to the analysis by *James et al.* [2015], may prove fruitful. The authors plan to explore this further in future work.

6.7.3 Summary

Our key findings are as follows:

1. There is a general trend towards wetting in the CMIP5 models across the annual cycle, and between October and May the increase in mean rainfall is significant between the future and present simulations at the 95% level.
2. In the models' future simulations there is general agreement that the rain band does not traverse as far south during SON and DJF, instead remaining in the southern half of the Congo Basin for longer than in the historical period.

3. In DJF, models tend to show wetting across the basin, but this ranges in magnitude from 2.3 mm season^{-1} in the model with the smallest change, to 160.4 mm season^{-1} in the model with the largest change; a difference of 158.1 mm season^{-1}.
4. High magnitude wetting is associated with an enhancement of uplift in the core convective region, while models with little rainfall change show a slight decrease in uplift. This is linked to a poleward expansion of the Hadley cell in wetting models, and a weakened Indian Ocean Walker cell, which has been identified across CMIP3 and CMIP5 models but is at odds with recent trends over the Congo Basin.
5. Models with the wettest change feature an enhanced low-level circulation in the future, with greater qflux convergence and qflux from the north and east.
6. It is likely that the enhanced qflux and qflux convergence is a result of both increases in q and a dynamical enhancement of low-level winds.
7. It is also likely that the warming West Indian Ocean acts as a greater source of q for the basin in the future in the wettest models. The plausibility of this signal should thus be assessed further.

Acknowledgements

The GCM data used in this study was made available through the Earth System Grid Federation (ESGF) Peer-to-Peer system (https://pcmdi.llnl.gov/search/cmip5/). The first author is fully funded by the UK Natural Environment Research Council

(NERC) via a Doctoral Training Programme (NE/L002612/1), and partly funded by a UK Met Office CASE studentship. Richard Washington is partly supported by NERC and the U.K. Government's Department for International Development (DfID) UMFULA project (NE/M020207/1). The authors acknowledge the helpful inputs of Callum Munday, Emma Howard, Rachel James and Neil Hart.

Supplementary material

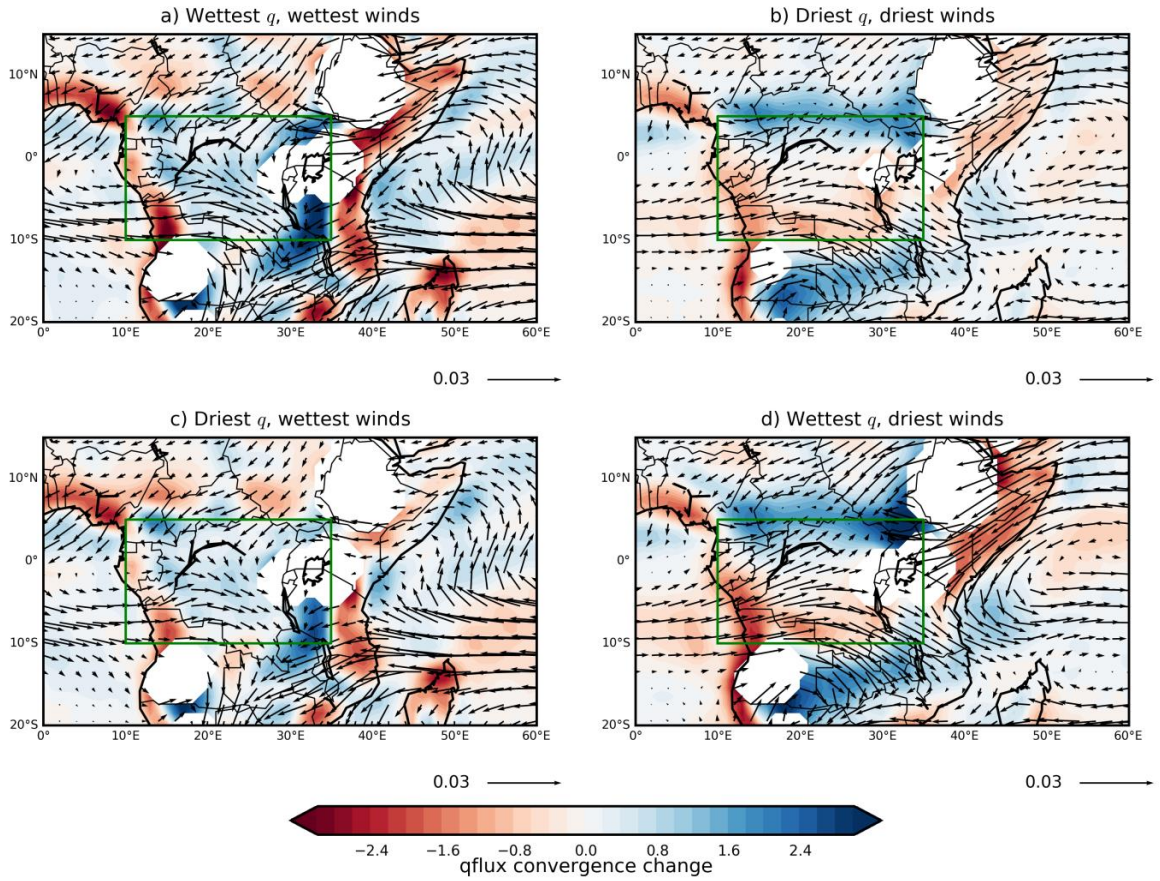

Figure 6.S1 - Long term mean DJF *qflux* convergence (10^{-8} kg kg^{-1} s^{-1}; shaded) and *qflux* (kg kg^{-1} m s^{-1}; vectors) at 850 hPa in (a) the wettest composite and (b) the driest composite. Swapped values of *q* and winds: (c) *q* from the driest models, winds from the wettest models; (d) *q* from the wettest models, winds from the driest models.

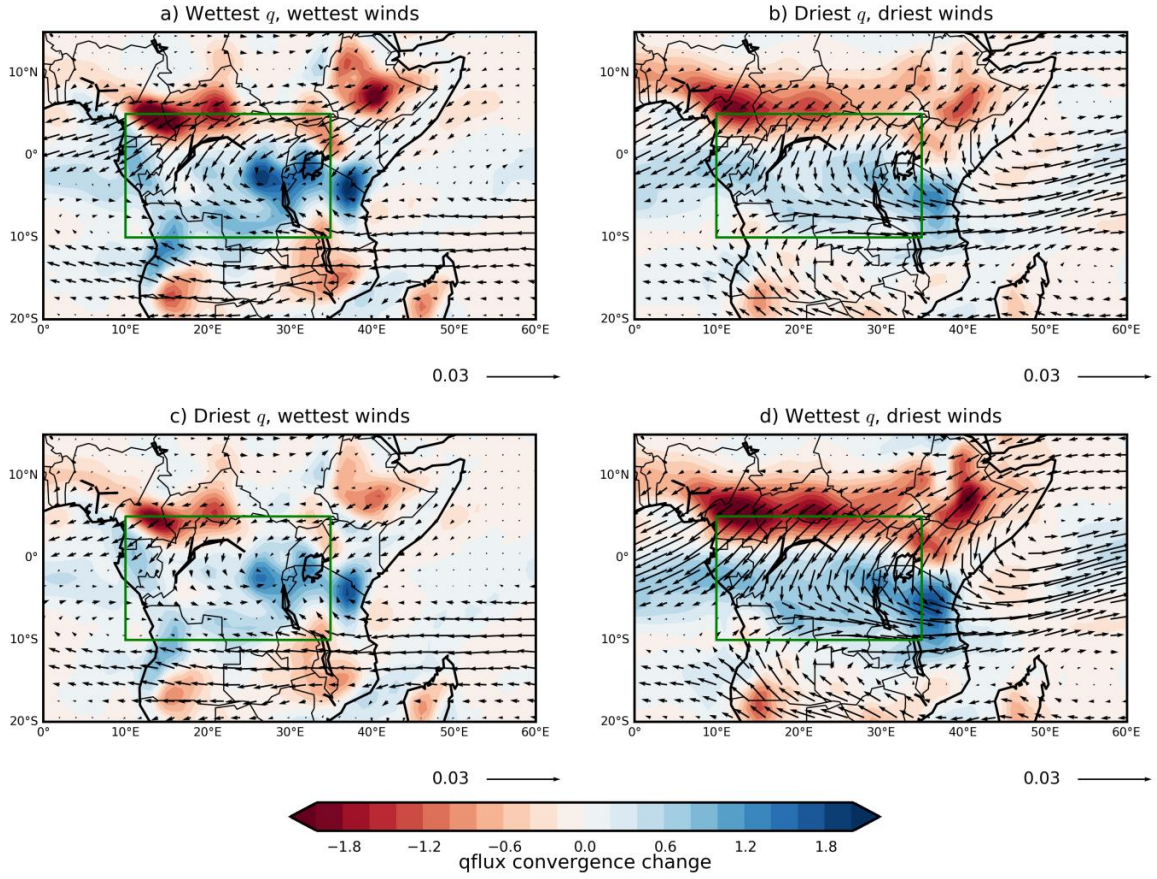

Figure 6.S2 - As in Figure 6.S1 but for 700 hPa.

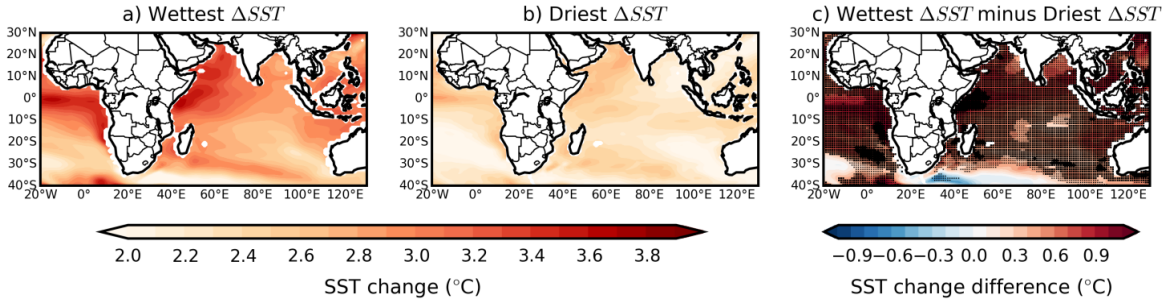

Figure 6.S3 - Future minus historical SST (°C; ΔSST) in (a) wettest composite, (b) driest composite; (c) wettest composite ΔSST minus driest composite ΔSST. RCP8.5 data for FGOALs is missing, so driest composite includes only 3 models. Stipples in (c) occur at gridboxes where: 1) all wettest composite values are larger or smaller than all driest composite values (large dots); 2) all wettest composite values are greater or smaller than the driest composite mean (squares); 3) driest composite values are greater or smaller than the wettest composite mean (crosses); and 4) both (2) and (3) are true (small dots). Due to missing data the dry composite contains only 3 models.

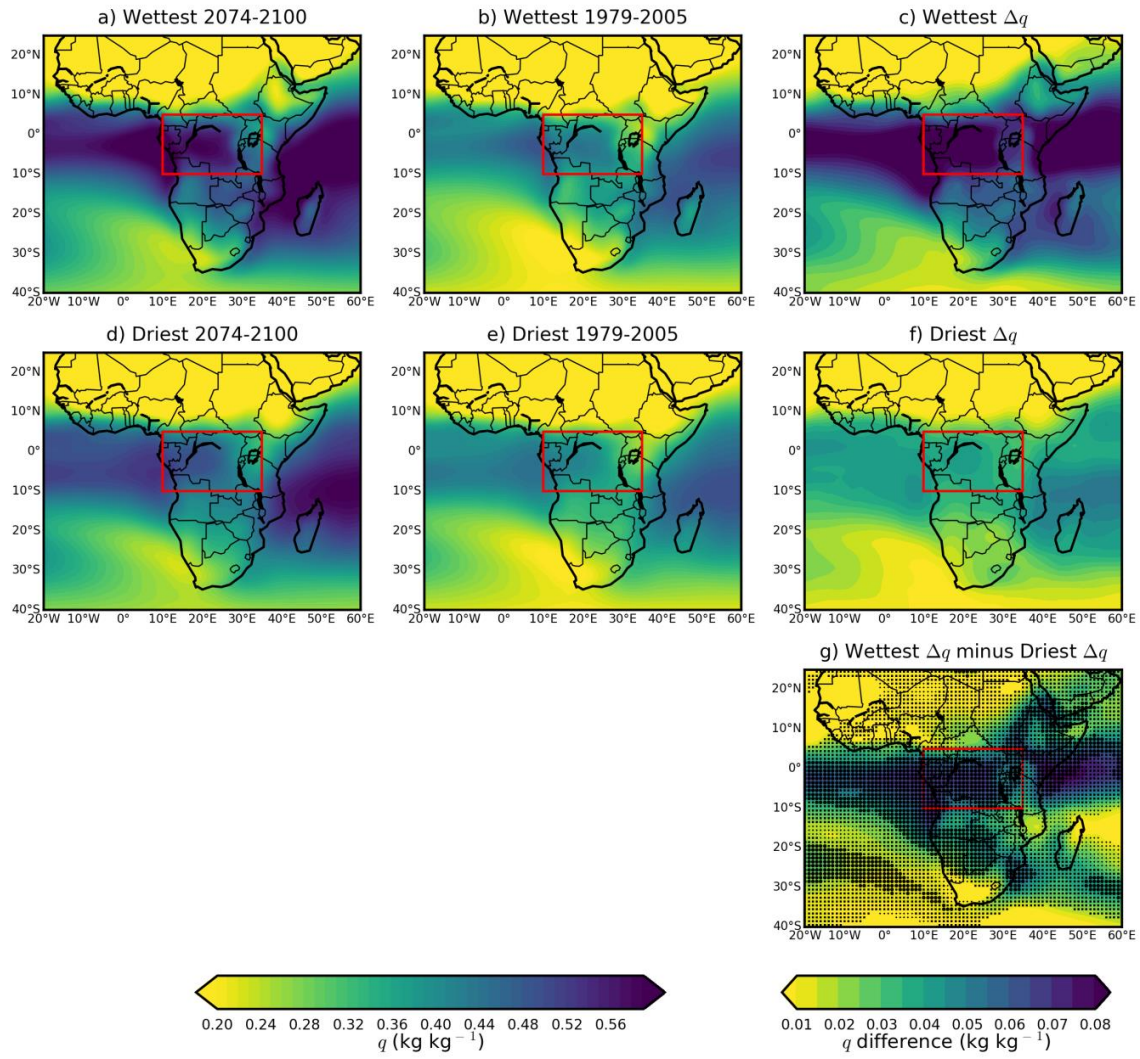

Figure 6.S4 - Long term mean DJF vertically integrated (surface to 300 hPa) q (kg kg^{-1}) in the wettest composite (top row) and the driest composite (middle row) in: (a), (d) 2074-2100; (b), (e) 1979-2005); and (c), (f) Δq; (g) wettest composite Δq minus driest composite Δq. Stipples in (c) and (f) indicate where all four models in the composite agree on the sign of change. Stipples in (g) occur at gridboxes where: 1) all wettest composite values are larger or smaller than all driest composite values (large dots); 2) all wettest composite values are greater or smaller than the driest composite mean (squares); 3) driest composite values are greater or smaller than the wettest composite mean (crosses); and 4) both (2) and (3) are true (small dots). Due to missing data the dry composite contains only 3 models

7 Conclusions

The importance of the Congo Basin in the global and regional African climate systems is undisputed. But, there has been limited scientific attention to the climate system of the Congo Basin, and even less attention to the capabilities of climate models in this region. This has led to a significant gap in our understanding of how the climate of the Congo Basin might change in the future. Very few papers have attempted to describe the likely future changes in the Congo Basin in numerical models, and the findings of such research has been limited by the large uncertainty stemming from model divergence over this region. Until this point, there has been little evidence to support including or excluding particular modelled projections of change, and so the scientific value that can be drawn from these tools as an ensemble is limited. The overall consequence of this is that there is a dearth of credible and reliable climate change information for decision-makers to use in long-term planning for the Congo Basin.

This thesis aimed to fill some of these knowledge gaps by developing an understanding of why and how models behave as they do in the Congo Basin, with regard to their representation of climatological rainfall. This has involved both evaluating the processes relating to rainfall in the historical period, in order to establish the *credibility* of climate models, as well as assessing the *plausibility* of projected rainfall change in the future period. It is hoped that the outputs of this research, and future work that builds on this thesis, will contribute directly to the provision of more reliable climate information for policy-makers.

This final chapter reviews the work undertaken in this thesis and offers some conclusions. The first two sections will synthesize results relating to the two

overarching aims of the thesis (assessing historical credibility and future plausibility). It will then tie together the conclusions that can be made from across the results chapters relating to the model evaluation methodology developed in this thesis, in order to answer the question: how effective is this methodology in data scarce regions such as the Congo Basin? Limitations of the approach will be discussed, before highlighting potentially fruitful avenues for further research.

7.1 Model behaviour in the historical period

This section discusses the research questions relating to model behaviour in the historical period, which were largely explored in Chapters 3 and 4:

i. To what extent can the large-scale processes of water vapour transport, provision and convergence explain inter-model differences in the representation of rainfall in the Congo Basin?
ii. Can the credibility of models be determined based on an assessment of regional processes related to rainfall?

This section will summarise the findings which pertain to these research questions, and will identify the implications of these findings for the rest of the thesis and future work.

7.1.1 To what extent can the large-scale processes of water vapour transport, provision and convergence explain inter-model differences in the representation of rainfall in the Congo Basin?

7.1.1.1 Characterising model differences

The first step in understanding climate model behaviour in the Congo Basin was to examine in detail the representation of rainfall across a suite of models, and to quantify the differences between them. The models were chosen from the CMIP5 ensemble [*Taylor et al.*, 2012]; one of the most widely used and accessible climate model datasets for use in climate change research. There has been very little research to date into the behaviour of these models in the Congo Basin, and even less explaining the variations in rainfall magnitude and distribution across models.

The analysis in Chapter 3 focussed on the representation of the mean-state of the Congo Basin climate system across CMIP5 models. It showed that while all models are able to capture some of the broad features of rainfall over the basin, such as the semi-annual rainfall cycle, there are stark differences in the mean magnitude of rainfall simulated across models. In some months (e.g. December) the difference in mean Congo Basin rainfall between the wettest and driest models differs by a factor of five, and in several cases, the dry season values of one model (e.g. ACCESS1-3, July, 4.7 mm day^{-1}) exceed the wet season values of another (e.g. GISS-E2-H-CC, April, 4.4 mm day^{-1}). This research also highlighted significant differences

in observational and reanalysis datasets over the same region (e.g. Figure 3.3), with some datasets differing by up to 3 mm day^{-1} in some months, underlining the difficulty of determining which models produce 'good' or 'bad' historical rainfall climatologies using traditional performance-based metrics.

Chapter 3 also demonstrated that there are stark differences in the spatial distribution of mean rainfall amongst models and across seasons. In particular, in the wet seasons (MAM and SON), models have different regions of rainfall maxima; some have high rainfall in the east of the basin, some in the west, and some have several patchy, disconnected areas of rainfall. The Congo Basin domain used in this thesis covers an area of over three million square miles, and so these distances are non-trivial. The distance from the eastern to western boundary is over 1500 miles; the equivalent of it raining in London or raining in Istanbul.

There are two related implications of the distributional differences observed across models. First, when the climatologies of individual models are averaged to produce an ensemble mean, the resulting ensemble mean climatology cancels out distinct east and west spatial distributions in individual models, and is therefore not representative of any individual model. This has **implications for the use of ensemble means** in this region. They are frequently used as a 'best-estimate' of the climatology, based on the assumption that errors in individual models will be cancelled out by the averaging process [*Hagedorn et al.*, 2005; *Palmer et al.*, 2005]. However, these results show that in the Congo Basin ensemble means are likely to be misleading, as the averaging process cancels out some significant differences across models. Further, given that the ensemble mean does not represent any

individual model climatologies in the historical period, it casts doubt on its utility in future projections in this region, and its use would have implications for projections of the spatial pattern of the rainfall response under warming.

Second, such stark differences in rainfall magnitude and distribution indicate that there may be **significant differences in the processes models use to produce or maintain rainfall**. As there are substantial distances involved, it is possible that models with rainfall maxima in the east versus rainfall maxima in the west may be under the influence of different physical processes, or different strengths of the same process. Given that the behaviour of such processes may be better observed or constrained in reanalysis data than rainfall, it follows that an investigation of these processes may offer insights into which models are more believable. Such an analysis was conducted in Chapter 3 and Chapter 4, and the findings are discussed below.

7.1.1.2 Links to large-scale circulation and moisture flux

Given the scarcity of observational rainfall data in the Congo Basin and the divergence in satellite and reanalysis rainfall estimates, this thesis sought to determine ways of assessing the capabilities of models without such data. Previous research has highlighted the importance of the large-scale circulation in driving Congo Basin rainfall variability in both observations [e.g. *Pokam et al.*, 2012; *Cook and Vizy*, 2015] and models [e.g. *Washington et al.*, 2013]. Such processes are a useful starting point for process-based analysis, as they are better constrained in reanalysis than the highly parameterised variable of rainfall. The remainder of

Chapter 3 therefore assessed the links between rainfall and the large-scale moisture circulation, in order to establish whether such processes could be used to help a) better understand model behaviour in this region and b) constrain the range of rainfall climatologies represented by models.

Significant relationships (at the 95% level) were found across models between mean Congo Basin low-level moisture flux convergence and rainfall in all seasons. These relationships varied by height and by season; in MAM the strongest rainfall/convergence relationship was found at 700 hPa ($r=0.70$, $p<0.05$) whilst in SON, JJA and DJF it was at 850 hPa (and $r=0.66$, $r=0.71$, and $r=0.81$ respectively; $p<0.05$). In addition, significant positive relationships were found between the amount of moisture entering the basin via particular basin boundaries and rainfall over the basin, including a significant relationship with qflux from the west in SON ($r=0.60$ at 700 hPa, $p<0.05$) and from the north and east during DJF ($r=0.82$ and $r=0.87$ respectively, at 850 hPa, $p<0.05$). This finding is in accordance with research into seasonal variations in the regional moisture circulation in reanalysis data: *Pokam et al.* [2012] found that MAM experiences a maximum in moisture flux convergence at mid- to upper-levels, associated with the AEJ-N, whereas during SON the maximum is at low-levels, and is associated with low-level westerly flux from the Atlantic Ocean.

The analysis of the links between rainfall and moisture identified two important considerations for process-based model evaluation in this region. First, seasonal variation in the strength of the rainfall/moisture relationship highlights the importance of conducting **seasonally-specific** assessments of model capabilities.

Previous research into the Congo Basin climate regime indicates that the relative influence of the large-scale circulation and regional circulation features on rainfall varies throughout the year; Chapter 3 found that the same occurs in models. In particular, there are key distinctions between the two rainy seasons, further highlighting the importance of not approaching this region from the traditional 'ITCZ paradigm' [*Nicholson*, 2017a], under which the rainy seasons might be expected to feature similar rainfall climatologies. It also raises the possibility that some models perform in some seasons than others.

In addition this work points to the importance of analysing circulation processes at **specific heights** in the atmosphere. Assessment of moisture usually focuses on the column-integrated field; however, as noted by *Pokam et al.* [2012], regional and global circulation features lead to a non-uniform distribution of moisture flux and convergence throughout the atmospheric column, and as such, rainfall variability is more related to moisture flux and moisture flux convergence at specific (particularly low-to-mid) levels in the atmosphere. Thus the advantage of analysing individual levels rather than column-integrated convergence is that the influence of circulation patterns at different heights, and associated processes, can be elucidated.

7.1.2 Can the credibility of models be determined based on an assessment of regional processes related to rainfall?

The first aim of this thesis is to determine the credibility of models in the Congo Basin. The findings in Chapters 3 and 4 suggest two ways in which this can be achieved; via the guidance of targeted observational campaigns, and via a process-based analysis of the credibility of the processes relating to rainfall amongst models. These are discussed below.

7.1.2.1 Targeted observations

The analysis of moisture flux in Chapter 3 identified key boundaries over which qflux is strongly correlated with model rainfall (Figure 3.15). In particular, the amount of qflux entering the basin from the west at low-levels is positively correlated with basin rainfall in SON, whilst during MAM and DJF, low-to-mid-level qflux across the northern and eastern boundaries is most important for explaining the spectrum of mean model rainfall over the basin. Given the strong link with rainfall, if qflux across these boundaries could be measured, the data could be used to confront models to determine which are reproducing qflux, and thus rainfall, correctly. Targeted measurements of qflux convergence in this region were originally suggested by *Washington et al.* [2013], and the findings of this thesis provide additional justification for such measurements by highlighting specific locations at the boundaries of the basin which would provide the most useful data with which to confront models. These locations have the benefit of being largely outside the barriers to access in the region. Such measurements could be collected via a flight campaign, or by in situ data collection using instruments such as Lidar. For the former, the identification of the most significant boundaries in individual seasons is particularly important as such campaigns are usually limited to 1-2

months of data collection. Short-term measurement campaigns or individual in situ sites are significantly less expensive than long-term, less-targeted weather data collection, and this thesis has shown they are likely to provide significant insights into climate model behaviour.

Efforts are already underway to begin targeted data collection of qflux based on the findings of this thesis. Funding from the Future Climate for Africa programme (£250K) was secured for a Lidar to be purchased and placed on a boundary of the Congo Basin in order to measure moisture flux. Yaoundé in Cameroon was chosen as the most appropriate location based on a number of factors: a significant relationship between qflux over this boundary and rainfall, particularly in SON; access to an ongoing power supply at the University of Yaoundé, and presence of collaborators in the area who can help maintain the instrument and manage data collection. The Lidar is in transit to Cameroon at the time of writing. There are also plans to install a second Lidar in the Turkana region of Kenya during the MAM rainy season, to measure moisture fluxes across the eastern boundary of the Congo Basin. This is hoped to give insights into the influence of topography on moisture fluxes between the Congo Basin and East Africa.

7.1.2.2 Assessing model credibility in the absence of observational rainfall data

While targeted observational campaigns may offer important insights for model evaluation and development, there remain practical and financial barriers to collecting observations across the majority of the Congo Basin. As such, the main

aim of this thesis was to develop a method of establishing model credibility in the absence of observational data. Chapter 4 thus described and deployed a methodology of process-based model evaluation that could be used in data scarce regions such as the Congo Basin. Given the importance of the rainy seasons, as well as a reasonable prior understanding of the processes related to rainfall in this season, SON was chosen as the season in which to apply this methodology in Chapter 4.

The first key finding of Chapter 4 was that there are large spatial variations between models in the location of rainfall, particularly in the zonal direction. The Atlantic coast and central east Congo Basin consistently emerged as regions of rainfall maxima in models, but were not consistently present, or at the same strength, in all models. Correlation analysis between rainfall in the east and west of the Congo Basin domain across models found that, throughout most of the year, model wetness is positively and significantly correlated between the east and west of the basin (ranging from $r=0.526$, $p=0.03$ to $r=0.732$, $p=0.001$), indicating that common processes may be driving model wetness across the basin as a whole. However, between August and November, model wetness is not correlated between each half of the basin, suggesting that the processes determining inter-model rainfall differences in the east may be distinct from those in the west. As a result, both halves of the basin required independent analysis. This finding highlights the importance of evaluating models with a regionally-specific focus, as the relative importance of processes can differ significantly even on relatively small spatial scales.

A process-based assessment was then conducted on each half of the basin in turn, focussing on composites of models from the extreme ends of the wet-to-dry spectrum. As previous studies have highlighted the importance of moisture sources, flux, and convergence, these processes were used as starting points. In particular, this chapter aimed to identify the role played by Atlantic and Indian Ocean SST biases, and associated moisture circulations, in explaining model rainfall differences. Warm tropical Atlantic SST biases were linked to high model rainfall in the west of the basin, via a chain of processes including enhanced evaporation and increased local convection. Given that this bias related to a chain of processes not observed in reality, the analysis suggested that models which are both wet and have a strong Atlantic SST bias are not producing credible rainfall climatologies. In contrast, model rainfall differences in the east were not sensitive to Atlantic SST biases; instead, circulation features such as the low-level westerlies and the AEJs were found to be the most important differentiators between wet and dry models. The dry models were unable to capture the distinct two jet structure of the AEJs in this season, indicating they are less credible than the wet models.

The findings in Chapter 4 indicate that a process-based method can be used to help determine model credibility. For this purpose, three aspects of the methodology proved particularly important. First, simply identifying the differences between composites or calculating correlations between variables across models is not enough to establish whether models are producing credible historical climatologies. It is vital to link the processes together in a **chain of processes** which lead to rainfall differences, as this gives insights into whether the rainfall is being produced for credible reasons. Without this step the physical links between

rainfall and other processes could be interpreted incorrectly. Second, linking model rainfall to **known biases** such as SST was found to be a useful way of assessing model credibility in the absence of observed rainfall data. SSTs are well observed in the satellite era, and biases in the eastern tropical oceans in coupled climate models are well-known [*Wang et al.*, 2014]. As the chain of processes related to high rainfall in the west Congo Basin is linked to spuriously high tropical Atlantic SSTs, this casts doubt on the representation of rainfall in those models. Finally, comparing the chain of processes linked to model wetness to **historical analogues** was also found to be useful in assessing model credibility. For example, in wet models in the west Congo Basin, high rainfall is related to high SSTs and enhanced local convection. However, while in observations wet years are related to anomalously warm SSTs, this is via a different set of processes [*Cook and Vizy*, 2015; *Neupane*, 2016]. This casts further doubt on the credibility of the wet coupled models, as they are not producing high magnitude rainfall via a known climatological process.

7.2 Plausibility of model future climate projections

The findings regarding model credibility in the historical period in Chapters 3 and 4 were intended to feed directly into an examination of the capabilities of models in projecting future climate change. The research in Chapters 5 and 6 thus attempted to answer the following research questions:

iii. Does model credibility in the historical period give insights into the plausibility of future projections?

iv. What processes contribute to inter-model uncertainty in future climate projections, and can an understanding of these processes help determine the plausibility of projections?

These are discussed in turn below.

7.2.1 Does model credibility in the historical period give insights into the plausibility of future projections?

This research question was tackled in Chapter 5, using the SON rainy season as a test-case for the process-based methodology developed throughout this thesis. Research which attempts to determine the most plausible climate change response from a suite of differing projections often works on the assumption that models which perform well in the historical period will produce more reliable or realistic future projections [*Rowell et al.*, 2016]. This is the underlying assumption of the majority of studies conducting performance-based model evaluation, as discussed in Section 1.4.2. However, it is not clear whether historical performance in terms of a metrics-based comparison to observations actually reduces the range of uncertainty in future projections [*Rowell et al.*, 2016]. The hypothesis in Chapter 5 is that categorising models based on the credibility of their historical climatology, as determined by a process-based assessment, may provide greater insights into the plausibility of different rainfall change signals.

Chapter 5 used the same composites of models as in Chapter 4: the extreme wet and dry models in the eastern and western subdomains of the basin. These composites featured significantly different rainfall climatologies in the historical period, which were found to be related to a range of regional processes. The analysis in Chapter 5 thus tests whether these differences in the historical period translate into differences the climate change signal. It does this by asking two questions of the composites: 1) does categorising models based on historical credibility make a difference to the rainfall change signal (ΔP)?; and 2) is the rainfall change signal in either composite related to changes in the same processes which drive rainfall differences in the historical period; and thus can anything be said about the plausibility of the rainfall change?

In the west Congo Basin, the analysis found that in both historically wet and historically dry models, the average rainfall change signal is similar. Both composites featured mean wetting over the whole domain (0.29 mm day $^{-1}$ in the wet composite, 0.34 mm day $^{-1}$ in the dry composite), with consistent wetting amongst composite members in the northern half of the domain (0.71 mm day $^{-1}$ and 0.79 mm day $^{-1}$ in the wet and dry composites respectively) and drying in the southern quarter of the domain (-0.54 mm day $^{-1}$ and -0.40 mm day $^{-1}$ in the wet and dry composites respectively). These changes are similar despite the large underlying climatological differences between the two composites, especially in terms of the tropical Atlantic SST bias, which is stronger and more equatorward in wet models. The analysis also found that excluding the most historically dubious models (i.e. the extremely wet models) from the overall CMIP5 sample did not reduce the overall spread in model rainfall signals (Figure 5.15).

The similarity between the west Congo Basin Δ*P* signal in both historically wet and dry models indicates that there is not a simple relationship between the strength of historical biases and the magnitude of rainfall change. However, a process-based analysis can still be utilised for two important purposes: first, to determine whether the processes causing wetting are the same across both composites, which would indicate a dominant, general response to warming across all models; and second, to determine whether the processes connected to rainfall change in either composite are plausible. In answer to the first, the analysis in Chapter 5 found that the north-western wetting signal in both wet and dry models is linked to a similar set of processes: enhanced tropical SST warming, particularly in the Gulf of Guinea, enhanced evaporation over the Gulf of Guinea, and enhanced low-level westerly qflux into the basin via the western boundary. Alongside the similar spatial pattern of change in many models (northern wetting and southern drying), this does indicate some common responses to warming amongst models during SON in the west Congo Basin.

The chain of processes connected to wetting in both composites is similar to the chain of processes leading to relative model wetness in the historical period: an enhanced source of q from warm SSTs, increased low level qflux into the basin, and enhanced qflux convergence. Whilst an enhancement of the low-level circulation into convective areas may be theoretically expected under a 'rich-gets-richer' mechanism of tropical rainfall change, the warming SSTs are also likely to be providing an enhanced moisture source to this low-level circulation in both composites. Given that increases in tropical Atlantic SSTs under warming build on

a large historical SST bias (up to 4.5 °C) in all but one model in the sample, the magnitude and pattern of this warming, and the resultant enhanced moisture supply, may not be credible in any of the analysed models. There is additional reason to be cautious as analysis of the omega field over the west Congo Basin finds that mean uplift actually decreases in this region (Figure 5.6), indicating that an enhanced supply of q will be an important contribution to the projected rainfall increases. If the enhanced q is coming from a spurious source, then the magnitude of the ΔP signal may not be plausible.

In contrast to the west, significant differences in the ΔP signal were found between the historically wet and dry models in the east Congo Basin. Wet models project mean wetting of 1.19 mm day^{-1} in the north of the eastern subdomain, while dry models only project rainfall increases of 0.43 mm day^{-1}, with one composite member projecting mean drying. Chapter 5 thus hypothesized that the processes causing distinct historical climatologies between the two composites may also be important for driving differences in rainfall change, and could therefore be used to establish the plausibility of the differing rainfall signals in the north east Congo Basin. The analysis found that for some important processes in the historical period, future changes are not significantly different between the wet and dry composite. For example, there are few significant differences between wet and dry models in their representation of changes to the South Atlantic High. In addition, as in the west composites, low-level westerly qflux into the basin increases in both composites, but again the signals are similar in both. These results suggest a common response to warming across models, but this response cannot explain the different rainfall signals in the east of the basin.

In the historical period, a key difference between wet and dry model climatologies is in their representation of the African Easterly Jets (Figure 4.16). Dry models feature a stronger and more equatorward AEJ-N, leading to a merging of the northern and southern component of the jet near the equator, and resulting in an export of moisture through the western boundary of the basin. Wet models feature two distinct and more poleward jets, more closely resembling the structure seen in reanalysis data during SON. In the future period, changes to the easterly winds were found to be associated with these underlying structures (Figure 7.1). In wet

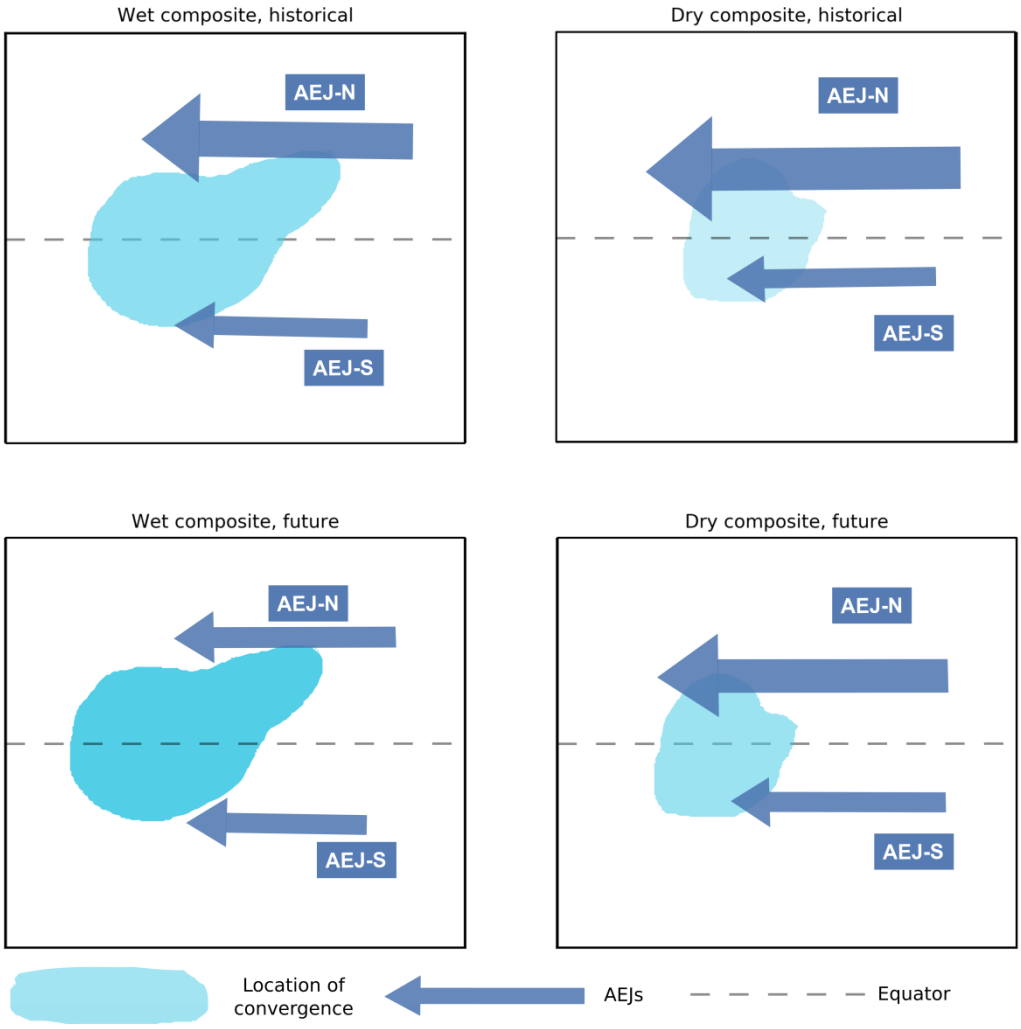

Figure 7.1 – Schematic of the difference between the location and strength of the AEJs in wet and dry models in Chapter 4 (top row) and the changes to the AEJs in the future described in Chapter 5 (bottom row).

models the AEJ-N weakens and the AEJ-S becomes more meridional, resulting in enhanced convergence in the north-east of the Congo Basin, co-locating with the main region of wetting. In the dry composite, the AEJ-N also weakens, but to a lesser extent than in the wet models. Importantly, changes in the AEJ-N occur in the historical equatorward location of the jet, resulting in less enhancement of convergence than in wet models, and continued export of moisture out of the basin. As the low rainfall change in dry models is linked to an underlying process which is not found to be credible compared to reanalysis, this analysis casts doubt on the plausibility of the relatively small ΔP signal in dry models.

The analysis in Chapter 5 found that, during SON, model credibility in the historical period has some bearing on rainfall change in some areas of the domain but not others. Further work is needed to assess the utility of this method in other seasons. This is discussed further in Section 7.3.

7.2.2 What processes contribute to inter-model uncertainty in future climate projections, and can an understanding of these processes help determine the plausibility of projections?

As described in Section 1.4.3.1, there are two ways of using process-based evaluation for understanding future change. The first, assessing the plausibility of rainfall signals in models based on their historical credibility, was tested in Chapter 5. The second, identifying the processes driving differences in rainfall

projections and using these to assess their plausibility, was tested in Chapter 6. The DJF dry season was chosen for this analysis, as it features the largest and most consistent rainfall change signal of any season. An additional justification was that there has been very little previous analysis on rainfall changes during the dry seasons in the Congo Basin, despite the vulnerability of the rainforest boundaries during these seasons [*Malhi et al.*, 2013]. The previous research that has been undertaken indicated small rainfall increases in the future in ensemble projections across all seasons [*Haensler et al.*, 2013a]; however, this approach masks the complex range of mean rainfall change produced by coupled models by the end of the century, which vary from 2.3 mm season $^{-1}$ to 160.4 mm season^{-1} during DJF. Chapter 6 thus provides the first comprehensive analysis of why different models produce different rainfall signals during DJF over the Congo Basin.

Research into the mechanisms of rainfall change over the tropics and Africa has indicated that dynamical mechanisms of change (as opposed to thermodynamic mechanisms) contribute most to uncertainty in the rainfall response to warming across models [e.g. *Chadwick et al.*, 2013; *Lazenby et al.*, 2018]. Chapter 6 thus focussed on identifying differences in dynamical processes related to the extreme ends of the inter-model spectrum of rainfall change. First, the vertical circulation was assessed. Models which experienced the wettest ΔP signal experienced significant increases in uplift in the future over the east Congo Basin and over the west Indian Ocean. This is matched with increased and extended subsidence in the northern subtropics and over subtropical southern Africa, and weakened uplift over the Maritime Continent. This latter result indicates a weakening of the Walker cell over the Indian Ocean in the wettest models, which previous research into

tropical changes in multi-model ensembles has indicated may be a response to warming [e.g. *Vecchi and Soden*, 2007; *Shongwe et al.*, 2011; *DiNezio et al.*, 2013]. In contrast, models with the driest Δ*P* signal featured reduced uplift over the east Congo Basin in the future, alongside smaller changes over the subtropics, the Indian Ocean, and the Maritime Continent.

Differences in the horizontal circulation were also found between the wettest and driest models. Models with the greatest wetting experience greater qflux convergence at low levels (700 and 850 hPa), as well as enhanced qflux entering the basin from the north and east compared to the driest models. Additional analysis confirms that these increases are a result of both increased winds and increased q in the wettest models (Figure 6.S1 and 6.S2). This indicates that both thermodynamical and dynamical responses to warming could contribute to differences in model rainfall responses, though there is evidence that the some of the increases in *q* are in part due to enhanced transport from outside the region (i.e. dynamical). The models with the greatest Δ*P* signal also feature greater increases in tropical SSTs, including in the west Indian Ocean, which may contribute to enhanced evaporation and thus an enhanced moisture supply into the basin through the eastern boundary. Further work is needed to disentangle these effects across individual models.

The next steps in this research are to determine which rainfall signal is most plausible over this region. A recent observational study by *Hua et al.* [2016] may offer some insights into this. The study finds that the recent observed drying trend over Central Africa (2000-2014) between April and June is associated with

enhanced uplift over the Maritime Continent, and reduced uplift over the Congo Basin. This is the same relationship found in this study between vertical motion over Central African and the Maritime Continent in wet models, though with an opposite signal. In one sense this is promising, as it indicates some models are able to capture the direction of the connection between these two regions. However, that models are projecting an opposite signal under future warming to that observed in recent decades may be a cause for concern. Further work is needed at a tropics-wide scale to determine whether an enhancement of uplift over the Congo Basin at the expense of convection over the Maritime Continent is a plausible scenario. This will be important for determining which models are producing the most plausible rainfall signals over the Congo Basin during DJF.

The future-focussed process-based analysis in Chapter 6 has proved promising, and similar analysis should be conducted in other seasons in the Congo Basin. Alongside deeper investigation into the plausibility of tropics-wide climate, this method is expected to prove fruitful for constraining the range of future rainfall change signals in the Congo Basin. Further work could add value to these findings; in particular, analysis of models' abilities to capture the processes associated with drying trends in the historical period may offer insights into whether the higher magnitude future wetting is plausible. This is similar to the approach taken by *James et al.* [2015] over the Sahel. The findings from Chapter 6 could also be strengthened by an improved understanding of the plausibility of processes related to rainfall in the historical period during DJF, as conducted in Chapter 5 for SON.

7.3 The value of process-based assessments

The process-based approach to model evaluation espoused in this thesis has been conducted in the context of increasing recognition within the climate science community of the scientific value in understanding how and why models behave as they do. This is reflected in a number of recent initiatives to improve our understanding of physical processes in models, such as an American Meteorological Society special collection on Process-Oriented Model Diagnostics, including analyses of moisture budgets [*Adames and Ming*, 2018], coupling biases [*Nagura et al.*, 2018] and teleconnections [*Henderson et al.*, 2017], and a "Model Diagnostics Task Force", put together by the US National Oceanic and Atmospheric Administration's (NOAA) "Model Diagnostics Task Force", to develop and implement process-based metrics at the model development stage. There has also been increasing recognition of the importance of regionally-focused process-based assessments, as called for by *James et al.* [2018] over Africa.

In the context of such work, this thesis hypothesized that a process-based approach would provide significant insights into the behaviour of climate models in the Congo Basin, and sought to advance a model evaluation methodology that is of particular use in data scarce regions. The ability of commonly used performance-based methods of model evaluation to provide insights into model behaviour is severely limited without long-term, homogenous rainfall data with which to compare models to. It was hypothesized that a process-based approach

would offer greater clarity in determining the credibility of models, with the overall aim of constraining the spectrum of model climatologies and future projections. This section will evaluate the overall effectiveness of the process-based approaches developed in this thesis, identifying its limitations and pointing to possible improvements for future work.

The analysis in this thesis provided a number of improvements upon traditional performance-based methods over the Congo Basin. In particular, the identification of chains of processes which link differences in regional processes to differences in rainfall across models has helped determine the reasons that some models have vastly different historical climatologies (Chapter 4) or future projections (Chapters 5 and 6). This provides additional information to correlation analysis, as it can give insight into the direction of the relationship, and the physical mechanisms linking variables together. Determining the chain of processes is particularly important when attempting to ascertain model credibility. The impetus behind the regional process-based evaluation in this thesis is that whilst observational rainfall data is severely limited in this region, we generally have a better understanding of large-scale regional processes such as the atmospheric circulation, and as a result these are better represented in reanalysis data. The method developed in this thesis allows for a comparison between the processes linked to rainfall in models and in reality, providing one measure of how credible the models may be. For example, in Chapter 4 a chain of processes was identified linking the warm SST bias in the tropical east Atlantic to rainfall in the west of the Congo Basin. These processes included enhanced evaporation in the tropical east Atlantic, strengthened low-level qflux and enhanced local convection. However, studies using reanalysis data at

interannual timescales have found that whilst wetting over the west Congo Basin is associated with anomalously warm SSTs, it is via a different chain of processes than the one identified across models [*Cook and Vizy*, 2015; *Neupane*, 2016]. This casts doubt on the credibility of models with high wetting here, as it is linked to a chain of processes not evident in reality.

In addition, linking differences in model rainfall to known model biases is another important way this method can be used to assess model credibility. In Chapter 4 the well-known positive SST bias in the tropical east Atlantic is linked via a chain of processes to model wetness in the west Congo Basin. This is likely a key reason why the chain of processes in this region in models differs to that in reality. The connection to this bias thus casts doubt on models which have both a strong bias and high rainfall in the west. Connecting inter-model differences to known model biases has also been utilised effectively in southern Africa, where a recent study by *Munday and Washington* [2018] linked model rainfall differences to biases in the representation of topography over Tanzania and Malawi. In addition to helping determine which models are the least credible, such an assessment can also be used to guide model development. The findings in Chapter 4 strongly indicate that improving modelled SSTs in the tropical east Atlantic will be vital for improving representations of Central African rainfall and reducing differences amongst models. Chapter 5 also shows that the extent to which future SST changes build on underlying SST biases is not fully understood, further highlighting the need to reduce this bias.

Two process-based approaches for assessing the plausibility of future rainfall changes in models were tested in this thesis. The first, in Chapter 5, assessed the extent to which grouping models by their historical credibility contributed to differences in their future climate signals and by extension, gave insights into the plausibility of those signals. This approach was found to be more effective in some parts of the Congo Basin domain than others during the test season of SON. In the east Congo Basin significant differences in the rainfall projections between of historically wet and historically dry models were found to relate to differences in the underlying climatological representation of the African Easterly Jets. In the west of the basin however, despite large underlying SST biases in the historical period driving significant rainfall differences, these did not translate into significantly different rainfall signals.

These findings suggest that where some models feature a substantial climatological bias and other models do not, the method may be useful, as future changes may build on the different underlying climatological states. However, where all models share a similar bias, as in the west Congo Basin, sampling models from across this spectrum does not provide significantly different results. It may be that a different sampling method is needed to understand the plausibility of projected changes in the west Congo Basin, such as sampling based on the strength or spatial pattern of the bias, as opposed to the strength of the rainfall climatology. It is also likely sampling models on their future change signal could provide additional insights to the plausibility of rainfall projections in the west Congo Basin in SON.

This latter approach, in which models are sampled on the basis of their climate change signal, proved useful in investigating the model spread in rainfall projections in DJF (Chapter 6). Chapter 6 identified the processes associated with the weakest and strongest wetting signals across models, finding strong links between rainfall and changes to the horizontal and vertical circulations. Whilst previous work has identified a weak mean wetting signal [*Haensler et al.*, 2013c; *Aloysius et al.*, 2016], this analysis offered the first insight into the processes most important for driving different magnitudes of rainfall change over the Congo Basin. The next step is to investigate further the likely changes in these processes under warming, to give insights into which rainfall signal is most plausible. For example, the results in Chapter 6 strongly suggest that investigating the plausibility of the response of Indian Ocean SSTs and convection to warming will help to constrain the likely rainfall response over the Congo Basin. In addition, the conclusions of Chapter 6 highlights that a better understanding of processes in the historical period, as conducted in Chapter 4 for SON, would aid an assessment of the plausibility of the processes future change. This could include an analysis of how well models capture trends and variability in reanalysis in the historical period.

Overall, the analysis in this thesis shows that a process-based approach to model evaluation can add significant scientific value, particularly in regions such as the Congo Basin where comparing model performance to severely limited observations lacks rigour. This thesis highlights the importance of regionally and seasonally specific model evaluation, as models which are credible in one season or subdomain are not necessarily credible in another. The conclusions from this thesis also raise fundamental questions regarding the extent to which we can trust,

and by extension, use, individual CMIP5 models in this region. Should the presence of a bias found to relate to rainfall in any model deem that model not credible? If we excluded all models with an Atlantic SST bias, this would leave only one model left to analyse. In which case, at what point do we deem a model 'credible enough' despite deficiencies? No model is perfect, but where should the line be drawn? These questions cannot be answered by this thesis alone, but will be important questions for the model evaluation community to discuss.

The process-based methodology advanced in this thesis also feeds into wider discussions within the climate science community about the value of a deeper understanding of model uncertainties. *Stevens and Bony* [2013] argue that a better understanding of physical processes in the Earth system will provide greater reductions in uncertainty than a more expansive representation of the system as a whole, which has for many years been the priority for the climate modelling community. Reducing uncertainty in model representations of physical processes over Central and southern Africa was a central aim of the Future Climate for Africa UMFULA (Uncertainty Reduction in Models for Understanding Development Applications), which this thesis contributed to extensively. Further, a recent EOS article by *Carslaw et al.* [2018] highlighted the lack of attention paid to model uncertainty stemming from the large number of degrees of freedom inherent within model simulations of multiple uncertain processes, and how little is being done between each generation of climate models to reduce this. Analysis using data from intercomparison projects, as in this thesis, goes some way towards sampling this uncertainty, but future work may need to include a much larger array of model versions, in order to fully sample model uncertainties [*Carslaw et*

al., 2018]. These discussions suggest a paradigm shift is needed, under which reducing model uncertainty is a top priority for the climate science community.

7.4 Avenues for future research

This thesis has contributed four new research papers to the scientific literature on coupled model capabilities in the Congo Basin, including two on future climate change, which has been severely understudied in spite of its importance in global and regional climate dynamics. However, there is still important work to be done to improve our understanding of climate model capabilities in this region. This final section will outline some of the priorities for future research in this region.

As the previous section highlights, there is a need for regionally- and seasonally-specific process-based evaluation in this region. Models which are credible in one season or subdomain are not necessarily credible in others, as the processes contributing to rainfall across the domain and throughout the annual cycle are not always the same. There is therefore a need for tailored process-based analysis to fit the research question at hand. This thesis focussed predominately on the SON wet season, but Chapter 3 also highlighted important features in the MAM wet season which are worthy of investigation. These include the influence of model representation of the East African highlands on moisture flux into and rainfall over the basin. In light of this, further work should also be conducted into the links between East Africa and the Congo Basin, particularly in MAM which is a wet season in both regions, and is at the centre of the 'East African paradox'. Recent

work has suggested that moisture advection from the Congo Basin into East Africa contributes to wetting in the latter in the future [*Giannini et al.*, 2018]; process-based evaluation in the future should look at connections between the two regions to help try and determine the plausibility of rainfall changes across equatorial Africa, and whether model credibility between the two regions is linked.

The thesis has highlighted the value of assessing models across multiple modelling centres, and future work should build on this. Whilst valuable work has been conducted assessing the capabilities of models from individual modelling groups, such as *James et al.*'s [2018] study on the UK Met Office's Unified Model, further work needs to be done to compare such findings across models from different modelling centres. Intercomparison projects such as CMIP have provided an essential framework for doing this; however, thus far, work has primarily focused on the ensemble mean of model outputs, with less attention paid to uncovering the physical reasons behind such model differences. *James et al.* [2018] call for a model evaluation "hub" for Africa in order to improve simulations of African climate across models. Given the large variability across models identified in this thesis, as well as the significant differences in processes driving these changes, such a hub would add to our understanding of model capabilities in this region significantly.

Future research should also assess the capabilities of models across a wider range of model datasets. This thesis has focussed on coarse resolution model data from the CMIP5 dataset, but very little analysis has been conducted into the capabilities of regional models in this region, and the extent to which they may be able to offer improvements on global models. Previous analysis using varying model

resolutions has found no obvious improvements over Africa as resolution increases [*Moufouma-Okia and Jones*, 2014], and so process-based evaluations should be conducted on RCMs and compared with the processes found in GCMs. The CORDEX dataset would be a good starting point for this analysis, as the results could be compared directly to the parent GCMs within CMIP5.

Analysis of high resolution, limited-area climate models will also be important, due to the predominance of convective rainfall in the Congo Basin, which occurs on much smaller spatial and temporal scales than GCMs or downscaled RCMs can capture. A good candidate for this analysis is the new CP4-Africa dataset, produced under Future Climate for Africa's IMPALA project. CP4-Africa is a pan-African convection-permitting climate simulation with 4.5 km horizontal resolution developed by the UK Met Office [*Stratton et al.*, 2018]. Initial analysis, conducted alongside this thesis, indicates significant differences between the climatology of the Congo Basin in the 4.5 km and 25 km version of the model. A central aim of all regional and high-resolution model analysis should be to determine whether higher-resolution models provide more credible historical climatologies and more plausible projections than GCMs [e.g. *Kendon et al.*, 2017]. Given the exponential increases in computing costs as resolution increases, identifying any such improvements will be important for justifying the development of such models.

This thesis has focussed on the mean-state of both historical and future climate in models, which is well-justified as the ability of models to represent higher-order variability and trends will depend ultimately on their ability to represent the mean-state. Nevertheless, it will be important for future work to assess both

higher-order variability and trends. In the Congo Basin the majority of rainfall is produced by systems which usually persist in the atmosphere for less than a day, and the ability of models to represent the variability of these systems will likely be an important contributor to model differences. There has also been limited research into the representation of interannual modes of variability such as ENSO and their teleconnections within models, though process-based analysis of these modes in other African regions has proved fruitful [e.g. *Dieppois et al.*, 2015]. It will also be important to analyse the ability of models to reproduce the processes associated with climatic trends, particularly in light of the drying trend observed in recent decades [*Sanga-Ngoie and Fukuyama*, 1996; *Laraque et al.*, 2001; *Malhi and Wright*, 2004]. *Hua et al.* [2016] have already identified some of the important processes related to this trend in observations, and future work could assess the ability of models to capture these processes. This will also be useful for assessing the plausibility of the wetting trend in many models, particularly in DJF, as it is of opposite sign to the recent observed trend.

Finally, this thesis has pointed to the importance of improving our understanding the Congo Basin climate regime in reality, in order to better assess the capabilities of models. Targeted observational campaigns, such as the ones described in Section 7.1.2.1 will be an important first step, and the outputs will be able to be used directly to assess the credibility of the circulation in models. There is currently important work being conducted into the distribution of convection over the Congo Basin in satellite data [*Hart and Washington*, forthcoming] and into the relationship between low-to-mid-level convergence and convection in reanalysis data [*Pokam and Washington*, forthcoming]. Such improvements will complement

the development of novel methodologies of model evaluation, such as the one developed in this thesis.

7.5 Concluding remarks

Climate models are the only tools available to understand how the climate of this important region might change in the future. As they are currently used, they provide some information regarding the range and degree of possible rainfall changes under warming, but limited insight into the plausibility of any of these changes over the Congo Basin. New approaches must be utilised in order to provide useful and usable information for regional decision-makers. This thesis presents several examples of such approaches, which can help improve our understanding of the plausibility of these signals and offer some constraints on the full spectrum of rainfall projections over the Congo Basin. There is much more work to be done, but this thesis has made an important contribution to understanding this severely understudied, yet hugely important region.

References

Abiodun, B. J., W. J. Gutowski, A. A. Abatan, and J. M. Prusa (2011), CAM-EULAG: A non-hydrostatic atmospheric climate model with grid stretching, *Acta Geophys.*, *59*(6), 1158–1167, doi:10.2478/s11600-011-0032-2.

Adames, Á. F., and Y. Ming (2018), Moisture and Moist Static Energy Budgets of South Asian Monsoon Low Pressure Systems in GFDL AM4.0, *J. Atmos. Sci.*, *75*(6), 2107–2123, doi:10.1175/JAS-D-17-0309.1.

Adler, R. F., G. J. Huffman, A. Chang, R. Ferraro, P.-P. Xie, J. Janowiak, B. Rudolf, U. Schneider, S. Curtis, D. Bolvin, A. Gruber, J. Susskind, P. Arkin, and E. Nelkin (2003), The Version-2 Global Precipitation Climatology Project (GPCP) Monthly Precipitation Analysis (1979–Present), *J. Hydrometeorol.*, *4*(6), 1147–1167, doi:10.1175/1525-7541(2003)004<1147:TVGPCP>2.0.CO;2.

Aguilar, E., a. A. Barry, M. Brunet, L. Ekang, a. Fernandes, M. Massoukina, J. Mbah, a. Mhanda, D. J. do Nascimento, T. C. Peterson, O. T. Umba, M. Tomou, and X. Zhang (2009), Changes in temperature and precipitation extremes in western central Africa, Guinea Conakry, and Zimbabwe, 1955-2006, *J. Geophys. Res. Atmos.*, *114*(2), 1–11, doi:10.1029/2008JD011010.

Akkermans, T., W. Thiery, and N. P. M. Van Lipzig (2014), The regional climate impact of a realistic future deforestation scenario in the congo basin, *J. Clim.*, *27*(7), 2714–2734, doi:10.1175/JCLI-D-13-00361.1.

Albrecht, R. I., S. J. Goodman, D. E. Buechler, R. J. Blakeslee, and H. J. Christian (2016), Where are the lightning hotspots on earth?, *Bull. Am. Meteorol. Soc.*, *97*(11), 2051–2068, doi:10.1175/BAMS-D-14-00193.1.

Alexander, M. A., I. Bladé, M. Newman, J. R. Lanzante, N. C. Lau, and J. D. Scott (2002), The atmospheric bridge: The influence of ENSO teleconnections on air-sea interaction over the global oceans, *J. Clim.*, *15*(16), 2205–2231, doi:10.1175/1520-0442(2002)015<2205:TABTIO>2.0.CO;2.

Allan, R. P. (2012), Regime dependent changes in global precipitation, *Clim. Dyn.*, *39*(3), 827–840, doi:10.1007/s00382-011-1134-x.

Allan, R. P., B. J. Soden, V. O. John, W. Ingram, and P. Good (2010), Current changes in tropical precipitation, *Environ. Res. Lett.*, *5*(2), 1–8, doi:10.1088/1748-9326/5/2/025205.

Allen, M. R., and W. J. Ingram (2002), Constraints on future changes in climate and the hydrologic cycle, *Nature*, *419*(6903), doi:10.1038/nature01092.

Aloysius, N. R., J. Sheffield, and E. F. Wood (2016), Evaluation of historical and future simulations of precipitation and temperature in Central Africa from CMIP5 climate models, *J. Geophys. Res. Atmos.*, *121*(1), 130–152, doi:10.1002/2015JD023656.

Alsdorf, D., E. Beighley, A. Laraque, H. Lee, R. Tshimanga, F. O'Loughlin, G. Mahï¿½, B. Dinga, G. Moukandi, and R. G. M. Spencer (2016), Opportunities for hydrologic research in the Congo Basin, *Rev. Geophys.*, *54*(2), 378–409, doi:10.1002/2016RG000517.

Anyah, R. O., and W. Qiu (2012), Characteristic 20th and 21st century precipitation and temperature patterns and changes over the Greater Horn of Africa, *Int. J. Climatol.*, *32*(3), 347–363, doi:10.1002/joc.2270.

Asefi-Najafabady, S., and S. Saatchi (2013), Response of African humid tropical forests to recent rainfall anomalies, *Philos. Trans. R. Soc. B Biol. Sci.*, *368*(1625), doi:10.1098/rstb.2012.0306.

Baccini, A., S. J. Goetz, W. S. Walker, N. T. Laporte, M. Sun, J. Hackler, P. S. A. Beck, R. Dubayah, M. A. Friedl, S. Samanta, and R. A. Houghton (2012), Estimated carbon dioxide emissions from tropical deforestation improved by carbon-density maps, *Nat. Clim. Chang.*, *2*(3), 182–185, doi:10.1038/nclimate1354.

Bain, C. L., K. D. Williams, S. F. Milton, and J. T. Heming (2014), Objective tracking of african easterly waves in met office models, *Q. J. R. Meteorol. Soc.*, *140*(678), 47–57, doi:10.1002/qj.2110.

Baker, N. C., and P. C. Taylor (2016), A framework for evaluating climate model performance metrics, *J. Clim.*, *29*(5), 1773–1782, doi:10.1175/JCLI-D-15-0114.1.

Bala, G., K. Caldeira, M. Wickett, T. J. Phillips, D. B. Lobell, C. Delire, and A. Mirin (2007), Combined climate and carbon-cycle effects of large-scale deforestation, *Proc. Natl. Acad. Sci.*, *104*(16), 6550–6555, doi:10.1073/pnas.0608998104.

Balagizi, C. M., M. M. Kasereka, E. Cuoco, and M. Liotta (2018), Influence of moisture source dynamics and weather patterns on stable isotopes ratios of precipitation in Central-Eastern Africa, *Sci. Total Environ.*, *628–629*, 1058–1078, doi:10.1016/j.scitotenv.2018.01.284.

Balas, N., S. E. Nicholson, and D. Klotter (2007), The relationship of rainfall variability in West Central Africa to sea-surface temperature fluctuation, *Int. J. Climatol.*, *27*(10), 1335–1349, doi:10.1002/joc.

Baumberger, C., R. Knutti, and G. Hirsch Hadorn (2017), Building confidence in climate model projections: an analysis of inferences from fit, *Wiley Interdiscip. Rev. Clim. Chang.*, *8*(3), 1–20, doi:10.1002/wcc.454.

Behera, S. K., J. J. Luo, S. Masson, P. Delecluse, S. Gualdi, A. Navarra, and T. Yamagata

(2005), Paramount impact of the Indian ocean dipole on the East African short rains: A CGCM study, *J. Clim.*, *18*(21), 4514–4530, doi:10.1175/JCLI9018.1.

Bell, J. P., A. M. Tompkins, C. Bouka-biona, I. S. Sanda, and B. E. T. Al (2015), A process-based investigation into the impact of the Congo basin deforestation on surface climate, , 1–19, doi:10.1002/2014JD022586.Received.

Beltrando, G., and P. Camberlin (1993), Interannual variability of rainfall in the eastern horn of Africa and indicators of atmospheric circulation, *Int. J. Climatol.*, *13*(5), 533–546, doi:10.1002/joc.3370130505.

Bentsen, M., I. Bethke, J. B. Debernard, T. Iversen, A. Kirkevag, Ø. Seland, H. Drange, C. Roelandt, I. A. Seierstad, C. Hoose, and J. E. Kristjansson (2013), The Norwegian earth system model, NorESM1-M—Part 1: description and basic evaluation of the physical climate, *Geosci. Model Dev. Discuss.*, *6*, 687–720, doi:10.5194/gmd-6-687-2013.

Biasutti, M., and A. H. Sobel (2009), Delayed Sahel rainfall and global seasonal cycle in a warmer climate, *Geophys. Res. Lett.*, *36*(23), 1–5, doi:10.1029/2009GL041303.

Biasutti, M., A. H. Sobel, and S. J. Camargo (2009), The role of the Sahara low in summertime Sahel rainfall variability and change in the CMIP3 models, *J. Clim.*, *22*(21), 5755–5771, doi:10.1175/2009JCLI2969.1.

Black, E., J. Slingo, and K. R. Sperber (2003), An Observational Study of the Relationship between Excessively Strong Short Rains in Coastal East Africa and Indian Ocean SST, *Mon. Weather Rev.*, *131*(1), 74–94, doi:10.1175/1520-0493(2003)131<0074:AOSOTR>2.0.CO;2.

Blamey, R. C., and C. J. C. Reason (2012), Mesoscale convective complexes over Southern Africa, *J. Clim.*, *25*(2), 753–766, doi:10.1175/JCLI-D-10-05013.1.

Boer, G. J., and S. J. Lambert (2001), Second-order space-time climate difference statistics, *Clim. Dyn.*, *17*(2–3), 213–218, doi:10.1007/PL00013735.

Bollasina, M. A., and Y. Ming (2013), The general circulation model precipitation bias over the southwestern equatorial Indian Ocean and its implications for simulating the South Asian monsoon, *Clim. Dyn.*, *40*(3–4), 823–838, doi:10.1007/s00382-012-1347-7.

Bombelli, A., M. Henry, S. Castaldi, S. Adu-Bredu, A. Arneth, A. De Grandcourt, E. Grieco, W. L. Kutsch, V. Lehsten, A. Rasile, M. Reichstein, K. Tansey, U. Weber, and R. Valentini (2009), An outlook on the Sub-Saharan Africa carbon balance, *Biogeosciences*, *6*(10), 2193–2205, doi:10.5194/bg-6-2193-2009.

Boschat, G., I. Simmonds, A. Purich, T. Cowan, and A. B. Pezza (2016), On the use of composite analyses to form physical hypotheses: An example from heat wave - SST associations, *Sci. Rep.*, *6*(June), 1–10, doi:10.1038/srep29599.

Bracegirdle, T. J., E. Shuckburgh, J. B. Sallee, Z. Wang, A. J. S. Meijers, N. Bruneau, T. Phillips, and L. J. Wilcox (2013), Assessment of surface winds over the atlantic, indian, and pacific ocean sectors of the southern ocean in cmip5 models: Historical bias, forcing response, and state dependence, *J. Geophys. Res. Atmos.*, *118*(2), 547–562, doi:10.1002/jgrd.50153.

Brands, S., S. Herrera, J. Fernández, and J. M. Gutiérrez (2013), How well do CMIP5 Earth System Models simulate present climate conditions in Europe and Africa?: A performance comparison for the downscaling community, *Clim. Dyn.*, *41*(3–4), 803–817, doi:10.1007/s00382-013-1742-8.

Brncic, T. M., K. J. Willis, D. J. Harris, and R. Washington (2007), Culture or climate? The relative influences of past processes on the composition of the lowland Congo rainforest, *Philos. Trans. R. Soc. B Biol. Sci.*, *362*(1478), 229–242,

doi:10.1098/rstb.2006.1982.

Brown, J. R., A. F. Moise, R. Colman, and H. Zhang (2016), Will a warmer world mean a wetter or drier Australian monsoon?, *J. Clim.*, *29*(12), 4577–4596, doi:10.1175/JCLI-D-15-0695.1.

Brubaker, K. L., D. Entekhabi, and P. S. Eagleson (1993), Estimation of continental precipitation recycling, *J. Clim.*, *6*(6), 1077–1089, doi:10.1175/1520-0442(1993)006<1077:EOCPR>2.0.CO;2.

Burde, G. I., A. Zangvil, and P. J. Lamb (1996), Estimating the role of local evaporation in precipitation for a two-dimensional region, *J. Clim.*, *9*(6), 1328–1338, doi:10.1175/1520-0442(1996)009<1328:ETROLE>2.0.CO;2.

Burpee, R. W. (1972), The Origin and Structure of Easterly Waves in the Lower Troposphere of North Africa, *J. Atmos. Sci.*, *29*(1), 77–90, doi:10.1175/1520-0469(1972)029<0077:TOASOE>2.0.CO;2.

Camberlin, P., and R. E. Okoola (2003), The onset and cessation of the "' long rains '" in eastern Africa and their interannual variability, *Theor. Appl. Climatol.*, *54*(1–2), 43–54, doi:10.1007/s00704-002-0721-5.

Camberlin, P., S. Janicot, and I. Poccard (2001), Seasonality and atmospheric dynamics of the teleconnection between African rainfall and tropical ocean surface temperatures, *Int. J. Climatol.*, *21*, 973–1005, doi:10.1002/joc.673.

Caminade, C., L. Terray, and E. Maisonnave (2006), West African monsoon response to greenhouse gas and sulphate aerosol forcing under two emission scenarios, *Clim. Dyn.*, *26*(5), 531–547, doi:10.1007/s00382-005-0083-7.

Carslaw, K. S., L. A. Lee, L. A. Regayre, and J. S. Johnson (2018), Climate Models Are Uncertain, but We Can Do Something About It, *Eos (Washington. DC).*

Chadwick, R., I. Boutle, and G. Martin (2013), Spatial patterns of precipitation

change in CMIP5: Why the rich do not get richer in the tropics, *J. Clim.*, *26*(11), 3803–3822, doi:10.1175/JCLI-D-12-00543.1.

Chou, C., and J. D. Neelin (2004), Mechanisms of Global Warming Impacts on Regional Tropical Precipitation*, *J. Clim.*, *17*(13), 2688–2701, doi:10.1175/1520-0442(2004)017<2688:MOGWIO>2.0.CO;2.

Chou, C., J. D. Neelin, J. Y. Tu, and C. T. Chen (2006), Regional tropical precipitation change mechanisms in ECHAM4/OPYC3 under global warming, *J. Clim.*, *19*(17), 4207–4223, doi:10.1175/JCLI3858.1.

Chou, C., J. Y. Tu, and P. H. Tan (2007), Asymmetry of tropical precipitation change under global warming, *Geophys. Res. Lett.*, *34*(17), 1–5, doi:10.1029/2007GL030327.

Chou, C., J. D. Neelin, C. A. Chen, and J. Y. Tu (2009), Evaluating the "rich-get-richer" mechanism in tropical precipitation change under global warming, *J. Clim.*, *22*(8), 1982–2005, doi:10.1175/2008JCLI2471.1.

Christensen, J. H., K. K. Kumar, E. Aldria, S.-I. An, I. F. a. Cavalcanti, M. De Castro, W. Dong, P. Goswami, A. Hall, J. K. Kanyanga, A. Kitoh, J. Kossin, N.-C. Lau, J. Renwick, D. B. Stephenson, S.-P. Xie, and T. Zhou (2013), Climate Phenomena and their Relevance for Future Regional Climate Change, in *Climate Change 2013: The Physical Science Basis. Contribution of Working Group I to the Fifth Assessment Report of the Intergovernmental Panel on Climate Change*, edited by T. F. Stocker, D. Qin, G.-K. Plattner, M. M. B. Tignor, S. K. Allen, J. Boschung, A. Nauels, Y. Xia, V. Bex, and P. M. Midgley, pp. 1217–1308, Cambridge University Press, Cambridge, United Kingdom and New York, NY, USA.

Christian, H. J., R. J. Blakeslee, D. J. Boccippio, W. L. Boeck, D. E. Buechler, K. T. Driscoll, S. J. Goodman, J. M. Hall, W. J. Koshak, D. M. Mach, and M. F. Stewart

(2003), Global frequency and distribution of lightning as observed from space by the Optical Transient Detector, *J. Geophys. Res.*, *108*(ACL 4), 1–15, doi:-10.1029/2002JD002347.

Ciais, P., A. Bombelli, M. Williams, S. L. Piao, J. Chave, C. M. Ryan, M. Henry, P. Brender, and R. Valentini (2011), The carbon balance of Africa: Synthesis of recent research studies, *Philos. Trans. R. Soc. A Math. Phys. Eng. Sci.*, *369*(1943), 2038–2057, doi:10.1098/rsta.2010.0328.

CKDN (2014), *The IPCC's Fifth Assessment Report: What's in it for Africa?*, London.

Collier, M., and P. Uhe (2012), CMIP5 datasets from the ACCESS1.0 and ACCESS1.3 coupled climate models, *CAWCR Tech. Rep. No. 059*, Centre for Australian Weather and Climate Research, doi:ISBN: 20978-1-922173-29-4.

Collier, P., G. Conway, and T. Venables (2008), Climate change and Africa, *Oxford Rev. Econ. Policy*, *24*(2), 337–353, doi:10.1093/oxrep/grn019.

Collins, M. (2017), Still weighting to break the model democracy, *Geophys. Res. Lett.*, *44*(7), 3328–3329, doi:10.1002/2017GL073370.

Collins, M., R. Knutti, J. Arblaster, J.-L. Dufresne, T. Fichefet, P. Friedlingstein, X. Gao, W. J. Gutowski, T. Johns, G. Krinner, M. Shongwe, C. Tebaldi, A. J. Weaver, and M. Wehner (2013), Long-term Climate Change: Projections, Commitments and Irreversibility, *Clim. Chang. 2013 Phys. Sci. Basis. Contrib. Work. Gr. I to Fifth Assess. Rep. Intergov. Panel Clim. Chang.*, 1029–1136, doi:10.1017/CBO9781107415324.024.

Collins, M. A. T. (2007), Ensembles and probabilities: A new era in the prediction of climate change, *Philos. Trans. R. Soc. A Math. Phys. Eng. Sci.*, *365*(1857), 1957–1970, doi:10.1098/rsta.2007.2068.

Cook, K. H. (1999), Generation of the African easterly jet and its role in determining

West African precipitation, *J. Clim.*, *12*(5 I), 1165–1184, doi:10.1175/1520-0442(1999)012<1165:GOTAEJ>2.0.CO;2.

Cook, K. H., and E. K. Vizy (2006), Coupled Model Simulations of the West African Monsoon System: Twentieth- and Twenty-First-Century Simulations, *J. Clim.*, *19*(15), 3681–3703, doi:10.1175/JCLI3814.1.

Cook, K. H., and E. K. Vizy (2015), The Congo Basin Walker circulation: dynamics and connections to precipitation, *Clim. Dyn.*, *47*(3–4), 697–717, doi:10.1007/s00382-015-2864-y.

Creese, A., and R. Washington (2016), Using qflux to constrain modeled Congo Basin rainfall in the CMIP5 ensemble, *J. Geophys. Res. Atmos.*, *121*(22), 13415–13442, doi:10.1002/2016JD025596.

Creese, A., and R. Washington (2018), A process-based assessment of CMIP5 rainfall in the Congo Basin: the September-November rainy season, *J. Clim.*, *31*(18), 7417–7439, doi:10.1175/JCLI-D-17-0818.1.

Dargie, G. C., S. L. Lewis, I. T. Lawson, E. T. A. Mitchard, S. E. Page, Y. E. Bocko, and S. A. Ifo (2017), Age, extent and carbon storage of the central Congo Basin peatland complex, *Nature*, *542*(7639), 86–90, doi:10.1038/nature21048.

Davey, M., M. Huddleston, K. Sperber, P. Braconnot, F. Bryan, D. Chen, R. Colman, C. Cooper, U. Cubasch, P. Delecluse, D. DeWitt, L. Fairhead, G. Flato, C. Gordon, T. Hogan, M. Ji, M. Kimoto, a. Kitoh, T. Knutson, M. Latif, H. Le Treut, T. Li, S. Manabe, C. Mechoso, G. Meehl, S. Power, E. Roeckner, L. Terray, a. Vintzileos, R. Voss, B. Wang, W. Washington, I. Yoshikawa, J. Yu, S. Yukimoto, and S. Zebiak (2002), STOIC: A study of coupled model climatology and variability in tropical ocean regions, *Clim. Dyn.*, *18*(5), 403–420, doi:10.1007/s00382-001-0188-6.

Dee, D. P., S. M. Uppala, A. J. Simmons, P. Berrisford, P. Poli, S. Kobayashi, U. Andrae, M. A. Balmaseda, G. Balsamo, P. Bauer, P. Bechtold, A. C. M. Beljaars, L. van de Berg, J. Bidlot, N. Bormann, C. Delsol, R. Dragani, M. Fuentes, A. J. Geer, L. Haimberger, S. B. Healy, H. Hersbach, E. V Hólm, L. Isaksen, P. Kållberg, M. Köhler, M. Matricardi, A. P. McNally, B. M. Monge-Sanz, J. J. Morcrette, B.-K. Park, C. Peubey, P. de Rosnay, C. Tavolato, J.-N. Thépaut, and F. Vitart (2011), The ERA-Interim reanalysis: configuration and performance of the data assimilation system, *Q. J. R. Meteorol. Soc.*, *137*(656), 553–597, doi:10.1002/qj.828.

Dezfuli, A. (2017), *Climate of Western and Central Equatorial Africa*.

Dezfuli, A. K., and S. E. Nicholson (2011), A note on long-term variations of the African easterly jet, *Int. J. Climatol.*, *31*(13), 2049–2054, doi:10.1002/joc.2209.

Dezfuli, A. K., and S. E. Nicholson (2013), The relationship of rainfall variability in western equatorial africa to the tropical oceans and atmospheric circulation. Part II: The boreal autumn, *J. Clim.*, *26*(1), 66–84, doi:10.1175/JCLI-D-11-00686.1.

Dezfuli, A. K., B. F. Zaitchik, and A. Gnanadesikan (2015), Regional atmospheric circulation and rainfall variability in south equatorial Africa, *J. Clim.*, *28*(2), 809–818, doi:10.1175/JCLI-D-14-00333.1.

Diedhiou, A., A. Bichet, R. Wartenburger, S. I. Seneviratne, D. P. Rowell, M. B. Sylla, I. Diallo, S. Todzo, N. E. Touré, M. Camara, B. N. Ngatchah, N. A. Kane, L. Tall, and F. Affholder (2018), Changes in climate extremes over West and Central Africa at 1.5°C and 2°C global warming, *Environ. Res. Lett.*, *(in press)*, doi:10.1088/1748-9326/aac3e5.

Diem, J. E., S. J. Ryan, J. Hartter, and M. W. Palace (2014), Satellite-based rainfall

data reveal a recent drying trend in central equatorial Africa, *Clim. Change*, *126*(1–2), 263–272, doi:10.1007/s10584-014-1217-x.

Dieppois, B., M. Rouault, and M. New (2015), The impact of ENSO on Southern African rainfall in CMIP5 ocean atmosphere coupled climate models, *Clim. Dyn.*, *45*(9–10), 2425–2442, doi:10.1007/s00382-015-2480-x.

DiNezio, P. N., G. A. Vecchi, and A. C. Clement (2013), Detectability of changes in the walker circulation in response to global warming, *J. Clim.*, *26*(12), 4038–4048, doi:10.1175/JCLI-D-12-00531.1.

Dong, B., J. M. Gregory, and R. T. Sutton (2009), Undestanding land-sea warming contrast in response to increasing greenhouse gases. Part I: Transient adjustment, *J. Clim.*, *22*(11), 3079–3097, doi:10.1175/2009JCLI2652.1.

Donner, L. J., B. L. Wyman, R. S. Hemler, L. W. Horowitz, Y. Ming, M. Zhao, J. C. Golaz, P. Ginoux, S. J. Lin, M. D. Schwarzkopf, J. Austin, G. Alaka, W. F. Cooke, T. L. Delworth, S. M. Freidenreich, C. T. Gordon, S. M. Griffies, I. M. Held, W. J. Hurlin, S. a. Klein, T. R. Knutson, A. R. Langenhorst, H. C. Lee, Y. Lin, B. I. Magi, S. L. Malyshev, P. C. D. Milly, V. Naik, M. J. Nath, R. Pincus, J. J. Ploshay, V. Ramaswamy, C. J. Seman, E. Shevliakova, J. J. Sirutis, W. F. Stern, R. J. Stouffer, R. J. Wilson, M. Winton, A. T. Wittenberg, and F. Zeng (2011), The dynamical core, physical parameterizations, and basic simulation characteristics of the atmospheric component AM3 of the GFDL global coupled model CM3, *J. Clim.*, *24*(13), 3484–3519, doi:10.1175/2011JCLI3955.1.

Druyan, L. M., and T. M. Hall (1996), The sensitivity of African wave disturbances to remote forcing, *J. Appl. Meteorol.*, *35*(7), 1100–1110, doi:10.1175/1520-0450(1996)035<1100:TSOAWD>2.0.CO;2.

Dufresne, J. L., M. a. Foujols, S. Denvil, A. Caubel, O. Marti, O. Aumont, Y. Balkanski,

S. Bekki, H. Bellenger, R. Benshila, S. Bony, L. Bopp, P. Braconnot, P. Brockmann, P. Cadule, F. Cheruy, F. Codron, A. Cozic, D. Cugnet, N. de Noblet, J. P. Duvel, C. Eth??, L. Fairhead, T. Fichefet, S. Flavoni, P. Friedlingstein, J. Y. Grandpeix, L. Guez, E. Guilyardi, D. Hauglustaine, F. Hourdin, A. Idelkadi, J. Ghattas, S. Joussaume, M. Kageyama, G. Krinner, S. Labetoulle, A. Lahellec, M. P. Lefebvre, F. Lefevre, C. Levy, Z. X. Li, J. Lloyd, F. Lott, G. Madec, M. Mancip, M. Marchand, S. Masson, Y. Meurdesoif, J. Mignot, I. Musat, S. Parouty, J. Polcher, C. Rio, M. Schulz, D. Swingedouw, S. Szopa, C. Talandier, P. Terray, N. Viovy, and N. Vuichard (2013), Climate change projections using the IPSL-CM5 Earth System Model: From CMIP3 to CMIP5, *Clim. Dyn.*, *40*(9–10), 2123–2165, doi:10.1007/s00382-012-1636-1.

Dunne, J. P., J. G. John, S. Shevliakova, R. J. Stouffer, J. P. Krasting, S. L. Malyshev, P. C. D. Milly, L. T. Sentman, A. J. Adcroft, W. Cooke, K. a. Dunne, S. M. Griffies, R. W. Hallberg, M. J. Harrison, H. Levy, A. T. Wittenberg, P. J. Phillips, and N. Zadeh (2013), GFDL's ESM2 global coupled climate-carbon earth system models. Part II: Carbon system formulation and baseline simulation characteristics, *J. Clim.*, *26*(7), 2247–2267, doi:10.1175/JCLI-D-12-00150.1.

Dunning, C. M., R. P. Allan, and E. Black (2017), Identification of deficiencies in seasonal rainfall simulated by CMIP5 climate models, *Environ. Res. Lett.*, *12*(11), doi:10.1088/1748-9326/aa869e.

Durack, P. J., S. E. Wijffels, and R. J. Matear (2012), Ocean Salinities Reveal Strong Global Water Cycle Intensification During 1950 to 2000, *Science (80-.).*, *336*(April), 455–458, doi:10.1126/science.1212222.

Dyer, E. L. E., D. B. A. Jones, J. Nusbaumer, H. Li, O. Collins, G. Vettoretti, and D. Noone (2017), Congo Basin precipitation: Assessing seasonality, regional

interactions, and sources of moisture, *J. Geophys. Res.*, *122*(13), 6882–6898, doi:10.1002/2016JD026240.

Easterbrook, S. (2012), Some CMIP5 statistics, Available from: http://www.easterbrook.ca/steve/2012/04/some-cmip5-statistics/ (Accessed 23 August 2018)

Eichhorn, A., and J. Bader (2016), Impact of tropical Atlantic sea-surface temperature biases on the simulated atmospheric circulation and precipitation over the Atlantic region: An ECHAM6 model study, *Clim. Dyn.*, *49*(5), 1–15, doi:10.1007/s00382-016-3415-x.

Endo, S., and T. Tozuka (2015), Two flavors of the Indian Ocean Dipole, *Clim. Dyn.*, *46*(April), 3371–3385, doi:10.1007/s00382-015-2773-0.

Engelbrecht, F., J. Adegoke, M. J. Bopape, M. Naidoo, R. Garland, M. Thatcher, J. McGregor, J. Katzfey, M. Werner, C. Ichoku, and C. Gatebe (2015), Projections of rapidly rising surface temperatures over Africa under low mitigation, *Environ. Res. Lett.*, *10*(8), doi:10.1088/1748-9326/10/8/085004.

Van Der Ent, R. J., H. H. G. Savenije, B. Schaefli, and S. C. Steele-Dunne (2010), Origin and fate of atmospheric moisture over continents, *Water Resour. Res.*, *46*(9), 1–12, doi:10.1029/2010WR009127.

Ernst, C., M. Philippe, V. Astrid, B. Catherine, C. Musampa, and D. Pierre (2013), National forest cover change in Congo Basin: Deforestation, reforestation, degradation and regeneration for the years 1990, 2000 and 2005, *Glob. Chang. Biol.*, *19*(4), 1173–1187, doi:10.1111/gcb.12092.

FAO (2011), *The State of Forests in the Amazon Basin, Congo Basin and Southeast Asia*.

Farnsworth, A., E. White, C. J. R. Williams, E. Black, and D. R. Kniveton (2011),

Understanding the Large Scale Driving Mechanisms of Rainfall Variability over Central Africa, in *African Climate and Climate Change*.

Fink, A. H. (2003), Spatiotemporal variability of the relation between African Easterly Waves and West African Squall Lines in 1998 and 1999, *J. Geophys. Res.*, *108*(D11), 4332, doi:10.1029/2002JD002816.

Flato, G., J. Marotzke, B. Abiodun, P. Braconnot, S. C. Chou, W. Collins, P. Cox, F. Driouech, S. Emori, V. Eyring, C. Forest, P. Gleckler, E. Guilyardi, C. Jakob, V. Kattsov, C. Reason, and M. Rummukainen (2013), Evaluation of Climate Models, in *Climate Change 2013: The Physical Science Basis. Contribution of Working Group I to the Fifth Assessment Report of the Intergovernmental Panel on Climate Change*, edited by T. F. Stocker, D. Qin, G.-K. Plattner, M. Tignor, S. K. Allen, J. Boschung, A. Nauels, Y. Xia, V. Bex, and P. M. Midgley, pp. 741–866, Cambridge University Press, Cambridge, United Kingdom and New York, NY, USA.

Flato, G. M. (2011), Earth system models: An overview, *Wiley Interdiscip. Rev. Clim. Chang.*, *2*(6), 783–800, doi:10.1002/wcc.148.

Folland, C. K., T. N. Palmer, and D. E. Parker (1986), Sahel rainfall and worldwide sea temperatures, 1901-85, *Nature*, *320*, 602–607, doi:10.1038/320602a0.

Fontaine, B., S. Janicot, and V. Moron (1995), Rainfall anomaly patterns and wind field signals over West Africa in August (1958-1989), *J. Clim.*, *8*(6), 1503–1510, doi:10.1175/1520-0442(1995)008%3C1503:RAPAWF%3E2.0.CO;2.

Fotso-Nguemo, T. C., R. Chamani, Z. D. Yepdo, D. Sonkoué, C. N. Matsaguim, D. A. Vondou, and R. S. Tanessong (2018), Projected trends of extreme rainfall events from CMIP5 models over Central Africa, *Atmos. Sci. Lett.*, *19*(2), 1–8, doi:10.1002/asl.803.

Fowler, H. J., S. Blenkinsop, and C. Tebaldi (2007), Linking climate change modelling to impacts studies: recent advances in downscaling techniques for hydrological modelling H., *Int. J. Climatol.*, *27*, 1547–1578, doi:10.1002/joc.1556.

Frierson, D. M. W., J. Lu, and G. Chen (2007), Width of the Hadley cell in simple and comprehensive general circulation models, *Geophys. Res. Lett.*, *34*(18), 1–5, doi:10.1029/2007GL031115.

Fuller, T. L., P. R. Sesink Clee, K. Y. Njabo, A. Tróchez, K. Morgan, D. B. Meñe, N. M. Anthony, M. K. Gonder, W. R. Allen, R. Hanna, and T. B. Smith (2018), Climate warming causes declines in crop yields and lowers school attendance rates in Central Africa, *Sci. Total Environ.*, *610–611*, 503–510, doi:10.1016/j.scitotenv.2017.08.041.

Funk, C., S. E. Nicholson, M. Landsfeld, D. Klotter, P. Peterson, and L. Harrison (2015), The Centennial Trends Greater Horn of Africa precipitation dataset, *Sci. Data*, *5*, doi:10.1038/sdata.2018.121.

Gent, P. R., G. Danabasoglu, L. J. Donner, M. M. Holland, E. C. Hunke, S. R. Jayne, D. M. Lawrence, R. B. Neale, P. J. Rasch, M. Vertenstein, P. H. Worley, Z. L. Yang, and M. Zhang (2011), The community climate system model version 4, *J. Clim.*, *24*(19), 4973–4991, doi:10.1175/2011JCLI4083.1.

Giannini, A., M. Biasutti, I. M. Held, and A. H. Sobel (2008), A global perspective on African climate, *Clim. Change*, *90*(4), 359–383, doi:10.1007/s10584-008-9396-y.

Giannini, A., B. Lyon, R. Seager, and N. Vigaud (2018), Dynamical and thermodynamic elements of modeled climate change at the East African margin of convection, *Geophys. Res. Lett.*, 992–1000,

doi:10.1002/2017GL075486.

Giorgi, F., C. Jones, and G. R. Asrar (2009), Addressing climate information needs at the regional level: the CORDEX framework, *Bull. - World Meteorol. Organ.*, *58*(3), 175–183.

Gleckler, P. J., K. E. Taylor, and C. Doutriaux (2008), Performance metrics for climate models, *J. Geophys. Res. Atmos.*, *113*(6), 1–20, doi:10.1029/2007JD008972.

Goddard, L., and N. E. Graham (1999), Importance of the Indian Ocean for simulating rainfall anomalies over eastern and southern Africa, *J. Geophys. Res.*, *104*, 19099, doi:10.1029/1999JD900326.

Grist, J. P., and S. Nicholson (2001), A Study of the Dynamic Factors Influencing the Rainfall Variability in the West African Sahel, *J. Clim.*, *14*(7), 1337–1359, doi:10.1175/1520-0442(2001)014<1337:ASOTDF>2.0.CO;2.

Grist, J. P., S. E. Nicholson, and A. I. Barcilon (2002), Easterly Waves over Africa. Part II: Observed and Modeled Contrasts between Wet and Dry Years, *Mon. Weather Rev.*, *130*(2), 212–225, doi:10.1175/1520-0493(2002)130<0212:EWOAPI>2.0.CO;2.

Guilyardi, E., A. Wittenberg, A. Fedorov, M. Collins, C. Wang, A. Capotondi, G. J. van Oldenborgh, and T. Stockdale (2009), Understanding El Niño in ocean-atmosphere general circulation models: Progress and challenges, *Bull. Am. Meteorol. Soc.*, *90*(3), 325–340, doi:10.1175/2008BAMS2387.1.

Gulizia, C., and I. Camilloni (2014), Comparative analysis of the ability of a set of CMIP3 and CMIP5 global climate models to represent precipitation in South America, *Int. J. Climatol.*, *35*(4), 583–595, doi:10.1002/joc.4005.

Haensler, A., F. Saeed, and D. Jacob (2013a), Assessing the robustness of projected

precipitation changes over central Africa on the basis of a multitude of global and regional climate projections, *Clim. Change*, *121*(2), 349–363, doi:10.1007/s10584-013-0863-8.

Haensler, A., D. Jacob, P. Kabat, and F. Ludwig (2013b), Assessment of projected climate change signals over central Africa based on a multitude of global and regional climate projections, in *Climate Change Scenarios for the Congo Basin*, Climate Service Center Report 11.

Haensler, A., F. Saeed, and D. Jacob (2013c), SUPP MAT Assessing the robustness of projected precipitation changes over central Africa on the basis of a multitude of global and regional climate projections, *Clim. Change*, *121*(2), 349–363, doi:10.1007/s10584-013-0863-8.

Hagedorn, R., F. J. Doblas-Reyes, and T. N. Palmer (2005), The rationale behind the success of multimodel ensembles in seasonal forecasting—I. Basic concept, *Tellus A Dyn. Meteorol. Oceanogr.*, *57*(3), 219–233, doi:10.1111/j.1600-0870.2005.00103.x.

Hamududu, B., and A. Killingtveit (2012), Assessing climate change impacts on global hydropower, *Energies*, *5*(2), 305–322, doi:10.3390/en5020305.

Hansen, J., M. Sato, and R. Ruedy (1997), Radiative forcing and climate response, , *102*, 6831–6864.

Hansingo, K., and C. J. C. Reason (2009), Modelling the atmospheric response over southern Africa to SST forcing in the southeast tropical Atlantic and southwest subtropical Indian Oceans, *Int. J. Climatol.*, *29*, 1001–1012, doi:10.1002/joc.

Harris, I., P. D. Jones, T. J. Osborn, and D. H. Lister (2014), Updated high-resolution grids of monthly climatic observations - the CRU TS3.10 Dataset, *Int. J. Climatol.*, *34*(3), 623–642, doi:10.1002/joc.3711.

Hart, N. C. G., and R. Washington (n.d.), Convective Outbreaks in the African rainbelt: Hotspots, Variability and Change,

Hart, N. C. G., C. J. C. Reason, and N. Fauchereau (2013), Cloud bands over southern Africa: Seasonality, contribution to rainfall variability and modulation by the MJO, *Clim. Dyn.*, *41*(5–6), 1199–1212, doi:10.1007/s00382-012-1589-4.

Hastenrath, S. (2000), Zonal circulations over the equatorial Indian Ocean, *J. Clim.*, *13*(15), 2746–2756, doi:10.1175/1520-0442(2000)013<2746:ZCOTEI>2.0.CO;2.

Hazeleger, W., C. Severijns, T. Semmler, S. Ştefănescu, S. Yang, X. Wang, K. Wyser, E. Dutra, J. M. Baldasano, R. Bintanja, P. Bougeault, R. Caballero, A. M. L. Ekman, J. H. Christensen, B. Van Den Hurk, P. Jimenez, C. Jones, P. Kållberg, T. Koenigk, R. McGrath, P. Miranda, T. Van Noije, T. Palmer, J. a. Parodi, T. Schmith, F. Selten, T. Storelvmo, A. Sterl, H. Tapamo, M. Vancoppenolle, P. Viterbo, and U. Willén (2010), EC-Earth: A seamless Earth-system prediction approach in action, *Bull. Am. Meteorol. Soc.*, *91*(10), 1357–1363, doi:10.1175/2010BAMS2877.1.

Heavens, N. G., D. S. Ward, and M. M. Natalie (2013), Studying and Projecting Climate Change with Earth System Models, *Nat. Educ. Knowl.*, *4*(5), 4.

Hegerl, G. C., E. Black, R. P. Allan, W. J. Ingram, D. Polson, K. E. Trenberth, R. S. Chadwick, P. A. Arkin, B. B. Sarojini, A. Becker, A. Dai, P. J. Durack, D. Easterling, H. J. Fowler, E. J. Kendon, G. J. Huffman, C. Liu, R. Marsh, M. New, T. J. Osborn, N. Skliris, P. A. Stott, P.-L. Vidale, S. E. Wijffels, L. J. Wilcox, K. M. Willett, and X. Zhang (2015), Challenges in Quantifying Changes in the Global Water Cycle, , (August), 1097–1116.

Held, I. M., and A. Y. Hou (1980), Nonlinear Axially Symmetric Circulations in a Nearly Inviscid Atmosphere, *J. Atmos. Sci.*, *37*(3), 515–533, doi:10.1175/1520-

0469(1980)037<0515:NASCIA>2.0.CO;2.

Held, I. M., and B. Soden (2006), Robust responses of the hydrological cycle to global warming, *J. Clim.*, *19*(21), 5686–5699, doi:10.1175/2010JCLI4045.1.

Held, I. M., T. L. Delworth, J. Lu, K. L. Findell, and T. R. Knutson (2005), Simulation of Sahel drought in the 20th and 21st centuries, *Proc. Natl. Acad. Sci. United States Am.*, *102*, 17891–17896.

Henderson, S. A., E. D. Maloney, and S. W. Son (2017), Madden-Julian oscillation Pacific teleconnections: The impact of the basic state and MJO representation in general circulation models, *J. Clim.*, *30*(12), 4567–4587, doi:10.1175/JCLI-D-16-0789.1.

Hirons, L., and A. Turner (2018), The impact of Indian Ocean mean-state biases on the representation of the East African short rains, *J. Clim.*, *in press.*, doi:10.1175/JCLI-D-17-0804.1.

Hirst, A. C., and S. Hastenrath (1983a), Atmosphere-Ocean Mechanisms of Climate Anomalies in the Angola-Tropical Atlantic Sector, *J. Phys. Oceanogr.*, *13*(7), 1146–1157, doi:10.1175/1520-0485(1983)013<1146:AOMOCA>2.0.CO;2.

Hirst, A. C., and S. Hastenrath (1983b), Atmosphere-Ocean Mechanisms of Climate Anomalies in the Angola-Tropical Atlantic Sector, *J. Phys. Oceanogr.*, *13*(7), 1146–1157, doi:10.1175/1520-0485(1983)013<1146:AOMOCA>2.0.CO;2.

Hoerling, M., J. Hurrell, J. Eischeid, and A. Phillips (2006), Detection and attribution of twentieth-century northern and southern African rainfall change, *J. Clim.*, *19*(16), 3989–4008, doi:10.1175/JCLI3842.1.

Houze, R. A. J. (2004a), Mesoscale Convective Systems, *Rev. Geophys.*, *42*, 1–43, doi:10.1029/2004RG000150.1.INTRODUCTION.

Houze, R. A. J. (2004b), Mesoscale Convective Systems, *Rev. Geophys.*, *42*, 1–43,

doi:10.1029/2004RG000150.1.INTRODUCTION.

Howard, E., and R. Washington (2018), Characterizing the Synoptic Expression of the Angola Low, *J. Clim.*, *31*(17), 7147–7166, doi:10.1175/JCLI-D-18-0017.1.

Hu, Y., and Q. Fu (2007), Observed poleward expansion of the Hadley circulation since 1979, *Atmos. Chem. Phys.*, *7*(19), 5229–5236, doi:10.5194/acp-7-5229-2007.

Hua, W., L. Zhou, H. Chen, A. Nicholson, Sharon E. Raghavendra, and Y. Jiang (2016), Possible causes of the Central Equatorial African long-term drought, *Environ. Res. Lett.*, *accpeted f*(12), 1–13, doi:10.1088/1748-9326/11/12/124002.

Hua, W., L. Zhou, H. Chen, S. E. Nicholson, Y. Jiang, and A. Raghavendra (2018), Understanding the Central Equatorial African long-term drought using AMIP-type simulations, *Clim. Dyn.*, *50*(3–4), 1115–1128, doi:10.1007/s00382-017-3665-2.

Huang, P., S. P. Xie, K. Hu, G. Huang, and R. Huang (2013), Patterns of the seasonal response of tropical rainfall to global warming, *Nat. Geosci.*, *6*(5), 357–361, doi:10.1038/ngeo1792.

Huang, Y., W. L. Chameides, and R. E. Dickinson (2007), Direct and indirect effects of anthropogenic aerosols on regional precipitation over east Asia, *J. Geophys. Res. Atmos.*, *112*(3), 1–17, doi:10.1029/2006JD007114.

Huffman, G. J., D. T. Bolvin, E. J. Nelkin, D. B. Wolff, R. F. Adler, G. Gu, Y. Hong, K. P. Bowman, and E. F. Stocker (2007), The TRMM Multisatellite Precipitation Analysis (TMPA): Quasi-Global, Multiyear, Combined-Sensor Precipitation Estimates at Fine Scales, *J. Hydrometeorol.*, *8*(1), 38–55, doi:10.1175/JHM560.1.

Jackson, B., S. E. Nicholson, and D. Klotter (2009), Mesoscale Convective Systems

over Western Equatorial Africa and Their Relationship to Large-Scale Circulation, *Mon. Weather Rev.*, *137*(4), 1272–1294, doi:10.1175/2008MWR2525.1.

James, R., and R. Washington (2013), Changes in African temperature and precipitation associated with degrees of global warming, *Clim. Change*, *117*(4), 859–872, doi:10.1007/s10584-012-0581-7.

James, R., R. Washington, and D. P. Rowell (2013), Implications of global warming for the climate of African rainforests, *Philos. Trans. R. Soc. Lond. B. Biol. Sci.*, *368*, 20120298.

James, R., R. Washington, and R. Jones (2015), Process-based assessment of an ensemble of climate projections for West Africa, *J. Geophys. Res.*, *120*(4), 1221–1238, doi:10.1002/2014JD022513.

James, R., R. Washington, B. Abiodun, G. Kay, J. Mutemi, W. Pokam, N. Hart, G. Artan, and C. Senior (2018), Evaluating climate models with an African lens, *Bull. Am. Meteorol. Soc.*, BAMS-D-16-0090.1, doi:10.1175/BAMS-D-16-0090.1.

Jeffrey, S. J., L. D. Rotstayn, M. A. Collier, S. M. Dravitzki, C. Hamalainen, C. Moeseneder, K. K. Wong, and J. I. Syktus (2013), Australia's CMIP5 submission using the CSIRO Mk3.6 model, *Aust. Meteorol. Oceanogr. J.*, *63*, 1–13, doi:10.22499/2.6301.001.

Ji, D., L. Wang, J. Feng, Q. Wu, H. Cheng, Q. Zhang, J. Yang, W. Dong, Y. Dai, D. Gong, R. H. Zhang, X. Wang, J. Liu, J. C. Moore, D. Chen, and M. Zhou (2014), Description and basic evaluation of Beijing Normal University Earth System Model (BNU-ESM) version 1, *Geosci. Model Dev.*, *7*(5), 2039–2064, doi:10.5194/gmd-7-2039-2014.

Jiang, J. H., H. Su, C. Zhai, V. S. Perun, A. Del Genio, L. S. Nazarenko, L. J. Donner, L.

Horowitz, C. Seman, J. Cole, A. Gettelman, M. A. Ringer, L. Rotstayn, S. Jeffrey, T. Wu, F. Brient, J. L. Dufresne, H. Kawai, T. Koshiro, M. Watanabe, T. S. Lécuyer, E. M. Volodin, T. Iversen, H. Drange, M. D. S. Mesquita, W. G. Read, J. W. Waters, B. Tian, J. Teixeira, and G. L. Stephens (2012), Evaluation of cloud and water vapor simulations in CMIP5 climate models Using NASA "A-Train" satellite observations, *J. Geophys. Res. Atmos.*, *117*(14), doi:10.1029/2011JD017237.

Johanson, C. M., and Q. Fu (2009), Hadley cell widening: Model simulations versus observations, *J. Clim.*, *22*(10), 2713–2725, doi:10.1175/2008JCLI2620.1.

Jones, C. D., J. K. Hughes, N. Bellouin, S. C. Hardiman, G. S. Jones, J. Knight, S. Liddicoat, F. M. O'Connor, R. J. Andres, C. Bell, K. O. Boo, A. Bozzo, N. Butchart, P. Cadule, K. D. Corbin, M. Doutriaux-Boucher, P. Friedlingstein, J. Gornall, L. Gray, P. R. Halloran, G. Hurtt, W. J. Ingram, J. F. Lamarque, R. M. Law, M. Meinshausen, S. Osprey, E. J. Palin, C. Parsons L., T. Raddatz, M. G. Sanderson, A. A. Sellar, A. Schurer, P. Valdes, N. Wood, S. Woodward, M. Yoshioka, and M. Zerroukat (2011), The HadGEM2-ES implementation of CMIP5 centennial simulations, *Geosci. Model Dev.*, *4*(3), 543–570.

Joseph, S., A. K. Sahai, B. N. Goswami, P. Terray, S. Masson, and J. J. Luo (2012), Possible role of warm SST bias in the simulation of boreal summer monsoon in SINTEX-F2 coupled model, *Clim. Dyn.*, *38*(7–8), 1561–1576, doi:10.1007/s00382-011-1264-1.

Jury, M. R., E. Matari, and M. Matitu (2009), Equatorial African climate teleconnections, *Theor. Appl. Climatol.*, *95*, 407–416.

Kalnay, E., M. Kanamitsu, R. Kistler, W. Collins, D. Deaven, L. Gandin, M. Iredell, S. Saha, G. White, J. Woollen, Y. Zhu, M. Chelliah, W. Ebisuzaki, W. Higgins, J. Janowiak, K. C. Mo, C. Ropelewski, J. Wang, a. Leetmaa, R. Reynolds, R. Jenne,

and D. Joseph (1996), The NCEP/NCAR 40-year reanalysis project, *Bull. Am. Meteorol. Soc.*, *77*(3), 437–471, doi:10.1175/1520-0477(1996)077<0437:TNYRP>2.0.CO;2.

Kalognomou, E. A., C. Lennard, M. Shongwe, I. Pinto, A. Favre, M. Kent, B. Hewitson, A. Dosio, G. Nikulin, H. J. Panitz, and M. Büchner (2013), A diagnostic evaluation of precipitation in CORDEX models over Southern Africa, *J. Clim.*, *26*(23), 9477–9506, doi:10.1175/JCLI-D-12-00703.1.

Kanamitsu, M., and T. N. Krishnamurti (1978), Northern Summer Tropical Circulation During Drought and Normal Rainfall Months, *Mon. Weather Rev.*, *106*, 331–347, doi:10.1175/1520-0493(1978)106<0331:NSTCDD>2.0.CO;2.

Kay, G., and R. Washington (2008), Future southern African summer rainfall variability related to a southwest Indian Ocean dipole in HadCM3, *Geophys. Res. Lett.*, *35*(12), L12701, doi:10.1029/2008GL034180.

Kendon, E. J., N. Ban, N. M. Roberts, H. J. Fowler, M. J. Roberts, S. C. Chan, J. P. Evans, G. Fosser, and J. M. Wilkinson (2017), Do convection-permitting regional climate models improve projections of future precipitation change?, *Bull. Am. Meteorol. Soc.*, *98*(1), 79–93, doi:10.1175/BAMS-D-15-0004.1.

Kent, C., R. Chadwick, and D. P. Rowell (2015), Understanding uncertainties in future projections of seasonal tropical precipitation, *J. Clim.*, 150317081728001, doi:10.1175/JCLI-D-14-00613.1.

Kim, D., K. Sperber, W. Stern, D. Waliser, I. S. Kang, E. Maloney, W. Wang, K. Weickmann, J. Benedict, M. Khairoutdinov, M. I. Lee, R. Neale, M. Suarez, K. Thayer-Calder, and G. Zhang (2009), Application of MJO simulation diagnostics to climate models, *J. Clim.*, *22*(23), 6413–6436, doi:10.1175/2009JCLI3063.1.

Kitchell, J. F., D. E. Schindler, R. Ogutu-ohwayo, P. N. Reinthal, S. E. Applications, N. May, I. D. E. Schindler, and I. R. Ogutu-ohwayo (2011), The Nile Perch in Lake Victoria : Interactions Between Predation and Fisheries THE NILE PERCH IN LAKE VICTORIA : INTERACTIONS BETWEEN PREDATION AND FISHERIES, *Ecol. Appl.*, *7*(2), 653–664.

Klein, S. A., Y. Zhang, M. D. Zelinka, R. Pincus, J. Boyle, and P. J. Gleckler (2013), Are climate model simulations of clouds improving? An evaluation using the ISCCP simulator, *J. Geophys. Res. Atmos.*, *118*(3), 1329–1342, doi:10.1002/jgrd.50141.

Knutti, R. (2010), The end of model democracy?, *Clim. Change*, *102*(3), 395–404, doi:10.1007/s10584-010-9800-2.

Knutti, R., R. Furrer, C. Tebaldi, J. Cermak, and G. A. Meehl (2010), Challenges in combining projections from multiple climate models, *J. Clim.*, *23*(10), 2739–2758, doi:10.1175/2009JCLI3361.1.

Knutti, R., J. Sedláček, B. M. Sanderson, R. Lorenz, E. M. Fischer, and V. Eyring (2017), A climate model projection weighting scheme accounting for performance and interdependence, *Geophys. Res. Lett.*, *44*(4), 1909–1918, doi:10.1002/2016GL072012.

Kotir, J. H. (2011), Climate change and variability in Sub-Saharan Africa: A review of current and future trends and impacts on agriculture and food security, *Environ. Dev. Sustain.*, *13*(3), 587–605, doi:10.1007/s10668-010-9278-0.

Lafon, T., S. Dadson, G. Buys, and C. Prudhomme (2013), Bias correction of daily precipitation simulated by a regional climate model: A comparison of methods, *Int. J. Climatol.*, *33*(6), 1367–1381, doi:10.1002/joc.3518.

Laing, A. G., and J. L. Evans (2015), Introduction to Tropical Meteorology, Available

from:
http://ftp.comet.ucar.edu/ootw/tropical/textbook_2nd_edition/index.htm (Accessed 16 August 2018)

Laing, A. G., R. E. Carbone, and V. Levizzani (2011), Cycles and Propagation of Deep Convection over Equatorial Africa, *Mon. Weather Rev.*, *139*(9), 2832–2853, doi:10.1175/2011MWR3500.1.

Laraque, A., G. Mahe, D. Orange, and B. Marieu (2001), Spatio-temporal variations in hydrological regimes within Central Africa during XXth Century, *J. Hydrol.*, *245*, 104–117.

Large, W. G., and G. Danabasoglu (2006), Attribution and impacts of upper-ocean biases in CCSM3, *J. Clim.*, *19*(11), 2325–2346, doi:10.1175/JCLI3740.1.

Lau, K. M., S. S. P. Shen, K.-M. Kim, and H. Wang (2006), A multimodel study of the twentieth-century simulations of Sahel drought from the 1970s to 1990s., *J. Geophys. Res.*, *111*(D7), D07111, doi:10.1029/2005JD006281.

Lawrence, D., and K. Vandecar (2015), Effects of tropical deforestation on climate and agriculture, *Nat. Clim. Chang.*, *5*(1), 27–36, doi:10.1038/nclimate2430.

Lazenby, M. J., M. C. Todd, and Y. Wang (2016), Climate model simulation of the South Indian Ocean Convergence Zone: mean state and variability, *Clim. Res.*, *68*(1), 59–71, doi:10.3354/cr01382.

Lazenby, M. J., M. C. Todd, R. Chadwick, and Y. Wang (2018), Future precipitation projections over central and southern Africa and the adjacent Indian Ocean: What causes the changes and the uncertainty?, *J. Clim.*, JCLI-D-17-0311.1, doi:10.1175/JCLI-D-17-0311.1.

Leduc, M., R. Laprise, R. de Elï¿½a, and L. Šeparović (2016), Is institutional democracy a good proxy for model independence?, *J. Clim.*, *29*(23), 8301–

8316, doi:10.1175/JCLI-D-15-0761.1.

Levin, N. E., E. J. Zipser, and T. E. Ceding (2009), Isotopic composition of waters from Ethiopia and Kenya: Insights into moisture sources for eastern Africa, *J. Geophys. Res. Atmos.*, *114*(23), 1–13, doi:10.1029/2009JD012166.

Lewis, S. L., G. Lopez-Gonzalez, B. Sonké, K. Affum-Baffoe, T. R. Baker, L. O. Ojo, O. L. Phillips, J. M. Reitsma, L. White, J. A. Comiskey, M.-N. Djuikouo K, C. E. N. Ewango, T. R. Feldpausch, A. C. Hamilton, M. Gloor, T. Hart, A. Hladik, J. Lloyd, J. C. Lovett, J.-R. Makana, Y. Malhi, F. M. Mbago, H. J. Ndangalasi, J. Peacock, K. S.-H. Peh, D. Sheil, T. Sunderland, M. D. Swaine, J. Taplin, D. Taylor, S. C. Thomas, R. Votere, and H. Wöll (2009), Increasing carbon storage in intact African tropical forests, *Nature*, *457*, 1003–1006.

Li, L. J., P. Lin, Y. Yu, B. Wang, T. Zhou, L. Liu, J. Liu, Q. Bao, S. Zu, W. Huang, K. Xia, Y. Pu, L. Dong, S. Shen, Y. Liu, N. Hu, M. Liu, W. Sun, X. Shi, W. Zheng, B. Wu, M. Song, H. Liu, X. Zhang, G. Wu, W. Xue, K. Huang, G. Yang, Z. Song, and F. Qiao (2013), The Flexible Global Ocean-Atmosphere-Land System Model, Grid-point Version 2: FGOALS-g2, *Adv. Atmos. Sci.*, *30*(3), 543–560, doi:10.1007/s00376-012-2140-6.

Liebmann, B., M. P. Hoerling, C. Funk, I. Bladé, R. M. Dole, D. Allured, X. Quan, P. Pegion, and J. K. Eischeid (2014), Understanding recent eastern Horn of Africa rainfall variability and change, *J. Clim.*, *27*(23), 8630–8645, doi:10.1175/JCLI-D-13-00714.1.

Lindesay, J. A. (1988), South African rainfall, the Southern Oscillation and a Southern Hemisphere semi-annual cycle, *J. Climatol.*, *8*(1), 17–30, doi:10.1002/joc.3370080103.

Liu, C., and E. J. Zipser (2005), Global distribution of convection penetrating the

tropical tropopause, *J. Geophys. Res. Atmos.*, *110*(23), 1–12, doi:10.1029/2005JD006063.

Lohmann, U., and J. Feichter (2004), Global indirect aerosol effects: a review, *Atmos. Chem. Phys. Discuss.*, *4*(6), 7561–7614, doi:10.5194/acpd-4-7561-2004.

Longandjo, G.-N. T. (2017), The Hydroclimate Variability of Central Africa: seasonal cycle, mechanisms, teleconnections and impacts on neighbouring regions, University of Cape Town.

Lu, J., G. A. Vecchi, and T. Reichler (2007), Expansion of the Headley cell under global warming, *Geophys. Res. Lett.*, *34*(6), L06805, doi:10.1029/2006GL028443.

Lyon, B., and D. G. Dewitt (2012), A recent and abrupt decline in the East African long rains, *Geophys. Res. Lett.*, *39*(2), 1–5, doi:10.1029/2011GL050337.

Ma, J., and S. P. Xie (2013), Regional Patterns of Sea Surface Temperature Change: A Source of Uncertainty in Future Projections of Precipitation and Atmospheric Circulation, *J. Clim.*, *26*(8), 2482–2501, doi:10.1175/JCLI-D-12-00283.1.

Ma, J., S. P. Xie, and Y. Kosaka (2012), Mechanisms for tropical tropospheric circulation change in response to global warming, *J. Clim.*, *25*(8), 2979–2994, doi:10.1175/JCLI-D-11-00048.1.

Ma, J., R. Chadwick, K.-H. Seo, C. Dong, G. Huang, G. R. Foltz, and J. H. Jiang (2018), Responses of the Tropical Atmospheric Circulation to Climate Change and Connection to the Hydrological Cycle, *Annu. Rev. Earth Planet. Sci.*, *46*(1), annurev-earth-082517-010102, doi:10.1146/annurev-earth-082517-010102.

Maidment, R. I., D. Grimes, R. P. Allan, E. Tarnavsky, M. Stringer, T. Hewison, R. Roebeling, and E. Black (2014), The 30 year TAMSAT African Rainfall Climatology And Time series (TARCAT) data set, *J. Geophys. Res. Atmos.*,

119(18), 10619–10644, doi:10.1002/2014JD021927.

Malhi, Yadvinder, S. Adu-bredu, R. A. Asare, S. L. Lewis, P. Mayaux, P. T. R. S. B, Y. Malhi, S. Adu-bredu, R. A. Asare, S. L. Lewis, and P. Mayaux (2013), African rainforests : past , present and future, *Philos. Trans. R. Soc. London B Biol. Sci.*, *368*(1625), doi:10.1098/rstb.2012.0312.

Malhi, Y., and J. Wright (2004), Spatial patterns and recent trends in the climate of tropical rainforest regions, *Philos. Trans. R. Soc. B Biol. Sci.*, *359*(1443), 311–329, doi:10.1098/rstb.2003.1433.

Markowski, P., and Y. Richardson (2011), *Mesoscale meteorology in midlatitudes (Vol. 2)*, John Wiley & Sons, Ltd., Hoboken, NJ.

Marsland, S. J., H. Haak, J. H. Jungclaus, M. Latif, and F. Roske (2003), The Max-Planck-Institute global ocean/sea ice model with orthogonal curvilinear coordinates, *Ocean Model.*, *5*(2), 91–127, doi:10.1016/S1463-5003(02)00015-X.

Martin, E. R., and C. Thorncroft (2015), Representation of African easterly waves in CMIP5 models, *J. Clim.*, *28*(19), 7702–7715, doi:10.1175/JCLI-D-15-0145.1.

Masson, D., and R. Knutti (2011), Climate model genealogy, *Geophys. Res. Lett.*, *38*(8), 1–4, doi:10.1029/2011GL046864.

Mayaux, P., J. F. Pekel, B. Desclée, F. Donnay, A. Lupi, F. Achard, M. Clerici, C. Bodart, A. Brink, R. Nasi, and A. Belward (2013), State and evolution of the African rainforests between 1990 and 2010, *Philos. Trans. R. Soc. B Biol. Sci.*, *368*(1625), doi:10.1098/rstb.2012.0300.

Maynard, K., and J. F. Royer (2004), Sensitivity of a general circulation model to land surface parameters in African tropical deforestation experiments, *Clim. Dyn.*, *22*(6–7), 555–572, doi:10.1007/s00382-004-0398-9.

McCollum, J. R., A. Gruber, and M. B. Ba (2000), Discrepancy between Gauges and Satellite Estimates of Rainfall in Equatorial Africa, *J. Appl. Meteorol.*, *39*(5), 666–679, doi:10.1175/1520-0450-39.5.666.

McSweeney, C. F., R. G. Jones, R. W. Lee, and D. P. Rowell (2014), Selecting CMIP5 GCMs for downscaling over multiple regions, *Clim. Dyn.*

Meehl, G. A., T. F. Stocker, W. D. Collins, P. Friedlingstein, A. T. Gaye, J. M. Gregory, A. Kitoh, R. Knutti, J. M. Murphy, A. Noda, S. C. B. Raper, I. G. Watterson, A. J. Weaver, and Z.-C. Zhao (2007a), Global Climate Projections, *Clim. Chang. 2007 Contrib. Work. Gr. I to Fourth Assess. Rep. Intergov. Panel Clim. Chang.*, 747–846, doi:10.1080/07341510601092191.

Meehl, G. A., T. F. Stocker, W. D. Collins, P. Friedlingstein, A. T. Gaye, J. M. Gregory, A. Kitoh, R. Knutti, J. M. Murphy, A. Noda, S. C. B. Raper, I. G. Watterson, A. J. Weaver, and Z.-C. Zhao (2007b), Global Climate Projections, *Clim. Chang. 2007 Contrib. Work. Gr. I to Fourth Assess. Rep. Intergov. Panel Clim. Chang.*, 747–846, doi:10.1080/07341510601092191.

Megevand, C., A. Mosnier, J. Hourticq, K. Sanders, N. Doetinchem, and C. Streck (2013), *Deforestation Trends in the Congo Basin*.

Mehran, A., A. Aghakouchack, and T. J. Phillips (2015), Evaluation of CMIP5 continental precipitation simulations relative to satellite-based gauge-adjusted observations, *J. Geophys. Res.*, 1695–1707, doi:10.1002/2013JD021152.Received.

Mosnier, A., P. Havlík, M. Obersteiner, K. Aoki, E. Schmid, S. Fritz, I. McCallum, and S. Leduc (2014), Modeling Impact of Development Trajectories and a Global Agreement on Reducing Emissions from Deforestation on Congo Basin Forests by 2030, *Environ. Resour. Econ.*, *57*(4), 505–525, doi:10.1007/s10640-012-

9618-7.

Moufouma-Okia, W., and R. Jones (2014), Resolution dependence in simulating the African hydroclimate with the HadGEM3-RA regional climate model, *Clim. Dyn.*, *44*(3–4), 609–632, doi:10.1007/s00382-014-2322-2.

Munday, C., and R. Washington (2017), Circulation controls on southern African precipitation in coupled models: The role of the Angola Low, *J. Geophys. Res. Atmos.*, *122*(2), 861–877, doi:10.1002/2016JD025736.

Munday, C., and R. Washington (2018), Systematic climate model rainfall biases over southern Africa: links to moisture circulation and topography, *J. Clim.*, JCLI-D-18-0008.1, doi:10.1175/JCLI-D-18-0008.1.

Munzimi, Y. A., M. C. Hansen, B. Adusei, and G. B. Senay (2015), Characterizing Congo basin rainfall and climate using Tropical Rainfall Measuring Mission (TRMM) satellite data and limited rain gauge ground observations, *J. Appl. Meteorol. Climatol.*, *54*(3), 541–555, doi:10.1175/JAMC-D-14-0052.1.

Nagura, M., J. P. Mccreary, and H. Annamalai (2018), Origins of coupled model biases in the Arabian Sea climatological state, *J. Clim.*, *31*(5), 2005–2029, doi:10.1175/JCLI-D-17-0417.1.

Neale, R. B., A. Gettelman, S. Park, C. Chen, P. H. Lauritzen, D. L. Williamson, A. J. Conley, D. Kinnison, D. Marsh, A. K. Smith, F. Vitt, R. Garcia, J. Lamarque, M. Mills, S. Tilmes, H. Morrison, P. Cameron-smith, W. D. Collins, M. J. Iacono, R. C. Easter, X. Liu, S. J. Ghan, P. J. Rasch, and M. a Taylor (2012), Description of the NCAR Community Atmosphere Model (CAM 5.0), *NCAR Tech. Notes*, National Center for Atmospheric Research.

Neelin, J. D., M. Munnich, H. Su, J. E. Meyerson, and C. E. Holloway (2006), Tropical drying trends in global warming models and observations, *Proc. Natl. Acad.*

Sci. U. S. A., *103*, 6110–6115, doi:10.1073/pnas.0601798103.

Nesbitt, S. W., R. Cifelli, and S. a. Rutledge (2006), Storm Morphology and Rainfall Characteristics of TRMM Precipitation Features, *Mon. Weather Rev.*, *134*(10), 2702–2721, doi:10.1175/MWR3200.1.

Neupane, N. (2016), The Congo Basin Zonal Overturning Circulation, *Adv. Atmos. Sci.*, *33*(June), 767–782, doi:10.1007/s00376-015-5190-8.1.

Newell, R. E., and J. W. Kidson (1984), African mean wind changes between sahelian wet and dry periods, *J. Climatol.*, *4*(1), 27–33, doi:10.1002/joc.3370040103.

Ngomanda, A., D. Jolly, I. Bentaleb, A. Chepstow-Lusty, M. Makaya, J. Maley, M. Fontugne, R. Oslisly, and N. Rabenkogo (2007), Lowland rainforest response to hydrological changes during the last 1500 years in Gabon, Western Equatorial Africa, *Quat. Res.*, *67*(3), 411–425, doi:10.1016/j.yqres.2007.01.006.

Nguyen, H., and J. P. Duvel (2008), Synoptic wave perturbations and convective systems over equatorial Africa, *J. Clim.*, *21*(23), 6372–6388, doi:10.1175/2008JCLI2409.1.

Niang, I., O. C. Ruppel, M. a. Abdrabo, A. Essel, C. Lennard, J. Padgham, and P. Urquhart (2014), Africa, in *Climate Change 2014: Impacts, Adaptation and Vulnerability. Part B: Regional Aspects. Contributions of the Working Group II to the Fifth Assessment Report of the Intergovernmental Panel on Climate Change.*, edited by V. R. Barros, C. B. Field, D. J. Dokken, M. D. Mastrandrea, K. J. Mach, T. E. Bilir, M. Chatterjee, K. L. Ebi, Y. O. Estrada, R. C. Genova, B. Girma, and and L. L. W. (eds. . E.S. Kissel, A.N. Levy, S. MacCracken, P.R. Mastrandrea, pp. 1199–1265, Cambridge University Press, Cambridge, United Kingdom and New York,

NY, USA.

Nicholson, S. E. (1980), The Nature of Rainfall Fluctuations in Subtropical West Africa, *Mon. Weather Rev.*, *108*, 473–487, doi:10.1175/1520-0493(1980)108<0473:TNORFI>2.0.CO;2.

Nicholson, S. E. (1986), The Spatial Coherence of African Rainfall Anomalies: Interhemispheric Teleconnections, *J. Appl. Meteorol. Climatol.*, *25*(10), 1365–1381.

Nicholson, S. E. (1997), An Analysis of the Enso Signal in the Tropical Atlantic and Western Indian Oceans, *Int. J. Climatol.*, *17*(4), 345–375, doi:10.1002/(SICI)1097-0088(19970330)17:4<345::AID-JOC127>3.0.CO;2-3.

Nicholson, S. E. (2015), Long-term variability of the East African “short rains” and its links to large-scale factors, *Int. J. Climatol.*, *35*(13), 3979–3990, doi:10.1002/joc.4259.

Nicholson, S. E. (2017a), The ITCZ and the seasonal cycle over equatorial Africa, *Bull. Am. Meteorol. Soc.*, *30*, 337–348, doi:10.1175/BAMS-D-16-0287.1.

Nicholson, S. E. (2017b), Climate and climatic variability of rainfall over eastern Africa, *Rev. Geophys.*, *55*(3), 590–635, doi:10.1002/2016RG000544.

Nicholson, S. E., and A. K. Dezfuli (2013), The relationship of rainfall variability in western equatorial Africa to the tropical oceans and atmospheric circulation. Part I: The boreal spring, *J. Clim.*, *26*(1), 45–65, doi:10.1175/JCLI-D-11-00653.1.

Nicholson, S. E., and D. Entekhabi (1986), The quasi-periodic behavior of rainfall variability in Africa and its relationship to the southern oscillation, *Arch. Meteorol. Geophys. Bioclimatol. Ser. A*, *34*(3–4), 311–348, doi:10.1007/BF02257765.

Nicholson, S. E., and D. Entekhabi (1987), Rainfall Variability in Equatorial and Southern Africa: Relationships with Sea Surface Temperatures along the Southwestern Coast of Africa, *J. Clim. Appl. Meteorol.*, *26*(5), 561–578, doi:10.1175/1520-0450(1987)026<0561:RVIEAS>2.0.CO;2.

Nicholson, S. E., and J. P. Grist (2003), The seasonal evolution of the atmospheric circulation over West Africa and equatorial Africa, *J. Clim.*, *16*(7), 1013–1030, doi:10.1175/1520-0442(2003)016<1013:TSEOTA>2.0.CO;2.

Nicholson, S. E., and J. Kim (1997), The relationship of the El Niño-Southern Oscillation to African rainfall, *Int. J. Climatol.*, *17*(117–135), 117–135.

Nicholson, S. E., B. Some, and B. Kone (2000), An Analysis of Recent Rainfall Conditions in West Africa, Including the Rainy Seasons of the 1997 El Nino and the 1998 La Nina Years, *J. Clim.*, *13*, 2628–2640, doi:10.1007/s10803-018-3505-1.

Nicholson, S. E., B. Some, J. McCollum, E. Nelkin, D. Klotter, Y. Berte, B. M. Diallo, I. Gaye, G. Kpabeba, O. Ndiaye, J. N. Noukpozounkou, M. M. Tanu, a. Thiam, a. a. Toure, and a. K. Traore (2003), Validation of TRMM and Other Rainfall Estimates with a High-Density Gauge Dataset for West Africa. Part II: Validation of TRMM Rainfall Products, *J. Appl. Meteorol.*, *42*(10), 1355–1368, doi:10.1175/1520-0450(2003)042<1355:VOTAOR>2.0.CO;2.

Nicholson, S. E., A. K. Dezfuli, and D. Klotter (2012), A two-century precipitation dataset for the continent of Africa, *Bull. Am. Meteorol. Soc.*, *93*(8), 1219–1231, doi:10.1175/BAMS-D-11-00212.1.

Nicholson, S. E., D. Klotter, A. K. Dezfuli, and L. Zhou (2018a), New rainfall data sets for the Congo Basin and surrounding regions., *J. Hydrometeorol.*, 1379–1396, doi:10.1175/JHM-D-18-0015.1.

Nicholson, S. E., C. Funk, and A. H. Fink (2018b), Rainfall over the African continent from the 19th through the 21st century, *Glob. Planet. Change*, *165*(May 2017), 114–127, doi:10.1016/j.gloplacha.2017.12.014.

Nikulin, G., C. Jones, F. Giorgi, G. Asrar, M. B??chner, R. Cerezo-Mota, O. B. Christensen, M. D??qu??, J. Fernandez, A. H??nsler, E. van Meijgaard, P. Samuelsson, M. B. Sylla, and L. Sushama (2012), Precipitation climatology in an ensemble of CORDEX-Africa regional climate simulations, *J. Clim.*, *25*(18), 6057–6078, doi:10.1175/JCLI-D-11-00375.1.

Niznik, M. J., and B. R. Lintner (2013), Circulation, moisture, and precipitation relationships along the south pacific convergence zone in reanalyses and CMIP5 models, *J. Clim.*, *26*(24), 10174–10192, doi:10.1175/JCLI-D-13-00263.1.

Nobre, P., and J. Srukla (1996), Variations of Sea Surface Temperature, Wind Stress, and Rainfall over the Tropical Atlantic and South America, *J. Clim.*, *9*(10), 2464–2479, doi:10.1175/1520-0442(1996)009<2464:VOSSTW>2.0.CO;2.

Nogherotto, R., E. Coppola, F. Giorgi, and L. Mariotti (2013), Impact of Congo Basin deforestation on the African monsoon, *Atmos. Sci. Lett.*, *14*(1), 45–51, doi:10.1002/asl2.416.

Ogallo, L. J., J. E. Janowiak, and M. S. Halpert (1988), Teleconnection between seasonal rainfall over East Africa and global sea surface temperature anomalies, *J. Meteorol. Soc. Japan*, *66*(6), 807–821, doi:10.2151/jmsj1965.66.6_807.

Okoola, R. E., and P. G. Ambenje (2003), Transition from the Southern to the Northern Hemisphere summer of zones of active convection over the Congo Basin, *Meteorol. Atmos. Phys.*, *84*(3–4), 255–265, doi:10.1007/s00703-003-

0002-6.

Okumura, Y., and S. P. Xie (2006), Some overlooked features of tropical atlantic climate leading to a new Niño-like phenomenon, *J. Clim.*, *19*(22), 5859–5874, doi:10.1175/JCLI3928.1.

Ongoma, V., H. Chen, and C. Gao (2018), Evaluation of CMIP5 twentieth century rainfall simulation over the equatorial East Africa, *Theor. Appl. Climatol.*, (Ipcc 2013), 1–18, doi:10.1007/s00704-018-2392-x.

ORSTOM (1978), *Précipitations journalières de l'origine des stations à 1972*, Paris.

Overland, J. E., M. Wang, N. A. Bond, J. E. Walsh, V. M. Kattsov, and W. L. Chapman (2011), Considerations in the selection of global climate models for regional climate projections: The Arctic as a case study, *J. Clim.*, *24*(6), 1583–1597, doi:10.1175/2010JCLI3462.1.

Palmer, T. N., F. J. Doblas-Reyes, R. Hagedorn, and A. Weisheimer (2005), Probabilistic prediction of climate using multi-model ensembles: from basics to applications, *Philos. Trans. R. Soc. B*, *360*(1463), 1991–1998, doi:10.1098/rstb.2005.1750.

Payne, S. W., and M. M. McGarry (1977), The Relationship of Satellite Inferred Convective Activity to Easterly Waves Over West Africa and the Adjacent Ocean During Phase III of GATE, *Mon. Weather Rev.*, *105*(4), 413–420, doi:10.1175/1520-0493(1977)105<0413:TROSIC>2.0.CO;2.

Pereira, L. (2017), Climate Change Impacts on Agriculture across Africa, *Oxford Res. Encycl. Environ. Sci.*, 1–34, doi:10.1093/acrefore/9780199389414.013.292.

Petersen, W. A., S. A. Rutledge, W. A. Petersen, and S. A. Rutledge (2001), Regional Variability in Tropical Convection: Observations from TRMM, *J. Clim.*, *14*(17), 3566–3586, doi:10.1175/1520-0442(2001)014<3566:RVITCO>2.0.CO;2.

Pinto, I., C. Lennard, M. Tadross, B. Hewitson, A. Dosio, G. Nikulin, H. J. Panitz, and M. E. Shongwe (2016), Evaluation and projections of extreme precipitation over southern Africa from two CORDEX models, *Clim. Change*, *135*(3–4), 655–668, doi:10.1007/s10584-015-1573-1.

Pinto, I., C. Jack, and B. Hewitson (2018), Process-based model evaluation and projections over southern Africa from Coordinated Regional Climate Downscaling Experiment and Coupled Model Intercomparison Project Phase 5 models, *Int. J. Climatol.*, (January 2017), 1–11, doi:10.1002/joc.5666.

Pokam, W., C. L. Bain, R. S. Chadwick, R. Graham, D. J. Sonwa, and F. M. Kamga (2014), Identification of Processes Driving Low-Level Westerlies in West Equatorial Africa, *J. Clim.*, *27*(11), 4245–4262, doi:10.1175/JCLI-D-13-00490.1.

Pokam, W. M., and R. Washington (n.d.), Mid-tropospheric circulation and rainfall variability over Central Africa,

Pokam, W. M., L. A. Tchotchou Djiotang, and F. K. Mkankam (2012), Atmospheric water vapor transport and recycling in Equatorial Central Africa through NCEP/NCAR reanalysis data, *Clim. Dyn.*, *38*(9), 1715–1729, doi:10.1007/s00382-011-1242-7.

Pokam, W. M., G.-N. Longandjo, W. Moufouma-Okia, J. P. Bell, R. James, D. A. D. Vondou, A. Haensler, T. C. F. Nguemo, G. M. Guenang, A. L. D. Tchotchou, P. H. Kamsu-Tamo, R. R. Takong, G. Nikulin, C. Lennard, and A. Dosio (2018), Consequences of 1.5° C and 2° C global warming levels for temperature and precipitation changes over Central Africa, *Environ. Res. Lett.*

Pomposi, C., Y. Kushnir, and A. Giannini (2015), Moisture budget analysis of SST-driven decadal Sahel precipitation variability in the twentieth century, *Clim.*

Dyn., *44*(11–12), 3303–3321, doi:10.1007/s00382-014-2382-3.

Prodhomme, C., P. Terray, S. Masson, T. Izumo, T. Tozuka, and T. Yamagata (2014), Impacts of Indian Ocean SST biases on the Indian Monsoon: As simulated in a global coupled model, *Clim. Dyn.*, *42*(1–2), 271–290, doi:10.1007/s00382-013-1671-6.

Räisänen, J. (2007), How reliable are climate models?, *Tellus, Ser. A Dyn. Meteorol. Oceanogr.*, *59*(1), 2–29, doi:10.1111/j.1600-0870.2006.00211.x.

Reason, C. J. C., and H. Mulenga (1999), Relationships between South African rainfall and SST anomalies in the southwest Indian Ocean, *Int. J. Climatol.*, *19*(15), 1651–1673, doi:10.1002/(SICI)1097-0088(199912)19:15<1651::AID-JOC439>3.0.CO;2-U.

Reason, C. J. C., W. Landman, and W. Tennant (2006), Seasonal to decadal prediction of southern African climate and its links with variability of the Atlantic ocean, *Bull. Am. Meteorol. Soc.*, *87*(7), 941–955, doi:10.1175/BAMS-87-7-941.

Reichler, T., and J. Kim (2008), How well do coupled models simulate today's climate?, *Bull. Am. Meteorol. Soc.*, *89*(3), 303–311, doi:10.1175/BAMS-89-3-303.

Rennick, M. A. (1976), The Generation of African Waves, *J. Atmos. Sci.*, *33*(10), 1955–1969, doi:10.1175/1520-0469(1976)033<1955:TGOAW>2.0.CO;2.

Richter, I. (2015), Climate model biases in the eastern tropical oceans: causes, impacts and ways forward, *Wiley Interdiscip. Rev. Clim. Chang.*, *6*(3), 345–358, doi:10.1002/wcc.338.

Richter, I., and S. P. Xie (2008), On the origin of equatorial Atlantic biases in coupled general circulation models, *Clim. Dyn.*, *31*(5), 587–598,

doi:10.1007/s00382-008-0364-z.

Richter, I., S. P. Xie, A. T. Wittenberg, and Y. Masumoto (2012), Tropical Atlantic biases and their relation to surface wind stress and terrestrial precipitation, *Clim. Dyn.*, *38*(5–6), 985–1001, doi:10.1007/s00382-011-1038-9.

Richter, I., P. Chang, T. Doi, T. Kataoka, M. Nagura, P. Oettli, S. de Szoeke, T. Tozuka, and Z. Xu (2016), An Overview of coupled GCM Biases in the Tropics, in *Indo-Pacific Climate Variability and Predictability*, edited by S. K. Behera and T. Yamagata, pp. 213–263, World Scientific.

Roehrig, R., D. Bouniol, F. Guichard, F. déric Hourdin, and J. L. Redelsperger (2013), The present and future of the west african monsoon: A process-oriented assessment of CMIP5 simulations along the AMMA transect, *J. Clim.*, *26*(17), 6471–6505, doi:10.1175/JCLI-D-12-00505.1.

Ropelewski, C. F., and M. S. Halpert (1987), Global and Regional Scale Precipitation Patterns Associated with the El Niño/Southern Oscillation, *Mon. Weather Rev.*, *115*(8), 1606–1626, doi:10.1175/1520-0493(1987)115<1606:GARSPP>2.0.CO;2.

Rowell, D. P. (2012), Sources of uncertainty in future changes in local precipitation, *Clim. Dyn.*, *39*(7–8), 1929–1950.

Rowell, D. P., and R. Chadwick (2018), Causes of the Uncertainty in Projections of Tropical Terrestrial Rainfall Change: East Africa, *J. Clim.*, JCLI-D-17-0830.1, doi:10.1175/JCLI-D-17-0830.1.

Rowell, D. P., and J. R. Milford (1993), On the generation of African squall lines, *J. Clim.*, *6*(6), 1181–1193, doi:10.1175/1520-0442(1993)006<1181:OTGOAS>2.0.CO;2.

Rowell, D. P., B. B. B. Booth, S. E. Nicholson, and P. Good (2015), Reconciling past

and future rainfall trends over East Africa, *J. Clim.*, *28*(24), 9768–9788, doi:10.1175/JCLI-D-15-0140.1.

Rowell, D. P., C. a. Senior, M. Vellinga, and R. J. Graham (2016), Can climate projection uncertainty be constrained over Africa using metrics of contemporary performance?, *Clim. Change*, *134*(4), 621–633, doi:10.1007/s10584-015-1554-4.

Saeed, F., A. Haensler, T. Weber, S. Hagemann, and D. Jacob (2013), Representation of extreme precipitation events leading to opposite climate change signals over the Congo basin, *Atmosphere (Basel).*, *4*(3), 254–271, doi:10.3390/atmos4030254.

Samba, G., and D. Nganga (2012), Rainfall variability in Congo-Brazzaville: 1932–2007, *Int. J. Climatol.*, *32*(6), 854–873, doi:10.1002/joc.2311.

Samba, G., D. Nganga, and M. Mpounza (2008), Rainfall and temperature variations over Congo-Brazzaville between 1950 and 1998, *Theor. Appl. Climatol.*, *91*, 85–97.

Sandjon, A. T., A. Nzeukou, and C. Tchawoua (2012), Intraseasonal atmospheric variability and its interannual modulation in Central Africa, *Meteorol. Atmos. Phys.*, *117*, 167–179, doi:10.1007/s00703-012-0196-6.

Sanga-Ngoie, K., and K. Fukuyama (1996), Interannual and longterm climate variability over the Zaire river basin during the last 30 years, *J. Geophys. Res.*, *101*(16), 351–360.

Schmidt, G. A., M. Kelley, L. Nazarenko, R. Ruedy, G. L. Russell, I. Aleinov, M. Bauer, S. E. Bauer, M. K. Bhat, R. Bleck, V. Canuto, Y. H. Chen, Y. Cheng, T. L. Clune, A. Del Genio, R. de Fainchtein, G. Faluvegi, J. E. Hansen, R. J. Healy, N. Y. Kiang, D. Koch, A. A. Lacis, A. N. LeGrande, J. Lerner, K. K. Lo, E. E. Matthews, S. Menon, R.

L. Miller, V. Oinas, A. O. Oloso, J. P. Perlwitz, M. J. Puma, W. M. Putman, D. Rind, A. Romanou, M. Sato, D. T. Shindell, S. Sun, R. A. Syed, N. Tausnev, K. Tsigaridis, N. Unger, A. Voulgarakis, M. S. Yao, and J. Zhang (2014), Configuration and assessment of the GISS ModelE2 contributions to the CMIP5 archive, *J. Adv. Model. Earth Syst.*, *6*(1), 141–184, doi:10.1002/2013MS000265.

Schneider, U., A. Becker, P. Finger, A. Meyer-Christoffer, B. Rudolf, and M. Ziese (2015), GPCC Full Data Reanalysis Version 7.0 at 0.5°: Monthly Land-Surface Precipitation from Rain-Gauges built on GTS-based and Historic Data, , doi:10.5676/DWD_GPCC/FD_M_V7_050.

Schott, F., J. Fischer, U. Garternicht, and D. Quadfasel (1997), Summer monsoon response of the Northern Somali Current, 1995, *Geophys. Res. Lett.*, *24*(21), 2565, doi:10.1029/97GL00888.

Schott, F. a., and J. P. McCreary (2001), The monsoon circulation of the Indian Ocean, *Prog. Oceanogr.*, *51*(1), 1–123, doi:10.1016/S0079-6611(01)00083-0.

Schubert, C. J., E. Durisch-kaiser, B. Wehrli, B. Thamdrup, P. Lam, and M. M. M. Kuypers (2006), Anaerobic ammonium oxidation in a tropical freshwater system (Lake Tanganyika), *Env. Microbiol*, *8*(10), 1857–1863, doi:10.1111/j.1462-2920.2006.001074.x.

Schumacher, C., and R. A. Houze (2003), Stratiform rain in the tropics as seen by the TRMM precipitation radar, *J. Clim.*, *16*(11), 1739–1756, doi:10.1175/1520-0442(2003)016<1739:SRITTA>2.0.CO;2.

Scoccimarro, E., S. Gualdi, A. Bellucci, A. Sanna, P. G. Fogli, E. Manzini, M. Vichi, P. Oddo, and A. Navarra (2011), Effects of tropical cyclones on ocean heat transport in a high-resolution coupled general circulation model, *J. Clim.*, *24*(16), 4368–4384, doi:10.1175/2011JCLI4104.1.

Seth, A., S. A. Rauscher, M. Biasutti, A. Giannini, S. J. Camargo, and M. Rojas (2013), CMIP5 projected changes in the annual cycle of precipitation in monsoon regions, *J. Clim.*, *26*(19), 7328–7351, doi:10.1175/JCLI-D-12-00726.1.

Shem, W. O. (2006), Biosphere-atmosphere interaction over the Congo Basin and its influence on the regional hydrological cycle, Georgia Institute of Technology.

Shepherd, T. G. (2014), Atmospheric circulation as a source of uncertainty in climate change projections, *Nat. Geosci.*, *7*(10), 703–708, doi:10.1038/NGEO2253.

Shongwe, M. E., G. J. van Oldenborgh, B. J. J. M. van den Hurk, B. de Boer, C. A. S. Coelho, and M. K. van Aalst (2009), Projected Changes in Mean and Extreme Precipitation in Africa under Global Warming. Part I: Southern Africa, *J. Clim.*, *22*(13), 3819–3837, doi:10.1175/2009JCLI2317.1.

Shongwe, M. E., G. J. van Oldenborgh, B. van den Hurk, and M. van Aalst (2011), Projected changes in mean and extreme precipitation in Africa under global warming. Part II: East Africa, *J. Clim.*, *24*(14), 3718–3733, doi:10.1175/2010JCLI2883.1.

Sorí, R., R. Nieto, S. M. Vicente-Serrano, A. Drumond, and L. Gimeno (2017), A Lagrangian perspective of the hydrological cycle in the Congo River basin, *Earth Syst. Dyn.*, *8*(3), 653–675, doi:10.5194/esd-8-653-2017.

Stainforth, D. A., T. E. Downing, R. Washington, A. Lopez, and M. New (2007), Issues in the interpretation of climate model ensembles to inform decisions, *Philos. Trans. R. Soc. A Math. Phys. Eng. Sci.*, *365*(1857), 2163–2177, doi:10.1098/rsta.2007.2073.

Stevens, B., and S. Bony (2013), What are Climate Models Missing?, , *340*(July),

183–187, doi:10.1126/science.1112699.

Stratton, R. A., C. A. Senior, S. B. Vosper, S. S. Folwell, I. A. Boutle, P. D. Earnshaw, E. Kendon, A. P. Lock, A. Malcolm, J. Manners, C. J. Morcrette, C. Short, A. J. Stirling, C. M. Taylor, S. Tucker, S. Webster, and J. M. Wilkinson (2018), A Pan-African convection-permitting regional climate simulation with the met office unified model: CP4-Africa, *J. Clim.*, *31*(9), 3485–3508, doi:10.1175/JCLI-D-17-0503.1.

Sun, Q., C. Miao, Q. Duan, H. Ashouri, S. Sorooshian, and K.-L. Hsu (2017), A review of global precipitation datasets: data sources, estimation, and intercomparisons, *Rev. Geophys.*, 1–29, doi:10.1002/2017RG000574.

Suzuki, T. (2011), Seasonal variation of the ITCZ and its characteristics over central Africa, *Theor. Appl. Climatol.*, *103*(1), 39–60, doi:10.1007/s00704-010-0276-9.

Sylla, M. B., F. Giorgi, E. Coppola, and L. Mariotti (2013), Uncertainties in daily rainfall over Africa: Assessment of gridded observation products and evaluation of a regional climate model simulation, *Int. J. Climatol.*, *33*(7), 1805–1817, doi:10.1002/joc.3551.

Taylor, K. E. (2001), Summarizing multiple aspects of model performance in a single diagram, *J. Geophys. Res.*, *106*(D7), 7183–7192, doi:10.1029/2000JD900719.

Taylor, K. E., R. J. Stouffer, and G. A. Meehl (2012), An Overview of CMIP5 and the Experiment Design, *Bull. Am. Meteorol. Soc.*, *93*(4), 495–498, doi:10.1175/BAMS-D-11-00094.1.

Tebaldi, C., and R. Knutti (2007), The use of the multi-model ensemble in probabilistic climate projections., *Philos. Trans. A. Math. Phys. Eng. Sci.*, *365*(1857), 2053–2075, doi:10.1098/rsta.2007.2076.

Tennant, W. (2003), An Assessment of Intraseasonal Variability from 13-Yr GCM Simulations, *Mon. Weather Rev.*, *131*(9), 1975–1991, doi:10.1175/1520-0493(2003)131<1975:AAOIVF>2.0.CO;2.

Thorncroft, C. D., and M. Blackburn (1999), Maintenance of the African easterly jet, *Q. J. R. Meteorol. Soc.*, *125*(555), 763–786, doi:10.1002/qj.49712555502.

Thorncroft, C. D., and B. J. Hoskins (1994), An idealized study of African easterly waves. I: A linear view, *Q. J. R. Meteorol. Soc.*, *120*(518), 953–982, doi:10.1002/qj.49712051809.

Tierney, J. E., C. C. Ummenhofer, and P. B. deMenocal (2015), Past and future rainfall in the Horn of Africa, *Sci. Adv.*, *1*(9), e1500682–e1500682, doi:10.1126/sciadv.1500682.

Titchner, H. A., and N. A. Rayner (2014), The Met Office Hadley Centre sea ice and sea surface temperature data set, version 2: 1. Sea ice concentrations, *J. Geophys. Res. Atmos.*, *119*, 2864–2889, doi:10.1002/2013JD020316.

Todd, M. C., and R. Washington (2004), Climate variability in central equatorial Africa: Influence from the Atlantic sector, *Geophys. Res. Lett.*, *31*(23), 1–4, doi:10.1029/2004GL020975.

Toracinta, E. R., and E. J. Zipser (2001), Lightning and SSM/I-ice-scattering mesoscale convective systems in the global tropics, *J. Appl. Meteorol.*, *40*(6), 983–1002, doi:10.1175/1520-0450(2001)040<0983:LASIIS>2.0.CO;2.

Trapp, R. J. (2013), *Mesoscale-convective processes in the atmosphere*, Cambridge University Press, Cambridge and New York.

Trenberth, K. E. (1998), Atmospheric moisture residence times and cycling: Implications for rainfall rates and climate change, *Clim. Change*, *39*(4), 667–694, doi:10.1023/A:1005319109110.

Uccellini, L. W., and D. R. Johnson (1979), The coupling of upper and lower tropospheric jet streaks and implications for the development of severe convective storms, *Mon. Weather Rev.*, *107*(6), 682–703, doi:10.1175/1520-0493(1979)107<0682:TCOUAL>2.0.CO;2.

Ummenhofer, C. C., A. Sen Gupta, M. H. England, and C. J. C. Reason (2009), Contributions of Indian Ocean sea surface temperatures to enhanced East African rainfall, *J. Clim.*, *22*(4), 993–1013, doi:10.1175/2008JCLI2493.1.

Vecchi, G. A., and B. J. Soden (2007), Global warming and the weakening of the tropical circulation, *J. Clim.*, *20*(17), 4316–4340, doi:10.1175/JCLI4258.1.

Vecchi, G. A., B. J. Soden, A. T. Wittenberg, I. M. Held, A. Leetmaa, and M. J. Harrison (2006), Weakening of tropical Pacific atmospheric circulation due to anthropogenic forcing, *Nature*, *441*(1), 73–76, doi:10.1038/nature04744.

Vigaud, N., Y. Richard, M. Rouault, and N. Fauchereau (2007), Water vapour transport from the tropical Atlantic and summer rainfall in tropical southern Africa, *Clim. Dyn.*, *28*(2–3), 113–123, doi:10.1007/s00382-006-0186-9.

Viste, E., D. Korecha, and A. Sorteberg (2013), Recent drought and precipitation tendencies in Ethiopia, *Theor. Appl. Climatol.*, *112*(3–4), 535–551, doi:10.1007/s00704-012-0746-3.

Vizy, E. K., and K. H. Cook (2001), Mechanisms by Which Gulf of Guinea and Eastern North Atlantic Sea Surface Temperature Anomalies Can Influence African Rainfall, *J. Clim.*, *14*(5), 795–821, doi:10.1175/1520-0442(2001)014<0795:MBWGOG>2.0.CO;2.

Vizy, E. K., and K. H. Cook (2012), Mid-twenty-first-century changes in extreme events over northern and tropical Africa, *J. Clim.*, *25*(17), 5748–5767, doi:10.1175/JCLI-D-11-00693.1.

Vizy, E. K., and K. H. Cook (2016), Understanding long-term (1982–2013) multi-decadal change in the equatorial and subtropical South Atlantic climate, *Clim. Dyn.*, *46*(7–8), 2087–2113, doi:10.1007/s00382-015-2691-1.

Vizy, E. K., K. H. Cook, J. Crétat, and N. Neupane (2013), Projections of a wetter sahel in the twenty-first century from global and regional models, *J. Clim.*, *26*(13), 4664–4687, doi:10.1175/JCLI-D-12-00533.1.

Vogel, C. (2005), "Seven fat years and seven lean years"? Climate change and agriculture in Africa, *IDS Bull.*, *36*(2), 30–35, doi:10.1111/j.1759-5436.2005.tb00192.x.

Voldoire, A., E. Sanchez-Gomez, D. Salas y Mélia, B. Decharme, S. Cassou, C. Sénési, S. Valcke, I. Beau, A. Alias, M. Chevallier, M. Déqué, J. Deshayes, H. Douville, E. Fernandez, G. Madec, E. Maisonnave, M. Moine, S. Planton, D. Saint-Martin, S. Szopa, S. Tyteca, R. Alkama, S. Belamari, A. Braun, L. Coquart, and F. Chauvin (2011), The CNRM-CM5.1 global climate model: description and basic evaluation, *Clim. Dyn.*, *40*(9), 2091–2121, doi:10.1007/s00382-011-1259-y.

Vondou, D. A., and A. Haensler (2017), Evaluation of simulations with the regional climate model REMO over Central Africa and the effect of increased spatial resolution, *Int. J. Climatol.*, *37*(March), 741–760, doi:10.1002/joc.5035.

van Vuuren, D. P., J. Edmonds, M. Kainuma, K. Riahi, A. Thomson, K. Hibbard, G. C. Hurtt, T. Kram, V. Krey, J. F. Lamarque, T. Masui, M. Meinshausen, N. Nakicenovic, S. J. Smith, and S. K. Rose (2011), The representative concentration pathways: An overview, *Clim. Change*, *109*(1), 5–31, doi:10.1007/s10584-011-0148-z.

Wahl, S., M. Latif, W. Park, and N. Keenlyside (2009), On the Tropical Atlantic SST warm bias in the Kiel Climate Model, *Clim. Dyn.*, *36*(5–6), 891–906,

doi:10.1007/s00382-009-0690-9.

Wang, C., L. Zhang, S.-K. Lee, L. Wu, and C. R. Mechoso (2014), A global perspective on CMIP5 climate model biases, *Nat. Clim. Chang.*, *4*(3), 201–205, doi:10.1038/NCLIMATE2118.

Washington, R., M. Harrison, D. Conway, E. Black, A. Challinor, D. Grimes, R. Jones, A. Morse, and M. Todd (2004), *African Climate Report: A report commissioned by the UK Government to review African climate science , policy and options for action*.

Washington, R., M. Harrison, D. Conway, E. Black, A. Challinor, D. Grimes, R. Jones, A. Morse, G. Kay, and M. Todd (2006), African Climate Change: Taking the shorter route, *Bull. Am. Meteorol. Soc.*, *87*(10), 1355–1366, doi:10.1175/BAMS-87-10-1355.

Washington, R., R. James, H. Pearce, W. M. Pokam, and W. Moufouma-Okia (2013), Congo Basin rainfall climatology: can we believe the climate models?, *Philos. Trans. R. Soc. Lond. B. Biol. Sci.*, *368*(1625), 20120296, doi:10.1098/rstb.2012.0296.

Watanabe, M., T. Suzuki, R. O'Ishi, Y. Komuro, S. Watanabe, S. Emori, T. Takemura, M. Chikira, T. Ogura, M. Sekiguchi, K. Takata, D. Yamazaki, T. Yokohata, T. Nozawa, H. Hasumi, H. Tatebe, and M. Kimoto (2010), Improved climate simulation by MIROC5: Mean states, variability, and climate sensitivity, *J. Clim.*, *23*(23), 6312–6335, doi:10.1175/2010JCLI3679.1.

Watanabe, S., T. Hajima, K. Sudo, T. Nagashima, T. Takemura, H. Okajima, T. Nozawa, H. Kawase, M. Abe, T. Yokohata, T. Ise, H. Sato, E. Kato, K. Takata, S. Emori, and M. Kawamiya (2011), MIROC-ESM: model description and basic results of CMIP5-20c3m experiments, *Geosci. Model Dev. Discuss.*, *4*(2), 1063–

1128, doi:10.5194/gmdd-4-1063-2011.

Watterson, I. G., J. Bathols, and C. Heady (2014), What influences the skill of climate models over the continents?, *Bull. Am. Meteorol. Soc.*, *95*(5), 689–700, doi:10.1175/BAMS-D-12-00136.1.

Webster, P. J. (1983), Large-scale structure of the tropical atmosphere, in *Large scale dynamical processes in the atmosphere*, edited by B. Hoskins and R. Pearce, pp. 235–275, Academic Press, New York, NY.

Werth, D., and R. Avissar (2005), The local and global effects of African deforestration, *Geophys. Res. Lett.*, *32*(12), 1–4, doi:10.1029/2005GL022969.

Williams, A. P., C. Funk, J. Michaelsen, S. A. Rauscher, I. Robertson, T. H. G. Wils, M. Koprowski, Z. Eshetu, and N. J. Loader (2012), Recent summer precipitation trends in the Greater Horn of Africa and the emerging role of Indian Ocean sea surface temperature, *Clim. Dyn.*, *39*(9–10), 2307–2328, doi:10.1007/s00382-011-1222-y.

Williams, a. P., and C. Funk (2011), A westward extension of the warm pool leads to a westward extension of the Walker circulation, drying eastern Africa, *Clim. Dyn.*, *37*(11–12), 2417–2435, doi:10.1007/s00382-010-0984-y.

Williams, C. A., N. P. Hanan, J. C. Neff, R. J. Scholes, J. A. Berry, A. S. Denning, and D. F. Baker (2007), Africa and the global carbon cycle, *Carbon Balance Manag.*, *13*(3), doi:10.1186/1750-0680-2-3.

Williams, E. R., and G. Sátori (2004), Lightning, thermodynamic and hydrological comparison of the two tropical continental chimneys, *J. Atmos. Solar-Terrestrial Phys.*, *66*(13–14 SPEC. ISS.), 1213–1231, doi:10.1016/j.jastp.2004.05.015.

WMO (2003) Twenty-first status report on implementation of the World Weather

Watch: Forty years of World Weather Watch. WMO Rep. 957

World Bank (2017a), World Development Indicators, Available from: http://wdi.worldbank.org/table (Accessed 6 September 2018)

World Bank (2017b), World Development Indicators,

Wu, T., W. Li, J. Ji, X. Xin, L. Li, Z. Wang, Y. Zhang, J. Li, F. Zhang, M. Wei, X. Shi, F. Wu, L. Zhang, M. Chu, W. Jie, Y. Liu, F. Wang, X. Liu, Q. Li, M. Dong, X. Liang, Y. Gao, and J. Zhang (2013), Global carbon budgets simulated by the Beijing Climate Center Climate System Model for the last century, *J. Geophys. Res. Atmos.*, *118*(10), 4326–4347, doi:10.1002/jgrd.50320.

Xie, P., and P. a. Arkin (1997), Global Precipitation: A 17-Year Monthly Analysis Based on Gauge Observations, Satellite Estimates, and Numerical Model Outputs, *Bull. Am. Meteorol. Soc.*, *78*(11), 2539–2558, doi:10.1175/1520-0477(1997)078<2539:GPAYMA>2.0.CO;2.

Xie, P., J. E. Janowiak, P. A. Arkin, R. Adler, A. Gruber, R. Ferraro, G. J. Huffman, and S. Curtis (2003), GPCP pentad precipitation analyses: an experimental dataset based on gauge observations and satellite estimates, *J. Clim.*, *16*(13), 2197–2214, doi:10.1175/2769.1.

Xie, S. P., and J. a. Carton (2004), Tropical Atlantic variability: Patterns, mechanisms, and impacts, *Geophys. Monogr. Ser.*, *147*, 121–142, doi:10.1029/147GM07.

Xie, S. P., C. Deser, G. A. Vecchi, J. Ma, H. Teng, and A. T. Wittenberg (2010), Global warming pattern formation: Sea surface temperature and rainfall, *J. Clim.*, *23*(4), 966–986, doi:10.1175/2009JCLI3329.1.

Xu, Z., P. Chang, I. Richter, W. Kim, and G. Tang (2014), Diagnosing southeast tropical Atlantic SST and ocean circulation biases in the CMIP5 ensemble,

Clim. Dyn., *43*, 3123–3145, doi:10.1007/s00382-014-2247-9.

Yang, D., and O. a. Saenko (2012), Ocean heat transport and its projected change in CanESM2, *J. Clim.*, *25*(23), 8148–8163, doi:10.1175/JCLI-D-11-00715.1.

Yang, Q., R. A. Houze, L. R. Leung, and Z. Feng (2017), Environments of Long-Lived Mesoscale Convective Systems Over the Central United States in Convection Permitting Climate Simulations, *J. Geophys. Res. Atmos.*, *122*(24), 13,288-13,307, doi:10.1002/2017JD027033.

Yang, W., R. Seager, M. a. Cane, and B. Lyon (2014), The East African long rains in observations and models, *J. Clim.*, *27*(19), 7185–7202, doi:10.1175/JCLI-D-13-00447.1.

Yang, W., R. Seager, M. A. Cane, and B. Lyon (2015a), The annual cycle of East African precipitation, *J. Clim.*, *28*(6), 2385–2404, doi:10.1175/JCLI-D-14-00484.1.

Yang, W., R. Seager, M. A. Cane, and B. Lyon (2015b), The rainfall annual cycle bias over East Africa in CMIP5 coupled climate models, *J. Clim.*, *28*(24), 9789–9802, doi:10.1175/JCLI-D-15-0323.1.

Yarnal, B. (1993), *Synoptic climatology in environmental analysis: A primer*, Belhaven Press, London.

Yin, L., R. Fu, E. Shevliakova, and R. E. Dickinson (2013), How well can CMIP5 simulate precipitation and its controlling processes over tropical South America?, *Clim. Dyn.*, *41*(11–12), 3127–3143, doi:10.1007/s00382-012-1582-y.

Yin, X., and A. Gruber (2010), Validation of the abrupt change in GPCP precipitation in the Congo River Basin, *2International J. Climatol.*, *30*, 110–119, doi:10.1002/joc.

Yukimoto, S., H. Yoshimura, M. Hosaka, T. Sakami, H. Tsujino, M. Hirabara, T. Y. Tanaka, M. Deushi, A. Obata, H. Nakano, Y. Adachi, E. Shindo, S. Yabu, T. Ose, and A. Kitoh (2011), Meteorological Research Institute-Earth System Model Version 1 (MRI-ESM1), Technical Reports No. 64.

Yukimoto, S., Y. Adachi, M. Hosaka, T. Sakami, H. Yoshimura, M. Hirabara, T. Y. Tanaka, E. Shindo, H. Tsujino, M. Deushi, R. Mizuta, S. Yabu, A. Obata, H. Nakano, T. Koshiro, T. Ose, and A. Kitoh (2012), A New Global Climate Model of the Meteorological Research Institute: MRI-CGCM3 - Model Description and Basic Performance, *J. Meteorol. Soc. Japan*, *90A*(0), 23–64, doi:10.2151/jmsj.2012-A02.

Zhang, X., F. W. Zwiers, G. C. Hegerl, F. H. Lambert, N. P. Gillett, S. Solomon, P. A. Stott, and T. Nozawa (2007), Detection of human influence on twentieth-century precipitation trends, *Nature*, *448*(7152), 461–465, doi:10.1038/nature06025.

Zhou, L., Y. Tian, R. B. Myneni, P. Ciais, S. Saatchi, Y. Y. Liu, S. Piao, H. Chen, E. F. Vermote, C. Song, and T. Hwang (2014), Widespread decline of Congo rainforest greenness in the past decade., *Nature*, *509*(7498), 86–90, doi:10.1038/nature13265.

Zipser, E. J., D. J. Cecil, C. Liu, S. W. Nesbitt, and D. P. Yorty (2006), Where are the Most Intense Thunderstorms on Earth?, *Bull. Am. Meteorol. Soc.*, *87*(8), 1057–1071, doi:10.1175/BAMS-87-8-1057.

Zuidema, P., P. Chang, B. Medeiros, B. P. Kirtman, R. Mechoso, E. K. Schneider, T. Toniazzo, I. Richter, R. J. Small, K. Bellomo, P. Brandt, S. De Szoeke, J. T. Farrar, E. Jung, S. Kato, M. Li, C. Patricola, Z. Wang, R. Wood, and Z. Xu (2016), Challenges and prospects for reducing coupled climate model sst biases in the

eastern tropical atlantic and pacific oceans: The U.S. Clivar eastern tropical oceans synthesis working group, *Bull. Am. Meteorol. Soc.*, *97*(12), 2305–2327, doi:10.1175/BAMS-D-15-00274.1.